Report Rapport

Atomic Energy
Control Board

Commission de contrôle
de l'énergie atomique

86-05414/

Atomic Energy Control Board
P.O. Box 1046
Ottawa, Canada
K1P 5S9

Commission de contrôle de l'énergie atomique
C.P. 1046
Ottawa, Canada
K1P 5S9

INFO-0180-1

INVESTIGATION OF THE EXPLOSION HAZARDS OF HYDROGEN SULPHIDE

(PHASE I)

Report Covering the Period
January 1984 to January 1985

A research report prepared for the
Atomic Energy Control Board
Ottawa, Canada

by

A.J. Saber and A. Sulmistras
Concordia University
Montreal, Canada

I.O. Moen
Defence Research Establishment Suffield
Ralston, Alberta

P.A. Thibault
Combustion Dynamics Ltd.
Ralston, Alberta

March 1986

Canada

Research report

INVESTIGATION OF THE EXPLOSION HAZARDS OF HYDROGEN SULPHIDE -- PHASE I

ABSTRACT

The results of Phase I of an investigation directed towards quantifying the explosion hazards of hydrogen sulphide in air are described. The first phase is focussed on detonation in free hydrogen sulphide/air clouds. Detonation properties, including velocity and pressure, have been calculated and compared with experimental results. The observed detonation structure together with critical tube diameter tests are used to assess the detonability of hydrogen sulphide/air mixtures relative to hydrogen and common hydrocarbon gases. Detailed chemical kinetic modelling of hydrogen sulphide combustion in air has been performed to correlate the detonation cell size data and to determine the influence of water vapour on the detonability of hydrogen sulphide in air. Calculations of the blast wave properties for detonation of a hydrogen sulphide/air cloud provide the data required to assess the blast effects of such explosions.

The key results are summarized in the main text, and detailed reports covering various aspects of hydrogen sulphide/air detonations are included in five appendices.

RÉSUMÉ

Le rapport présente les résultats de la première phase d'une étude sur la quantification des dangers d'explosion de l'hydrogène sulfuré dans l'air. La première phase traitait principalement de l'explosion de nuages libres d'hydrogène sulfuré dans l'air. Les propriétés de l'explosion, y compris la vitesse et la pression, ont été calculées et comparées à des résultats d'expérience. La structure observée du nuage qui explose et les épreuves de diamètre critique des tubes sont utilisées pour évaluer la capacité d'explosion des mélanges d'hydrogène sulfuré et d'air par rapport à l'hydrogène et aux gaz communs d'hydrocarbone. Une modélisation chimique cinétique détaillée de la combustion de l'hydrogène sulfuré dans l'air a été effectuée pour mettre en corrélation les données dérivées de la grosseur des cellules après l'explosion et pour déterminer l'influence de la vapeur d'eau sur la capacité d'explosion de l'hydrogène sulfuré dans l'air. Les calculs des propriétés des ondes d'explosion de l'hydrogène sulfuré dans l'air fournissent les données requises pour évaluer les effets de telles explosions.

Les résultats les plus importants sont résumés dans le texte principal et les rapports détaillés de divers aspects de l'explosion de l'hydrogène sulfuré dans l'air sont inclus dans les cinq annexes.

DISCLAIMER

The Atomic Energy Control Board is not responsible for the accuracy of the statements made or opinions expressed in this publication, and neither the Board nor the authors assume liability with respect to any damage or loss incurred as a result of the use of the information contained in this publication.

TABLE OF CONTENTS

Page

ABSTRACT i
DISCLAIMER i
TABLE OF CONTENTS iii
LIST OF TABLES v
LIST OF FIGURES vi

A. INTRODUCTION .... 1.

B. HYDROGEN SULPHIDE COMBUSTION CHEMISTRY .... 2.

C. DETONATION PROPERTIES .... 3.

D. BLAST FROM DETONATION OF H_2S/AIR CLOUDS .... 5.

E. CONCLUSION .... 6.

APPENDICES

APPENDIX A	"Investigation of the Explosion Hazards of Hydrogen Sulphide", by A.J. Saber, A. Sulmistras and I.O. Moen. Report A, covering the period: 10 January 1984 to 15 October 1984, partially prepared with respect to Supply and Services Canada Contract No.: OSG.97702-R-3-7856, Serial No.: 8SG83-00152, 15 October 1984.
APPENDIX B	"Detonations in Hydrogen Sulphide-Air Cloud", by A. Sulmistras, I.O. Moen and A.J. Saber. Suffield Memorandum No. 1140, Defence Research Establishment Suffield, Ralston, Alberta, April 1985.
APPENDIX C	"Chemical Kinetics and Cellular Structure of Detonations in Hydrogen Sulphide and Air", by J.E. Shepherd, A. Sulmistras, A.J. Saber and I.O. Moen. Submitted to 10th International Colloquium on Dynamics of Explosions and Reactive Systems, August 4-9, 1985, Berkeley, CA, U.S.A. Prepared February 25, 1985.
APPENDIX D	"Detonations in Hydrogen Sulphide-Air Clouds, with Comparisons to Other Fuel-Air Mixtures", by A. Sulmistras, I.O. Moen and A.J. Saber. Presented at the Joint Technical Meeting of the Central and Western States Sections of the Combustion Institute, San Antonio, Texas, April 22-23, 1985.
APPENDIX E	"Blast Properties of H_2S-Air Detonations", by Paul Thibault, Combustion Dynamics Ltd. Report, Ralston, Alberta, April 1985.

LIST OF TABLES

TABLE I Toxicity Table for Hydrogen Sulphide (H_2S)

TABLE II Estimates of Flammability Limits for Selected Fuel-Air Mixtures

TABLE III Detonation Parameters for Fuel-Air Mixtures

TABLE IV Characteristic Pressures and Impulses from Detonation of a 10 m Radius Hemispherical Cloud of Stoichiometric Hydrogen-Sulphide in Air

LIST OF FIGURES

FIGURE 1 Burning Velocity of Hydrogen Sulphide-Air and Methane-Air Flames.

FIGURE 2 Chapman-Jouguet (C-J) Detonation Velocity for Various Fuel-Air Mixtures.

FIGURE 3 Chapman-Jouguet (C-J) Detonation Pressure Ratio for Various Fuel-Air Mixtures.

FIGURE 4 Comparison of Detonation Cell Structures in Hydrogen Sulphide-Air and Butane-Air Mixtures.

FIGURE 5 Detonation Cell Parameters for Hydrogen Sulphide in Air.

FIGURE 6 Critical Tube Diameters for Detonations in Various Fuel-Air Mixtures.

A. INTRODUCTION

Hydrogen sulphide (H_2S) is both an asphyxiant and an irritant. It has a molecular weight of 34.08 kg/kgmole and, at normal temperature (20°C) and pressure (101.3 kPa), the material is a clear colourless gas. In concentrations of about 1 part per million (ppm), 0.0001%, it is "evil smelling" with the characteristic odour of "rotten eggs". It is the constituent that makes sour gas "sour".

The toxicity of hydrogen sulphide is summarized in Table I. The allowable threshold for 8 hours exposure, the Threshold Limit Value (TLV) is 10 ppm in air. Above 10 ppm, protective equipment must be worn.

Hydrogen sulphide is produced, stored, and used in the chemical process industry. In particular, large quantities (thousands of tonnes) of hydrogen sulphide are used in the Gridler-Sulphide process for the production of deuterium oxide (heavy water) in plants licenced by the Atomic Energy Control Board (AECB). Heavy water is an essential material for the operation of CANDU nuclear reactors. Hydrogen sulphide is flammable in air at normal conditions in concentrations from about 4.3 to 45%, by volume. It is therefore necessary to assess realistically the potential hazard, if spilled hydrogen sulphide is ignited. If ignition occurs immediately, a diffusion flame results and the rate of burning is controlled by the mixing of fuel with air. The hazards of diffusion flames are dominated by thermal radiation from the burning fireball. However, without immediate ignition, a fuel/air cloud can develop. The cloud will be fuel lean at the outer perimeter and fuel rich near the source of the spill. Parts of this cloud are potentially explosive, and, if ignited, these parts can either detonate or burn, depending on the characteristics of the ignition source, the reactivity of the fuel/air mixtures and the geometry of the cloud.

Detonations, the most devastating explosion possible, are characterized by both high combustion velocity (~ 1700 m/s) and large pressure changes (~ 15 atm). On the other hand, laminar flames are typically associated with relatively low burning velocities (~ 0.5 m/s) and small pressure changes (~ 10^{-3} atm).

However, flames can be accelerated to high velocities by turbulence and confinement effects. These latter effects depend on the obstacle and confinement configuration, and the flow field into which the flame propagates, as well as the nature of the reactant mixture.

The present investigation is directed toward quantifying the explosion hazards of hydrogen sulphide in air, relevant to the environment of heavy water plants licenced by the Atomic Energy Control Board. The present report describes the work on detonations which is now complete. Investigations of flame acceleration and potential for transition to detonations are now in progress.

B. HYDROGEN SULPHIDE COMBUSTION CHEMISTRY

Some of the relevant physical and chemical properties of hydrogen sulphide and related compounds are discussed in Appendix A. Of particular relevance to the present study are the combustion properties in air. The flammability limits in air for hydrogen sulphide are compared with those of selected common gaseous fuels in Table II. The flammability limits of H_2S in air are relatively wide with a lower limit of 4.3% H_2S by volume and an upper limit of 45% H_2S. Within these limits H_2S will burn. The rate of burning as characterized by the laminar burning velocity depends on the H_2S/air composition, with a maximum velocity of 0.41 m/s at stoichiometric composition. The burning velocities for other compositions are compared with those for methane/air mixtures in Figure 1. The equivalence ratio ϕ is defined as the ratio of fuel/air divided by the ratio of fuel/air at stoichiometric composition. For H_2S/air mixtures, the relative amount of H_2S and air on a volumetric (or molar) basis can be expressed in terms of ϕ as follows:

$$\phi H_2S + 7.14 \text{ Air.}$$

In terms of the blast produced, laminar burning represents a relatively benign form of combustion. However, the potential for flame acceleration and possibly transition to detonation in obstacle and confined areas remain to be clarified. Detonations represent the potentially most damaging form of explosion and it is therefore important to characterize this type of explosion and to determine the susceptibility of H_2S/air to detonation.

C. DETONATION PROPERTIES

Both experimental measurements and theoretical calculations of properties of detonations in H_2S/air have been performed. Measurements were also performed for detonations in butane/air for comparison, and calculations were performed for a variety of fuel/air mixtures. Calculated detonation velocities (C-J velocities) and pressure ratios across the detonation waves (C-J pressure ratios) for these fuel/air mixtures are plotted as a function of fuel/air equivalence ratio in Figures 2 and 3, respectively. Values at stoichiometric compositions are given in Table III. The detonation velocity in H_2S/air at stoichiometric composition is 1647 m/s with an associated detonation pressure ratio of 15.3. These values are slightly smaller than those for the common hydrocarbon fuels (i.e., acetylene, ethylene, propane, butane and methane) and hydrogen, but in terms of the potential damage due to detonation of a cloud, these differences are insignificant.

As described in Appendix B, the measured detonation velocities and pressures are in good agreement with the calculated Chapman-Jouguet (C-J) values. The calculated values can therefore be used to predict the equilibrium detonation properties. These equilibrium detonation properties can be used to calculate the blast wave produced from detonation of a fuel/air cloud (see Appendix E). However, they provide no information on the susceptibility of a given fuel/air mixture to detonation.

Detailed discussions of the susceptibility of a given mixture to detonation are given in Appendix B, with a more concise summary in Appendix D. Essentially, the relative detonation hazard of a fuel/air mixture can be characterized by three different parameters, corresponding to: i) the critical initiation energy, E_c, or equivalently the mass of high explosive required to initiate a detonation, ii) the critical tube diameter, d_c, for a detonation to propagate from a round tube into a surrounding cloud, and iii) the characteristic dimension , S, of the detonation cellular structure. Extensive investigations over the past 10 years have established empirical correlations between these parameters, so that based on the measurement of one of the parameters, the relative detonation hazard can be assessed.

The experiments performed to assess the relative detonation hazards of H_2S in air are described in Appendix D. These experiments showed that the minimum critical tube diameter for H_2S in air was greater than 0.9 m, which implies that H_2S is less susceptible to detonation than butane ($d_c = 0.7$ m) and propane ($d_c \approx 0.9$ m) but more susceptible than methane ($d_c = 3.6$ m). A more quantitative measure of the relative susceptibility was obtained by measuring the characteristic width of the detonation cells. Typical smoked-foil records obtained for detonations in stoichiometric butane/air and two hydrogen sulphide/air mixtures are shown in Figure 4. It is clearly seen that the cell widths associated with butane/air detonations are considerably smaller than those for H_2S in air. At stoichiometric composition, the cell widths in butane and H_2S mixtures are about 55 mm and 100 mm, respectively. Estimates of the corresponding critical tube diameters based on 13S are therefore 0.7 m and 1.3 m, respectively. This is consistent with the failure of detonations in H_2S/air to successfully transmit from a 0.9 m tube, whereas detonations in butane/air were re-established after emerging from the tube.

The cell widths, and critical tube diameters for various fuel/air mixtures at stoichiometric composition, are given in Table III. The critical tube diameters range from 0.115 m for acetylene to an estimated value of 3.6 m for methane, with hydrogen sulphide being slightly less susceptible to detonation ($d_c = 1.3$ m) than propane ($d_c = 0.9$ m).

Away from stoichiometric composition (12.3% H_2S by volume), the detonation cell size increases as the mixture becomes less susceptible to detonation. The experimentally measured cell diameters for different compositions are compared with the prediction based on a scaled induction zone length in Figure 5. The calculation of the induction length is based on a detailed chemical kinetic model of hydrogen sulphide combustion. The chemical kinetic model as well as correlations of various chemical length scales with the detonability properties of H_2S/air are described in Appendix C. The chemical kinetic model has also been used to calculate the influence of water vapour on the detonability of H_2S/air. It is found that water vapour has a retarding effect on the reaction. The reaction zone length, and thus the predicted cell size, increases by a factor of 1.1, 1.4 and 2.1 for 1, 5 and 10% water vapour dilution, respectively.

The critical tube diameters for H_2S/air based on 13S estimates and those for other fuels, are plotted vs equivalence ratio in Figure 6. This figure again illustrates the relative insensitivity of H_2S/air mixtures to detonation.

Empirical correlations relating the critical tube diameter to the critical initiation energy are used in Annex B to obtain a lower bound of 80 g of tetryl solid explosives for initiation of detonation in an unconfined H_2S/air cloud. It is therefore unlikely that detonation could accidentally occur in such a cloud. However, most accidental spills occur in environments with obstacles and partially confined spaces. In such environments, flame acceleration and localized explosions will play an important role in assessing the detonation hazards. Such situations will be investigated in Phase II of this project. However, based on the results obtained to date, it can be concluded that transition to detonation is less likely with hydrogen sulphide fuel than with most common gaseous fuels except methane.

D. BLAST FROM DETONATION OF H_2S CLOUDS

The characteristics of the blast wave due to detonation of a stoichiometric H_2S/air cloud have been calculated using a one-dimensional finite difference code with flux-corrected transport. The results of these calculations, including pressure-time histories at various positions from a 10 m radius hemispherical cloud, are described in Appendix E. Some of the key results are summarized in Table IV. The blast wave overpressure decreases from a maximum of 14.3 atm within the cloud to less than 0.1 atm at a distance of 150 m from the cloud. The corresponding impulse decreases from about 70 atms•ms at the center to about 2 atm•ms at 150 m. Also given in Table IV are the dynamic pressures and impulses as well as normally reflected pressures.

A more complete description of the blast wave properties is given in Appendix E. Most of the results are for a 10 m radius hemispherical cloud. However, procedures for scaling to different cloud sizes are described in detail. For off stoichiometric compositions and for comparison with other fuels, scaling with detonation energy can be used to obtain estimates of the blast overpessure and positive impulse. The detonation energy release for various fuels at stoichiometric compositions are given in Table III. This energy also provides a basis for comparing the far-field blast wave from the detonation of an equivalent energy high explosive charge. Comparisons of the blast wave properties from high explosive charges and H_2S/air clouds given in Appendix E (Figures 23 and 24) show that energy equivalency provides a reasonable estimate of the blast overpressure and positive impulse outside the cloud.

E. CONCLUSION

The detonation properties of hydrogen sulphide in air have been investigated experimentally and theoretically, and compared with the detonation properties of common hydrocarbon fuels (acetylene, ethylene, propane, butane, methane) and hydrogen.

Calculated detonation velocities and pressures agree well with those observed experimentally. The maximum velocities and pressures at stoichiometric H_2S/air composition are slightly smaller than the corresponding values for other fuels, but in terms of the damage potential due to detonation of a fuel/air cloud, these differences are insignificant.

Critical tube diameter experiments have shown that the minimum critical tube diameter is greater than 0.9 m. The minimum diameter cell diameter for H_2S/air mixtures is found to be 100 mm, giving an estimate of 1.3 m for the minimum critical tube diameter. This means that H_2S is less sensitive to detonation than hydrogen and most common hydrocarbon mixtures, with the exception of methane.

A lower bound of 80 g of tetryl solid explosive is obtained for initiation of detonation in an unconfined H_2S/air cloud. It is therefore unlikely that detonation could occur in such a cloud. The role of obstacles and confinement in enhancing the potential for transition or onset of detonation will be investigated in Phase II of this project. Based on the results obtained so far, it can be concluded that the onset of detonation in H_2S/air clouds is less likely than in fuel/air clouds based on other more common gaseous fuels, with the exception of methane.

The blast wave properties at various distances from detonation in a hemispherical hydrogen sulphide/air cloud have been calculated. Standard blast parameters such as the overpressure, positive impulse and positive duration as well as other properties of relevance to structural response calculations have been reported. Detailed pressure-time histories are also included.

In summary, the detonation properties of hydrogen sulphide in air have been characterized and compared with the properties of other fuel/air mixtures. Phase I of this project has therefore been completed. Planning for Phase II is now underway. In this second phase, flame acceleration and transition to detonation in various obstacle and confinement environments will be investigated.

TABLE I

TOXICITY TABLE
FOR HYDROGEN SULPHIDE (H_2S)

1 PPM = 0.0001% (1/10,000 of 1%)	CAN SMELL
10 PPM = 0.001% (1/1,000 of 1%)	ALLOWABLE FOR 8 HOURS EXPOSURE THRESHOLD LIMIT VALUE (T.L.V.)

IF THE LEVEL IS ABOVE 10 PPM, THEN PROTECTIVE EQUIPMENT MUST BE WORN

100 PPM = 0.01% (1/100 OF 1%)	KILLS SMELL IN 3 TO 15 MINUTES IRRITATION OF EYES AND THROAT
200 PPM = 0.02% (2/100 OF 1%)	KILLS SMELL RAPIDLY BURNS EYES AND THROAT
500 PPM = 0.05% (5/100 OF 1%)	LOSES SENSE OF REASONING AND BALANCE STOPPAGE OF BREATHING IN 2 TO 15 MINUTES VICTIM NEEDS ARTIFICIAL RESPIRATION
700 PPM = 0.07% (7/100 OF 1%)	UNCONSCIOUS QUICKLY BREATHING WILL STOP AND DEATH RESULTS UNLESS RESCUED IMMEDIATELY
1000 PPM = 0.1% (1/10 OF 1%)	UNCONSCIOUS AT ONCE BRAIN DAMAGE UNLESS RESCUED PROMPTLY

1% = 10,000 PPM

PPM - PARTS OF GAS PER MILLION PART OF AIR BY VOLUME

TABLE II

ESTIMATES OF FLAMMABILITY LIMITS FOR SELECTED FUEL-AIR MIXTURES

Fuel		Flammability Limits (Volume % in Air)
Methane	CH_4	5.3 - 15.0
Acetylene	C_2H_2	2.5 - 81.0
Ethylene	C_2H_4	3.1 - 32.0
Propane	C_3H_8	2.2 - 9.5
Pentane	C_5H_{12}	1.5 - 7.8
Hydrogen	H_2	4.0 - 75.0
Hydrogen Sulphide	H_2S	4.3 - 45.0

TABLE III

DETONATION PARAMETERS FOR FUEL-AIR MIXTURES

(Stoichiometric Composition; Initial Pressure 1 atm; Initial Temperature 298.15K)

Fuel	% Fuel By Volume	Detonation Pressure Ratio	Velocity (m/s)	Energy Release (MJ/kg mixture)	Initiation Energy (g tetryl)	Critical Tube Diameter (m)	Cell Width (mm)
Acetylene (C_2H_2)	7.75	19.1	1864	2.44	1.25	0.115	9.8
Hydrogen (H_2)	29.6	15.6	1968	2.82	1.1	0.20	15
Ethylene (C_2H_4)	6.54	18.4	1822	2.35	10 NO GO 15 GO	0.43	28
Ethane (C_2H_6)	5.66	18.0	1825	2.31	30 NO GO 40 GO	~ 0.9	54 - 62
Propylene (C_3H_6)	4.46	18.5	1809	2.31	12.5	0.7	--
Propane (C_3H_8)	4.03	18.3	1798	2.29	50 NO GO 80 GO	0.9	69
n-Butane (C_4H_{10})	3.13	18.4	1796	2.28	50 NO GO 80 GO	~ 0.7 (13 S)	50 - 62
Methane (CH_4)	9.48	17.2	1801	2.31	22×10^3 (estimate)	3.6 (13 S)	280 ± 30
Hydrogen Sulphide (H_2S)	12.3	15.3	1647	1.96	>80	1.3 (13 S)	100
Hexane (C_6H_{14})	Aerosol	18.6	1795	2.28	25	--	--

TABLE IV

CHARACTERISTIC PRESSURES AND IMPULSES FROM DETONATION OF A 10 m RADIUS HEMISPHERICAL CLOUD OF STOICHIOMETRIC HYDROGEN SULPHIDE IN AIR

Radius (m)	Maximum Overpressure (atm)	Normally Reflected Pressure (atm)	Dynamic Pressure* (atm)	Positive Impulse (atm·ms)	Dynamic Impulse (atm·ms)
1.000	14.2585	35.917	5.656	69.5435	.8812
2.500	14.2585	35.917	5.656	64.7787	1.2929
5.000	14.2585	35.917	5.656	54.6684	1.9250
7.500	14.2585	35.917	5.656	45.3759	2.5763
10.000	14.2585	35.917	5.893	34.8111	7.4131
12.500	5.3546	24.633	5.701	23.6805	8.7341
15.000	3.5418	14.223	3.082	18.5077	8.1959
17.500	2.5468	9.169	1.729	14.9287	7.4559
20.000	1.9450	6.427	1.067	13.2050	6.1160
22.500	1.5183	4.660	.696	12.0268	4.6630
25.000	1.2548	3.654	.484	11.0731	3.6298
27.500	1.0541	2.936	.350	10.2257	2.8835
30.000	.9075	2.439	.264	9.4998	2.3293
35.000	.6903	1.752	.157	8.2903	1.5960
40.000	.5731	1.406	.111	7.3379	1.1482
50.000	.4144	.967	.059	5.9596	.6583
75.000	.2292	.502	.018	4.0372	.2396
100.000	.1534	.326	.008	3.0402	.1184
125.000	.1128	.236	.004	2.4384	.0693
150.000	.0881	.182	.002	2.0338	.0448

* $\frac{1}{2}(\rho u^2)$, where ρ is the density and u is the flow velocity.

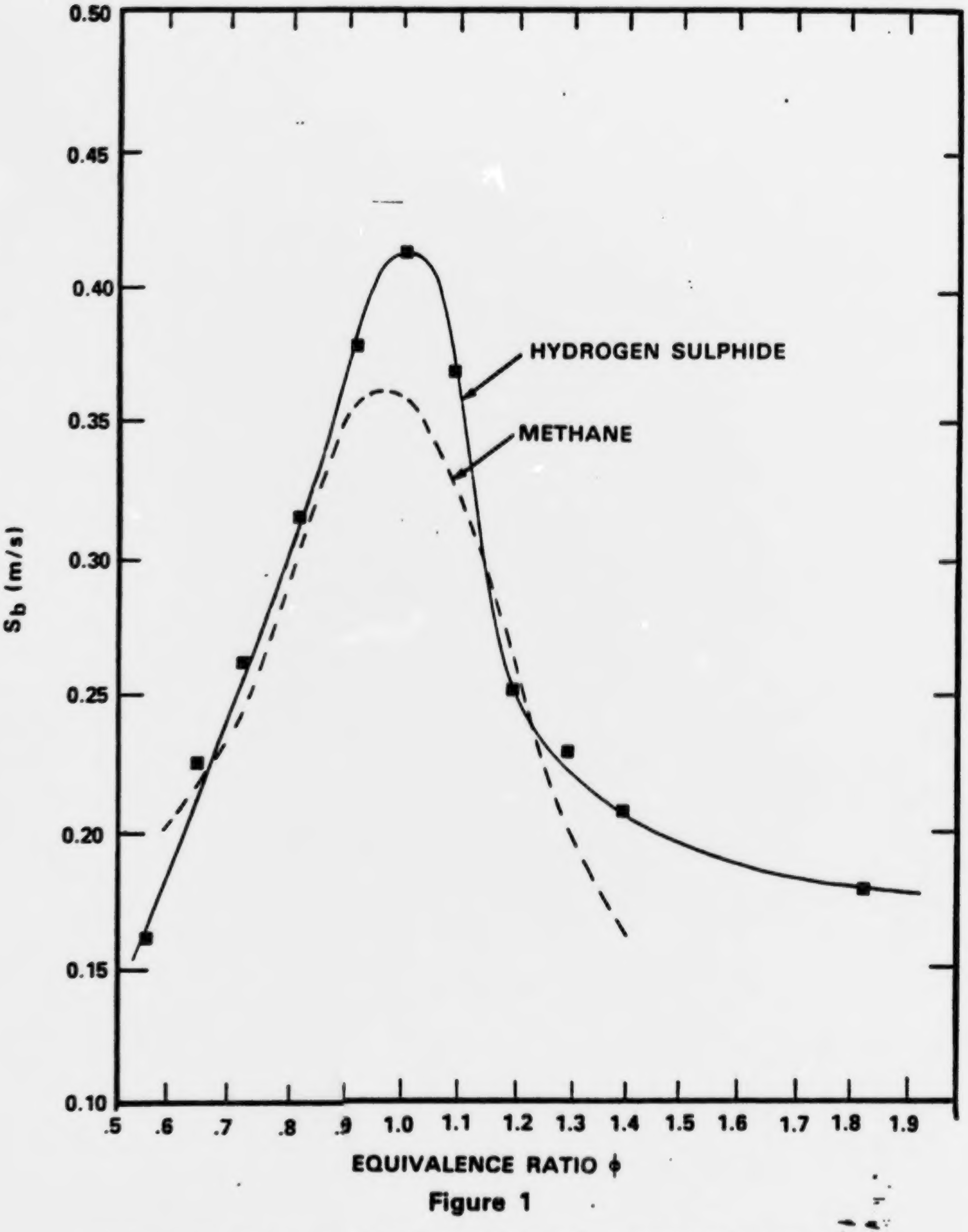

Figure 1

BURNING VELOCITIES OF HYDROGEN SULPHIDE-AIR AND METHANE-AIR FLAMES

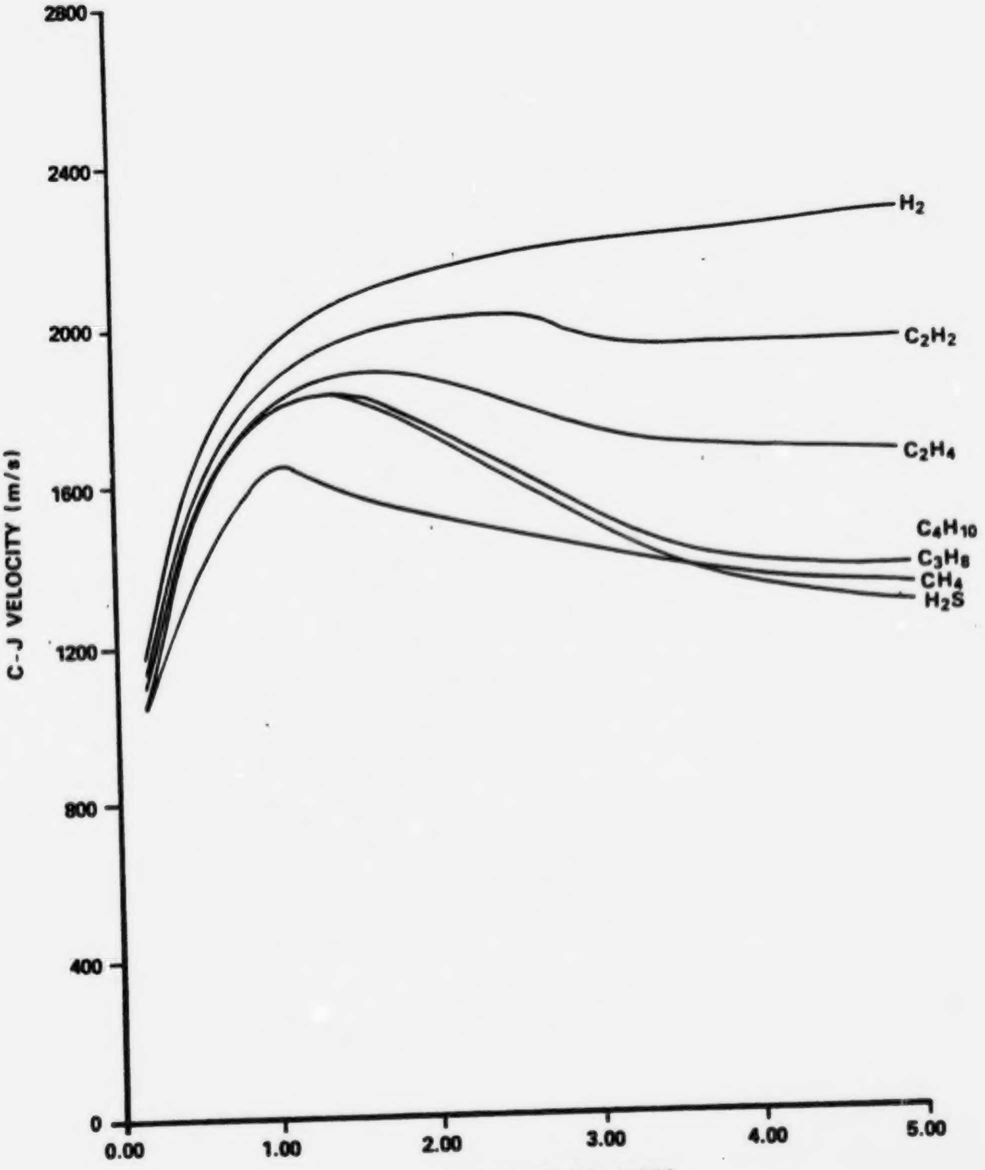

Figure 2

CHAPMAN-JOUGUET (C-J) DETONATION VELOCITY FOR VARIOUS FUEL-AIR MIXTURES

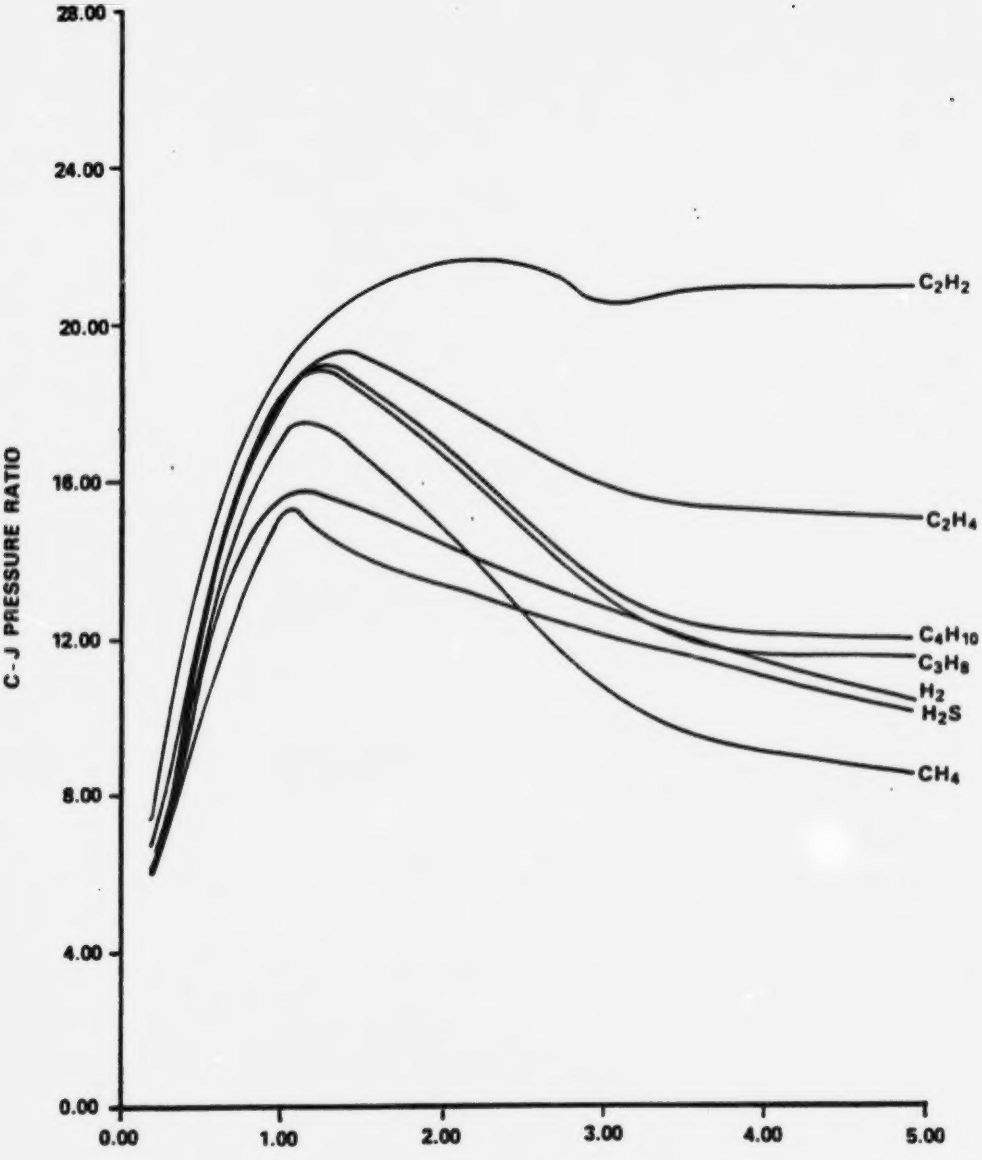

Figure 3

CHAPMAN-JOUGUET (C-J) DETONATION PRESSURE RATIO FOR VARIOUS FUEL-AIR MIXTURES

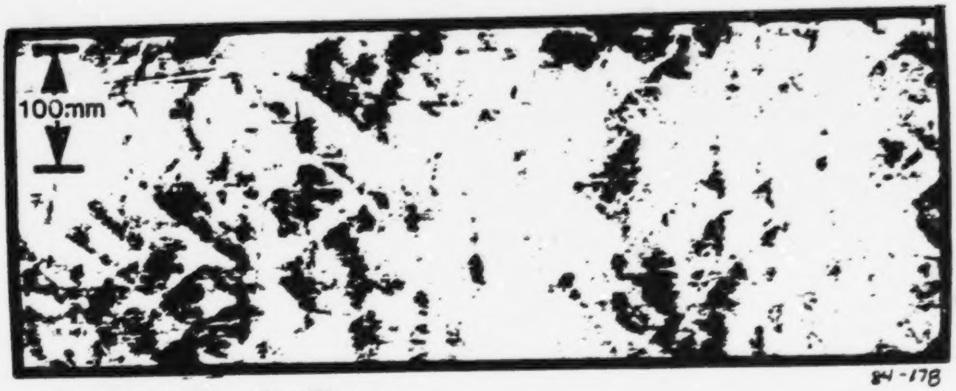

84-178

BUTANE - 3.16% S ~ 55 mm

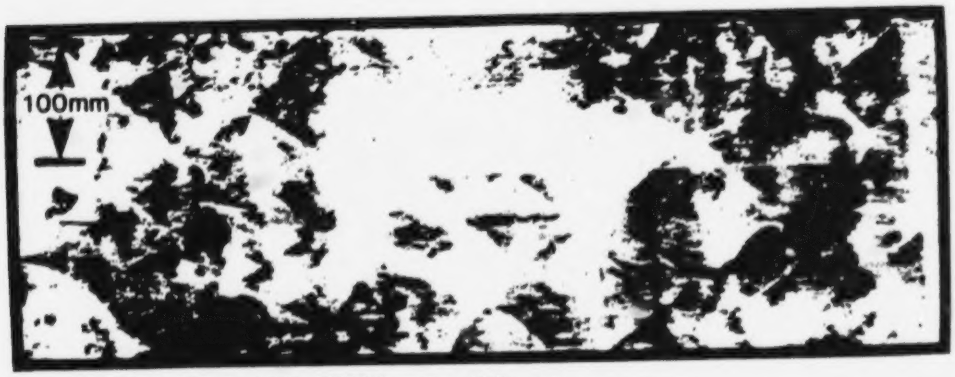

HYDROGEN SULPHIDE - 14.2% S ~ 110 mm

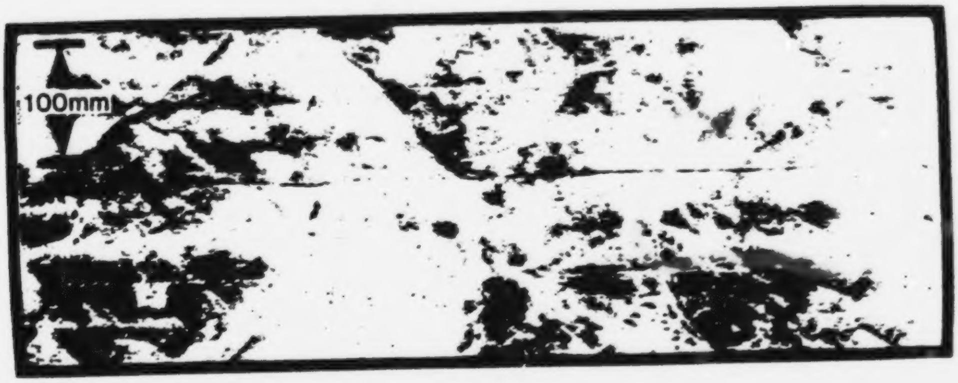

HYDROGEN SULPHIDE - 10.0% S ~ 275 mm

Figure 4. COMPARISON OF CELL STRUCTURES

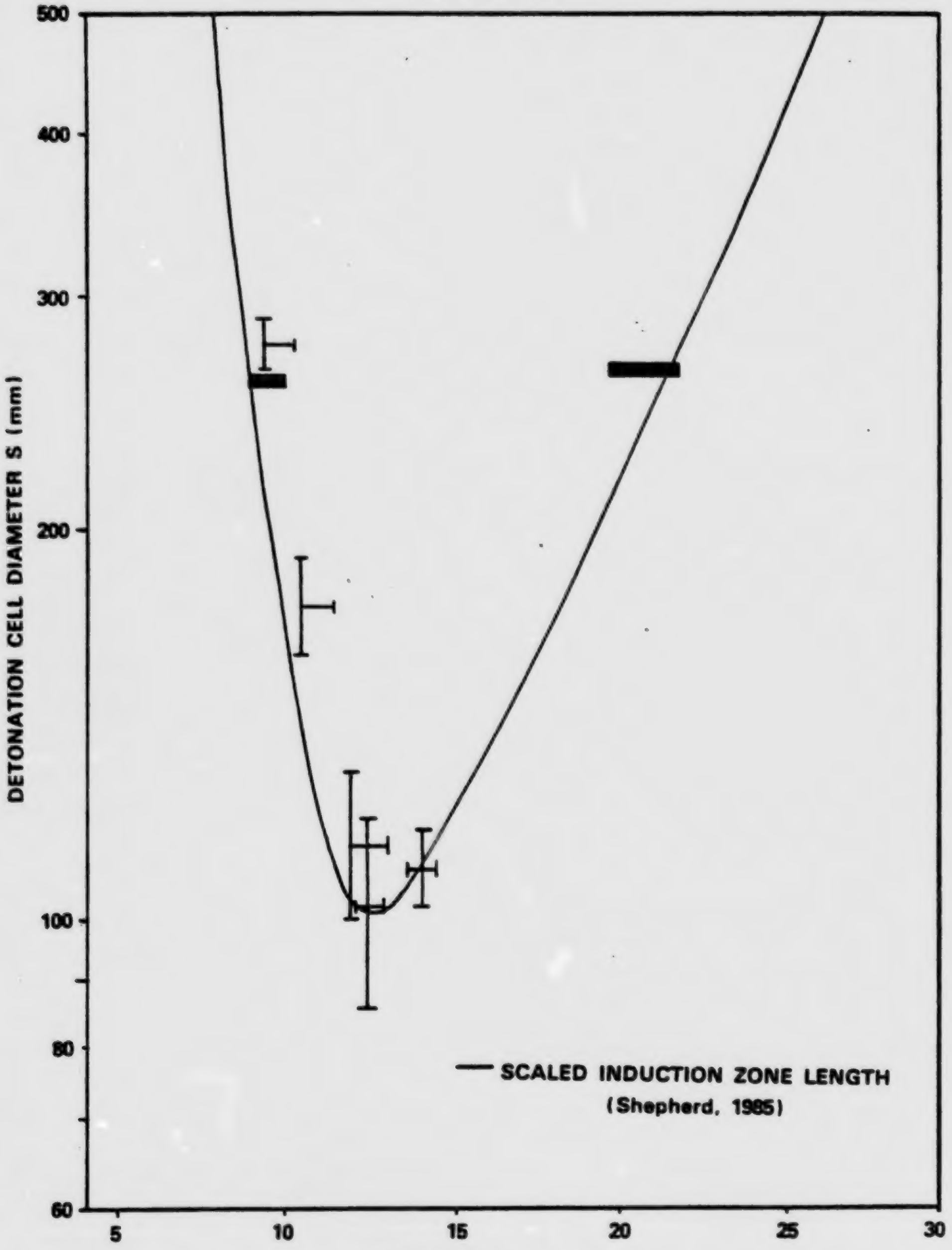

Figure 5

DETONATION CELL DIAMETERS FOR HYDROGEN SULPHIDE IN AIR

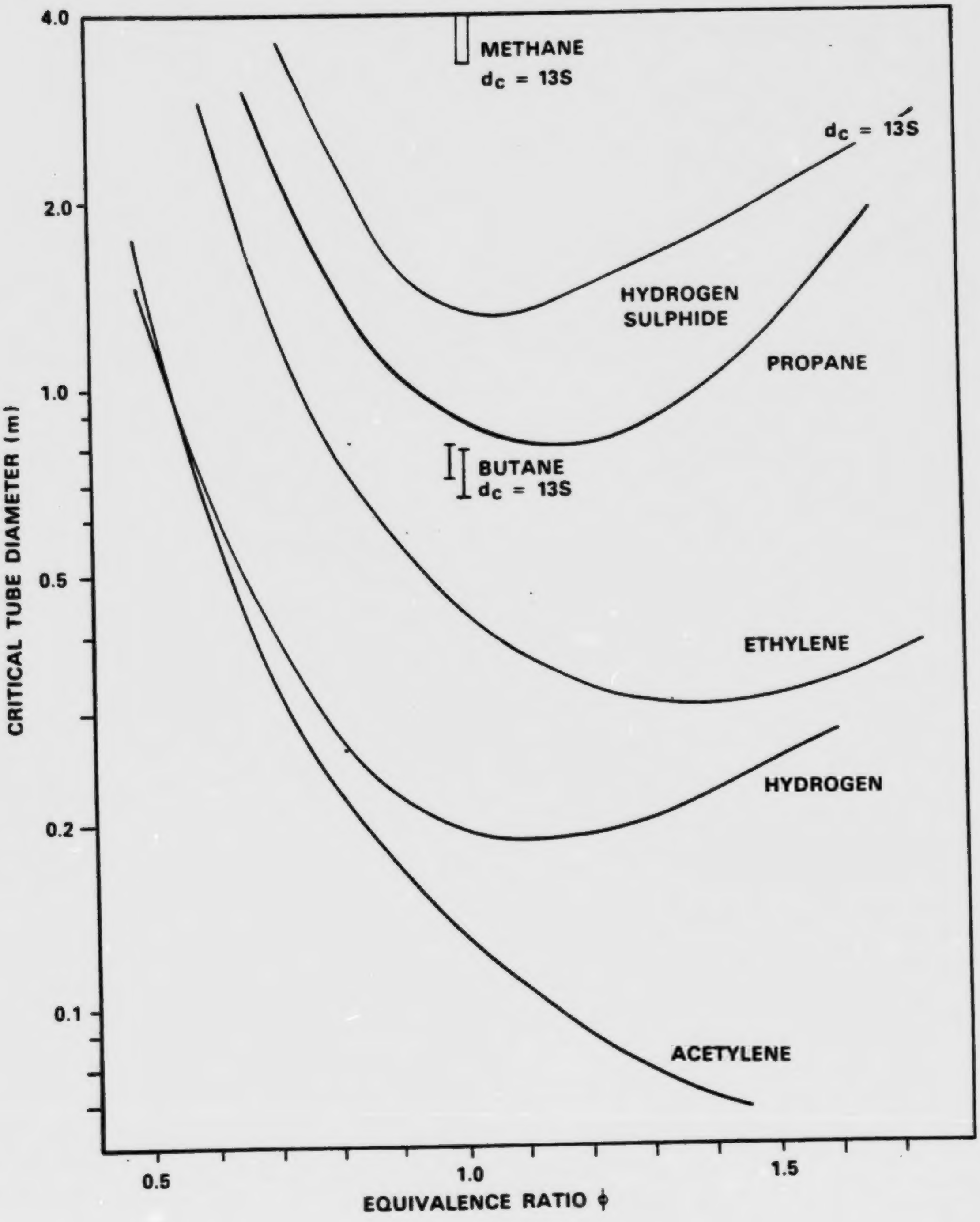

4.0
2.0
1.0
0.5
0.2
0.1
CRITICAL TUBE DIAMETER (m)
METHANE
d_c = 13S
d_c = 13S
HYDROGEN SULPHIDE
PROPANE
BUTANE
d_c = 13S
ETHYLENE
HYDROGEN
ACETYLENE
0.5
1.0
1.5
EQUIVALENCE RATIO ϕ

FIGURE 6

APPENDIX A

Investigation of the Explosion Hazards of Hydrogen Sulphide

by

A.J. Saber, A. Sulmistras and I.O. Moen.

INVESTIGATION OF THE EXPLOSION HAZARDS OF HYDROGEN SULPHIDE (H_2S)

Report A
Covering The Period:
10 January 1984 to 15 October 1984

by

Aaron Jaan Saber, Ph.D.,
Eng.(Quebec),P.Eng.(Ontario)

and

Albert Sulmistras

Mechanical Engineering Department
Concordia University
1455 de Maisonneuve Boulevard West
Montreal, Quebec H3G 1M8

and

Ingar O. Moen, Ph.D.
Head, Shock and Blast Group

Military Engineering Section
DefenceResearch Establishment, Suffield
Ralston, Alberta T0J 1R0

15 October 1984

INVESTIGATION OF THE EXPLOSION HAZARDS OF HYDROGEN SULPHIDE (H_2S)

Report A
Covering The Period:
10 January 1984 to 15 October 1984

prepared by

Aaron Jaan Saber, Ph.D.,
Eng.(Quebec),P.Eng.(Ontario)

and

Albert Sulmistras

Mechanical Engineering Department
Concordia University
1455 de Maisonneuve Boulevard West
Montreal, Quebec H3G 1M8

and

Ingar O. Moen, Ph.D.
Head, Shock and Blast Group

Military Engineering Section
DefenceResearch Establishment, Suffield
Ralston, Alberta T0J 1R0

15 October 1984

This report has been prepared partially with respect to Supply and Services Canada Contract Number: 03SG.97702-R-3-7856, Serial Number: 8SG83-00152, entitled "Investigation of the Explosion Hazards of Hydrogen Sulphide (H_2S)," dated 10 January 1984; Scientific Authority Dr. Ingar Moen, Science Contracting Officer R. Tingley.

The authors reserve the rights to the contents of this report as indicated on page 2 of Schedule "A" to the contracting document cited above.

It is requested that reference to this report be made in the following form:

> Saber, A.J., Sulmistras, A., Moen, I.O., "Investigation of the Explosion Hazards of Hydrogen Sulphide (H_2S)," Report A, covering the period: 10 January 1984 to 15 October 1984, partially prepared with respect to Supply and Services Canada Contract Number: 03SG.97702-R-3-7856, Serial Number: 8SG83-00152, 15 October 1984.

ABSTRACT

Hydrogen sulphide (H_2S) properties and chemistry are introduced. Then, discussions of (a) hydrogen sulphide combustion and flame propagation; (b) detonation effects (Chapman-Jouguet conditions), and the principles used in determining the change of fluid properties due to detonation; (c) computation of hydrogen sulphide - air explosion fluid properties at Chapman-Jouguet properties; (d) physical properties of detonation including cell size; and (e) and general principles of blast. Calculations performed show that hydrogen sulphide - air mixtures have Chapman-Jouguet detonation properties that are the same order of magnitude as hydrogen and typical hydrocarbon fuels in air. From the results it can be concluded that detonation of hydrogen sulphide - air mixtures can be compared to those of butane, but are less detonable.

Disclaimer (as required by the Atomic Energy Control Board):

> The Atomic Energy Control Board is not responsible for the accuracy of the statements made or opinions expressed in this publication and neither the Board nor the Authors nor the Defence Research Establishment Suffield (DRES) nor Concordia University assume liability with respect to any damage or loss incurred as a result of the use made of the information covered in this publication.

TABLE OF CONTENTS

FRONTISPIECE
TITLE PAGE i
ABSTRACT iii
DISCLAIMER iv
TABLE OF CONTENTS v
LIST OF TABLES xi
LIST OF FIGURES xii

A. INTRODUCTION TO THE INVESTIGATION 1
    1. Goals of the Investigation 1
    2. Report Scope and Summary 2

B. INTRODUCTION TO THE EXPLOSION HAZARDS OF HYDROGEN SULPHIDE 3
    1. Hydrogen Sulphide and Its Use 3
    2. Hydrogen Sulphide in a Heavy Water Plant 3
    3. Flammability Limits 4
    4. Heats of Combustion 4
    5. Combustion Mechanisms 5
    6. Explosions Modes 6
    7. Explosion Situations 6
    8. Examples of Vapour Cloud Explosion Incidents 6
    9. The Hydrogen Sulphide Question 7

C. SELECTED PREVIOUS REPORTED WORK 8

D. HYDROGEN SULPHIDE 9

1. Toxicity Outline of Hydrogen Sulphide 9

2. Outline of Physical and Thermodynamic Properties . 10

3. Hydrogen Sulphide Overall Chemistry 11

4. Assays of Hydrogen Sulphide 11

5. The Sulphydryl (-S-H) Radical 11

E. HYDROGEN SULPHIDE COMBUSTION IN DRY AIR 13

1. The Composition of Dry Air 13

2. Overall Combustion of Hydrogen Sulphide in Air .. 13

2.1 Equivalence Ratio 14

3. Chemistry of Other Constituents Involved 15

3.1 Oxygen Chemistry 15

3.2 Atomic Oxygen 15

3.3 Ozone 16

3.4 Oxides and Peroxides 16

3.5 Oxonium Compounds 16

3.5.1 The Hydronium Ion 17

4. Sulphur Chemistry 17

4.1 Sulphur Oxides 17

4.1.1 Sulphur Dioxide (SO_2) 18

4.1.2 Sulphur Trioxide (SO_3) 18

4.1.3 Disulphur Trioxide (S_2O_3) 19

4.1.4 Sulphur Monoxide (SO) 19

4.1.5 Disulphur Heptoxide (S_2O_7) 19

4.1.6 Sulphur Tetroxide (SO_4) 19

5. Nitrogen Chemistry 19

  5.1 Dinitrogen Oxide (N_2O) 20

  5.2 Nitrogen Monoxide (NO) 20

  5.3 Nitrogen Trioxide (NO_3) 21

  5.4 Nitrogen Dioxide (NO_2) 21

  5.5 Dinitrogen Tetroxide (N_2O_4) 21

  5.6 Dinitrogen Pentoxide (N_2O_5) 22

  5.7 Other Oxides of Nitrogen 22

6. Compounds of Nitrogen and Sulphur 22

F. FLAMMABILITY REPORTS FOR HYDROGEN SULPHIDE 23

1. Early Flammability Reports 23

2. Flammability in Other Atmospheres 23

3. Burning Velocity Details 24

  3.1 Burning Velocity in Dry Air 24

  3.2 Burning Velocity in Wet Air 24

4. Burning Velocity of Other Fuels 24

5. Acceleration of Flames 25

6. Transition to Detonation 25

G. RANKINE-HUGONIOT CALCULATIONS 26

1. The Overall Chemical Reactions 26

2. The Rankine-Hugoniot Approach 27

3. Definitions and Parameters 28

3.1 Statement of the Problem 29

3.2 Rankine-Hugoniot Relations 30

3.2.1 The Rayleigh Line 30

3.2.2 The Hugoniot Curve 31

3.2.3 Mach Number 33

3.2.4 The Chapman-Jouguet Condition 34

4. Rankine-Hugoniot Solutions 34

4.1 Chapman-Jouguet Pressure Ratio 36

4.2 Chapman-Jouguet Specific Volume Ratio 36

4.3 Chapman-Jouguet Temperature Ratio 36

4.4 Chapman-Jouguet Mass Flow Rate 36

4.5 Chapman-Jouguet Mach Number 36

5. Sample Calculations 37

5.1 Calculation of Gas Properties 37

5.2 Calculation of Enthalpy of Reaction 38

5.3 Calculation of Detonation Ratios and Product Properties 40

6. Frozen - Shock Properties 43

7. Remarks 45

H. EQUILIBRIUM PROPERTIES OF DETONATED H_2S IN AIR 46
1. Detonation Products 46
1.1 Product Classification 47
1.2 Detonation Product Discussion 47
2. Combustion Energy Release 48
3. Detonation Temperature Ratio 48
4. Detonation Pressure Ratio 49
5. Detonation Velocity 50
6. Mach Number 50
7. Remarks on Comparison with Other Fuels 50

I. PHYSICAL DETONATION PROPERTIES 52
1. Cell Size 52
2. Critical Tube Diameter 53
3. Critical Initiation Energy 53
4. Remarks 55

J. BLAST WAVE CALCULATIONS 56
    1. Blast Wave Characterization 56
        1.1 Direct Blast Characterization 56
        1.2 Blast Impulse Characteristics 57
        1.3 Blast Regions 58
        1.4 Detonation Effect Scaling 59
    2. Hydrogen Sulphide Blast Wave Parameters 59
        2.1 Shock Wave Overpressure 60
        2.2 Positive Impulse 60
    3. Hydrogen Sulphide Blast Wave Calculations 60

K. CONCLUDING REMARKS 61

L. ACKNOWLEDGEMENTS 62

M. REFERENCES 63

N. TABLES 71
O. FIGURES 96

List of Tables.

B.1 Hydrogen Sulphide Inventory at Bruce Heavy Water Plant.
B.2 Estimates of Flammability Limits of Some Stoichiometric Fuel-Air Mixtures.
B.3 Estimates of Enthalpy of Reaction of Some Stoichiometric Fuel-Air Mixtures.

D.1 The Ultimate Analysis of Hydrogen Sulphide.
D.2 Toxicity Table for Hydrogen Sulphide.
D.3 Physical and Thermodynamic Properties of Hydrogen Sulphide.
D.4 Hydrogen Bond Lengths with Sulphur and Oxygen.
D.5 Some Bond Angles in Sulphur Compounds.

E.1 Composition of the Atmosphere.
E.2 The Gravimetric Analysis of Dry Air.
E.3 Properties of Hydrogen Compounds of Sulphur and Oxygen.
E.4 Physical Constants for Oxygen.
E.5 The Normal Oxides of Nitrogen.

F.1 Flammability Limits of Hydrogen Sulphide In Air (1 per cent Water Vapour) in Closed Tubes as Reported by Coward and Jones.

G.1 Enthalpies of Formation.
G.2 Specific Heat Ratios.

H.1 Summary of Detonation Properties for Hydrogen Sulphide in Air.
H.2 Hydrogen Sulphide Combustion in Air Detonated product (Equilibrium - Final) Condition Product Mixture.
H.3 Species Considered in Detonation Product Calculation.
H.4 Classification for Species Production of Hydrogen Sulphide Detonation in Air Against Equivalence Ratio.
H.5 Chapman-Jouguet Condition Parameter Values for Some Stoichiometric Fuel-Air Mixtures.

I.1 Detonability Parameter Values for Selected Fuels in Air at Stoichiometric Concentrations.

J.1 Calculated Scaling Values for Hydrogen Sulphide and Air Detonation.

List of Figures.

B.1 Layout of Bruce Heavy Water Plant.

D.1 The Sulphur Cycle.

F.1 Burning Velocity of Hydrogen Sulphide in Dry Air.
F.2 Burning Velocity of Hydrogen Sulphide in Wet and Dry Air.
F.3 Burning Velocity of Methane in Dry Air.

G.1 Structure Through a Detonation Wave.
G.2 Schematic for Control Volume Detonation Analysis.
G.3 The Rayleigh Line.
G.4 The Hugoniot Curve.
G.5 The Simultaneous Solution of Mass, Momentum and Energy Equations.
G.6 The ZND Solution for Detonation.

H.1 Chapman-Jouguet Energy Release vs. Equivalence Ratio.
H.2 Chapman-Jouguet Temperature Ratio vs. Equivalence Ratio.
H.3 Chapman-Jouguet Pressure Ratio vs. Equivalence Ratio.
H.4 Chapman-Jouguet Velocity vs. Equivalence Ratio.

I.1 Detonation Cell Structure.
I.2 Transverse Wave Structure of a Detonation.
I.3 Variation of Cell Size with Equivalence Ratio.
I.4 Development of a Detonation Wave from a Tube.
I.5 Dependence of Critical Tube Diameter on Equivalence Ratio.

J.1 Canonical Blast Wave Character.
J.2 Blast Wave Overpressure Ratio for Hydrogen Sulphide Detonation in Air.
J.3 Blast wave Overpressure Ratio for Ethylene Detonation in Air.
J.4 Scaled Positive Impulse for Hydrogen Sulphide Detonation in Air.
J.5 Scaled Positive Impulse for Ethylene Detonation in Air.

A. Introduction to the Investigation.

This investigation is directed toward quantifying the explosion hazards of hydrogen sulphide (H_2S) in air relevant to the environment of heavy water plants licenced by the Atomic Energy Control Board (AECB). The approach involves comparison of the explosive ability of hydrogen sulphide to that of other materials, particularly hydrocarbons and hydrogen, that have been studied elsewhere and have comparable heats of combustion.

A.1 Goals of the Investigation.

The goal of this investigation is the establishment of quantitative details of the explosion hazard of hydrogen sulphide in air.

Specific objectives are:

(a) Experimentally determine the detonability of hydrogen sulphide - air mixtures relative to that of selected "common" hydrocarbon - air mixtures, by performing "large-scale" tests;

(b) Calculate the detonation properties of hydrogen sulphide - air mixtures;

(c) Compare measured hydrogen sulphide detonability with calculations;

(d) Calculate blast wave characteristics of hydrogen sulphide - air explosions;

(e) Search and review the literature for

  (1) Combustion properties of hydrogen sulphide - air mixtures,
  (2) Explosion properties of hydrogen sulphide - air mixtures, and
  (3) Flame acceleration and transition-to-detonation in fuel - air mixtures;

(f) Identify particularly hazardous obstacle and/or confinement configurations, based on literature search and reviews; and

(g) Identify and draft plans for tests to fill gaps in available hydrogen sulphide combustion data for

(1) Flame speed,
(2) Flame acceleration,
(3) Transition-to-detonation, and
(4) Evaluation of existing models for flame acceleration and transition to detonation.

A.2 Report Scope and Summary.

This report begins with an outline of the use of hydrogen sulphide and its particular application in heavy water production. Next comes a comparison of hydrogen sulphide to hydrocarbon and hydrogen fuel mixtures in air. The the problem of vapour cloud explosions of fuels in air is then discussed.

The report continues with background information on hydrogen sulphide chemistry, detonation properties, blast effects and flame propagation. The report also outlines calculated estimates of product formation, energy release and blast effects due to detonation of mixtures of hydrogen sulphide in air.

The report follows on with definitions of the dynamic properties used for quantification of detonation sensitivity of gaseous media.

Comparison data for flame acceleration and transition-to-detonation are presented for other combustible gases are provided.

Finally, the experimental procedures for determination of the detonation sensitivity of hydrogen sulphide are outlined.

B. Introduction to the Explosion Hazards of Hydrogen Sulphide.

In this section, hydrogen sulphide is introduced and its effectiveness as a fuel is compared to that of the hydrocarbons and to hydrogen. This discussion is followed an outline of the physical mechanisms associated with the chemistry of combustion, their effects (blast) and their classification. Next, vapour cloud explosion cases are briefed.

B.1 Hydrogen Sulphide and Its Use.

Hydrogen sulphide (H_2S, molecular weight 34.08 kg/kgmole) is a clear colourless gas at normal temperature (20C) and pressure (101.3kPa). When first encountered, in concentrations of about 1 to 100 parts per million (ppm) in air, the material has an offensive smell generally described as comparable to "rotten eggs."[1,2] The gas is both toxic[1,2] and flammable.[3-10]

Hydrogen sulphide results from the decomposition of metal sulphides and albuminous matter. It is found in the areas of mineral springs, sewers, gas and oil wells and some mines. Hydrogen sulphide is also a by-product of several industrial processes, including the production of synthetic rubber and viscose rayon and in petroleum refining, dying and leather-treating.[2]

Industrial applications of hydrogen sulphide include the preparation of sulphides; the production of sulphur-bearing organic compounds; copper, cadmium and titanium from spent chemical process catalysts; the formulation of extreme-pressure lubricants; and the preparation of rare-earth phosphors used in colour television tubes.[3]

A specific use of hydrogen sulphide, the one of interest in this investigation, is in the application of the Girdler-Sulphide process for the separation of heavy water (deuterium oxide, D_2O) from fresh water,[11] as undertaken at facilities licenced by the Atomic Energy Control Board (AECB).

B.2 Hydrogen Sulphide in a Heavy Water Plant.

One example heavy water separation facility, Bruce Heavy Water Plant, has a hydrogen sulphide inventory estimated at 3390 tonnes, distributed as shown in Table B.1.[12] The plant layout is shown in Figure B.1. Located on the eastern shore of Lake

Huron (Southwestern Ontario), the plant components are dominated by sets of vertical cylindrically shaped process tanks. These tanks rise to over 70 metres above grade.[12] The vertical process tanks and other plant units are interconnected by process and service piping ranging from 0.05 to 1.3 metres diameter.

B.3 Flammability Limits.

It has been established that hydrogen sulphide is combustible in air.[4-10] In general, gaseous chemicals which disperse in air can form mixtures that can support combustion on their own, that is can react or can have combustion proceed once started, without any further external ignition mechanism. These mixtures are called "flammable." Flammable mixtures of one gas (fuel) in air (oxidiser) can have a variety of proportions ranging, continuously, from a lower limit where the mole ratio of fuel to the total is at the minimum capable of supporting combustion to an upper limit where the mole ratio of fuel to the total mixture is at a maximum.

Examples of chemicals that form flammable mixtures in air include hydrogen sulphide (H_2S), hydrogen (H_2), acetylene (C_2H_2), ethylene (C_2H_4), methane (CH_4), propane (C_3H_8), and butane (C_4H_{10}).[4] Estimates of flammability limits for these chemicals are outlined in Table B.2.[4] They vary from a wide range of 2.3 to 81 per cent for acetylene in air to a narrow range of 1.9 to 8.5 per cent for butane in air. The flammability limit for hydrogen sulphide ranges from about 4.3 to 45 per cent in air. These data show that the flammability of hydrogen sulphide is comparable to that of hydrocarbon gases and hydrogen.

B.4 Heats of Combustion.

When a flammable mixture burns energy associated with chemical bonds is released.[13,14] This energy depends on the proportion of fuel to air in the mixture. In the case where the proportions of fuel and oxidiser result in the consumption of all the fuel and the production of stable chemical species, the mixtures are called "stoichiometric."[15,16] In the case of hydrogen the stable product is water (H_2O), for hydrocarbons the stable products are water and carbon dioxide (CO_2) and for hydrogen sulphide the stable products are water and sulphur dioxide (SO_2). Stoichiometric mixtures of the fuels listed in Table B.2[17] and the energy released when the reaction occurs at normal temperature and pressure are shown in Table B.3.[17] For hydrocarbons, the enthalpies of reaction for stoichiometric conditions vary over a ten per cent range from about 2.29 MJ/kg of mixture for propane in air to about 2.44 MJ/kg of mixture for acetylene in air. The corresponding value for hydrogen is 2.82 MJ/kg of mixture and for hydrogen sulphide the enthalpy of reaction is about 1.96 MJ/kg of mixture, only 10 per cent lower than that of the lowest energy hydrocarbon.

The flammability limits and the enthalpy of reaction show that the overall mixtures and resultant energies for hydrogen sulphide combustion in air approximate those of hydrogen and the hydrocarbons.

B.5 Combustion Mechanisms.

The mechanisms of combustion depend mainly on the way the reactants begins to burn or is ignited.[18] When combustion is maintained by raising the temperature of reactants to the ignition point by heat feedback from the reaction zone, the mechanism is called "deflagration," and the flame propagates subsonicly into the gaseous reactants.[15,16,19] Next, when ignition is accomplished using shock heating of the reactants, the mechanism is called "detonation," and the flame propagates supersonicly into the unreacted fuel-air mixture.

The gasdynamics of combustion depends on the boundary conditions. This is particularly the case when the combustion propagates subsonicly, that is with a Mach less than one. In this case any disturbance in the flow propagates as a wave with the local speed of sound. In the relatively cool unburned gas, the wave propages at a slow speed of sound. In the relatively hot burned products the wave propages at a higher velocity, albeit with a unity Mach number. As a consequence, deflagrations may have their flames distorted by confinement and obstacles.

For typical hydrocarbon-air mixtures, the initial laminar low velocity flames are less than 1 m/s,[20] where Mach numbers are about in the range from 0.001 to 0.01 and the fluid dynamics can be well treated as an incompressible flow.[21,22] These flames can be accelerated,[20,23-26] can become turbulent and can have flame speeds accelerated by over two orders of magnitude to over 100 m/s, to Mach numbers in the range of 0.3, where the fluid dynamics must be treated compressibility. Next, given sufficient acceleration, the flame velocity may become supersonic, Mach numbers of the order of 5, and the combustion is considered to have undergone transition to detonation.[27-30]

B.6 Explosion Modes.

In the laminar, low Mach number case, the pressure change across the flame may be neglected. On the other hand, in both the subsonic accelerated case and the detonation case, the pressure change across the flame is not negligible and may be propagated into the environment.

When the pressure change exceeds 0.02 Pa, the sound pressure level is about 60 db and the effect is an audible roar.[31] Below this level the combustion need not be considered explosive. Above a 120 db sound pressure level, 20 Pa pressure change, the pressure change is called "blast" and body and structural damage may result. These pressure changes can be found in accelerated flames[32,33] and as a consequence of detonation.

B.7 Explosion Situations.

There are four basic classifications for gas phase explosions:

(1) Open (Unconfined Vapour Cloud Explosion - UVCE);
(2) Partially confined;
(3) Confined; and
(4) Boiling Liquid Evapourating Vapour Explosion (BLEVE);

The first three categories are associated with spills or mixtures of flammable materials in air and their boundary conditions. The fourth classification is associated with a container of a high vapour pressure substance that ruptures and flash evapourates. This causes little blast damage, but may result in "rocketing" of the container.[34] In the BLEVE case, if the substance that escapes is a fuel and ignites immediately, a fireball can be produced.[34]

B.8 Examples of Vapour Cloud Explosion Incidents.

There are many examples of disasterous incidents that have been classified as vapour cloud explosions.[35] Some that have been investigated include the fuels listed in Table B.2: Hydrogen (1975), ethylene (1964), propane (1965), methane (1963) and butane (1957).

One case, the NYPRO works at Flixborough, England, occurred in 1971.[36] In this case, an unconfined vapour cloud explosion (UVCE) resulted from the ignition of about 40 tonnes of liquid petroleum gas spilled by the catastrophic failure of a large-diameter pipe. Ignition occurred within 2 minutes due to a Deisel truck with the motor running, located about 100 meters from the spill point. The flame propagated backward to the point of release.

Eighty people were injured, 20 were killed, buildings collapsed or were structurally distorted, windows were blown out at 200 meters, acrid smoke drifted from the site and water was polluted. Over $US(1979)200,000,000 damage was claimed for compensation.

B.9 The Hydrogen Sulphide Question.

Hydrogen sulphide combustion and physical properties compare to those of materials that have a demonstrated history of vapour cloud incidents. For that reason investigation of the explosion hazard of hydrogen sulphide is considered necessary.

C. Selected Previous Reported Work.

Investigations of the combustion of hydrogen sulphide have been reported since 1909.[37] The work reported an autoignition temperature of stoichiometric hydrogen sulphide in air at 292°. Work was subsequently reported in the period from 1924 to 1927, by Jones and White and their co-workers.[38] In general, these early reported studies discussed the laminar premixed combustion of hydrogen sulphide in air.

Later studies of hydrogen sulphide combustion centre around the combustion of hydrogen sulphide emissions recovered from coke-ovens or other coal-fired heaters.[39] These studies examine the oxidation of sulphur-bearing compounds under various experimental conditions.[40,41] The results of these investigations have been summarized by Glassman.[15]

Detailed investigations of the combustion of hydrogen sulphide in air, including measurements of the flammability limits and initial estimates of the detonation properties and flame acceleration have been carried out by Lee and his co-workers at McGill University. These studies include the work of Kincler on "The Influence of Water Sprays on H_2S-Air Flames."[42]

This investigation is directed toward the effects of hydrogen sulphide explosion in air. It therefore rests on the combustion studies above and extends the work to large scale at environmental conditions. Where relevant, other work is cited below.

D. Hydrogen Sulphide.

There are a number of sulphides, including polysulphides and hydrosulphides, of which hydrogen sulphide H_2S is the most common.[1] Hydrogen sulphide occurs naturally in the gases of volcanoes, sulphur springs, undersea vents, swamps and stagnant bodies of water.[3]

Hydrogen sulphide (H_2S) is a clear colourless gas.[43] It has an unpleasant smell, generally described as that of "rotten eggs." Furthermore, hydrogen sulphide is extremely poisonous and forms a dangerous explosive mixture with air.[44] The ultimate analysis of hydrogen sulphide (Table D.1) shows that the mass ratio of hydrogen to sulphur is 0.05915 to 0.94085.

Hydrogen sulphide is constantly being formed and broken down in the "sulphur cycle" (Figure D.1.)[45] The illustration shows how sulphur and sulphates are related through their processing in the biosphere. Sulphates are washed into the seas from which hydrogen sulphide is released. The hydrogen sulphide enters the atmosphere, from which sulphur returns to the Earth and its surface in the form of oxides and and sulphates. These sulphur compounds are then processed by bacteria in the soil and are subsequently ingested by plants and animals. The sulphur compounds then return to the soil through excretion and death for the cycle to continue.

D.1 Toxicity Outline of Hydrogen Sulphide.

Hydrogen sulphide is both an irritant and an asphyxiant.[44] As Table D.2 shows, at low concentrations, 1 to 10 parts per million (ppm), hydrogen sulphide presence in air can be detected by a smell with the characteristic odour of "rotten eggs."[46]. The allowable threshold for 8 hours exposure, the Threshold Limit Value (TLV) is 10 ppm. Above 10 ppm, protective equipment must be worn.

At higher concentrations, the action of the gas on the nervous system reveals itself. First, depression and then, in still higher amounts, the respiratory centre is paralysed. At 100 ppm, the sense of smell is desensitized in 3 to 15 minutes and there is irritation of the eyes and throat. At 200 ppm, the sense of smell is lost rapidly and the eyes and throat burn. At 500 ppm, the sense of balance is lost, reasoning is incapacitated and breathing stops in 2 to 15 minutes. Victims at this stage require artificial respiration.

At 700 ppm, victims are quickly unconcious and will die unless rescued immediately. At 1000 ppm, victims are unconcious at once, and will suffer brain damage unless rescued promptly.

Fatal hydrogen sulphide poisoning may occur even more rapidly than that following exposure to a similar concentration of hydrogen cyanide.

D.2 Outline of Physical and Thermodynamic Properties.

At standard temperature and pressure (20° and 101.3 kPa). The molecular weight of H_2S is 34.080 kg/kgmole, and the boiling point at atmospheric pressure is -60.75°C (212.41°K). The physical and thermodynamic properties of hydrogen sulphide are outlined in Table D.3.[1,3]

Hydrogen sulphide is denser than air (1.1906 times greater) and is readily condensed as a colourless liquid. The vapour pressure of hydrogen sulphide is 10.3 ata at 0°C. The critical temperature is 100.4°C, the critical pressure is 89 ata, and the critical density is 0.37 g/litre.

Hydrogen sulphide is highly soluble in water: 1 volume of water can absorb 4.65 volumes of hydrogen sulphide at 0°C, 3.44 volumes at 10°C, 2.75 volumes at 18°C and 2.61 at 20°C. A crystalline hydrate $H_2S.(23/4)H_2O$ is formed at low temperatures.

Hydrogen sulphide forms the root of the polysulphides and hydrogen polysulphides. These materials, of the form H_2S_x, may have multiple sulphur bonds.

Hydrogen sulphide also forms addition compounds with other substances, including numerous halides.

Liquid hydrogen sulphide is an excellent solvent for organic materials, but a poor solvent for inorganic substances. It has a small dielectric constant and ionizes only slightly.

D.3 Hydrogen Sulphide Overall Chemistry.

Hydrogen sulphide may be formed by the direct combination of the elements:

$$S + H_2 = H_2S + 4.8 \text{ kcal/gmole} \qquad (D.1)$$

and decomposes at high temperatures with the reverse of reaction D.1

Hydrogen sulphide reacts with most metals, forming the corresponding sulphides, especially when heated or in the presence of water. It also forms sulphides when heated with many oxides.

D.4 Assays of Hydrogen Sulphide.

Hydrogen Sulphide can be assayed by its spontaneous and rapid incorporation into acid solution with methylene blue by reaction with N,N-dimethyl-p-phenylene diamine and $FeCl_3$. The methylene blue formed is then assayed spectrophotometrically at 650 - 670 nm.[45]

D.5 The Sulphydryl (-S-H) Radical.

Sulphur takes on a variety of group forms with other elements.[43] Two of these group forms are sulphydryl (-S-H) and disulphide (-S-S-).[45] The sulphydryl and disulphide groups are found typically in thiols and disulphides. (The term "thio" indicates that a sulphur atom has been substituted for an oxygen atom in a parent species, as found for example in the thiosulphate ion, $S_2O_3^=$).[47] These are a variety of methods available for analysis of these latter groups.

The chemical reactions of the thiols are ultimately the result of the electronic structure around the -S-H radical group.[49] The most fundamental characteristics are the bond lengths and the bond angles. These determine the light absorption properties and the ability to ionize and react.[13]

Thiols have a greater acidity and a lesser ability to form hydrogen bonds and double bonds than their oxygen brothers.[45] This is because sulphur has a larger atomic spacial extent (volume) and therefore is less electronegative than oxygen. Consequently, the bond length is longer and the dissociation energy for the -S-H bond is less than the -O-H bond. The bond lengths for sulphur and oxygen bonds with hydrogen are outlined in Table D.4. Some bond angles are given in Table D.5.[45]

Organic sulphides of the form R-SH, where R is an organic radical, are "evil smelling compounds" called mercaptans.[48] Hydrogen sulphide (H_2S) is the simplest mercaptan H-SH. It is present in traces in the unpolluted atmosphere (0.07-0.32 parts per 10^{-9}).[45] In general, the combustion of sulphur produces sulphur oxides and trioxides which, combined with steam produce highly corrosive acids.[48]

SH groups, are chemically the most active groups found in living organism cells, forming, among other things, a wide range of stable metallic complexes.

E. Hydrogen Sulphide Combustion in Dry Air.

In this section, the composition of air is discussed, followed by an outline of hydrogen sulphide combustion in air.

E.1 The Composition of Dry Air.

The combustion of hydrogen sulphide mixtures with and in air involves the chemical substances that air contains. By volumetric analysis, as given in Table E.1a, air is 20.946% molecular oxygen (O_2), 78.084% molecular nitrogen (N_2), with the balance (0.97%) other chemicals: carbon dioxide, carbon monoxide, argon, helium, and neon, for example. At low enough temperatures and pressures, the perfect gas assumptions apply and the volumetric analysis is equivalent to the molar analysis.

For calculation purposes, the minor constituents are neglected and air is presumed to have the composition shown in Table E.1b.

The gravimetric analysis of air is shown in Table E.2.

The gas constant for air is approximately 287.04 J/kg-K and the specific heat ratio is about 1.40062.

E.2 Overall Combustion of Hydrogen Sulphide in Air.

The hydrogen sulphide flame in air is blue and the combustion when oxygen is plentiful or fuel is lean produces water and sulphur dioxide. The reaction with the oxygen component in air can be described by:

$$H_2S + (3/2)O_2 = H_2O + SO_2 \qquad (E.1)$$

When oxygen starved or fuel rich the system produces water and sulphur:

$$H_2S + (1/2)O_2 = H_2O + S \qquad (E.2)$$

As Equation (B.2) shows, complete combustion of hydrogen sulphide in sufficient air produces water (H_2O) and sulphur dioxide (SO_2).

The overall reaction can be written as

$$H_2S + 1.5 \times (O_2 + 3.774N_2) = H_2O + SO_2 + 5.661N_2 \qquad (E.3)$$

In this reaction, the stable products of complete combustion are water (H_2O) and sulphur dioxide (SO_2). The equation shows that for these products to be formed, one mole of hydrogen sulphide with a molecular weight of 34 combines with 1.5 moles of molecular oxygen (molecular weight 32) and 5.661 moles of molecular nitrogen (molecular weight 28) for a total molecular weight of 206.508. The stoichiometric mass ratio of fuel to air is approximately 34/206 = 0.165.

E.2.1 Equivalence Ratio.

In combustion problems, ratios of fuel to air in reactant systems are compared to ratios of the same fuel to air where combustion is presumed to go to completion without residual fuel and/or oxidiser remaining, i.e., to the formation of a system of stable (unreacting) products. The parameter for comparison is called the equivalence ratio: the mass ratio of fuel to oxidizer with the balanced or stoichiometric mass ratio of fuel to oxidiser. The equivalence ratio can be expressed quantitatively as

$$\emptyset = \frac{[\text{fuel/air}]}{[\text{fuel/air}]_{\text{Stoichiometric}}} \qquad (E.4)$$

where fuel/air is the fuel to air mass, volume or molar ratio. For hydrogen sulphide stoichiometric composition is defined in air by the complete reactive to water (H_2O) and sulphur dioxide (SO_2) as

$$H_2S + 1.5(O_2 + 3.774N_2) = (H_2O + SO_2) + 5.661N_2 \qquad (E.5)$$

The mixture of hydrogen sulphide in air with an equivalence ratio $\emptyset$ is therefore given by $\emptyset H_2S + 1.5(O_2 + 3.774N_2)$. In this reaction, each mole of hydrogen sulphide requires 7.161 moles of air for complete combustion.

The stoichiometric molar or volume percentage of fuel to the fuel and air mixture is about 12.3% and the corresponding mass fraction is about 8%.

E.3 Chemistry of Other Constituents Involved.

The individual atoms from the oxygen and nitrogen molecules in air can become involved in combustion of hydrogen sulphide. For this reason, the chemistry of these materials is outlined here.

E.3.1 Oxygen Chemistry.

Oxygen and sulphur are both members of Group VIA of the periodic table of elements. The group members have a tendency to assume two electrons to assume inert gas configuration. All Group VIA members have distinctly electronegative behaviour with electropositive materials. For example, both oxygen and sulphur can combine with hydrogen as negatively bivalent elements forming water (H_2O) and hydrogen sulphide (H_2S), whose properties are outlined in Table E.3.

An important member of Group VIA, oxygen (O) not only supports combustion by combining with fuels, it also supports respiration and is vital for life. The atmosphere contains approximately 20.946% oxygen by volume (Table E.1), subject only to local changes.

Liquid oxygen is pale blue and non-conducting, and the solid is light blue in colour. Oxygen reactions are regarded as relatively slow at normal temperature and pressure (20C and 1 atmosphere). Oxygen is invariably diatomic in the gas state. Some physical constants for oxygen are shown in Table E.4.[43]

E.3.2 Atomic Oxygen.

Atomic oxygen (O) is formed in glow discharges of molecular oxygen at low pressures. It is relatively unreactive with hydrogen (H_2), methane (CH_4), hydrogen cyanide (HCN) and carbon monoxide (CO). However, atomic oxygen is relatively reactive with hydrogen bromide (HBr), hydrogen sulphide (H_2S), carbon sulphide (CS_2), methyl-chloride (CH_3Cl), dimethyl-chloride (CH_2Cl_2), and trimethyl-chloride ($CHCl_3$). Products of the reaction of atomic oxygen with organic compounds at low temperatures are not stable.

Activated oxygen can be formed from atomic oxygen by the collisional photo-deexcitation of excited molecules.

E.3.3 Ozone.

Ozone (O_3) is a triangular molecule of oxygen. It is recognized by its sharp, tickling smell. It is found in the Earth's atmosphere, at elevations of 20 to 60 km.[50] Ozone can be produced when wet, moist phosphorus is slowly oxidized in air. It can also be prepared by passing an electrical discharge through molecular oxygen.[47]

In high concentrations, ozone is corrosive on respiratory organs, since it reacts readily with organic compounds. Finally, ozone reacts with many substances that are nonreactive in molecular oxygen.

The process for preparation of ozone from molecular and atomic oxygen is

$$O_2 + O = O_3 + 24\ \mathrm{kcal/gmole} \qquad (E.6)$$

The decomposition of ozone can be dangerously explosive:

$$O_3 = (3/2)O_2 + 34.2\ \mathrm{kcal/gmole} \qquad (E.7)$$

but at ordinary temperatures, the decomposition is generally very slow.

E.3.4 Oxides and Peroxides.

The compounds of elements with oxygen are called oxides and peroxides. One class of oxides is formally derived by the replacement of hydrogen in water (H_2O). They include water, chlorine oxide (Cl_2O), nitrogen monoxide (NO), diboron trioxide (B_2O_3), and sulphur dioxide (SO_2). The oxides are usually gaseous and are mostly formed between oxygen and the non-metallic elements. Most oxides have thermal stability.

In addition to normal oxides, oxygen elements can be bonded to one another and to other elements to form "peroxides." The characteristic of peroxides is the radical $- O - O -$. An example is hydrogen peroxide ($HO - OH$).

E.3.5 Oxonium Compounds.

Oxides and peroxides can react with other substances. In one case, the potentially trivalent character of the oxygen atom allows bonding with three ligands.[43] The compound formed then involves the addition of the ligands, dissociation of the resultant molecule into positive and negative ions, and the subsequent electrovalent bonding of those ions.

E.3.5.1 The Hydronium Ion.

One form of oxonium ion is $H_2O...HX$ or $[H_3O]X$, based on the positive ion $[H_3O]^+$. The hydronium ion is the active radical in acids.

E.4 Sulphur Chemistry.

Sulphur is found in the elemental state in natural resource deposits. Sulphur in the bound hydrogen sulphide form is contained in coal gas, coke oven gas, water gas, producer gas, and smoke stack gas. As hydrogen sulphide (H_2S), sulphur often escapes from the ground as a gas, particularly in volcanic zones.[43] Volcanic gases frequently also contain sulphur dioxide (SO_2) the culprit compound in acid rain.[51] The bound sulphur can be removed by treatment with iron oxide as a purifier; although superior removal is achievable in wet processes.[43]

Sulphur makes up about 0.03 per cent of the Earth's crust; the oceans contain about 0.09 per cent sulphur; and coal contains 0.5 to over 3.0 per cent sulphur by dry weight.[52,53]

Sulphur exists in a variety of forms in nature. The form stable at ordinary temperature, rhombic (alpha-sulphur), is yellow, has a density of 2.06 g/cc, a hardness of 2.5, and a specific heat of 0.172 cal/g-K. Above 110°C, sulphur melts to form a yellow liquid. The complex details of its modifications and metamorphoses can be examined in the literature.[43]

E.4.1 Sulphur Oxides.

Sulphur forms four normal oxides: sulphur dioxide (SO_2), sulphur trioxide (SO_3), disulphur trioxide (S_2O_3), and sulphur monoxide (SO). It also forms two peroxides: disulphur heptoxide (S_2O_7) and sulphur tetroxide (SO_4). Sulphur trioxide is the anhydride of sulphuric acid (H_2SO_4) and sulphur dioxide is that of sulphurous acid (H_2SO_3). The salts of the acids are called sulphates and sulphites, respectively.

E.4.1.1 Sulphur Dioxide (SO_2).

Sulphur dioxide is formed when sulphur is burned in air:

$$S + O_2 = SO_2 + 70.9 \text{ kcal/gmole } (20^{\circ}C, 1 \text{ ata}) \qquad (E.8)$$

It is also formed by the combustion of sulphides in air.

Sulphur dioxide is a colourless gas with a strong, pungent smell. It does not burn and it does not support combustion on its own, although it will combine with oxygen in the presence of suitable catalysts. Nevertheless, it is toxic, if inhaled.

At relatively low pressures, sulphur dioxide's behaviour deviates strongly from the ideal gas law.

E.4.1.2 Sulphur Trioxide (SO_3)

Sulphur trioxide is formed in the combustion of sulphide ores in air. Both sulphur dioxide and sulphur trioxide are formed. However, in the presence of oxygen, the sulphur dioxide combines to make the trioxide:

$$SO_2 + (1/2) O_2 = SO_3 + 23.2 \text{ kcal/gmole} \qquad (E.9)$$

Sulphur trioxide is actively hygroscopic and forms sulphuric acid:

$$SO_3 + H_2O = H_2SO_4 + 21.28 \text{ kcal/gmole (at } 20^{\circ}C) \qquad (E.10)$$

As a consequence, sulphur trioxide can be explosive in the presence of water; can unbind water from many substances; and can char organic materials. The trioxide in the presence of water generally forms a thick fog limiting its ability to combine further due to the relatively low mobility of the droplets compared to any gas streams. However, once the sulphuric acid is formed, it relatively low vapour pressure reduces the fog production tendency and the reaction can readily occur.

E.4.1.3 Disulphur Trioxide (S_2O_3).

Disulphur trioxide can be obtained from the action of elemental sulphur on anhydrous sulphur trioxide.

E.4.1.4 Sulphur Monoxide (SO).

Sulphur monoxide is a colourless gas. It can be formed by the action of glow discharges on sulphur dioxide. It does not react with oxygen at ordinary temperature, but does decompose, albeit slowly, in the presence of sulphur. Sulphur monoxide does appear as an intermediate species in the formation of sundry compounds.

E.4.1.5 Disulphur Heptoxide (Sulphur Heptoxide, S_2O_7).

Disulphur heptoxide can be formed by the action of a relatively low-pressure electric discharge on a mixture of oxygen and sulphur dioxide. It can also be prepared by the action of ozone on sulphur dioxide or sulphur trioxide.[43] The compound forms oily droplets in air and readily decomposes, especially in the presence of water, releasing oxygen.

E.4.1.6 Sulphur Tetroxide (SO_4).

Sulphur tetroxide is a strong oxidiser. It was first found formed by the action of electric discharges on a mixture of sulphur dioxide and oxygen.[43]

E.5 Nitrogen Chemistry.

Nitrogen, with an atomic weight of 14.008, is a colourless, inert gas at normal temperature and pressure (1 atmosphere, 20°C); and has no taste or smell. Indeed, even at 3000°C, molecular nitrogen is barely dissociated. Nitrogen belongs to group VA of the periodic table;[43] whose other members include Phosphorus (P, molecular weight MW=30.975), Arsenic (As, MW=74.91), Antimony (Sb, MW=121.76) and Bismuth (Bi, MW=209.00).

Chemically, nitrogen exhibits valencies from 1 to 5 although its principal oxydation state with oxygen is three (3). Toward hydrogen, nitrogen is exclusively trivalent.[43] The hydroxides of nitrogen are acidic. It is noted here that nitric sulphides N_4S_4 and N_2S_5 decompose explosively when heated.

While the sulphur oxides are associated with the combustion of sulphur-containing compounds, the nitrogen compounds, oxides of nitrogen designated generically as NO_x, are by-products of combustion where air is involved. In this section, the chemistry of nitrogen is introduced, with a view to participation in hydrogen sulphide combustion.

The atmosphere, as was illustrated in Table E.1, is approximately 78% molecular nitrogen (N_2) by volume. In addition to its presence in the molecular form in air, elemental nitrogen is found in the traces of ammonia (NH_3) and nitric acid (HNO_3) in the atmosphere.[43]

The normal oxides of nitrogen are shown in Table E.5,[43] and are discussed below.

E.5.1 Dinitrogen Oxide (N_2O).

Dinitrogen oxide or "nitrous oxide" (N_2O) is a colourless gas with a sweet but weak smell and a sweet taste. In small amounts it induces laughter (hence the name "laughing gas), but is narcotic in large quantities. Although initiation is difficult, substances that combust readily with oxygen will burn as vigourously in dinitrogen oxide. Furthermore, dinitrogen oxide and molecular hydrogen in equal molar amounts will explode when ignited:

$$N_2O + H_2 = N_2 + H_2O(gas) + 77.5\ kcal \qquad (E.11)$$

A mixture of dinitrogen oxide with ammonia (NH_3) also explodes:

$$3N_2O+2NH_3= 4N_2+3H_2O(gas) \qquad (E.12)$$

E.5.2 Nitrogen Monoxide (NO).

Nitrogen monoxide (NO), also called "nitric oxide," is a product of nitrogen combustion:

$$N_2 + O_2 = 2NO \qquad (E.13)$$

At relatively high temperatures the product (NO) is favoured, while at lower temperatures, the process favours the reactants. Indeed, in order to form nitrogen monoxide, the reaction must be carried out at high temperatures (about 3000°C) and quickly quenched to retain the product. At normal atmospheric conditions (101.3 kPa, 20°), the rate of decomposition of nitrogen monoxide is slow and the material is "metastable."[43]

E.5.3 Nitrogen Trioxide (NO_3).

Nitrogen trioxide (dinitrogen trioxide), N_2O_3, is called the "anhydride of nitric acid." The compound can be formed by reversal of the following two reactions:

$$N_2O_3 = NO + NO_2 \qquad (E.14)$$

$$2N_2O_3 = 2NO + N_2O_4 \qquad (E.15)$$

E.5.4 Nitrogen Dioxide (NO_2).

Nitrogen dioxide may be readily formed by the oxidation of nitrogen monoxide:

$$2NO + O_2 = NO_2 \qquad (E.16)$$

Nitrogen dioxide is a brown-red, very poisonous gas, with a characteristic smell. The colour deepens as the gas is heated and polymerizes to nitrogen tetroxide:

$$2NO_2 = N_2O_4 \qquad (E.17)$$

Nitrogen dioxide is a powerful oxidant: potassium, phosphorus and sulphur will burn in it. Furthermore, a mixture of nitrogen dioxide and carbon disulphide (CS_2) can be made to detonate violently.[43]

E.5.5 Dinitrogen Tetroxide (N_2O_4).

As was mentioned above, dinitrogen tetroxide (N_2O_4) is a polymer derived from the combustion of nitrogen dioxide (NO_2). Dinitrogen tetroxide is a colourless gas.

E.5.6 Dinitrogen Pentoxide (N_2O_5).

Dinitrogen pentoxide, also called "nitrogen pentoxide" (N_2O_5), is an unstable solid. Having a melting point at one atmosphere of 30°C and a boiling point of 50°C, it may explode without any apparent stimulus.[43]

E.5.7 Other Oxides of Nitrogen.

It has been deduced, from a variety of observations, that there are more oxides of nitrogen than the six listed above.[43] In general, the oxides that appear due to the combustion of nitrogen are designated by the general formula NO_x.[54] They are the class of material responsible for "photochemical smog."

E.4 Compounds of Nitrogen and Sulphur.[43]

Nitrogen forms two compounds with sulphur. These are S_4N_4 (tetrasulphur tetranitride, sulphur nitride) and S_4N_2 (tetrasulphur dinitride).

Tetrasulphur tetranitride is a strongly endothermal compound which can decompose explosively through both shock and thermal heating:

$$S_4N_4 \; = \; 4S + 2N_2 + 128 \text{ kcal/kgmole} \qquad \text{(E.18)}$$

Tetrasulphur dinitride is a by-product of the decomposition of S_4N_4. It explodes when heated and at normal conditions decomposes slowly.

F. Flammability Reports for Hydrogen Sulphide.

The burning velocity of hydrogen sulphide has been reported since the 1920's. In general, this velocity is defined as the velocity os the flame front relative to the fresh gas immediately ahead of it in a direction normal to the flame front.[42]

F.1 Early Flammability Reports.

The flammability of hydrogen sulphide has been reported by Coward and Jones and reported in their bulletin.[4]

In a horizontal tube 6 cm. in diameter and open at both ends the limits of hydrogen sulphide in air were 5.9 and 27.2 per cent.[5] In closed tubes 1.5 metres in length and of different diameters the limits for mixtures containing 1 per cent water vapour are indicated in Table F.1.[6]

The limits in a closed horizontal tube, 4.5 cm wide and 75 cm long long with spark at the centre, are given as 3.1 and 45.1 per cent.[7] The great difference between these figures and the corresponding values in Table F.1 was not discussed by Coward and Jones.

F.2 Flammability in Other Atmospheres.

In addition to the combustion of hydrogen sulphide in air at one atmosphere, data for flammability in atmospheres of (a) nitrogen and oxygen, (b) air and carbon dioxide, and (c) nitric oxide were reported.

The lower limit of flammability of hydrogen sulphide in nitrogen and oxygen, with downward propagation of flame in a closed glass tube 150 cm in length and 5 cm in diameter, falls steadily from 6.60 per cent in 15.6 per cent oxygen to 4.93 in 66.6 per cent oxygen.[12]

With increasing amounts of carbon dioxide added to air, the limits of hydrogen sulphide approach and ultimately meet. In a closed horizontal tube 4.5 cm wide and 75 cm long with spark ignition at the centre, about 25 per cent of carbon dioxide in the mixture is sufficient to prevent any mixture inflaming completely, and about 36 per cent prevents partial inflammation.[9]

The limits of hydrogen sulphide in nitric oxide, with downward propagation of flame in a tube 18 mm in diameter, are approximately 20 and 55 per cent.[10]

F.3 Burning Velocity Details.

Measurements of burning velocity of dry hydrogen sulphide mixtures in air were made by J. Kincler.[42]

F.3.1 Burning Velocity in Dry Air.

In Figure F.1 are Kinkler results compared with those of Clark[55] and Gibbs and Calcote.[56] The Kincler data have their maximum at unity equivalence ratio (stoichiometric), at about 41.1 cm/s. At the 7 per cent and 20 per cent levels of hydrogen sulphide in air, the velocities are about 16 and 18 cm/s, respectively.

F.3.2 Burning Velocity in Wet Air.

Water saturated with hydrogen sulphide was sprayed into a flammability tube in order to determine the burning velocity in wet air.[42] These results are compared to those for hydrogen sulphide in dry air are shown in Figure F.2. First, the burning velocity maxima occur at about unity equivalence ratio. The velocity in wet air is about 32 cm/s, approximately 25% lower than the dry air case. Next, as the flammability limits are approached, the burning velocities become equal.

F.4 Burning Velocity of Other Fuels.

In order to compare the flame propagation properties of hydrogen sulphide with those of other materials, selected data have been assembled from the literature. The first of these is the flame propagation velocity for methane in air, shown in Figure F.3.[42] Other data show flame velocities range from 0.4 m/s for methane (CH_4) and propane (C_3H_8) to 2.7 m/s for hydrogen (H_2). [42]

F.5 Acceleration of Flames.

Flame acceleration due to turbulence[23] and confinement[24] have been observed in hydrocarbons and hydrogen. Since hydrogen sulphide burning velocities are similar to those of the hydrocarbons and hydrogen and since the enthalpy of reaction and transport properties compare, it is expected that hydrogen sulphide flames can also be accelerated. It is planned to investigate this.

F.6 Transition to Detonation.

Flames of various chemical systems have been observed to accelerate and transition to detonation.[27-30] It is also planned to investigate this possibility.

G. Rankine-Hugoniot Calculations.

Combustion is due to the release of energy when matter reacts chemically. This energy is used by the matter involved to (a) raise its temperature and (b) change its pressure. These effects can be estimated by balancing the mass, momentum and energy in the reactants with those in the products. The Rankine-Hugoniot relations are a set of equations used to estimate these balances for the case of a steady process.

The first step involved is the identification of the reactant and product species. Then, the quantity of energy released can be calculated from the quantities and properties of the reactants and of the products. Using this energy release along with a balance of the mass and momentum of the reactants and products, the final state of the fluid after combustion can be estimated.

It is pointed out here that Rankine-Hugoniot analyses are simplified estimates of overall effects and are generally applied only to the detonation case.[19]

G.1 The Overall Chemical Reactions.

In this section, the relationship between reactant and product species is modelled by the overall chemical reaction. In the case of equivalence ratio less than or equal to unity, that is, when the reacting system is either fuel lean (or conversely air rich) or has ideal proportions for complete combustion, the chemical reaction is

$$\emptyset H_2S + 1.5(O_2+3.774N_2) = \emptyset(H_2O+SO_2) + 5.661N_2 + (1-\emptyset)O_2 \qquad (G.1)$$

In this case, all the hydrogen sulphide is consumed. The products are water (H_2O) and sulphur dioxide (SO_2), and residual, unused molecular oxygen (O_2) remains for equivalence ratios $\emptyset$ less than unity and there is no unused molecular oxygen for unity equivalence ratio. Molecular nitrogen (N_2) is presumed unreacted.

On the other hand, when the equivalence ratio is slightly greater than unity, that is when the reacting system is fuel rich, the overall chemical balance is modelled as

$$\phi H_2S + (O_2+3.774N_2) = \phi(H_2O+SO) + 3.774N_2 + (\phi-1)H_2S \qquad (G.2)$$

Here, all the molecular oxygen is used, however there is residual hydrogen sulphide fuel and the products are water and sulphur monoxide (SO).

Finally, when the equivalence ratio is much greater than unity, that is when the reacting system is very fuel rich, the overall chemical reaction is modelled as

$$\phi H_2S + 0.5(O_2+3.774N_2) = \phi(H_2O+S) + 1.887N_2 + (\phi-1)H_2S \qquad (G.3)$$

In this last case, there is residual fuel, but the products are sulphur (S) and water.

In the case of unity equivalence ratio, that is where the hydrogen sulphide and air concentrations are matched to presumed ideal complete overall reaction, the fuel mass fraction is about 0.142 and the fuel mole fraction is about 0.123.

The energy released is then expressed as the difference in the enthalpies of formation of the product and reactant species involved.

G.2 The Rankine-Hugoniot Approach.

Detonation properties of mixtures of hydrogen sulphide in air are the consequence of equilibrium balances of the overall mass, momentum and energy of the fluid system across the boundaries of a control volume of unknown extent. These properties can be estimated by using the Rankine-Hugoniot relations.[15,16,19] These relations are an explicit equation set that relate the upstream to the downstream dynamic properties of the fluid and and thermodynamic properties of the media. The approach "provides a framework within which plane deflagration and detonation waves may be investigated."[19] In this approach, transport properties of viscosity and thermal conductivity are neglected.

The analysis assumes (a) plane (1-dimensional) combustion without rotation or vorticity; (b) stationary mass flow rate; (c) no viscosity or (d) diffusion; (e) adiabaticity between the subject fluid and the environment; and (f) rates of reaction can be neglected when estimating the difference in system properties across the combustion zone. Briefly, the Rankine-Hugoniot approach gives the change in properties across the detonation when all the chemical and kinetic energy due to the combustion process has been converted to directed kinetic energy and enthalpy;[57] but makes no statement about the rates of any processes involved, or about the physical space required for the conversion.

The solution to the Rankine-Hugoniot equation set includes (a) the detonation velocity and (b) Mach number relative to the unburned medium; the (c) temperature and (d) pressure ratios across the zone of the event. Furthermore, by judicious definition of the zones of interest, intermediate (e) temperature ratio and (f) pressure ratios due to shock compression, but prior to combustion inside the detonation wave, can be estimated.

The result shows the nature of the blast wave due to a detonation. From this, (g) total impulse (the overall pressure loading effect due to a blast) - and both positive and negative impulse - can be calculated, assuming that the event time for the detonation is small compared to the times for the exterior blast dynamic effects and that the blast effects are evaluated far enough from the detonation source that the event can be treated as though it occurs at a point.

In this section, detonations are defined, the Rankine-Hugoniot relations presented, and sample calculations given for a hydrogen sulphide detonation case, assuming the overall complete ideal gas reaction.

G.3 Definitions and Parameters.

In order to detail its effects, the general character of a detonation is presented in the form of a problem statement. This is followed by discussion of the Rankine-Hugoniot relations. Then comes an outline of the solution of the equation set and the establishment of equilibrium thermodynamic, Chapman-Jouguet, conditions following the event.

Next, cases of hydrogen sulphide fuel to air ratio are defined using the equivalence ratio, the comparison between the fuel - air ratio presumed for ideal complete combustion without either excess air or excess fuel the available fuel - air ratio.

Finally, sample calculations are presented for the stoichiometric, unity equivalence ratio case.

G.3.1 Statement of the Problem.

A homogeneous mixture of a combustible medium is presumed available. For combustion to ensue, specific events must occur. These events centre around the establishment of a high enough temperature to initiate combustion processes. This initial temperature threshold, ignition, can be delivered to the medium in a variety of ways. However, for combustion to be maintained the reaction ignition must be continuously available to unburned reactants. In the case where the threshold temperature is provided solely by the reactant combustion process, the event is called deflagration. On the other hand, if the ignition temperature is provided by a shock wave incident on the unreacted medium, raising the local temperature above the combustion threshold, the event is called detonation. In this latter case, reactions can proceed without the requirement for energy feedback from the combustion zone into the unreacted gaseous medium.

A typical structure through a detonation is illustrated in Figure G.1. The figure is drawn with the axis parallel to the local combustion propagation direction at an instant in time. The detonation is divided into two zones (I) a shock zone and (II) a deflagration zone. In the shock zone, the thermodynamic properties of the combustible gas are elevated by shock heating to levels above those required for ignition. Usually, the shock heating occurs quickly compared to the reaction rates so the chemical composition does not change through the shock and the chemical composition is deemed "frozen." Following the shock, the media react in the deflagration zone, with corresponding changes in composition. The process combustion train propagates into the unreacted material as a wave. This class of phenomenon is called a ZND structure after Ze'eldovich, von Neumann and Doring.[19] The structure can be modelled by balancing mass, momentum and energy across the entire detonation and then across the shock region alone.

G.3.2 Rankine-Hugoniot Relations.

To analyse the detonation, a homogeneous solution of reactants is presumed to react with a locally plane front. In that case, the situation can be sketched schematically as shown in Figure G.2. The wave is presumed to be steady and is viewed in a frame of reference that moves with the reaction front and so appears motionless with respect to the front. Furthermore, the detonation zone is presumed isolated within a control volume and is one-dimensional. As a result, all property changes occur in the control volume and are established as functions of the axial dimension "x" only.

The initial conditions of the fluid include the thermodynamic variables of temperature T_1 and pressure P_1, which completely define the state for a single-phase, single component fluid; and bulk velocity u_1, from which the kinetic energy is derived. The enthalpy (h), the density (r), and the specific volume (v) are given for convenience. The exit conditions with subscript "2", as well as the inlet velocity u_1 are unknown. No statement about the rate of the reaction and hence the physical extent (thickness) of the detonation is made. However, since all events are presumed to occur in the combustion zone, the control volume does not have to define the extent of the detonation, but merely enclose it.

G.3.2.1 The Rayleigh Line.

The Rayleigh line is a one-dimensional statement of the mass balance across the combustion zone.

Presuming one dimensionality, the continuity equation for stationary flow through the control volume shown in Figure G.2 is

$$m = r_1 u_1 = r_2 u_2 \qquad (G.4)$$

That is, mass flux m is the product of the density r and velocity u. Furthermore, in the steady case, the mass flux (the mass flow rate per unit area) m must be constant.

Next, neglecting body forces and surface forces including viscosity; dynamic effects are presumed to be only those associated with pressure p and mass flux ru^2. Consequently, the one-dimensional momentum flux equation form of Newton's Second Law of Motion is

$$P_1 + r_1 u_1{}^2 = P_2 + r_2 u_2{}^2 \qquad (G.5)$$

Rearranging Equation (G.5) and using Equation (G.4) to eliminate velocity from the momentum flux terms gives

$$p_2 - p_1 = -m^2 (1/r_2 - 1/r_1) \qquad (G.6)$$

Equation (G.6) expresses the pressure p_2 at the exit of the control volume in terms of the change of specific volume ($v=1/r$), the mass flux(m) and the initial pressure (p_1). The equation has two constants p_1 and $1/r_1$, which completely define the thermodynamic state of the incoming fluid and is in the form of a straight line with slope $-m^2$. This relationship is called the Rayleigh line.

The Rayleigh line is sketched in Figure G.3 on $p,1/r$ axes. The line passes through the point $p_1,1/r_1$ which represents the known thermodynamic conditions of the unreacted medium ahead, upstream, of the detonation zone. Next, since the mass flow for the steady case is always real, the slope of the Rayleigh line $-m^2$ is always negative. Therefore, as Figure G.3 illustrates, the downstream, after combustion, thermodynamic state must have a higher pressure along with a lower specific volume or a lower pressure along with a higher specific volume, than the initial unreacted condition.

G.3.2.2 The Hugoniot Curve.

Associated with the mass and momentum in the form of the Rayleigh line is the energy equation in the form of the Hugoniot curve. The energy equation, an expression of the First Law of Thermodynamics, can be written in control volume form as

$$h_1 + u_1^2/2 + q = h_2 + u_2^2/2 + w_{c.v.} \qquad (G.7)$$

where the specific enthalpy $h = e + p/r$ is the sum of the internal energy e and the flow work p/r; q is the heat added to the flowing fluid mass moving through the control volume, and $w_{c.v.}$ is the control volume work per unit mass.

The velocity terms are replaced using the continuity equation (G.4). Furthermore, if the system flowing is adiabatic and no external control volume work is supplied to the environment

$$h_2 - h_1 = [1/2][(1/r_1) + (1/r_2)][p_2 - p_1] \qquad (G.8)$$

This expression, Equation (G.8) is called the Hugoniot curve. The Hugoniot curve expresses the enthalpy difference between the initial and final states of the system flowing through the control volume.

Now, the enthalpy terms in the Hugoniot curve represent the total enthalpy of the entering material (state 1) and leaving material (state 2). In the case where these two materials are different, such as when reactants enter the control volume, but products leave, the enthalpies are actually the sum of the enthalpies of formation (h_f^o) and sensible heat:

$$h = h_f^o + \int_{T^o}^{T} c_p dT \qquad (G.9)$$

In this equation the definition of enthalpy is used, where c_p is the specific heat at constant pressure and T is temperature.

Consequently, Equation (G.8) becomes

$$-h_{rp}^o + \{\int_{T^o}^{T_2} c_{p2} dT - \int_{T^o}^{T_1} c_{p1} dT\} = [1/2][(1/r_1)+(1/r_2)][p_1 - p_2] \qquad (G.10)$$

In Equation (G.10),

$$-h_{rp}^o = h_{f2}^o - h_{f1}^o \qquad (G.11)$$

$$= q$$

the enthalpy of reaction, equal to the thermodynamic heat energy available to the system, q, is the difference between the enthalpies of formation of products h_{f2}^o and reactants h_{f1}^o, respectively, at a standard temperature condition T^o.

As shown in Figure G.4, in the case where there is no reaction, the Hugoniot curve passes through the initial conditions $(p_1, 1/r_1)$. On the other hand, when the reactants are changed into products and the enthalpy of reaction is released, the curve does not pass through the initial state.

The reactants and products are modelled as ideal gases

$$p = r(R^o/M)T \qquad (G.12)$$

with constant specific heats. Then, Equation (G.10) becomes

$$-h_{rp}^o + [k_2/(k_2-1)](R^o/M_2)[T_2-T^o]-[k_1/(k_1-1)](R^o/M_1)[T_1-T^o]$$
$$= [1/2][(1/r_1)+(1/r_2)][p_1 - p_2] \qquad (G.13)$$

If the individual molecular weights M_1 and M_2 are replaced by their average M, and specific heat ratios k_1 and k_2 by their average k, and the gas constant by an average value R^o/M; Equation (G.13) becomes

$$-h_{rp}^{o} + [k/(k-1)](R^o/M)[T_2-T_1] = [1/2][(1/r_1)+(1/r_2)][p_1 - p_2] \qquad (G.14)$$

Finally, using the ideal gas law, Equation (G.12), the Hugoniot curve expression becomes

$$-h_{rp}^{o} + [k/(k-1)](p_2/r_2-p_1/r_1) = [1/2][(1/r_1)+(1/r_2)][p_1 - p_2] \qquad (G.15)$$

G.3.2.3 Mach Number.

The Mach number is a dimensionless measure of fluid velocity u compared to the local speed of sound c. The speed of sound is the speed at which an infinitessimal disturbance propagates in a medium. The speed of sound for an ideal gas is estimated as

$$c = [k\ (R^o/M)\ T]^{1/2} \qquad (G.16)$$

where R^o is the universal gas constant (8.314 kJ/kgmole-K), and M is the molecular weight of the medium. As a consequence, the Mach number is

$$M = u / c \qquad (G.17)$$

When the Mach number is less than unity ($M < 1$), the velocity is called subsonic, when the Mach number is unity the velocity is sonic, and when the Mach number exceeds unity the velocity is called supersonic.

In the case of a combustion with a process front that moves into the reactants at subsonically, the reaction is called a deflagration.[18] In a deflagration, a pressure wave moves ahead of the combustion front. When the combustion wave moves into the reactants at or above their speed of sound, the reaction zone and the pressure wave move together at the same sonic or supersonic velocity. This process is called a detonation.

The Mach number is the single parameter which most closely characterizes the combustion effect. The higher the Mach number the higher the velocity of the combustion wave into the reactant mixture, and the higher the velocity the larger the pressure change across the combustion wave and the larger the effect on the environment.

The Rankine-Hugoniot analysis has been successfully applied only to the detonation case.[19]

The solutions for the Chapman-Jouguet conditions are given below, in terms of the dimensionless ratios.

G.3.2.4 The Chapman-Jouguet Condition.

The state at which the mass flow and momentum are balanced with the energy equation is called the Chapman-Jouguet condition, after the investigators who originally and independently found the solution.[19] Using Rankine-Hugoniot analysis, the Chapman-Jouguet condition is the intersection of the Rayleigh line which models the mass flow of the system passing through the control volume and the Hugoniot curve which describes the enthalpy difference across the reaction zone.

This situation is shown schematically in Figure G.5. The Chapman-Jouguet condition is the tangent of the Rayleigh line to the Hugoniot curve. If the mass flow were higher as represented by a steeper slope of the Rayleigh line, then the reaction would not provide enough energy to maintain the higher mass flow and the fluid would slow down to the tangent condition. Conversely, if the mass flow were lower then the slope of the Rayleigh line would be less steep and the energy release would be utilized to speed up the flow of the system. The stable, balanced condition is therefore confirmed to be at the tangent of the two curves.

The Mach number of the detonation into the reactants always exceeds unity.

(Readers are referred to Reference [19] for more sophisticated and detailed explanations and derivations.)

G.4 Rankine-Hugoniot Solutions.

The Rankine-Hugoniot relations can be solved using several methods.[18,19] An accepted and general way is the use of dimensionless ratios. First, (a) the post-combustion properties of the fluid are expressed as ratios of the initial variables, and (b) other properties where needed are related to measurable initial values. Then, the equations are derived for ideal gas mixtures with identical upstream and downstream molecular weights and specific heat ratios.

The dimensionless ratios are defined below:

Following the approach of Williams[19], dimensionless ratios are first defined:

(a) Dimensionless pressure ratio

$$p = p_2/p_1 \qquad (G.18)$$

Here, the final pressure p_2 is compared to the initial pressure p_1.

(b) Dimensionless specific volume

$$v = v_2 / v_1$$

$$= r_1/r_2 \qquad (G.19)$$

In this case, the final specific volume v_2 is compared to the initial specific volume v_1, and is expressed in terms of a ratio of initial density r_1 to final density r_2.

(c) Dimensionless enthalpy of reaction

$$a = -h_{rp}^{o} r_1/p_1 \qquad (G.20)$$

The enthalpy of reaction for the combustion process h_{rp}^{o} is compared to the flow work r_1/p_1 associated with the entry of the reactants into the combustion zone.

(d) Dimensionless mass flow rate

$$\dot{y} = m^2/p_1 r_1 \qquad (G.21)$$

The dimensionless flow rate compares momentum flux mu = ru^2 to the initial pressure of the reactants p_1.

(e) The Mach number

$$M = u / c$$

The Mach number, as indicated above, is the measure of velocity u of a wave with respect to the speed of sound of the material c into which propagation is occurring.

The solution set for the Rankine-Hugoniot relations for Chapman-Jouguet detonation are given below.

G.4.1 Chapman-Jouguet Pressure Ratio.

The Chapman-Jouguet detonation pressure solution is expressed dimensionlessly as

$$p = 1 + a\,[k-1]\,\{1 + [1+(2k)/(a(k^2-1))]^{1/2}\} \qquad (G.22)$$

G.4.2 Chapman-Jouguet Specific Volume Ratio.

The Chapman-Jouguet specific volume ratio is

$$v = 1 + a\,[(k-1)/k]\,\{1 - [1+(2k)/(a(k^2-1))]^{1/2}\} \qquad (G.23)$$

G.4.3 Chapman-Jouguet Temperature Ratio.

The Chapman-Jouguet temperature ratio is

$$T = p\,v \qquad (G.24)$$

G.4.4 Chapman-Jouguet Mass Flow Rate.

The dimensionless Chapman-Jouguet mass flow rate is expressed as

$$y = k + a\,(k^2-1)\,\{1 + [1+(2k)/(a(k^2-1))]^{1/2}\} \qquad (G.25)$$

G.4.5 Chapman-Jouguet Mach Number.

The Mach number for propagation of Chapman-Jouguet waves into the reactant material is

$$M = \{1 + [a(k^2 - 1)]/(2k)\}^{1/2} + \{[a(k^2-1)]/[2k]\}^{1/2} \qquad (G.26)$$

G.5 Sample Calculations.

The following are sample calculations for detonation of a unity equivalence ratio mixture of hydrogen sulphide in air, based on the above formulae. Required data to undertake the calculations are given in Tables G.1 and G.2 for hydrogen sulphide, molecular oxygen, molecular nitrogen, sulphur dioxide, water vapour and other fuels and products of interest.

G.5.1 Calculation of Gas Properties.

The next step in the estimation of detonation end states requires determination of reactant and product molecular weights and determination of their average value.

The reactant molecular weight is

$$M_1 = \frac{M(H_2S) + 1.5[M(O_2) + 3.774M(N_2)]}{n(H_2S) + n(O_2) + n(N_2)} \qquad (G.27a)$$

$$= \frac{34.08 + 1.5\,[31.9988 + 3.774(28.0134)]}{1 + 1.5[1 + 3.774]}$$

$$= 29.49 \text{ kg/kgmole}$$

The product molecular weight is:

$$M_2 = \frac{M(H_2O) + M(SO_2) + 5.661M(N_2)}{n(H_2O) + n(SO_2) + n(N_2)} \qquad (G.27b)$$

$$= \frac{18.0152 + 64.0588 + 5.661(28.0134)}{1 + 1 + 5.661}$$

$$= 31.41 \text{ kg/kgmole}$$

Although the difference in molecular weights is about 7 per cent, the average molecular weight can be used for the calculation estimates. The average molecular weight is:

$$
\begin{aligned}
M &= [M_1 + M_2]/2 \\
&= [29.49 + 31.41] / 2 \\
&= 30.45 \ \ \text{kg/kgmole.}
\end{aligned}
\tag{G.28}
$$

The gas constant $R = R^o/M$ is estimated using the average molecular weight:

$$
\begin{aligned}
R &= R^o / M \\
&= 8.314 \ (\text{kJ/kgmole-K}) \ / \ 30.45 \ \ (\text{kg/kgmole}) \\
&= 273.03 \ \ \text{J} \ / \ [\text{kg-K}]
\end{aligned}
\tag{G.29}
$$

The reactant density at the initial standard conditions of atmospheric pressure of 101.3 kPa and 20C for ambient temperature is calculated using the ideal gas law Equation (G.12)

$$
\begin{aligned}
r_1 &= P_1 \ / \ RT \\
&= 101.3 \ \text{kPa} \ / \ [273.03 \ (\text{J/kg-K}) \ (273.15+20) \ \text{K}] \\
&= 1.266 \ \ \text{kg/m}^3.
\end{aligned}
\tag{G.30}
$$

G.5.2 Calculation of Enthalpy of Reaction.

The enthalpy of reaction is determined based on the overall stoichiometric reaction, Equations (G.1) to (G.3). The enthalpy of formation of the reactants h_{f1}^{o} is the total of the products of enthalpy of formation of each reactant species multiplied with the amount of each species present in the chemical balance. (The enthalpies of reaction are listed in Table G.1 for a variety of chemical reactants.[58,59])

For hydrogen sulphide in air, the enthalpy of formation of the reactant set is

$$h_{f1}^{o} = n(H_2S)M(H_2S)h_f^o(H_2S)+n(O_2)M(O_2)h_f^o(O_2)+n(N_2)M(N_2)h_f^o(N_2) \qquad (G.31)$$

$$= (1)34.08(-591.14)+1.5[(1)31.9988(0)+(3.774)28.0134(0)]$$

$$= -20146.1 \text{ kJ / mole of reactants}$$

The enthalpy of formation of the product set is

$$h_{f2}^{o} = n(H_2O)M(H_2O)h_f^o(H_2O)+n(SO_2)M(SO_2)h_f^o(SO_2)+n(N_2)M(N_2)h_f^o(N_2) \qquad (G.32)$$

$$= (1)18.0152(-13423.6)+(1)64.0588(-4633.89)+(5.661)28.0134(0)$$

$$= -538670 \text{ kJ / mole of products}$$

Therefore, the enthalpy of reaction from Equation (G.11) is

$$h_{rp}^{o} = -538670 - (-20146.1)$$

$$= -518524 \text{ kJ / mole of reactants}$$

The negative value signals that this amount of energy must be removed from the system in order to maintain the reference temperature at its level of 20C.

The enthalpy of reaction may be expressed in several ways. Two of these ways are:

(1) for each unit mass of (H_2S) fuel:

$$h_{rp}^{o}(H_2S) = -518524/34.08$$

$$= -15214.9 \text{ kJ/kg}(H_2S)$$

(2) for each unit mass of reactant mixture:

$$h_{rp}^{o}(H_2S) = -518524/\{34+1.5[(1)32+(3.774)28]\}$$

$$= -2154.57 \text{ kJ/kg(reactant mixture)}$$

Using the enthalpy of reaction, the initial density and the initial pressure, the dimensionless reaction energy from Equation (G.20) is

$$a = -h^{o}_{rp}\, r_1 / p_1 \qquad (G.33)$$

$$= 2154.57\ (kJ/kg)\ 1.266\ (kg/m^3) / [101.3\ kN/m^2]$$

$$= 26.92$$

G.5.3 Calculation of Detonation Ratios and Product Properties.

The detonation ratios (jumps) are calculated using the gas properties.

First, specific heat ratios are calculated for both reactants and products and then averaged as follows:

$$k_1 = \frac{k(H_2S) + 1.5[k(O_2) + 3.774\ k(N_2)]}{n(H_2S) + n(O_2) + n(N_2)} \qquad (G.34a)$$

$$= \frac{1.32 + 1.5[1.401 + 3.774(1.404)]}{1 + 1.5(1 + 3.774)}$$

$$= 1.393$$

$$k_2 = \frac{k(H_2O) + k(SO_2) + 5.661\ k(N_2)}{n(H_2O) + n(SO_2) + n(N_2)} \qquad (G.34b)$$

$$= \frac{1.329 + 1.29 + 5.661(1.404)}{1 + 1 + 5.661}$$

$$= 1.379$$

The average specific heat ratio is

$$k = [k_1 + k_2]/2 \qquad (G.35)$$

$$= [1.393 + 1.379]/2$$

$$= 1.386$$

The Chapman-Jouguet detonation pressure ratio is

$$p = 1 + a\,[k-1]\,\{1 + [1+(2k)/(a(k^2-1))]^{1/2}\} \tag{G.36}$$

$$= 1 + 26.92(1.386-1)\{1+[1+(2(1.386))/(26.92(1.386^2-1))]^{(1/2)}\}$$

$$= 22.35$$

As a result, from Equation (G.18), the pressure following the detonation is

$$P_2 = p\,(p_1) \tag{G.37}$$

$$= 22.35\,(101.3)$$

$$= 2263.6 \text{ kPa}$$

The Chapman-Jouguet specific volume ratio from Equation (G.19) is

$$v = 1 + a\,[(k-1)/k]\,\{1 - [1+(2k)/(a(k^2-1))]^{1/2}\} \tag{G.38}$$

$$= 1+26.92[(1.386-1)/1.386]\{1-[1+2(1.386)/(26.92(1.386^2-1))]^{1/2}\}$$

$$= 0.592$$

Therefore, the specific volume following the entire detonation wave is

$$v_2 = v\,/\,r_1 \tag{G.39}$$

$$= 0.592/1.266$$

$$= 0.468 \text{ m}^3/\text{kg}$$

The Chapman-Jouguet temperature ratio is

$$T = p\,v \tag{G.40}$$

$$= 22.36\,(0.592)$$

$$= 13.23$$

causing the final temperature calculation to show

$$T_2 = T\ (T_1) \qquad (G.41)$$

$$= 13.23\ (293.15)$$

$$= 3877.9 \quad K$$

$$\text{or} \quad = 3604.8 \quad C$$

The dimensionless mass flow rate at the Chapman-Jouguet solution point is

$$y = k + a\ (k^2-1)\ \{1 + [1+(2k)/(a(k^2-1))]^{1/2}\} \qquad (G.42)$$

$$= 1.386+26.92(1.386^2-1)\{1+[1+2(1.386)/(26.92(1.386^2-1))]^{1/2}\}$$

$$= 52.32$$

Consequently, the mass flow rate is

$$m_1 = [y\ p_1\ r_1]^{1/2} \qquad (G.43)$$

$$= [52.32(101.3)1000(1.266)]^{1/2}$$

$$= 2589.8 \quad kg/s$$

The initial Mach number for Chapman-Jouguet waves from Equation (G.26) is

$$M = \{1 + [a(k^2 - 1)]/(2k)\}^{1/2} + \{[a(k^2-1)]/[2k]\}^{1/2} \qquad (G.44)$$

$$= \{1+[26.92(1.386^2-1)]/(2(1.386))\}^{1/2} +$$

$$+\{[26.92(1.386^2-1)]/[2(1.386)]^{1/2}$$

$$= 6.14$$

The speed of sound for reactant gases is calculated as

$$c = [k\ (R^o/M)\ T]^{1/2} \qquad (G.45)$$

$$= [1.386\ (273.1)\ (293.15)]^{1/2}$$

$$= 333.1 \quad m/s$$

Then, the Chapman-Jouguet velocity of the detonation wave into the unreacted medium is

$$u = M_o c \tag{G.46}$$

$$= 6.14\ (333.1)$$

$$= 2046\ \text{m/s}$$

As an independent check on the results of the calculation, the initial Mach number is also calculated using the mass flow rate. From the mass flow rate and the initial density, the detonation front velocity is

$$u_1 = m_1 / r_1 \tag{G.47}$$

$$= 2589.8 / 1.266$$

$$= 2046\ \text{m/s}$$

The Mach number calculated on this mass flow basis is

$$M_1 = u_1 / c \tag{G.48}$$

$$= 2046 / 333.1$$

$$= 6.14$$

The difference in Mach number calculations is small.

G.6 Frozen - Shock Properties.

Once the changes in properties across the entire reaction zone have been calculated, the mass, momentum and energy balances are known. With this knowledge, information about the initial, shock region of the process can be discerned. The approach assumes that the reaction rates for the chemical process are zero and the mixture composition does not change in the shock zone. The post-shock - pre-combustion properties are not in equilibrium and are called "frozen".

The effects of the shock alone are calculated using the ZND formulation. The basis is the use of the mass flow rate calculated at the Chapman-Jouguet point for the entire detonation wave with the Hugoniot curve without combustion energy release. As Figure G.6 shows, the Rayleigh line is tangent to the Hugoniot curve with heat release, at condition 2. The slope of this Rayleigh line gives the mass flux for the detonation. The intersection of that Rayleigh line to the Hugoniot curve without heat release, at condition s, gives the thermodynamic conditions at the interface of the shock zone (I) and the reaction (detonation) zone (II). Hybrid calculations of this kind give the frozen properties of the unreacted medium.

The approach involves the simultaneous solution of Equation (G.6), the Rayleigh line; with Equation (G.8), the Hugoniot curve. The condition demands that the mass flow rate be determined from the overall detonation calculation Equation (G.36). The relationship between the specific volume following the shock but prior to the deflagration and the initial pressure and temperature is

$$v_s = 1/r_s \tag{G.49}$$

$$= \frac{g(p_1+m^2v_1) \pm ((gp_1-(g-1)m^2v_1{}^2)^2+2m^2q(1-2g))^{1/2}}{m^2(2g-1)} \tag{G.50}$$

Here,

$$g = k / (k - 1) \tag{G.51}$$

and q is the heat transfer from the system to the environment: In the case where there is combustion, $q = h^o_{rp}$ is the enthalpy of reaction.

Now, in the case where there is no reaction, the shock, q is zero and Equation G.50 reduces to

$$v_s^+ = \frac{g(p_1+m^2v_1)}{m^2(2g-1)} \tag{G.52a}$$

for the positive radical value, and to

$$v_- = v_1 \tag{G.52b}$$

for the negative radical.

The solutions to Equations (G.52) for specific volume and (G.6) for the associated pressure are:

$$(v_+, p) = (0.145\ m^3/kg,\ 4428\ kPa)$$

for the shocked condition; and

$$(v_-, p) = (0.790\ m^3/kg,\ 101.3\ kPa)$$

namely the initial condition.

It is noted here that the shocked pressure exceeds the equilibrium pressure following the detonation reactions by about a factor of two. This shock pressure is observed over a time that is short compared to those associated with combustion and is called the von Neumann "spike".

The balance of the property changes through the detonation, that is, those in the deflagration zone, follow the shocked reactant.

Now, actual detonations (a) are three-dimensional and have rotation, (b) have viscosity and (c) have diffusive effects, (d) are not fully adiabatic with the environment, and (e) have complex internal reactions. As a result, the locus of ZND conditions through the detonation, as shown in Figure G.6, is softened from initial (1) to final (2) conditions. The actual locus is approximated by the dashed lines in the illustration.

G.7 Remarks.

Viewed from the outside, in a detonation, a supersonic shock wave pressurizes the reactants, heats them, and puts them in motion. However, the deflagration takes the shocked gases, reacts them, raises their temperature again, but depressurizes them and changes their velocity to that of the speed of sound associated with their new (final) temperature. The higher pressure for the shocked reactants than in the fully combusted products, is called the von Neumann spike.

The ideal calculations offered in this section give clues to the equilibrium conditions that result due to a detonation event. However, the values differ markedly from reality since (a) ideal gas behaviour is assumed, and (b) products are prescribed by a one-step chemical reaction. More precise predictions require more detail. These more detailed calculations are performed by computer. The computer model allows determination of reaction products based on minimization of the Gibbs' free energy[60,61] and gives more complete results than are outlined above.

Solutions for five equivalence ratios (0.5, 0.75, 1.0, 2.0, and 4.0) have been undertaken at DRES and the results are discussed in the next section.

H. Equilibrium Properties of Detonated H_2S in Air.

Detailed estimates of detonation properties of mixtures of hydrogen sulphide in air have been calculated using the Rankine-Hugoniot relation approach, by employing a "complex chemical reaction computer code."[68]

The calculation assumes (a) 1-dimensional combustion without rotation or vorticity; (b) stationary mass flow rate; (c) inviscid; (d) adiabatic flows; where (e) the rates of reaction are neglected in favour of changes in properties as discontinuities across the combustion zone.

Calculations have been performed at The Defence Research Establishment Suffield (DRES) using the an equilibrium composition computer code. They include (a) detonation enthalpy, (b) detonation pressure, (c) detonation temperature, (d) detonation Mach number, (e) detonation velocity, and (f) detonation products. Results are presented as a function of equivalence ratio. Hydrogen sulphide - air compositions with equivalence ratios of 0.5, 0.75, 1.0, 2.0, and 4.0 have been used. The initial conditions are a temperature of 20C (293.15K) and an ambient pressure of 101.3 kPa. For reference, the results of the calculation are summarized in Tables H.1 and H.2.

H.1 Detonation Products.

Detonation products are determined from a list of specific chemical species that must be specified. These specified species are listed in Table H.3. The prescribed composition of air has been given in Table E.1b. Specified product species whose mole fraction was less than $5(10^{-6})$ are neglected. The major products are sulphur dioxide (SO_2) and water (H_2O), with residual molecular nitrogen (N_2).

H.1.1 Product Classification.

Product species have been classified according to their production behaviour as a function of equivalence ratio. The behaviour as a function of equivalence ratio is shown in Table H.4. The classes are:

(A) Maximum production at unity equivalence ratio:

SO_2, H, O, OH;

(B) Maximum production between 0.5 and unity equivalence ratio:

NO;

(C) Maximum production between unity and 4.0 equivalence ratio:

CO, SO, SH, SN, S;

(D) Increasing production with increasing equivalence ratio:

H_2O, H_2S;

(E) Decreasing production with increasing equivalence ratio:

CO_2, H_2, NO_2, S_2O, SO_3, N_2, O_2, A; and

(F) Minimum production at unity equivalence ratio:

S_2.

H.1.2 Detonation Product Discussion.

For all five cases considered, molecular nitrogen (N_2) forms the major product of the reactant mixture. However, categorized under Class E, molecular nitrogen residual decreases as a function of increasing equivalence ratio. The next dominating product species is water vapour (H_2O). The production of water, Class D, increases with equivalence ratio. The third major product species is sulphur dioxide (SO_2). Sulphur dioxide is categorized in Class A and exhibits a maximum of about 12.2% at unity equivalence ratio. Finally, the fourth major product is residual hydrogen sulphide (H_2S) fuel. The residual fuel, Class D, increases with equivalence ratio

Other major products, those with product mole fraction greater than or equal to 1 per cent are sulphur monoxide (Class C), unreacted argon (Class E), molecular hydrogen (Class E) and bimolecular sulphur (Class F).

The equilibrium calculations show that atmospheric molecular nitrogen and atmospheric carbon dioxide both participate in the formation of equilibrium products of detonation of hydrogen sulphide in air.

Two points are noted here: (1) both water and sulphur dioxide exist in combination as products for hydrogen sulphide detonation in air and at unity equivalence ratio they represent 12.2% (SO_2) and 11.9% (H_2O), respectively; and (2) hydrogen sulphide residuals increase with equivalence ratio and, in particular, at equivalence ratios of 2 and over exceed 1% (10,000 ppm).

Following the detonation event, the combustion products vent to and mix with ambient air. As a consequence, species short-lived in an oxygen-rich environment are greatly reduced in number and species that are long-lived are dispersed.

H.2 Combustion Energy Release.

The total combustion energy release is illustrated in Figure H.1 The diagram shows a gradual, almost linear increase in thermal energy output with per cent hydrogen sulphide to a maximum of about 2000 kJ/kg of mixture, corresponding to about 14,000 kJ/kg of hydrogen sulphide, at an equivalence ratio of unity. The thermal energy then decreases on the fuel rich side to about 1000 kJ/kg when the equivalence ratio is 2. The decrease of thermal energy output is associated with incomplete reaction of the hydrogen sulphide with air leaving unburned H_2S as well as other species produced in intermediary reactions.

Figure H.1 also shows the thermal energy release for other fuels including hydrogen (H_2), acetylene (C_2H_2), ethylene (C_2H_4), butane (C_4H_{10}), propane (C_3H_8) and methane (CH_4). Except for acetylene, all fuels show their thermal release maxima at about unit equivalence ratio. Furthermore, they all fall in the range of about 2000 to 3200 kJ/kg of combustible mixture.

H.3 Detonation Temperature Ratio.

The energy release of hydrogen sulphide detonation in air increases the sensible energy of the combustion system. The increase is shown along with those of selected other fuels as a ratio of final equilibrium system product temperature to initial temperature of the reactants in Figure H.2. Just as for thermal energy release, the product to reactant temperature ratio increases with equivalence ratio (volume per cent H_2S) and shows a maximum in the vicinity of the unity equivalence ratio. The maximum temperature ratio is about 9. This lies at the bottom of the range 9 to 11 shown for all six fuels considered. The deviation of the curve from linear is due to the sharing of the reaction heat between the sensible energy (temperature) and the directed kinetic energy of motion combustion gives to the product mass stream.

The intermediate temperature ratio due to the shock zone (I), but prior to the reaction zone (II) shows a maximum of about 5 when the equivalence ratio is unity.

The maximum overall detonation temperature ratio, at an equivalence ratio of unity is about 9. Therefore, when the reactants enter combustion at 20°C (293.16°K) the products leave at about 9(293.16)°K or about 2360°H. Such a high product temperature readily offers thermal energy to the environment.

H.4 Detonation Pressure Ratio.

Detonation increases the local thermodynamic pressure inside the combustion stream. The final product to initial reactant detonation pressure ratio is shown in Figure H.3. Like both the thermal energy release and the product temperature, the pressure ratio is shown for six other fuel mixed with air. All fuels shown maxima in pressure ratio at about unity equivalence ratio. The maximum pressure ratio calculated for hydrogen sulphide for the planar detonation wave, under the assumptions outlined above, is about 15. This ratio falls at the low end of fuels considered and is about the same value as that of hydrogen. The maximum pressure ratio is shown for acetylene at about 22, only 50 per cent higher. It is noted here that thermodynamic pressure scales approximately with temperature.

The shock effects alone also cause the pressure to increase. However, the internal effects are more drastic than the overall detonation pressure change. In general, the shock pressurization of the reactants is a factor of two greater than the overall detonation pressure effect. For example, at the maximum pressure change condition, when the equivalence ratio is one, the detonation pressure ratio is about 15, however, the shock pressure ratio is nearly 30.

Furthermore, in addition to the thermodynamic pressure, there is a dynamic "momentum flux" pressure associated with the directed kinetic energy of the product stream. This momentum flux augments the effect which a stopped product stream causes.

H.5 Detonation Velocity.

As has been mentioned, the thermal energy release is shared between the sensible heat, represented by temperature, and the directed kinetic energy. The directed kinetic energy is a function of the velocity.

The detonation velocity as mentioned in Section B, is the measure of the detonation wave propagation into the unreacted medium. The wave velocity is shown in Figure H.4 for a range of equivalence ratios of hydrogen sulphide and other fuels in air. As for the other products properties, velocity increases with equivalence ratio to a maximum of about 1650 m/s when the equivalence ratio is 1. This is at the low end of the Chapman-Jouguet velocity range of about 1600 to 2000 m/s for the fuels considered. The round form of the curve occurs since (a) the velocity is proportional to the square root of the directed kinetic energy and (b) the total thermal energy release is shared between the thermodynamic and dynamic modes.

Following the wave, the medium has acquired a velocity due to the thermal energy delivered to the products. Like the other overall effects, the post detonation velocity has a maximum at the unity equivalence ratio reactant composition. The velocity maximum is about 920 m/s.

H.6 Mach Number.

The variation of Mach number with hydrogen sulphide concentration increases with equivalence ratio to a maximum of about 4.8 when the equivalence ratio is unity. It is noted here that Mach number is directly proportional to system velocity, but inversely proportional to the square root of system temperature. The Mach number of the products following the detonation is unity.

H.7 Remarks on Comparison with Other Fuels.

In general, hydrogen sulphide exhibits overall detonation properties that are of the same order as hydrogen and common hydrocarbon fuels, in air. The hydrogen sulphide, however, falls at the low end of the range for (a) combustion energy release,

(b) temperature increase, (c) pressure ratio, and (d) detonation velocity. The behaviour does not appear to be unusual as compared to other fuels.

I. Physical Detonation Properties.

In this section, the detonation wave itself is discussed. The discussion focusses on the dynamic properties of the wave and the wave structure. These dynamic properties are (1) cell size, (2) critical tube diameter,and (3) critical initiation energy. The relationships between these properties that have been proposed elsewhere are outlined with reference to measurements made on selected hydrocarbons and hydrogen.

I.1 Cell Size.

When a soot-coated mylar, aluminum, steel or otherwise suitable sheet or plate is placed in a tube filled with a detonable gas and detonation of the gas is achieved, a cellular pattern is "written" on the plate (Figure I.1).[62] These cells are complex patterns that are related to the moving axial and transverse shocks within the propagating front. Nevertheless, as shown in Figure I.2, the cells may be quantified by defining L_c the cell length in the direction of propagation of the wave, and s the transverse width of the cell.[63]

Although cell patterns are complex and distinguishing individual cells may be subjective, work by Lee,[62] Knystautas,[64] Moen,[65] and Murray[66] demonstrate that cell structure is not only related to the dynamics of wave propagation but also to the mechanisms that cause detonation. As a result, the cell size s is used to characterize detonation mechanisms. The cell sizes for several hydrocarbons in air at stoichiometric conditions are shown in Table I.1. The cell size for ethane (C_2H_6) and propane (C_3H_8) at 54-62 mm and 69 mm, respectively, are about equal. The cell size for acetylene (C_2H_2) is much smaller at about 9.8 mm, and that for methane (CH_4) of 280 mm is much larger than the chain alkanes.

A survey for the determination of cell size at atmospheric pressure for detonable fuel solutions in air has been carried out by Knystautas.[64] The measurements show how cell size s varies with equivalence ratio ϕ. As Figure I.3 shows, the variation is typically convex-downward with the minimum cell size occuring at stoichiometric conditions ($\phi = 1$). Lee states that the most sensitive condition is at stoichiometric and "the minimum cell size usually occurs at the most detonable condition of ϕ=1."

It is pointed out here that despite the value of cell size for characterization of detonation, there is no analytical methodology for predicting cell size based on mixture thermochemistry. Furthermore, the determination of cell size is sufficiently subjective that statistical methods have to be used to compute "average" cell sizes written on large foils. Nevertheless, cell size is of sufficient importance and is related to detonability that its measurement is planned for investigation of hydrogen sulphide behaviour.

I.2. Critical Tube Diameter.

The second dynamic parameter is critical tube diameter d_c. The critical tube diameter, like the detonation cell size, remains an empirical notion. Experimentally, a planar detonation wave may propagate through a detonable gas contained in a right circular cross-section tube (Figure I.4). The tube opens at the upstream end into an unconfined solution of the same detonable material. The planar wave from the tube is transformed into a spherical wave in the unconfined zone if the tube diameter exceeds a critical value d_c. If $d<d_c$, the initial planar wave decouples from the shock and a planar deflagration results.

It was found by Mitranov and Soloukin [67] that the critical tube diameter in a circular tube is thirteen times the detonation cell size: $d_c = 13s$.

The dependence of critical tube diameter on equivalence ratio,

$$d_c = d_c(\phi) \tag{I.1}$$

is illustrated in Figure I.5. The solid curves are the cell size data from Figure I.3 multiplied by 13. It is noted here that despite the apparent acceptance of $d_c = 13s$, the acceptance is not universal.

I.3. Critical Initiation Energy.

(The following discussion is extracted from Lee[62], with minor changes and deletions.)

Experimentally, it is found that for a given mixture at given initial conditions, a definite quantity of energy must be used to initiate a detonation that will become a combustion wave propagating at the Chapman-Jouguet detonation velocity. If the ignition energy is insufficient, then the reaction zone decouples from the shock and a deflagration ensues.

According to Lee,[62] in descending order of sensitivity fall C_2H_2, H_2, C_2H_4, and the alkanes C_3H_8, C_2H_6 and C_4H_{10}.

In estimating the detonation energy, it is first recognized that the critical tube diameter is a minimum at unity equivalence ratio. Next, it is acknowledged that the unity equivalence ratio is recognized as a most sensitive condition for fuel solutions in air.[68]

Although there are a number of experimental parameters that may influence the initiation energy, so long as the time for energy deposition is short compared to a characteristic time of the blast wave. The characteristic time for the blast wave is

$$t_c = R_c/c_o \tag{I.2}$$

where the explosion length R_c is

$$R_c = (E_o/p_o)^{1/3} \tag{I.3}$$

There are various theories for critical energy.[69] A relationship between cell size and critical energy was obtained by Matsui and Lee using the critical tube diameter and the concept of work done.[70] In this case,

$$E_c = \pi\ p_1\ u_1\ d_c^3 / [24\ c_1] \tag{I.4}$$

where p_1, u_1, and c_1 are the pressure, particle velocity and acoustic velocity at the Chapman-Jouguet point. Using the Rankine-Hugoniot relations at the Chapman-Jouguet point and the 13s correlation for d_c, Equation (I.4) can be written as

$$E_c = 2197\ \pi\ r_o\ D^2\ s^3 / [24\ k(k+1)] \tag{I.5}$$

Other models have been developed and give similar relationships with different values for the numerical constants. For all these theories, the key relationship is that the critical energy is proportional to the cube of the cell size (s) and the cube of the critical tube diameter (d_c).

The agreement between theory and practice[71] have been reported as "reasonably good."[62]

I.4. Remarks.

The cell size s has been demonstrated to be characteristic of the dynamics of the detonation process. Furthermore, the link between the cell size and the critical tube diameter d_c is expressed as $s = 13\ d_c$.

For later comparison with hydrogen sulphide data to be measured, the cell size (s), critical tube diameter (d_c), and characteristic blast scale (R_c) are shown in Table I.2 for five hydrocarbons and hydrogen.

The limitations of the use of the dynamic properties lie in the lack of a comprehensive theory for the prediction of cell size and critical tube diameter; and the subjective nature of the determination of cell size.

In any event, the usefulness of these dynamic properties make them valuable operationally in characterising detonable gas mixtures and solutions. Indeed, it is for this reason that large-scale measurements of the critical tube diameter for hydrogen sulphide mixtures in air are planned.

J. Blast Wave Calculations.

According to Baker, et al.[34] "The general properties of an explosion which govern the strength, duration and other characteristics of the resulting blast wave must ... include at least its total energy, E; its energy density E/V; and the rate of energy release, i.e., its power. ... It has been found that the blast wave can be correlated by a single parameter, the total energy source, irrespective of the energy density or the power of the source." This energy source is compared to the mass of TNT that has the equivalent energy, where the energy of TNT is 4520 kJ/kg.[34]

Now, blasts effect people, animals, plants, the environment and structures; and since "the blast wave can be correlated by a single parameter;" the effects should be related to quantities that are straightforward to measure and predict. Quantities that are straightforward to measure are the shock front arrival times and the pressure vs time history of the blast at a specified location.

J.1 Blast Wave Characterization.

Following Baker et al.,[34] and Held[72] the properties defined and measured for the characterization of a blast wave are those of the undisturbed or side-on wave as it propagates through the environment, viz., the air. These properties are defined below and are illustrated in Figure J.1.

J.1.1 Direct Blast Characteristics.

The direct characteristics of the blast are:

(a) p_o - ambient, atmospheric pressure;

(b) p^+ - positive, overpressure, extremum;

(c) p^+-p_o - differential overpressure;

(d) p^- - negative, underpressure, extremum;

(e) p^--p_o - differential underpressure;

(f) t_a - blast arrival time;

(g) t^+ - overpressure decay time; and

(h) t^- - underpressure relaxation time.

As the illustration (Figure J.1) shows, the pressure is ambient until t_a, when the blast, shock front arrives. The local pressure then rises rapidly reaching p^+ for maximum absolute pressure value of $p^+ + p_o$. The positive overpressure decays to ambient over a time t^+, that is $t_a + t^+$ from initiation; to cross over the ambient pressure level: This period is called the positive phase. Next, an underpressure situation ensues, during which a partial vacuum is created. The underpressure remains for a time t^- for relaxation to the ambient pressure level. The relaxation is complete at $t_a + t^+ + t^-$ from initiation. The negative pressure period is called the suction or negative phase.

J.1.2 Blast Impulse Characteristics.

The total effect of the overpressure and suction (negative) phases are expressed by the pressure differential integrals between ambient and the positive and negative portions of the blast pressure time history.

The positive integral, expressed as the differential pressure from t_a to $t_a + t^+$ is the positive impulse I^+:

$$I^+ = \int_{t_a}^{t_a + t^+} [p(t) - p_o]\, dt \qquad (J.1)$$

The negative integral, expressed at the differential pressure from $t_a + t^+$ to $t_a + t^+ + t^-$ is the negative impulse I^-:

$$I^+ = \int_{t_a + t^+}^{t_a + t^+ + t^-} [p(t) - p_o]\, dt \qquad (J.2)$$

J.1.3 Blast Regions.

There are three regions of interest in blast effects due to explosions of gaseous fuel air mixtures. They are (a) internal, (b) near field, and (c) far field:

(a) Internal -	within the gaseous, burned fuel-air mixture;
(b) Near Field -	outside the gaseous, burned fuel-air mixture, but unburned and near to it, where the source geometry must be acknowledged; and
(c) Far Field -	far enough from the source that the entire fuel-air source region may be treated as a point impulse.

In the first region, internal, the blast effects on the unreacted fuel-air mixture are considered.

The near field region occurs close to the origin of the explosion. In the near field, the positive pressures are large compared to the suction phase pressure. Furthermore, in the case of a gaseous fuel-air explosive such as hydrogen sulphide, the near field may indeed be considered the region of unreacted affected by the blast of detonated material.

The far field is the region sufficiently distant from the source of the blast that the origin can be treated as a point.

The regions are distinguished from one another. However, because of the complex physical interactions between the detonation source and the environment actual boundaries do not exist and distinctions are not clear.

J.1.4 Detonation Effect Scaling.

The detonation and its effects are scaled by several parameters:

(a) $R_o = [\ E\ /\ p_o\ ]^{1/3}$ - the characteristic explosion length, where E is the total energy available from the reactant material and p_o is ambient pressure. This characteristic length represents a distance over which the energy release in combustion is equal to the work required to move atmospheric air the same distance;

(b) $\triangle p/p_o$ - the blast differential pressure ratio, where $\triangle p$ is the blast differential pressure;

(c) $\triangle p_s/p_o$ - the blast differential overpressure ratio, where $\triangle p_s = p(t)-p_o$ during the overpressure period from t_a to t_a+t^+ and p_o is again ambient pressure; and

(d) $I^+c_o/[p_oV^{1/3}]$ - the blast dimensionless positive impulse, where I^+ is defined in Equation (J.1), c_o is the local ambient speed of sound, V is the volume of the cloud of gaseous detonable reactants, and p_o is the ambient pressure.

These scaling factors are used for the characterization of the blast effects of hydrogen sulphide in air.

J.2 Hydrogen Sulphide Blast Wave Parameters.

The blast wave effects for hydrogen sulphide detonation in air have been calculated. The calculations are based on a hemispherical bag of hydrogen sulphide in air of 10 metres radius

(V = 2094 m^3). For the five equivalence ratios used for the detonation calculations in Section C (0.5, 0.75, 1.0, 2.0, and 4.0), the mass of the mixture, the calculated unit enthalpy the total energy in the bag (E) and the detonation explosion characteristic length (R_0) are shown in Table J.1.

The stoichiometric hydrogen sulphide in air condition has a TNT equivalent of about 43 per cent and a characteristic length of 36.6 metres. For comparison, the same mass of TNT has a characteristic length of 48.3 metres. Also shown in Table J.1, for comparison, are the results of the ideal calculation, where the characteristic scale length is 38.3 metres and the TNT equivalent is about 51 per cent.

J.2.1 Shock Wave Overpressure.

The integrated positive pressure, the positive impulse, is scaled as shown above; in Figure J.2. The illustration shows the decrease of the overpressure with distance scaled by the cube root of bag radius. The results lie in a narrow band in the region between the detonability limits of hydrogen sulphide. This shows that a single curve may be used for blast effect calculations.

The results are similar to those for the ethylene - air mixture as shown in Figure J.3; where blast effects have been shown for the mixtures at grade and elevated above it.

J.2.2 Positive Impulse.

The positive impulse I^+ has been calculated and scaled for hydrogen sulphide combustion in Figure J.4. The results fall between the detonability bands and compare with results for ethylene in air (Figure J.5).

J.3 Hydrogen Sulphide Blast Wave Calculations.

Blast wave calculations have been performed at DRES using a finite difference approach.[73] The method has previously been used for the calculation of blast wave effects for fuel - air explosives.[74] They are discussed in an associated report by Dr. P. Thibault.

K. Concluding Remarks.

Included in this report are discussions of (a) hydrogen sulphide chemistry, combustion and flame propagation; (b) detonation, and the principles used in determining the change of fluid properties due to detonation (Chapman-Jouguet calculations); (c) computation of Chapman-Jouguet properties; (d) physical properties of detonation including cell size; and (e) and general principles of blast.

Calculations performed show that hydrogen sulphide - air mixtures have Chapman-Jouguet detonation properties that are the same order of magnitude as hydrogen and typical hydrocarbon fuels in air. These results can be coupled with experimental determination of the hydrogen sulphide - air cell size in an accompanying report.

From the results it can be concluded that detonation of hydrogen sulphide - air mixtures can be compared to those of butane, but are less detonable.

The next reporting period focusses on flame acceleration and transition to detonation (particularly due to obstacles) and spill tests.

L. Acknowledgements.

The Investigators have been assisted by and want to thank Dr. Paul A. Thibault, who has contributed to this project by preparing the blast modelling computer code and has performed the blast wave calculations. Dr. Thibault is currently engaged in other contract work at DRES.

M. References.

1. Subcommittee on Hydrogen Sulfide, Committee on Medical and Biologic Effects of Environmental Pollutants, Division of Medical Sciences, Assembly of Life Sciences, National Research Council, Hydrogen Sulfide, University Park Press, Baltimore, Maryland, 1979.

2. The Canadian Association of Oilwell Drilling Contractors, Hydrogen Sulphide Training - Awareness-Alert, offered 26 - 28 March 1984 at DRES by B. Emeneau (AECL - Glace Bay).

3. Kirk-Othmer Encyclopedia of Chemical Technology, Third Edition, Volume 22, John Wiley and Sons, New York, New York, 1978, pp. 114-122.

4. Coward, H.F., Jones, G.W., "Limits of Flammability of Gases and Vapors," United States Bureau of Mines, Bulletin 503, United States Government printing Office, Washington, D.C., 1952.

5. Jones, G.W., Yant, W.P., Berger, L.B., "Explosibility of Hydrogen Sulphide," Industrial Engineering Chemistry, Volume 16, 1924, pp. 353-355.

6. White, A.G., "Limits for the Propagation of Flame in Inflammable Gas-Air Mixtures. I. Mixtures of Air and One Gas at Ordinary Temperature and Pressure," Journal of the Chemical Society, Volume 125, 1924, pp. 2387-2396.

7. Popov, P.V., Bezzub, K.E., "The Combustibility of Hydrogen Sulphide and Its Mixtures with Carbon Dioxide," Transactions of the Scientific Institute of Fertilizers and Insectofungicides, U.S.S.R., Number 135, 1939, pp.92-98.

8. White, A.G., "The Burning of Carbon Disulphide near the Limit for the Propagation of Flame with Some Remarks on the Ignition Point of Sulphur," Journal of the Chemical Society, 1927, pp. 793-802.

9. Popov, P.V., Bezzub, K.E., "The Combustibility of Hydrogen Sulphide and Its Mixtures with Carbon Dioxide," Transactions of the Scientific Institute of Fertilizers and Insectofungicides, U.S.S.R., Number 135, 1939, pp.92-98.

10. van der Wal, M.J., "Explosive and Non-Explosive Reactions between Nitrogen Oxides and Flammable Gases," Rec. travaux chimiques Bas Pays, Volume 53, 1934, pp. 97-117.

11. Katz, J.J., "Deuterium and Tritium," in Encyclopedia of Chemical Technology, edited by Kirk, R.E.,, Othmer, D.F., Third Edition, Volume 7, Wiley-Interscience, New York, New York, 1963, pp. 539-564.

12. "Probabilistic Consequence Assessment of Hydrogen Sulphide Releases from a Heavy Water Plant - Scope Determination," prepared by Monserco Ltd, Mississauga, Ontario, Atomic Energy Control Board Report INFO-0102-1, Ottawa, Ontario, 20 January 1983.

13. Daniels,F., Alberty, R.A., Physical Chemistry, Second Edition, John Wiley & Sons Inc, New York, 1961.

14. Moelwyn-Hughes, E.A., Physical Chemistry, Second Revised Edition, Pergamon Press, Oxford, U.K., 1961.

15. Glassman, I., Combustion, Academic Press, New York, 1977.

16. Strehlow, R.A., Combustion Fundamentals, McGraw-Hill Book Company, New York, New York, 1984.

17. Sulmistras, A., Moen, I.O., Saber, A.J., "Detonations in Hydrogen Sulphide-Air Clouds, PCN No. 27C50, Suffield Memorandum 1140 (Unclassified), Defence Research Establishment Suffield, Ralston, Alberta, October 1984.

18. Saber, A.J., "Combustion Terminology," Engineering Digest, Volume 30, Number 8, September 1984, pp. 19-25.

19. Williams, F.A., Combustion Theory, Addison-Wesley Publishing Company, Reading, Massachusetts, 1965.

20. Moen, I.O., Donato, M., Knystautas, R., Lee, J.H., "Flame Acceleration Due to Turbulence Produced by Obstacles," Combustion and Flame, Volume 39, pp. 21-32, 1980.

21. John, James E.A., Gas Dynamics, Allyn and Bacon, Inc., Boston, Massachusetts, 1969.

22. Shapiro, Ascher A., The Dynamics and Thermodynamics of Compressible Fluid Flow, Volume I, The Ronald Press Company, New York, New York, 1959.

23. Moen, I.O., Donato, M., Knystautas, R., Lee, J.H., Wagner, H.Gg., "Turbulent Flame Propagation and Acceleration in the Presence of Obstacles," Gasdynamics and Explosions, edited by Bowen J.Ray, Manson, N., Oppenheim Antoni K., Soloukin, R.I., Volume 75 of Progress in Astronautics and Aeronautics, American Institute of Aeronautics and Astronautics, pp. 33-47, New York, New York, 1981.

24. Chan, C., Moen, I.O., Lee, J.H.S., "Influence of Confinement on Flame Acceleration Due to Repeated Obstacles," Combustion and Flame, Volume 49, January 1983, pp. 27-39.

25. Hjertager, B.H., Fuhre, K., Parker, S.J., Bakke, J.R., "Flame Acceleration of Propane-Air in a Large-Scale Obstructed Tube," prepared for presentation at "9th International Colloquium on Dynamics of Explosions and Reactive Systems," Poitiers, France, 3-8 July 1983.

26. Chan, C.K., Lee, J.H., Knystautas, R., "Turbulent Flame Propagation in Obstacle-Filled Tubes," paper submitted for presentation to the 20th Symposium (International) on Combustion, Ann Arbor, Michigan, 12-17 August 1984,

27. Lee, J.H.S., Knystautas, R., Freiman, A., "High Speed Turbulent Deflagrations and Transition to Detonation in H_2-Air Mixtures," Combustion and Flame, Volume 56, pp. 227-239, 1984.

28. Hasson, A., Avinor, M., Burcat, A., "transition from Deflagration to Detonation, Spark Ignition, and Detonation Characteristics of Ethylene-Oxygen Mixtures in a Tube," Combustion and Flame, Volume 49, pp. 13-26, 1983.

29. Lee, J.H.S., Moen, I.O., "The Mechanism of Transition from Deflagration to Detonation in Vapor Cloud Explosions," Progress in Energy and Combustion Science, Volume 6, pp. 359-389, 1980.

30. Urtiew, P.A., Oppenheim, A.K., "Experimental Observations of the Transition to Detonation in an Explosive Gas," Proceedings of the Royal Society A, Volume 295, pp. 13-25, 1966.

31. Deathrage, Bruce H., "auditory and Other Sensory Forms of Information Processing," in Human Engineering Guide to Equipment Design, Revised Edition, edited by Van Cott, Harold P., Kincade, Robert G., American Institutes for Research, Superintendent of Documents, Washington, DC, 1972.

32. Chan, C., Lee, J.H.S., Moen, I.O., Thibault, P., "Turbulent Flame Acceleration and Pressure Development in Tubes," in *Proceedings of the First Specialist Meeting (International) of the Combustion Institute*, Bordeaux, France, 20-24 July 1981, pp. 479-484.

33. Moen, I.O., Lee, J.H.S., "Pressure Development Due to Turbulent Flame Propagation in Large-Scale Methane-Air Explosions," *Combustion and Flame*, Volume 47, pp. 31-52, 1982.

34. Baker, W.E., Cox, P.A., Westine, P.S., Kulesz, J.J., Strehlow, R.A., *Explosion Hazards and Evaluation*, Fundamental Studies in Engineering Series, Volume 5, Elsevier Scientific Publishing Company, Amsterdam, Holland, 1983, pg. 109.

35. Davenport, J.A., "A Survey of Vapor Cloud Incidents," *Loss Prevention*, Volume 11, technical manual prepared by the editors of *Chemical Engineering Progress*, September 1977, pp. 39-49.

36. Marshall, V.C., "Unconfined-Vapor-Cloud Explosions," *Chemical Engineering*, June 1982.

37. Dixon, H.B., Coward, H.F., *Journal of the Chemical Society*, Volume 95, pp. 514ff., 1909.

38. Flockenhaus, von C., "Rates of Flame Propagation of Hydrogen Sulphide/Air Mixtures," *Gas Warme International*, Volume 18, Number 4, April 1969.

39. Vesselman, S.G., Nikolayev, N.N., "Conditions for Minimum Nitrogen Oxides Formation During the Burning of Hydrogen Sulphide," *Coke and Chemistry U.S.S.R.*, Number 11, 1970, pp. 42-45.

40. Merryman, E.L., Levy, A., "Disulphur and the Lower Oxides of Sulphur in Hydrogen Sulphide Flames," *The Journal of Physical Chemistry*, Volume 76, Number 14, 1972, pp. 1925-1931.

41. Wendt, J.O.L., Ekmann, J.M., "Effect of Fuel Sulfur Species on Nitrogen Oxide Emissions from Premixed Flames," *Combustion and Flame*, Volume 25, pp. 355-360, 1975.

42. Kincler, J., "The Influence of Water Sprays on H_2S-Air Flames," M.Eng. Thesis, McGill University, Montreal, Quebec 1980.

43. Remy, H., Treatise on Inorganic Chemistry, Elsevier Publishing Company, Amsterdam, 1956.

44. Sax, N.Irving., Dangerous Properties of Industrial Materials, Van Nostrand Reinhold Company, New York, New York, 1968.

45. Jocelyn, P.C., Biochemistry of the SH Group, Academic Press Inc, New York, New York, 1972.

46. "Hydrogen Sulfide in the Atmospheric Environment: Scientific Criteria for Assessing Its Effects on Environmental Quality," Panel on Hydrogen Sulfide, Subcommittee on Air, Associate Committee on Scientific Criteria for Environmental Quality, National research Council of Canada, Publication Number NRCC 18467, Ottawa, Ontario, K1A 0R6.

47. Mahan, B.H., University Chemistry, Addison-Wesley Publishing Company, Reading, Massachusetts, 1965.

48. Munro, L.A., Chemistry in Engineering, Prentice-Hall Inc, Englewood Cliffs, New Jersey, 1964.

49. Davydov, A.S., Quantum Mechanics, Translated from the Russian by I.S. Schensted, NEO Press, Ann Arbor, Michigan, 1966.

50. Wallace, J.M., Hobbs, P.V., Atmospheric Science, An Introductory Survey, Academic Press, Inc., New York, New York, 1977.

51. Record, F.A., Bubenick, D.U., Kindya, R.J., Acid Rain Information Book, Noyes Data Corporation, Park Ridge, New Jersey, 1982.

52. Chemical Engineer's Handbook, Fifth Edition, Edited by Perry, Robert H., Chilton, Cecil H., McGraw-Hill Book Company, New York, New York, 1973, "Fuels, Chapter 9," page 9.4.

53. 1980 Annual Book of ASTM Standards, Part 26, "Gaseous Fuels; Coal and Coke; Atmospheric Analysis," ASTM Designation D3177-75, "Standard Test Methods for Total Sulfur in the Analysis Sample of Coal and Coke," American Society for Testing and Materials, Philadelphia, Pennsylvania, 1980, pp. 400-406.

54. Thompson, D., Brown, T.D., Beer, J.M., "NO_x Formation in Combustion," Combustion and Flame, Volume 19, 1972, pp. 69-79.

55. Chamberlin, D.S., Clark, D.R., "Industrial Engineering Chemistry," Volume 20, pp. 1016ff., 1928.

56. Gibbs, G.J., Calcote, H.F., "Journal of Chemical Engineering," Volume 4, pp. 226ff., 1959.

57. Saber, A.J., "MECH N619 - Combustion," class notes.

58. Perry, R.H., Chilton, C.K., Chemical Engineer's Handbook, Fifth Edition, McGraw-Hill Publishing Company, New York, New York, 1973, pg. 3-134.

59. CRC Handbook of Chemistry and Physics, Edited by Weast, W.C., Astle, M.J., CRC press Inc, Boca Raton, Florida, 1980, d67-d79.

60. Daniels, F., Alberty, R.A., Physical Chemistry, John Wiley and Sons, New York, 1961, pg. 103.

61. Vincenti, W.G., Kruger, Jr., C.H., Introduction to Physical Gas Dynamics, John Wiley and Sons, New York, 1965, pp. 70-75.

62. Lee, J.H.S., "Dynamic Parameters of Gaseous Detonations," undated report.

63. Fickett, W., Davis, W.C., Detonation, University of California Press, Berkeley, California, 1979.

64. Knystautas, R., Guirao, C., Lee, J.H.S., Sulmistras, A., "...paper..." submitted to 9th International Colloquium on Dynamics of Explosions and Reactive Systems, Poitiers, France, July 1983.

65. Moen, I.O., Thibault, P., Funk, J., Ward, S., and Rude, G.M., "Detonation Length Scales for Fuel-Air Explosives," paper for 9th International Colloquium on Dynamics of Explosions and Reactive Systems, Poitiers, France, July 1983.

66. Murray, S.B., Lee, J.H.S., "The Influence of Yielding Confinement on Large-Scale Ethylene-Air Detonations," paper for 9th International Colloquium on Dynamics of Explosions and Reactive Systems, Poitiers, France, July 1983.

67. Mitronov, V.V., Soloukin, R.I., Soviet Physics - Doklady, Volume 9, Number 12, 1965, pg. 1085.

68. Matsui, H., Lee, J.H.S., "On the Measure of the Relative Detonation Hazards of Gaseous Fuel-Oxygen and Air Mixtures," 17th Symposium (International) on Combustion, The Combustion Institute, 1978, pp. 1269-1980.

69. Lee, J.H.S., Annual Reviews of Physics and Chemistry, Volume 28, 1977, pp. 75-104.

70. Lee, J.H.S., Matsui, H., Combustion and Flame, Volume 28, pp. 61-66.

71. Lee, J.H.S., Knystautas, R., Guirao, C.M., "The Link between Cell Size, Critical Tube Diameter, Initiation Energy and Detonability Limits," in Fuel-Air Explosions Proceedings, Edited by J.H.S. Lee and C.M. Guirao, University of Waterloo Press, Waterloo, Ontario, 1982.

72. Held, M., "TNT - Equivalent," Propellants, Explosives, Pyrotechnics, Volume 8, 1983, pp. 158-167.

73. Sod, G.A., "A Survey of Several Finite Difference Methods for Systems of Nonlinear Hyperbolic Conservation Laws," Journal of Computational Physics, Volume 27, 1978, pp. 1 - 31.

74. Moen, I.O., Thibault, P.A., Funk, J.W., "Blast Waves from Non-Spherical Fuel-Air Explosions," Defence Research Establishment Suffield, Research Note Number 278 "to be published in the Proceedings of the 8th International Symposium on Military Application of Blast Simulation, Spiez, Switzerland, 20-24 June 1983."

75. CRC Handbook of Chemistry and Physics, Edited by Weast, W.C., Astle, M.J., CRC press Inc, Boca Raton, Florida, 1980, pp. F217-F218.

76. Handbook of Chemistry and Physics, 60th Edition, West, R.C., and Astle, M.J., eds., CRC Press, Inc., Boca Raton, Florida, 33431, 1980, pp. F-211.

77. Record, F.A., Bubenick, D.U., Kindya, R.J., Acid Rain Information Book, Noyes Data Corporation, Park Ridge, New Jersey, 1982.

78. Stull, D.R., et al., "JANAF Thermochemical Tables," United States Department of Commerce, National Bureau of Standards, Report Number NTIS PB168370, August 1965.

79. Karapet'yants, M.Kh., Karapet'yants, M.L., Thermodynamic Constants of Inorganic and Organic Compounds, translated by J. Schworach, Ann Arbor - Humphrey Scientific Publications, London, 1970.

80. Chase, M.W., et al., "JANAF Thermochemical Tables," 1974 supplement, Journal of Physical and Chemical Reference Data, Volume 3, Number 2, American Chemical Society, National Bureau of Standards, Washington, D.C., 1974.

81. Choa, J., et al., "JANAF Thermochemical Tables," First Addendum, United States Department of Commerce, National Bureau of Standards, Report Number NTIS PB168370-1, August 1966.

82. Perry, R.H., Chilton, C.K., Chemical Engineer's Handbook, Fifth Edition, McGraw-Hill Publishing Company, New York, New York, 1973, pg. 3-134.

83. Gordon, S., McBride, B.J., "Computer Program for Calculation of Complex Chemical Equilibrium Compositions, Rocket Performance, Incident and Reflected Shocks, and Chapman-Jouguet Detonations," National Aeronautics and Space Administration Report Number SP-273, Washington, DC, 1971.

84. Moen, I.O., Thibault, P.A., Funk, J.W., Ward, S.A., Rude, G.M., "Detonation Length Scales for Fuel - Air Explosives," Defence Research Establishment Suffield, Ralston, Alberta, Research Note Number 271, submitted to the 9th International Colloquium on Dynamics of Explosions and Reactive Systems, February 1982.

N. Tables.

TABLE B.1

HYDROGEN SULPHIDE INVENTORY AT BRUCE HEAVY WATER PLANT

(data from: Reference [12])

Quantity (Tonnes)	Location	Physical State
2160	Enriching units(4);	Approximately 90% gaseous at 2080 kPa (about 21 atmospheres)
	including interconnecting pipes and associated equipment	
1130	H_2S storage and unloading area	Approximately 51% at 32C and 39% at 128C
100	H_2S recovery area	Primarily gas
<1	Interconnecting pipes	Primarily gas at 2350 kPa (about 23 atm)

TABLE B.2

ESTIMATES OF FLAMMABILITY LIMITS OF SOME FUEL-AIR MIXTURES [4,16]

Fuel		Flammability Limits Per Cent by Volume
Methane	CH_4	5.3 - 15.0
Acetylene	C_2H_2	2.5 - 81.0
Ethylene	C_2H_4	3.1 - 32.0
Propane	C_3H_8	2.2 - 9.5
Pentane	C_5H_{12}	1.5 - 7.8
Hydrogen	H_2	4.0 - 75.0
Hydrogen Sulphide	H_2S	4.3 - 45.0

TABLE B.3

ESTIMATES OF ENTHALPY OF REACTION OF SOME STOICHIOMETRIC FUEL-AIR MIXTURES [17]

		Per Cent of Fuel by Volume	Enthalpy (MJ/kg of Mixture)
Acetylene	C_2H_2	7.75	2.44
Hydrogen	H_2	29.6	2.82
Ethylene	C_2H_4	6.54	2.35
Ethane	C_2H_6	5.66	2.31
Propylene	C_3H_6	4.46	2.31
Propane	C_3H_8	4.03	2.29
n-Butane	C_4H_{10}	3.13	2.30
Methane	CH_4	9.48	2.31
Hexane	C_6H_{14}	Aerosol	2.28
Hydrogen Sulphide	H_2S	12.3	1.96

TABLE D.1

THE ULTIMATE ANALYSIS OF HYDROGEN SULPHIDE (H_2S)

1. Basis: kilogram-mole.

2. Analysis of hydrogen sulphide (H_2S)

Element	Atomic Weight	x	Number of Atoms	=	Kilograms per Kgmole
Sulphur (S)	32.064		1		32.064
Hydrogen (H)	1.008		2		2.016
TOTAL					34.080

3. Ultimate Analysis:

Element	Kilograms per Kgmole	Kilogram Ratio		Mass Ratio
Sulphur (S)	32.064	32.064/ 34.080	=	0.94085
Hydrogen (H)	2.016	2.016/ 34.080	=	0.05915
SUM				1.00000

TABLE D.2

TOXICITY TABLE FOR HYDROGEN SULPHIDE

1 ppm	=	0.0001%	(1/10,000 of 1%)	Can Smell
10 ppm	=	0.001%	(1/1000 of 1%)	Allowable for 8 Hours Exposure **THRESHOLD LIMIT VALUE**

If the level is above 10 ppm,
then protective equipment MUST be worn

100 ppm	=	0.01%	(1/100 of 1%)	Kills Smell in 3 to 15 Minutes Irritation of Eyes and Throat
200 ppm	=	0.02%	(2/100 of 1%)	Kills Smell Rapidly Burns Eyes and Throat
500 ppm	=	0.05%	(5/100 of 1%)	Loses Sense of Reasoning and Balance Stoppage of Breathing in 2 to 15 Minutes Victim Needs Artificial Respiration
700 ppm	=	0.07%	(7/100 of 1%)	Unconscious Quickly Breathing Will Stop and Death Results Unless Rescued Immediately
1000 ppm	=	0.1%	(10/100 of 1%)	Unconscious at Once Brain Damage Unless Rescued Promptly

1% = 10,000 ppm

ppm — Parts of Gas per Million Parts of Air by Volume

TABLE D.3

PHYSICAL AND THERMODYNAMIC PROPERTIES OF H_2S[1,3]

Molecular Weight	34.08
Melting Point (°C)	-85.60
Boiling Point (°C)	-60.75
Enthalpy of Fusion (kJ/gmole)	2.375
Enthalpy of Vapourization (kJ/gmole)	18.67
Density at -60°C (kg/m^3)	993.0
Specific Gravity (air = 1)	1.19
Critical Temperature (°C)	100.4
Critical Pressure (kPa)	9020
Critical Density (kg/m^3)	368.1
Gibbs Free Energy of Formation (kJ/gmole at 25°C)	-33,600
Enthalpy of Formation (kJ/gmole at 25°C)	-20,600
Entropy (kJ/kgmole at 25°C)	205.7
Specific Heat at Constant Pressure (kJ/kgmole-K at 25°C)	34.2
Autoignition Temperature in Air (°C)	about 260
Explosive Range in Air (volume %, at 25°C)	
Lower Limit	4.6[4]
Upper Limit	46
Vapour Pressure (kPa)	
-60°C	102.7
-40°C	256.6
-20°C	546.6
0°C	1033
10°C	1428
20°C	1780
30°C	2391
40°C	2859
50°C	3697
60°C	4347
70°C	5379
80°C	6483
90°C	7354
100°C	8985
Solubility in Water (kg/100kg Solution at 101.3 kPa Total Pressure)	
0°C	0.710
10°C	0.530
20°C	0.398

TABLE D.4

HYDROGEN BOND LENGTHS WITH SULPHUR AND OXYGEN[51,52]

Parameter	Bond	X = Sulphur	X = Oxygen
Bond Length (Å)	X - H	1.33	0.96
	X - X	1.8 - 2.1	1.48 (in H_2O_2) 1.227 (in O_2^{+}) 1.26 (in O_2^{-}) 1.49 (in $O_2^{=}$) 1.208 (in O_2)
	X - C	1.82	1.43
Dissociation Energy (kcal/gmole)	X - H	89	100
	X - X	73	40 - 45
	X - C	73	77
Electronegativity (Lithium = 1)	X	2.6	3.5

TABLE D.5

SOME BOND ANGLES IN SULPHUR COMPOUNDS [45]

Compound	Bond	Bond Angle
Hydrogen Sulphide	H - S - H	92°20'
Aliphatic Thiol	H - S - C	100°
Aliphatic Sulphide	C - S - C	105°
Aromatic Thiol	H - S - C	109°
Disulphide	S - S - C	103° to 107°
Trisulphide	S - S - S	105° approx.

TABLE E.1

COMPOSITION OF THE ATMOSPHERE

(a) CONSTITUTION OF DRY ATMOSPHERIC AIR BY VOLUME[76]

Chemical Constituent	Content (per cent)	Content (ppm)
N_2	78.084±0.004	
O_2	20.946±0.002	
CO_2	0.033±0.001	
A	0.934±0.001	
Ne		18.18±0.04
He		5.24±0.004
Kr		I.14±0.01
Xe		0.087±0.001
H_2		0.5
CH_4		2
N_2O		0.5±0.1

(b) MOLAR CONSTITUTION OF DRY ATMOSPHERIC AIR USED FOR CALCULATIONS

Chemical Constituent	Molar Content (per cent)
N_2	78.087
O_2	20.946
CO_2	0.033
A	0.934

TABLE E.2

THE GRAVIMETRIC ANALYSIS OF DRY AIR

1. Basis: 100 kilograms.
2. Set up an analysis table:

	Constituents				Totals
	N_2	O_2	A	CO_2	
Volume Per Cent	78.087	20.946	0.934	0.033	100.00
Mole Fraction	0.78087	0.20946	0.00934	0.00033	1.0000
	x	x	x	x	
Kg-Mole Mass (constituents)	14.007(2) [28.01]	15.999(2) [32.00]	39.948 [39.85]	12.0112+15.999(2) [44.01]	
	V	V	V	V	
Air Kg-Mole Mass	21.875 +	6.703 +	0.373 +	0.015	28.965
Mass Ratio	$\frac{21.875}{28.965}$	$\frac{6.703}{28.965}$	$\frac{0.373}{28.965}$	$\frac{0.015}{28.965}$	
	0.7552	0.2314	0.0129	0.0005	1.0000
Kg/kg O_2	$\frac{0.7552}{0.2314}$	$\frac{0.2314}{0.2314}$	$\frac{0.0129}{0.2314}$	$\frac{0.0005}{0.2314}$	
	3.2637	1.0000	0.0557	0.0022	
	3.3216 <——<<				
Mole Ratio	$\frac{0.7809}{0.2095}$	$\frac{0.2095}{0.2095}$	$\frac{0.0093}{0.2095}$	$\frac{0.0003}{0.2095}$	
	3.7280	1.0000	0.0446	0.0016	
	3.7741 <——<<				

Notes:

(1) Assumed that the molecular weights of the small fraction constituents of air are in the nitrogen (N_2) air fraction.

(2) Molecular weights base on ${}_6C^{12}$.

TABLE E.3

PROPERTIES OF HYDROGEN COMPOUNDS OF OXYGEN AND SULPHUR

	H_2O	H_2S
Melting Point (C)	0.0	-85.6
Boiling Point (C)	100.0	-60.75
Critical Temperature (C)	366.0	100.4
Heat of Fusion (kcal/gmole)	1.430	0.5676
Heat of Vapourization (kcal/gmole)	9.715	4.463
Density at Boiling Point (g/cc)	0.958	0.993
Surface Tension at Boiling Point (dynes/cm)	58.9	28.7
Heat of Formation (at 20C and const press) (kcal/gmole)	68.35	4.8
Free Energy of Formation (at 25C) (kcal/mole)	-56.72	8.42

TABLE E.4

PHYSICAL CONSTANTS FOR OXYGEN [77]

Mass (g/litre at 0C and 1 atmosphere, 45° latitude)	1.42895
Boiling Point (C)	-183.0
Melting Point (C)	-218.9
Density of Solid at -252C	1.426
Density (relative to air = 1)	1.1053
Density of Liquid at Boiling Point (g/cc)	1.118
Critical Temperature (C)	-118.8
Critical Pressure (atmospheres)	49.7
Critical Density (g/c)	0.430
c_p of Gas at 20C (cal/g-K)	0.2184
c_v of Gas at 20C (cal/g-K)	0.183
$k = c_p/c_v$	1.395
c_p of Liquid at -200C	0.395
c_p of Solid at -222C	0.336
c_p of Solid at -25C	0.078
Heat of Vapourization of Liquid at Boiling Point (cal/g)	51
Heat of Fusion of Solid at Melting Point (cal/g)	3.3
Thermal Conductivity at 0C (cal/sec-K)	0.0000570
Solubility in Water at 0C (volumes in 1 volume of water)	0.0491
Solubility in Water at 20C (volumes in 1 volume of water)	0.0311
Solubility in Water at 100C (volumes in 1 volume of water)	0.0170

TABLE E.5

NORMAL OXIDES OF NITROGEN [43]

Formula	Name	Heat of Formation (kcal/g-mole)		
		Gas	Liquid	Solid
N_2O	dinitrogen oxide (nitrous oxide)	-19.6	-15.6	-
NO	nitrogen monoxide (nitric oxide)	-21.6	-	-
N_2O_3	nitrogen trioxide (dinitrogen trioxide)	-20.0	-10.6	-
NO_2	nitrogen dioxide	-8.0	-	-
N_2O_4	nitrogen tetroxide (dinitrogen tetroxide)	-2.4	+6.8	-
N_2O_5	nitrogen pentoxide (dinitrogen pentoxide)	-1.2	+3.6	+11.9

TABLE F.1

LIMITS OF FLAMMABILITY OF HYDROGEN SULPHIDE IN AIR (1 PER CENT WATER VAPOUR) IN CLOSED TUBES AS REPORTED BY COWARD AND JONES[6]

Tube Diameter (cm)	Direction of Flame Propagation					
	Upward		Horizontal		Downward	
	Lower	Higher	Lower	Higher	Lower	Higher
5.0	4.40	44.5	5.40	26.6	6.05	19.8
7.5	4.30	45.5	5.30	35.0	5.85	21.3

TABLE G.1

ENTHALPIES OF FORMATION

Ref.	Substance	Molecular Weight	Enthalpy of Formation	
		(kg/kgmole)	(Mcal/kgmole)	(kJ/kg)
78	H_2S	34.080	-4.184	-591.14
79	CH_4	16.0426	-17.895	-4667.1
79	C_2H_6	30.07	-20.236	-2815.68
79	C_3H_8	44.096	-24.82	-2355.02
80	C_2H_4	28.05	+12.54	+1870.49
78	C_2H_2	26.038	+54.19	+8707.69
78	H_2	2.0158	0.0	0.0
	O_2	31.9988	0.0	0.0
	N_2	28.0134	0.0	0.0
78	H_2O	18.0152	-57.7979	-13423.64
79	SO_2	64.0588	-70.947	-4633.89
81	CO_2	44.0098	-94.054	-8941.49
81	CO	28.0104	-26.42	-3946.49
80	SO	48.0594	+1.167	+101.6
81	S(cry)	32.06	0.0	0.0
81	S(gas)	32.06	+66.20	+8639.43
78	C(graphite)	12.011	0.0	0.0
78	C(gas)	12.011	+170.89	+59529.08

TABLE G.2

SPECIFIC HEAT RATIOS
(Reference 82)

Substance	Specific Heat Ratio
Air	1.403
H_2S	1.32
CH_4	1.31
C_2H_6	1.22
C_2H_4	1.255
C_2H_2	1.26
H_2	1.410
O_2	1.401
N_2	1.404
H_2O	1.329
SO_2	1.29
CO_2	1.304

TABLE H.1

SUMMARY OF DETONATION PROPERTIES FOR HYDROGEN SULPHIDE IN AIR

Calculated by Method of Reference [83]

Initial Conditions:

Temperature (K)	298.15
Pressure (kPa)	101.30

Equivalence Ratio	.500	.750	1.000	2.000	4.000
Shock Mach Number	3.978	4.505	4.830	4.539	4.116
Detonation Velocity, m/s	1366.000	1541.400	1647.000	1530.600	1365.500
Reaction Enthalpy, kJ/kg	1145.100	1621.900	1962.800	1610.900	1212.900

Unburned Reactants (Initial - 1) Conditions:

Hydrogen Sulphide (%)	7.591	10.970	14.110	24.731	39.654
Molecular Weight (M1,kg/kgmole)	29.299	29.450	29.592	30.081	30.798
Density (rho1,kg/m**3)	1.197	1.204	1.209	1.229	1.259
Specific Heat Ratio (gamma)	1.394	1.391	1.388	1.380	1.368
Mass Flux (kg/m**2-s)	1635.566	1845.580	1972.019	1832.648	1634.967

Shocked Reactant (Frozen - Intermediate - s) Conditions:

Ps/P1	18.595	23.985	27.651	24.333	19.864
Ts/T1	3.760	4.454	4.893	4.363	3.689
rhos/rho1	4.945	5.385	5.651	5.577	5.384
gammas	1.317	1.301	1.291	1.283	1.276
us (Velocity, m/s)	276.330	283.220	291.450	274.440	253.600

Detonated Product (Equilibrium - Final - 2) Conditions:

P2/P1	10.172	13.086	15.260	13.319	10.894
T2/T1	6.144	7.846	9.009	7.652	6.120
rho2/rho1	1.712	1.749	1.787	1.765	1.746
M2/M1	1.034	1.049	1.055	1.014	.981
gamma2	1.267	1.233	1.188	1.210	1.218
a2 (Sonic Velocity, m/s)	797.900	881.400	921.700	867.400	782.300
u1-us (Velocity Difference, m/s)	1089.670	1258.180	1355.550	1256.160	1111.900

TABLE H.2

HYDROGEN SULPHIDE COMBUSTION IN AIR
DETONATED PRODUCT (EQUILIBRIUM - FINAL) CONDITION
PRODUCT MIXTURE

Equivalence Ratio:		0.5	0.75	1.00	2.00	4.00
Species				Mole Fraction		
A	Argon	.00903	.00887	.00865	.00740	.00588
CO	Carbon Monoxide	.00000	.00001	.00008	.00016	.00011
CO_2	Carbon Dioxide	.00032	.00031	.00022	.00010	.00010
H	Atomic Hydrogen	.00000	.00006	.00112	.00052	.00003
H_2	Molecular Hydrogen	.00000	.00033	.00672	.04726	.06131
H_2O	Water (gas)	.06731	.09756	.11940	.15889	.21547
H_2S	Hydrogen Sulphide	.00000	.00000	.00002	.01236	.07313
NO	Nitrogen Monoxide	.00331	.00801	.00430	.00005	.00000
NO_2	Nitrogen Dioxide	.00002	.00001	.00000	.00000	.00000
N_2	Molecular Nitrogen	.75305	.73715	.72070	.61881	.49134
O	Atomic Oxygen	.00002	.00036	.00055	.00000	.00000
OH	Hydroxyl Radical	.00031	.00294	.00504	.00027	.00001
O_2	Molecular Oxygen	.09916	.04500	.00400	.00000	.00000
S	Monatomic Sulphur	.00000	.00000	.00010	.00101	.00010
SH	Thiol Radical	.00000	.00000	.00007	.00480	.00293
SN	Sulphur Nitride	.00000	.00000	.00000	.00002	.00000
SO	Sulphur Monoxide	.00000	.00026	.00746	.01691	.00237
SO_2	Sulphur Dioxide	.06683	.09894	.12150	.07665	.02155
SO_3	Sulphur Trioxide	.00064	.00019	.00004	.00000	.00000
S_2	Diatomic Sulphur	.00000	.00000	.00002	.05205	.12291
S_2O	Disulphur Monoxide	.00000	.00000	.00001	.00272	.00275
Total Mole Fraction		1.00000	1.00000	1.00000	.99998	.99999

TABLE H.2

HYDROGEN SULPHIDE COMBUSTION IN AIR DETONATED PRODUCT (EQUILIBRIUM - FINAL) CONDITION PRODUCT MIXTURE

Equivalence Ratio:		0.5	0.75	1.00	2.00	4.00
Species		Mole Fraction				
A	Argon	.00903	.00887	.00865	.00740	.00588
CO	Carbon Monoxide	.00000	.00001	.00008	.00016	.00011
CO_2	Carbon Dioxide	.00032	.00031	.00022	.00010	.00010
H	Atomic Hydrogen	.00000	.00006	.00112	.00052	.00003
H_2	Molecular Hydrogen	.00000	.00033	.00672	.04726	.06131
H_2O	Water (gas)	.06731	.09756	.11940	.15889	.21547
H_2S	Hydrogen Sulphide	.00000	.00000	.00002	.01236	.07313
NO	Nitrogen Monoxide	.00331	.00801	.00430	.00005	.00000
NO_2	Nitrogen Dioxide	.00002	.00001	.00000	.00000	.00000
N_2	Molecular Nitrogen	.75305	.73715	.72070	.61881	.49134
O	Atomic Oxygen	.00002	.00036	.00055	.00000	.00000
OH	Hydroxyl Radical	.00031	.00294	.00504	.00027	.00001
O_2	Molecular Oxygen	.09916	.04500	.00400	.00000	.00000
S	Monatomic Sulphur	.00000	.00000	.00010	.00101	.00010
SH	Thiol Radical	.00000	.00000	.00007	.00480	.00293
SN	Sulphur Nitride	.00000	.00000	.00000	.00002	.00000
SO	Sulphur Monoxide	.00000	.00026	.00746	.01691	.00237
SO_2	Sulphur Dioxide	.06683	.09894	.12150	.07665	.02155
SO_3	Sulphur Trioxide	.00064	.00019	.00004	.00000	.00000
S_2	Diatomic Sulphur	.00000	.00000	.00002	.05205	.12291
S_2O	Disulphur Monoxide	.00000	.00000	.00001	.00272	.00275
Total Mole Fraction		1.00000	1.00000	1.00000	.99998	.99999

TABLE H.3

SPECIES CONSIDERED IN DETONATION PRODUCT CALCULATION

A	CH_2O	CN_2	CS_2	C_2H_6	C_3O_2
CHO	HO_2	H_2O_2	NCO	NO_2	N_2O_4
O_2	SH	S_2	C(s)	CH_3	CO
C_2	C_2N	C_4	HNCO	H_2	H_2S
NH	NO_3	N_2O_5	SN	O_3	S_2O
C	CH_4	COS	C_2H	C_2N_2	C_5
HNO	$H_2O(s)$	$H_2SO_4(l)$	NH_2	N_2	N_3
S(s)	SO	S_8	CH	CN	CO_2
C_2H_2	C_2O	H	HNO_2	$H_2O(l)$	H_2SO_4
NH_3	N_2H_4	O	S(l)	SO_2	C_3H_8
CH_2	CNN	CS	C_2H_4	C_3	HCN
HNO_3	H_2O	N	NO	N_2O	OH
S	SO_3	$C_6H_6(l)$			

TABLE H.4

CLASSIFICATIONS FOR SPECIES PRODUCTION OF HYDROGEN SULPHIDE DETONATION IN AIR AGAINST EQUIVALENCE RATIO (Ø)

Class	Form	Mole Fraction		
		> 1.0%	1.0- 0.1%	< 0.1%
A	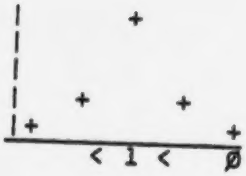	SO_2	H OH	O
B	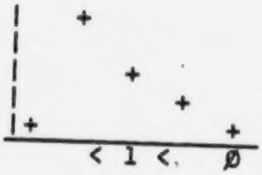		NO	
C	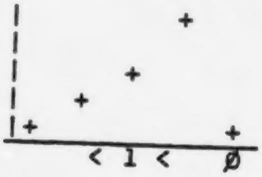	SO	O SH	CO SN
D	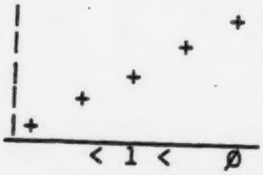	H_2O H_2S		
E	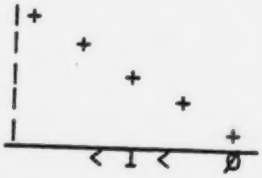	A H_2 N_2	S_2O	SO_3 CO_2 NO_2 O_2
F	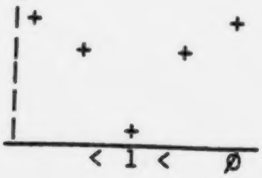	S_2		

TABLE H.5

DETONATION PARAMETERS OF SOME STOICHIOMETRIC FUEL-AIR MIXTURES

(Initial Conditions: 25C, 101.3 kPa)

Fuel		Mole Percent at Unity Equivalence Ratio	Volume of Fuel-Air Cloud per kg of Fuel (m^3)	Detonation Pressure (atm)	Detonation Velocity (m/s)	Detonation Energy (MJ/kg of fuel)
Methane	CH_4	9.48	-	-	-	-
Acetylene	C_2H_2	7.75	12.1	18.1	1860	35.4
Ethylene	C_2H_4	6.53	13.3	17.4	1850	37.5
Propane	C_3H_8	4.02	13.8	17.4	1798	37.9
Pentane	C_5H_{12}	2.55	-	-	-	-
Ethylene Oxide	C_2H_4O	-	7.2	18.4	1831	23.1
Propylene Oxide (aerosol)	C_3H_6O	-	8.0	17.7	1780	25.0
Hydrogen	H_2	29.50	-	-	-	-
Hydrogen Sulphide	H_2S	12.30	5.9	15.3	1650	13.9
TNT	-	-	-	$\sim 10^5$	5000-6000	4.2

TABLE I.1

DETONABILITY PARAMETER VALUES FOR SELECTED FUELS IN AIR AT STOICHIOMETRIC CONCENTRATIONS

(Reference [84])

Fuel	Formula	Cell Size (mm)	Critical Tube (m)
Acetylene	C_2H_2	9.8	0.12
Ethylene	C_2H_4	28.0	0.43
Propane	C_3H_8	69.0	0.90
Ethane	C_2H_6	54-62	~0.9
Methane	CH_4	280.0	3.2-4.1
Hydrogen	H_2	15.0	0.20
Hydrogen Sulphide	H_2S	?	?

TABLE J.1

CALCULATED SCALING VALUES FOR HYDROGEN SULPHIDE AND AIR DETONATION

Equivalence Ratio	Bag Volume (m^3)	Density (kg/m^3)	Mass (kg)	Unit Energy (kJ/kgmix)	Unit Energy (kJ/kgfuel)	Total Energy (E) (MJ)	Scaling Length $Ro = (E/po)^{1/3}$ (m)
.500	2094	1.197	2506.518	1145.1	15067	2.87	30.486
.750	2094	1.204	2521.176	1621.9	14744	4.08	34.303
1.000	2094	1.209	2531.646	1962.8	13920	4.96	36.606
2.000	2094	1.229	2573.526	1610.9	6493	4.14	34.461
4.000	2094	1.259	2636.346	1212.9	3051	3.19	31.604

O. Figures.

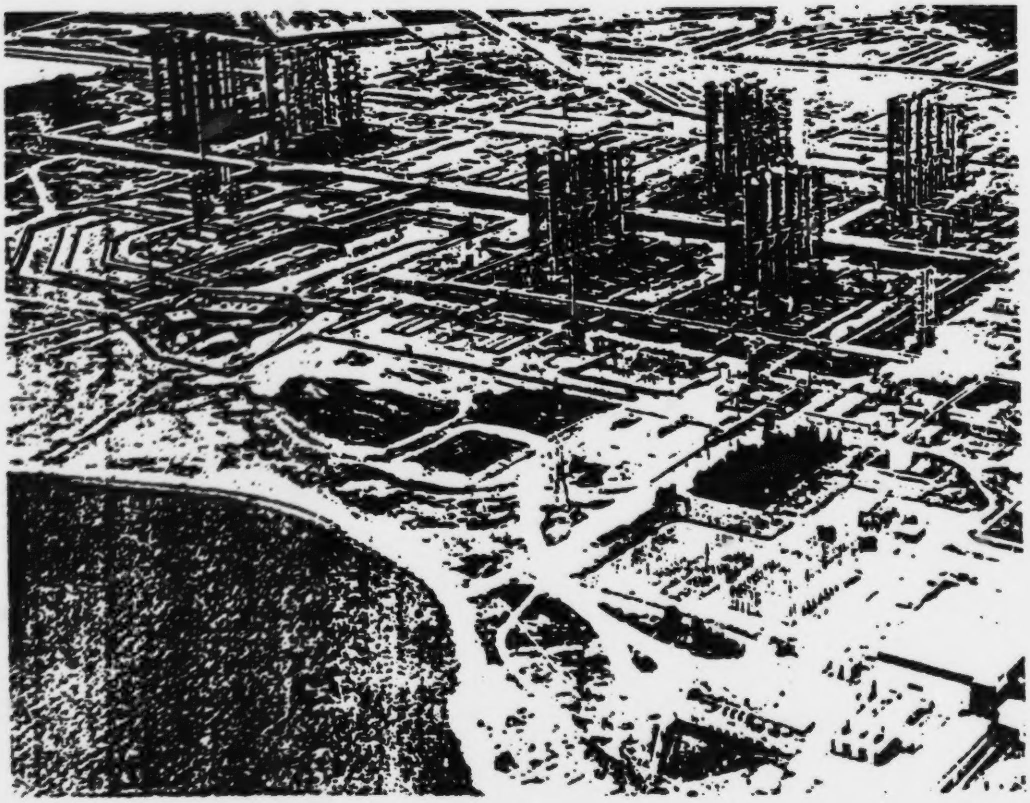

FIGURE B.1

LAYOUT OF
BRUCE HEAVY WATER PLANT

Located on the eastern shore of Lake Huron, Ontario, the Bruce Heavy Water plant components are dominated by sets of vertical process tanks rising to elevations of over 70 metres above the local grade. The vertical process tanks and other plant units are interconnected by process and service piping ranging from 0.05 to 1.3 metres diameter.

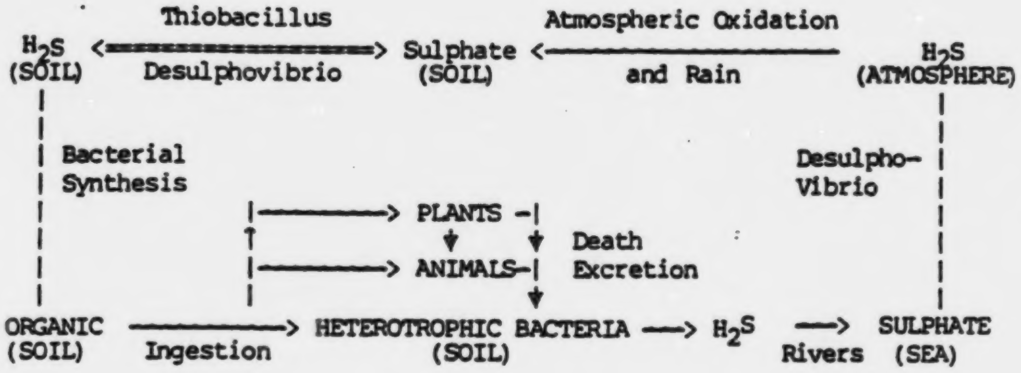

FIGURE D.1

THE SULPHUR CYCLE [45]

Hydrogen sulphide is constantly being formed and broken down in the "sulphur cycle." The illustration shows how sulphur and sulphates are related through their processing in the biosphere. Sulphates are washed into the seas from which hydrogen sulphide is released. The hydrogen sulphide enters the atmosphere, from which sulphur returns to the Earth and its surface in the form of oxides and and sulphates. These sulphur compounds are then processed by bacteria in the soil and are subsequently ingested by plants and animals. The sulphur compounds then return to the soil through excretion and death for the cycle to continue.

[Note: This illustration has been included for completeness in the discussion of hydrogen sulphide chemistry.]

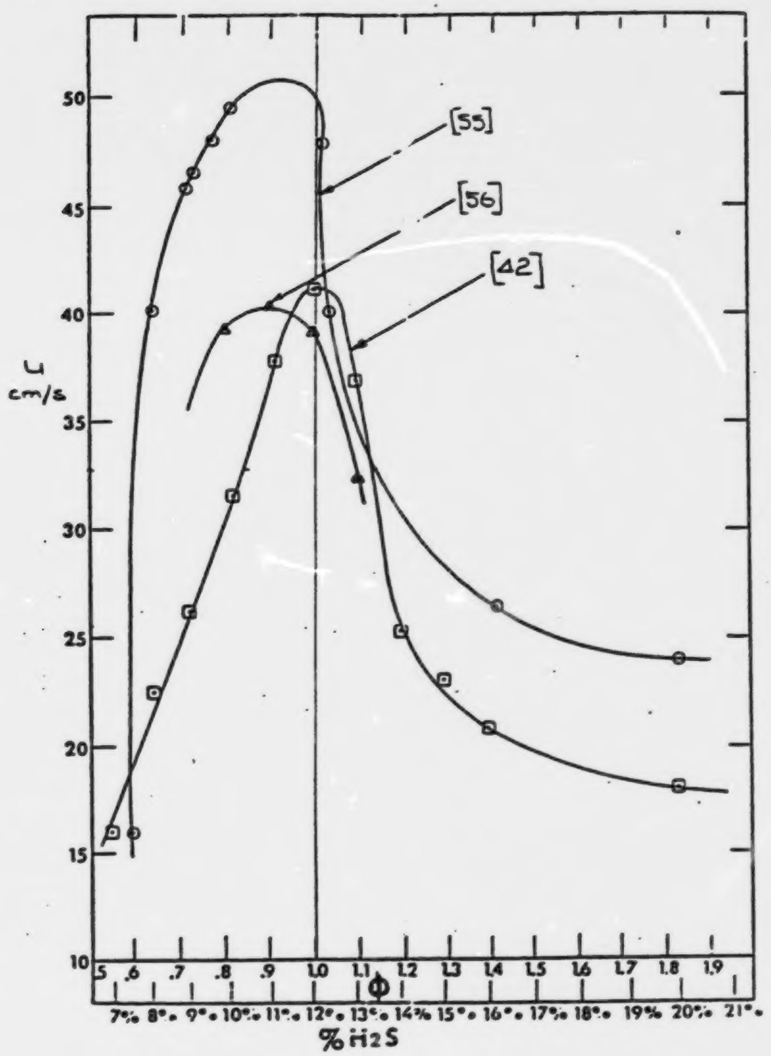

FIGURE F.1

BURNING VELOCITY OF HYDROGEN SULPHIDE IN AIR [42]

Results for the burning velocity of dry hydrogen sulphide mixtures in air from Kincler[42] are shown. The results are compared with those of Clark[55] and Gibbs and Calcote.[56] The Kincler data have their maximum at unity equivalence ratio (stoichiometric), at about 41.1 cm/s. At the 7 per cent and 20 per cent levels of hydrogen sulphide in air, the velocities are about 16 and 18 cm/s, respectively.

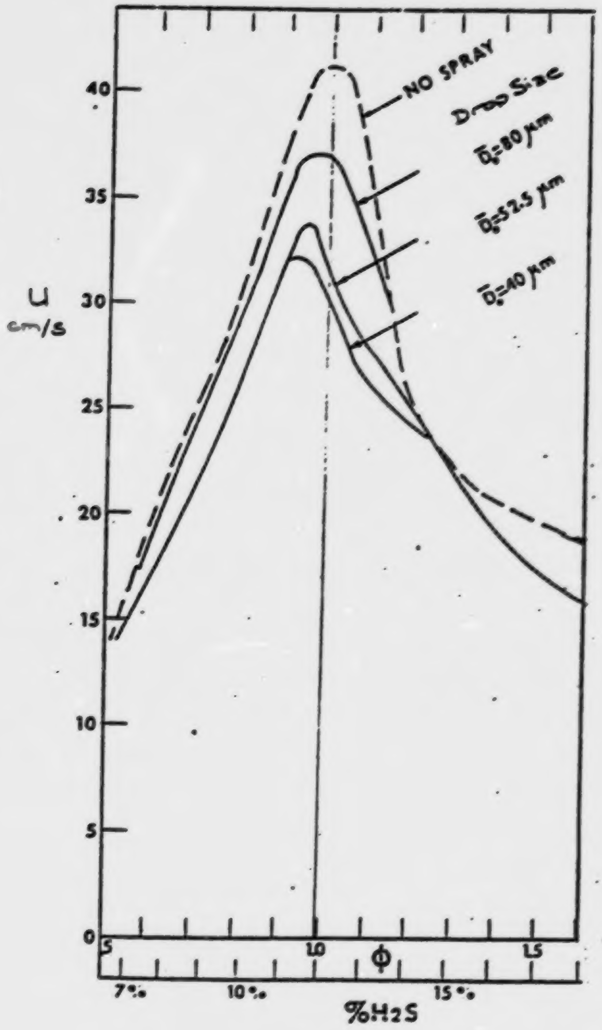

FIGURE F.2

BURNING VELOCITY OF HYDROGEN SULPHIDE
IN WET AND DRY AIR

Water saturated with hydrogen sulphide was sprayed into a flammability tube in order to determine the burning velocity in wet air.[42] These are compared to those for hydrogen sulphide in dry air. First, the burning velocity maxima occur at about unity equivalence ratio. The velocity in wet air is about 32 cm/s, approximately 25% lower than the dry air case. Next, as the flammability limits are approached the effect of water diminishes.

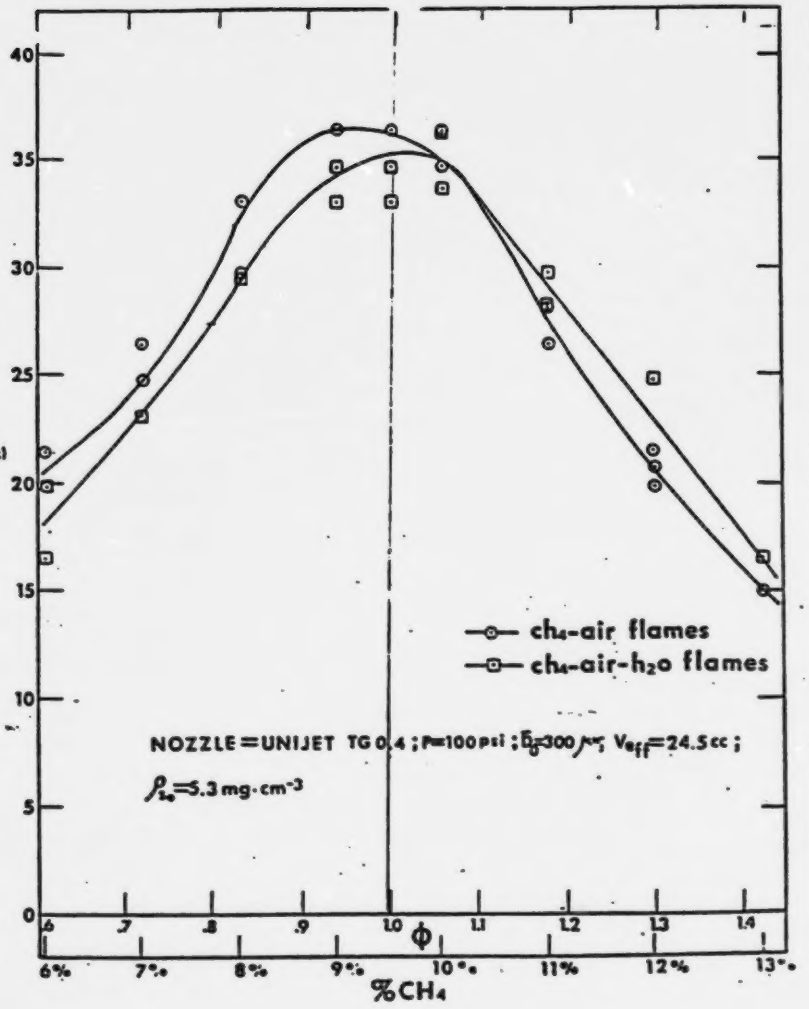

FIGURE F.3

BURNING VELOCITY OF METHANE

Results for the burning of dry methane mixtures in air from Kincler [42] are shown. The results are compared with those of other investigators in the Kincler reference. The Kincler data show maximum velocity at about unity equivalence ratio. This maximum is about 36 cm/s.

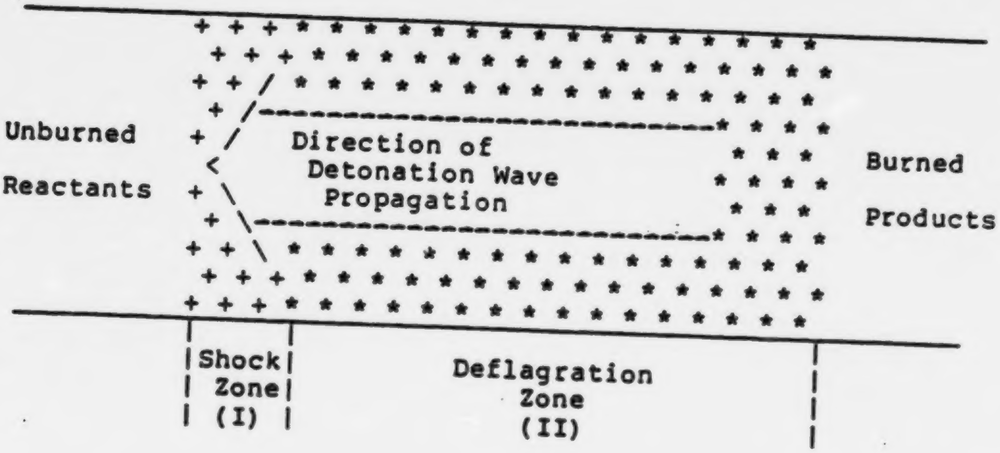

FIGURE G.1

STRUCTURE THROUGH A DETONATION WAVE

A typical structure through a detonation is illustrated. The figure is drawn with the axis parallel to the local combustion propagation direction at an instant in time. The detonation is divided into two zones (I) a relatively thin shock zone and (II) a deflagration zone. In the shock zone, the thermodynamic properties of the combustible are elevated by shock heating to levels above those required for ignition. However, the shock heating occurs quickly compared to the reaction rates so the chemical composition does not change through the shock. The chemical composition is called "frozen." Following the shock, the media combust in the deflagration zone, with corresponding changes in composition. The process combustion train propagates into the unreacted as a wave.

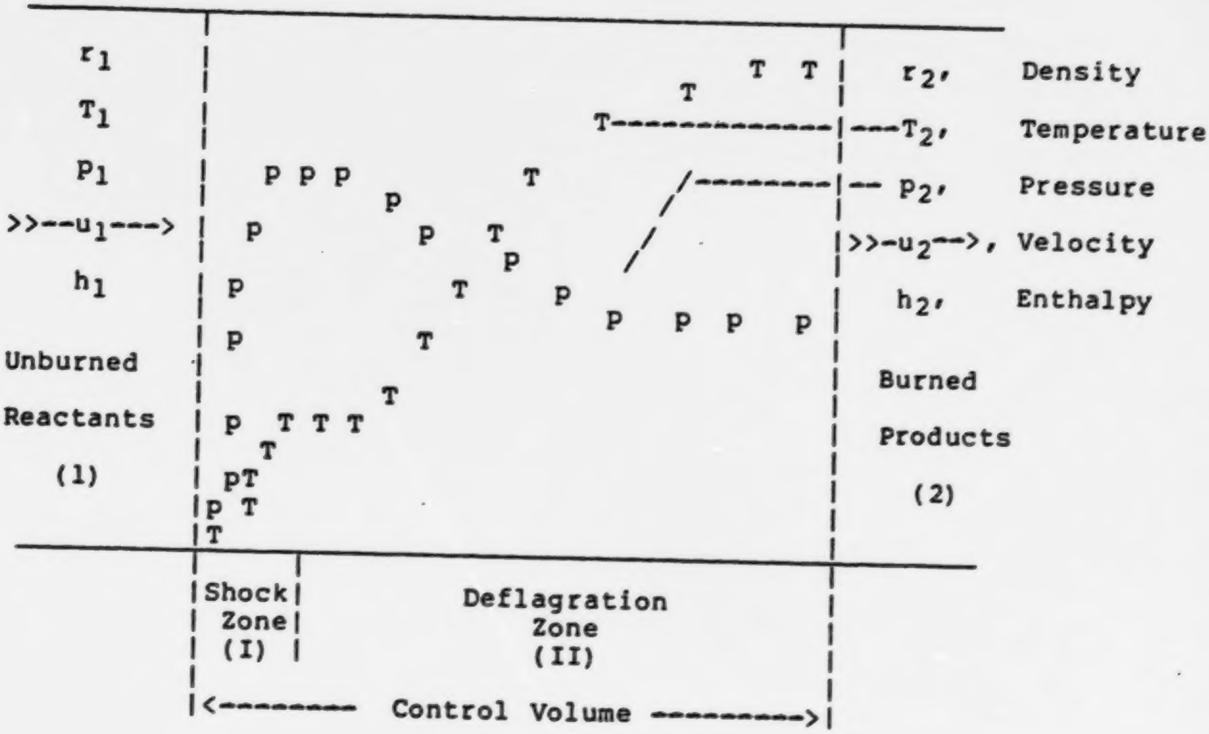

FIGURE G.2

SCHEMATIC FOR CONTROL VOLUME DETONATION ANALYSIS

The detonation situation is sketched schematically. The wave is presumed to be steady and so can be viewed in a frame of reference motionless with respect to the front. Furthermore, the wave is presumed to be planar so that all properties are functions of the axial dimension "x" only. To analyse the situation, the detonation zone is presumed isolated in a control volume. The initial conditions of the fluid include the density r_1, temperature T_1, pressure P_1, velocity u_1 and enthalpy h_1. The exit conditions with subscript "2", as well as the inlet velocity are unknown. No statement about the rate of the reaction and hence the physical extent (thickness) of the detonation is made. However, since all events are presumed to occur in the combustion zone, the control volume does not have to define the extent of the detonation, but merely enclose it.

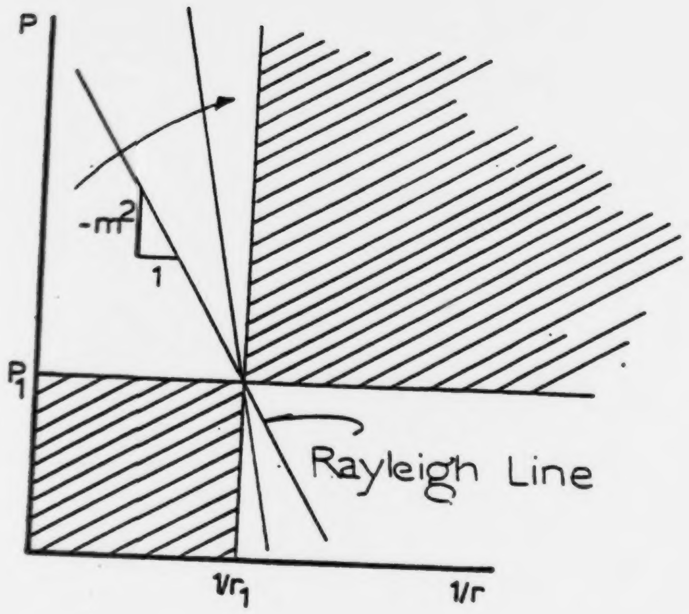

FIGURE G.3

THE RAYLEIGH LINE

The Rayleigh line represents the momentum and continuity equations. It is shown here, sketched on p,1/r axes. The Rayleigh line passes through the point $p_1, 1/r_1$, the initial condition of the reactant fluid. This point represents the known thermodynamic conditions of the unreacted medium ahead, upstream, of the detonation zone. The slope of the Rayleigh line is a constant $-m^2$ for a given mass flow. Consequently, any final condition that the fluid system assumes must lie on the staright line and can only assume conditions that have either both higher pressure and lower specific volume or lower pressure and higher specific volume. Next, the actual slope is determined from the combustion energy release and the properties of the product species. This requires of the energy equation.

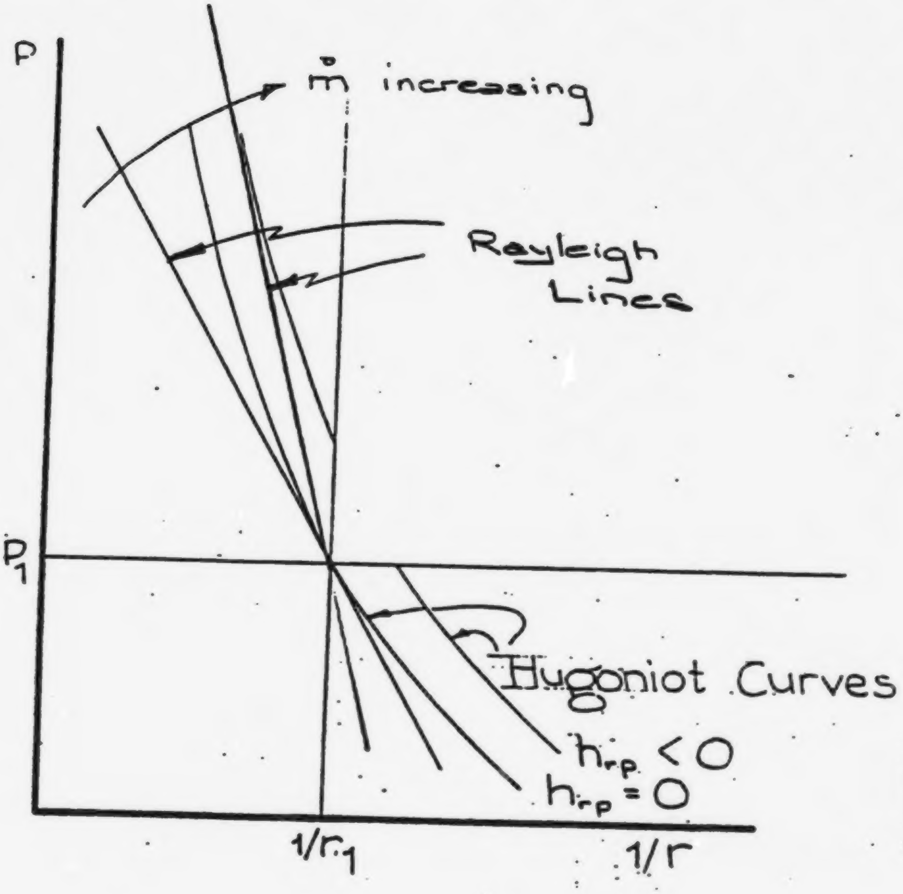

FIGURE G.4

THE HUGONIOT CURVE

In the case where there is no reaction, the Hugoniot curve passes through the initial conditions $(p_1, 1/r_1)$. On the other hand, when the reactants are changed into products and the enthalpy of reaction is released, the Hugoniot curve does not pass through the initial state. The mass flow, as represented by the slope of the Rayleigh line, must adjust to reflect the energy change due to the reaction.

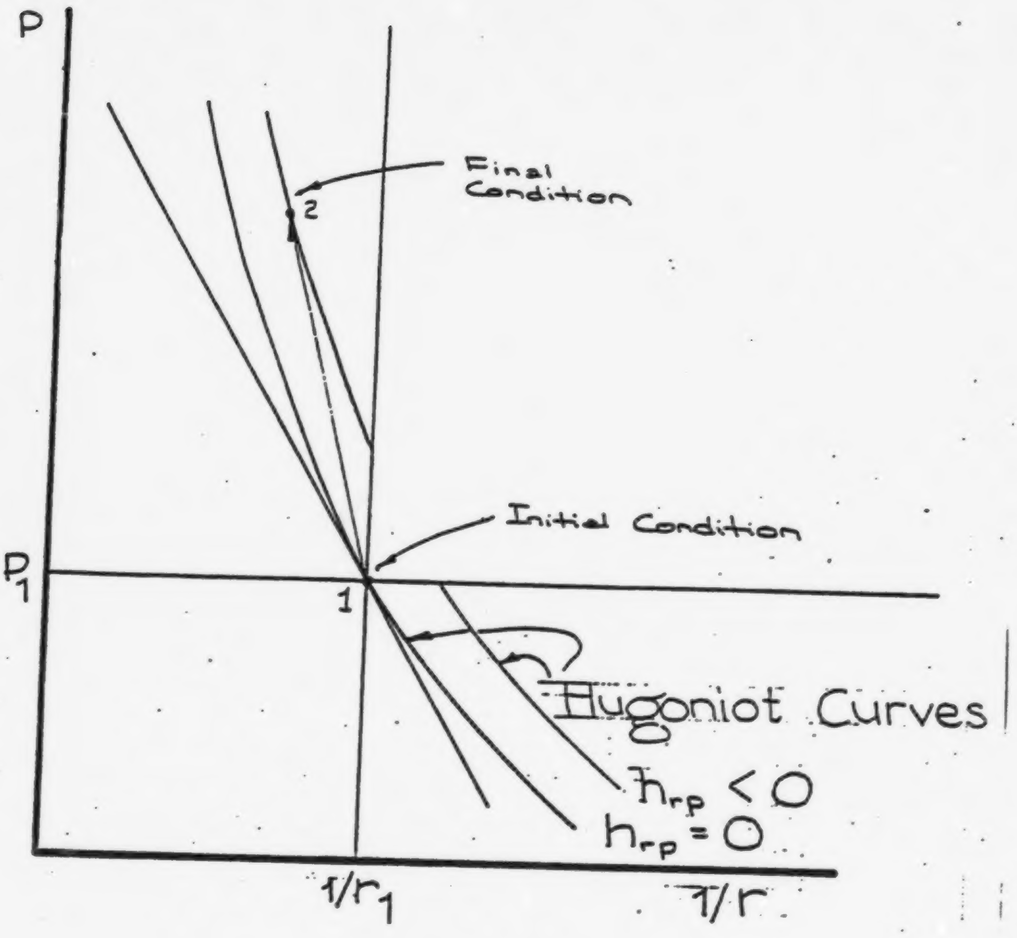

FIGURE G.5

THE SIMULTANEOUS SOLUTION OF MASS, MOMENTUM AND ENERGY RELATIONS

The mass flow of the system passing through the control volume characterises the Rayleigh line passing through the initial conditions. Similarly, the difference in enthalpy between the initial and final states of the system characterise the Hugoniot curve. The condition that satisfies both conservation characterization criteria is the intersection of the two curves. The intersection gives the condition at exit from the control volume. There are two apparent solutions shown. Both these solutions satisfy the momentum and energy criteria. However, only one solution the Chapman-Jouguet condition is stable.

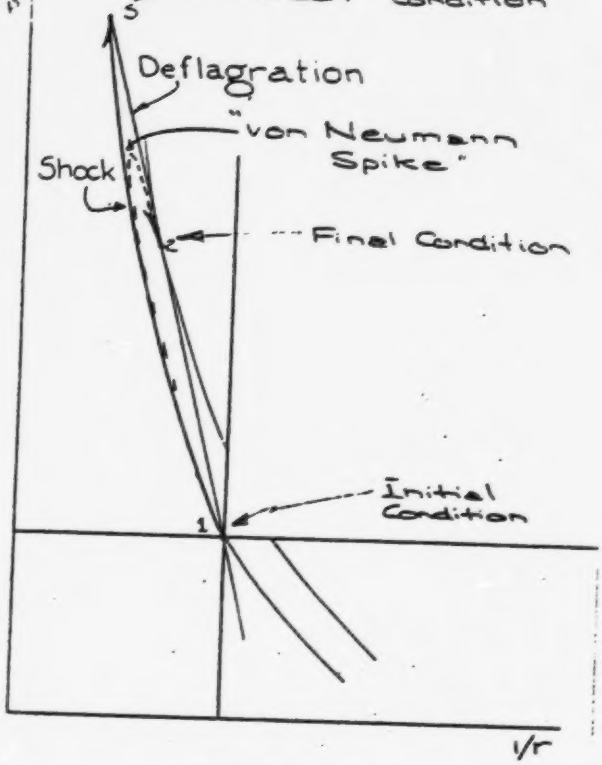

FIGURE G.6

THE ZND SOLUTION FOR DETONATION

Once the changes in properties across the entire reaction zone have been calculated, the mass, momentum and energy balances are known. With this knowledge, the post-shock:pre-combustion condition of the system can be calculated. The approach assumes that the mass flow is determined by the overall changes in the system including combustion, but in the shock there are no chemical reactions. As the figure shows, the overall Rayleigh line is tangent to the Hugoniot curve with heat release, at condition 2 and its slope gives the mass flux for the detonation. The intersection of that Rayleigh line to the Hugoniot curve without heat release, at condition s, gives the thermodynamic conditions at the interface of the shock zone (I) and the reaction (detonation) zone (II). It is noted here that the shocked pressure exceeds the equilibrium pressure following the detonation reactions. This shock pressure is observed over a time that is short compared to those associated with combustion and is called the von Neumann "spike". The actual process is approximated by the dashed line.

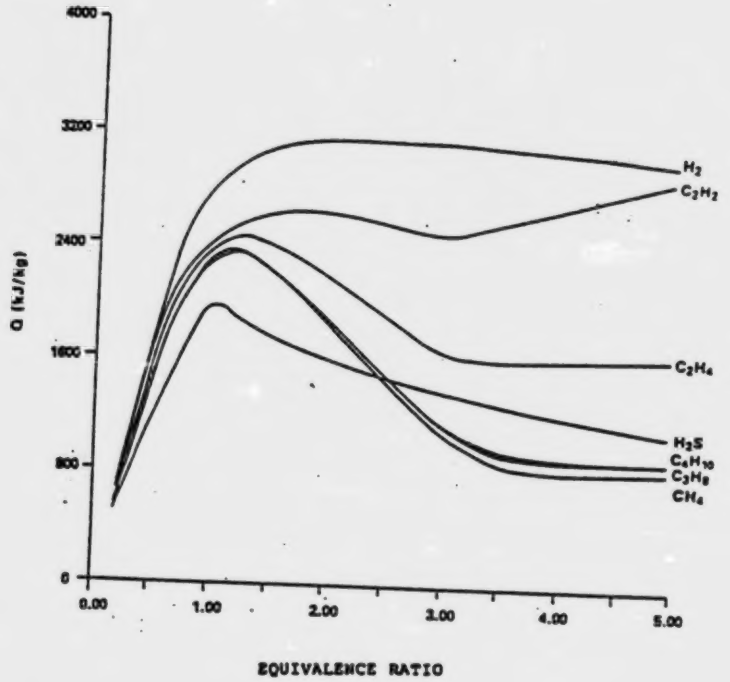

FIGURE H.1

CHAPMAN-JOUGUET ENERGY RELEASE vs EQUIVALENCE RATIO

The diagram shows a gradual, almost linear increase in thermal energy output with per cent hydrogen sulphide to a maximum of about 2000 kJ/kg of mixture, corresponding to about 14,000 kJ/kg of hydrogen sulphide, at an equivalence ratio of unity. The thermal energy then decreases on the fuel rich side to about 1000 kJ/kg when the equivalence ratio is 2. The decrease of thermal energy output is associated with incomplete reaction of the hydrogen sulphide with air leaving unburned H_2S as well as other species produced in intermediary reactions. Also shown are the thermal energy release for other fuels including hydrogen (H_2), acetylene (C_2H_2), ethylene (C_2H_4), butane (C_4H_{10}), propane (C_3H_8) and methane (CH_4). Except for acetylene, all fuels show their thermal release maxima at about unit equivalence ratio. Furthermore, they all fall in the range of about 2000 to 3200 kJ/kg of combustible mixture.

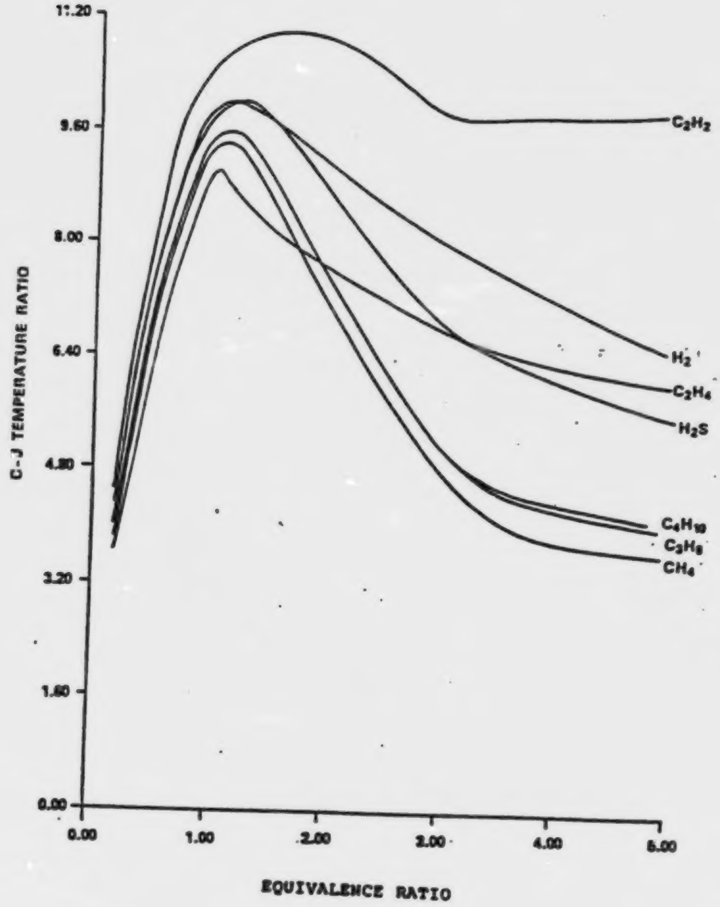

FIGURE H.2

CHAPMAN-JOUGUET TEMPERATURE RATIO vs EQUIVALENCE RATIO

The energy release of hydrogen sulphide detonation in air increases the sensible energy of the combustion system. The increase is shown along with those of selected other fuels as a ratio of final equilibrium system product temperature to initial temperature of the reactants in the figure. Just as for thermal energy release, the product to reactant temperature ratio increases with equivalence ratio (volume per cent H_2S) and shows a maximum in the vicinity of the unity equivalence ratio. The maximum temperature ratio is about 9. This lies at the bottom of the range 9 to 11 shown for all six fuels considered. The deviation of the curve from linear is due to the sharing of the reaction heat between the sensible energy (temperature) and the directed kinetic energy of motion combustion gives to the product mass stream.

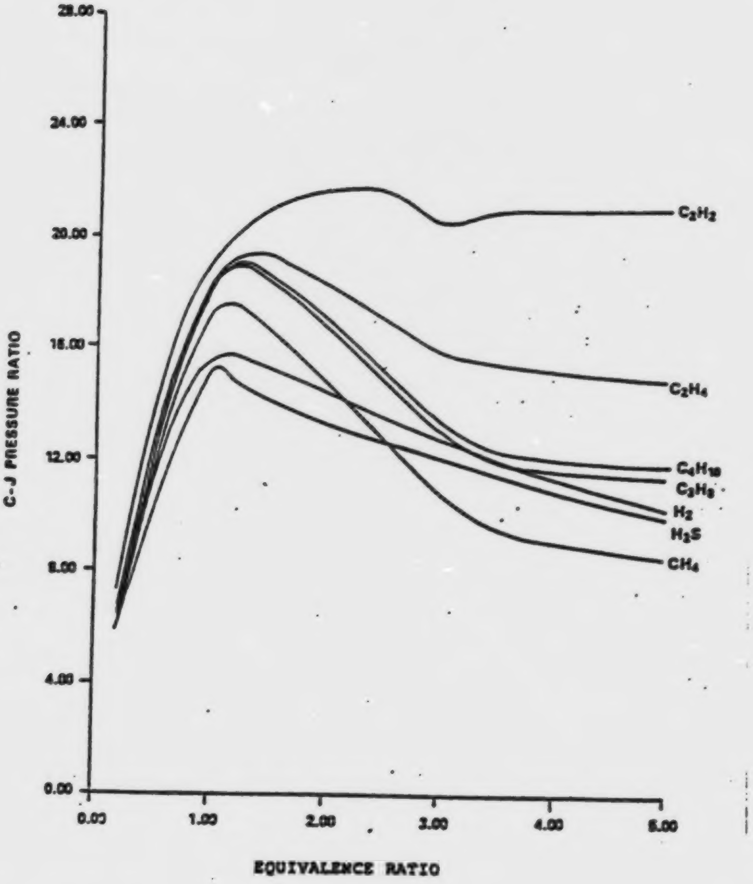

FIGURE H.3

CHAPMAN-JOUGUET PRESSURE RATIO vs EQUIVALENCE RATIO

Detonation increases the local thermodynamic pressure inside the combustion stream. The final product to initial reactant detonation pressure ratio is shown above. Like both the thermal energy release and the product temperature, the pressure ratio is shown for six other fuel mixed with air. All fuels shown maxima in pressure ratio at about unity equivalence ratio. The maximum pressure ratio calculated for hydrogen sulphide for the planar detonation wave, under the assumptions outlined above, is about 15. This ratio falls at the low end of fuels considered and is about the same value as that of hydrogen. The maximum pressure ratio is shown for acetylene at about 22, only 50 per cent higher. It is noted here that thermodynamic pressure scales approximately with temperature.

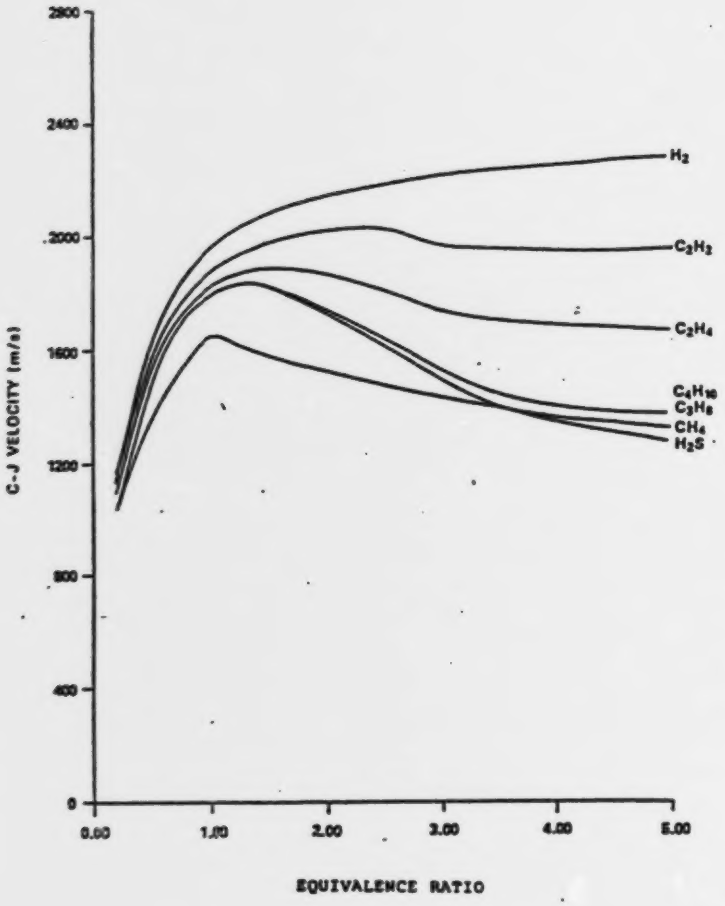

FIGURE H.4

CHAPMAN-JOUGUET VELOCITY vs EQUIVALENCE RATIO

The detonation velocity is the measure of the detonation wave propagation into the unreacted medium. This velocity is shown in the illustration for a range of equivalence ratios of hydrogen sulphide and other fuels in air. As for the other products properties, velocity increases with equivalence ratio to a maximum of about 1650 m/s when the equivalence ratio is 1. This is at the low end of the Chapman-Jouguet velocity range of about 1600 to 2000 m/s for the fuels considered. The round form of the curve occurs since (a) the velocity is proportional to the square root of the directed kinetic energy and (b) the total thermal energy release is shared between the thermodynamic and dynamic modes.

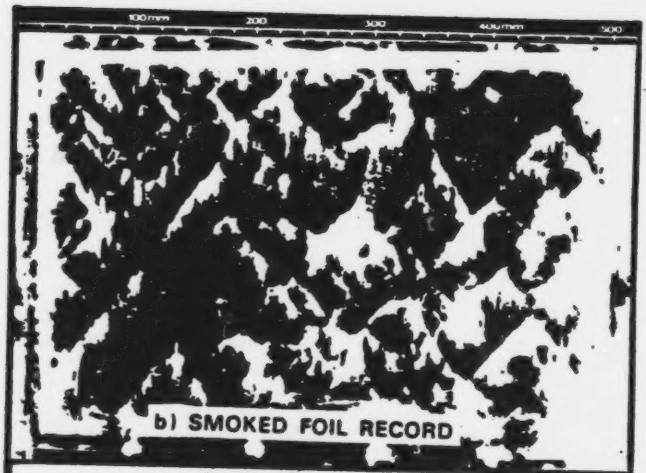

b) SMOKED FOIL RECORD

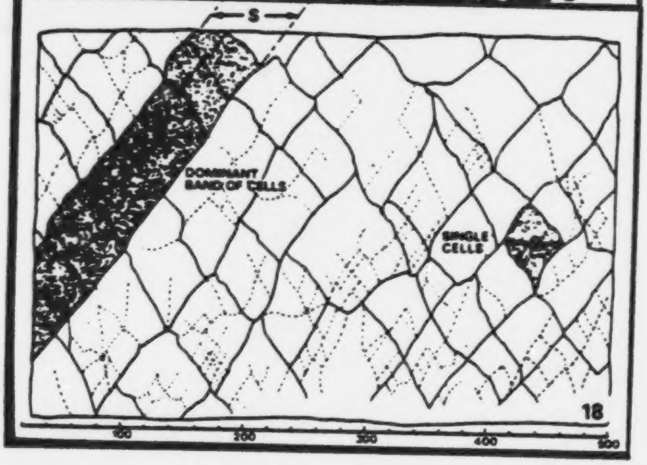

c) INTERPRETATION OF SMOKED FOIL RECORD

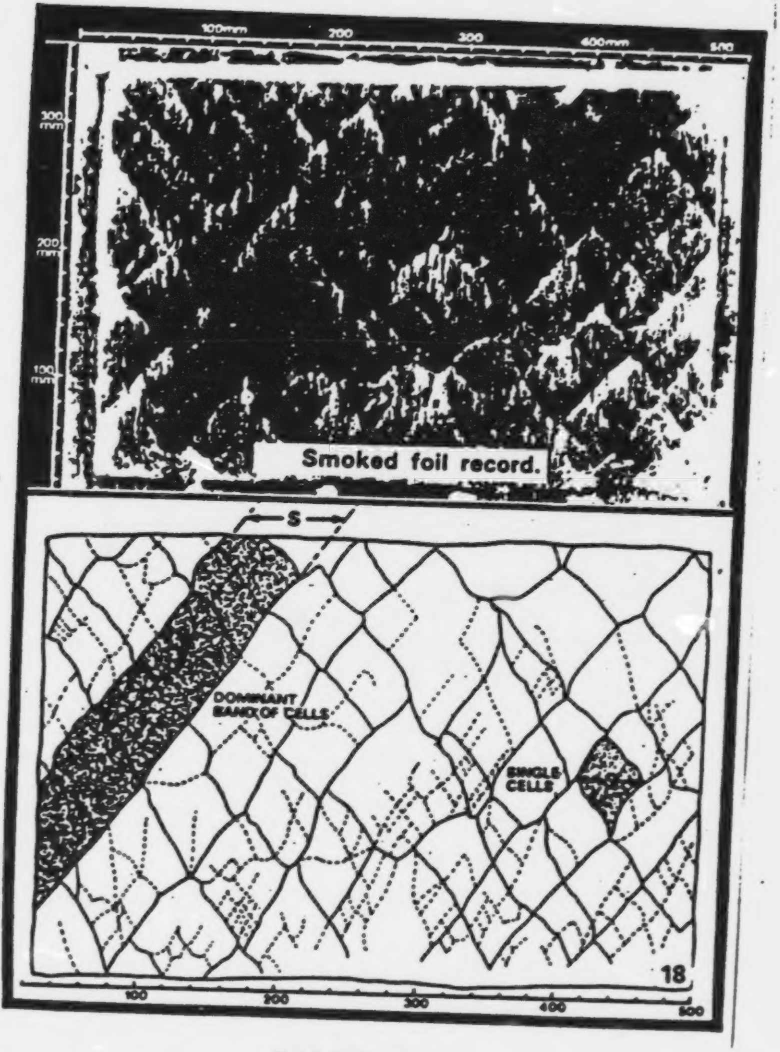

FIGURE I.1

DETONATION CELL STRUCTURE

When a soot-coated mylar, aluminum, steel or other plate is placed in a tube filled with a detonable gas and detonation of the gas is achieved, a cellular pattern is "written" on the plate.[16,62,71] These cells are complex patterns that are related to the moving axial and transverse shocks within the propagating front.

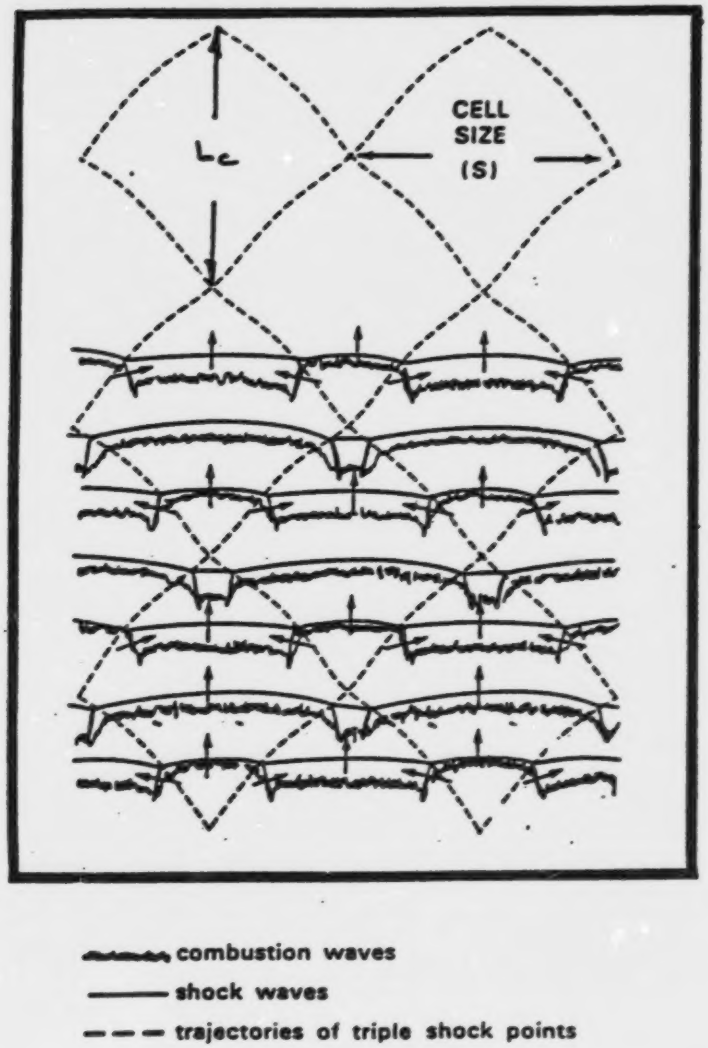

FIGURE I.2

TRANSVERSE WAVE STRUCTURE THROUGH A DETONATION

As shown,the cells may be quantified by defining L_c the cell length in the direction of propagation of the wave, and s the transverse width of the cell.[63]

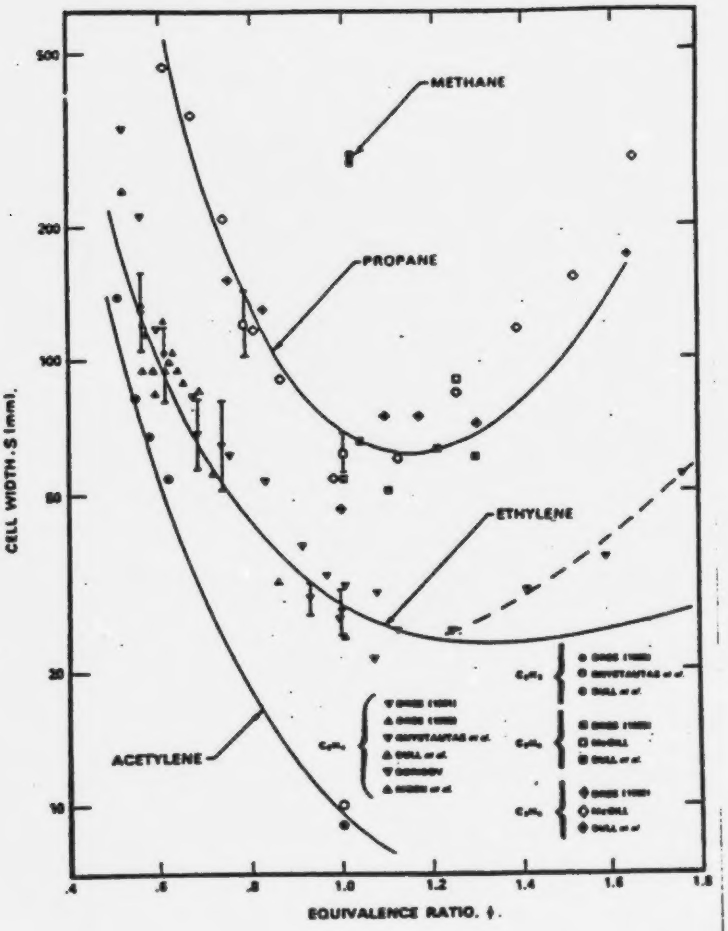

FIGURE I.3

VARIATION OF CELL SIZE WITH EQUIVALENCE RATIO

As illustration shows, the variation of cell size s with equivalence ratio ϕ is typically convex-downward with the minimum cell size occuring at stoichiometric conditions ($\phi = 1$).[68]

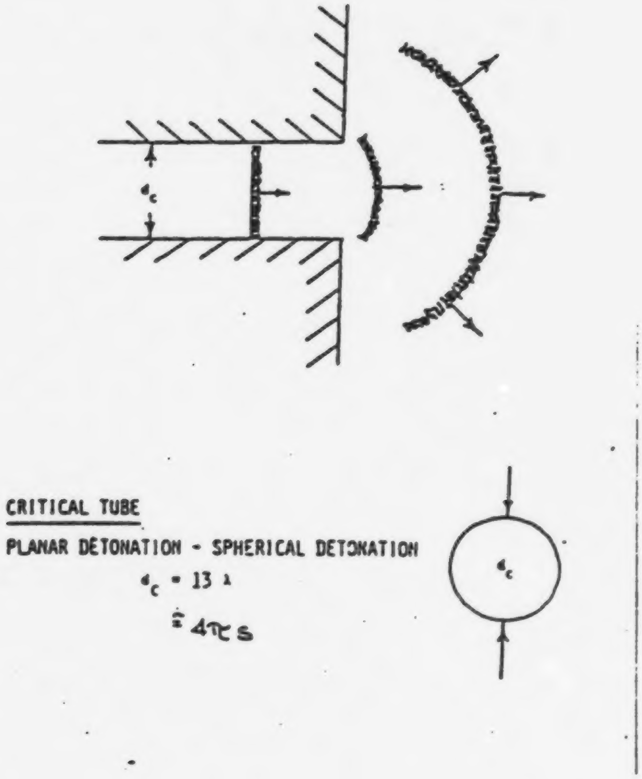

FIGURE I.4

DEVELOPMENT OF A DETONATION WAVE FROM A TUBE

Experimentally, a planar detonation wave may propagate through a detonable gas contained in a right circular cross-section tube. The tube opens at the upstream end into an unconfined solution of the same detonable material. The planar wave from the tube is transformed into a spherical wave in the unconfined if the tube diameter exceeds a critical value d_c. If $d<d_c$, the initial planar wave decouples from the shock and a planar deflagration results.

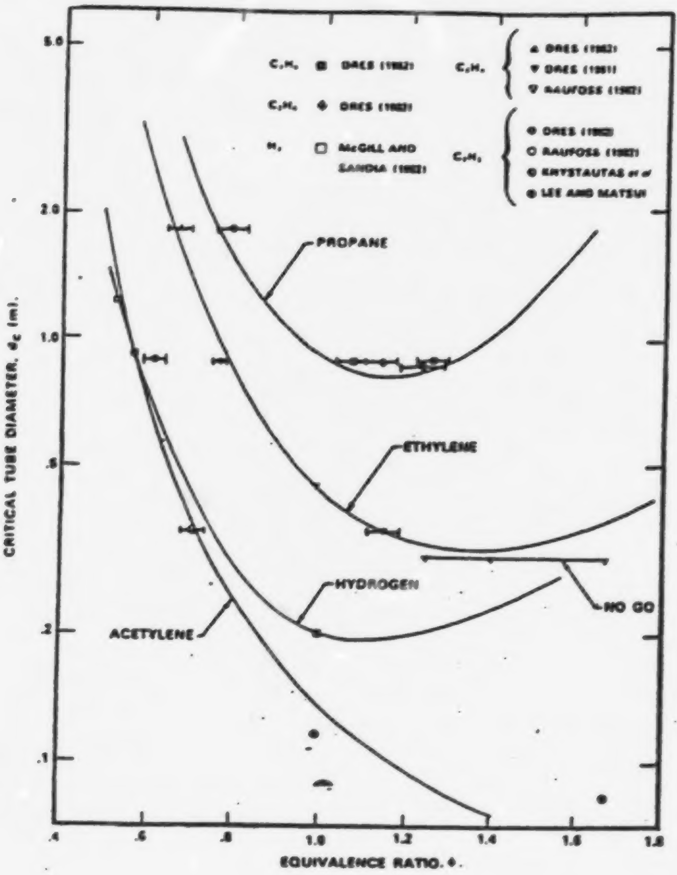

FIGURE I.5

DEPENDENCE OF CRITICAL TUBE DIAMETER ON EQUIVALENCE RATIO

The dependence of critical tube diameter on equivalence ratio, $d_c = d_c(\Phi)$ is illustrated. The solid curves are fits to the data. It is noted here that despite the apparent acceptance of $d_c = 13s$, the acceptance is not universal.

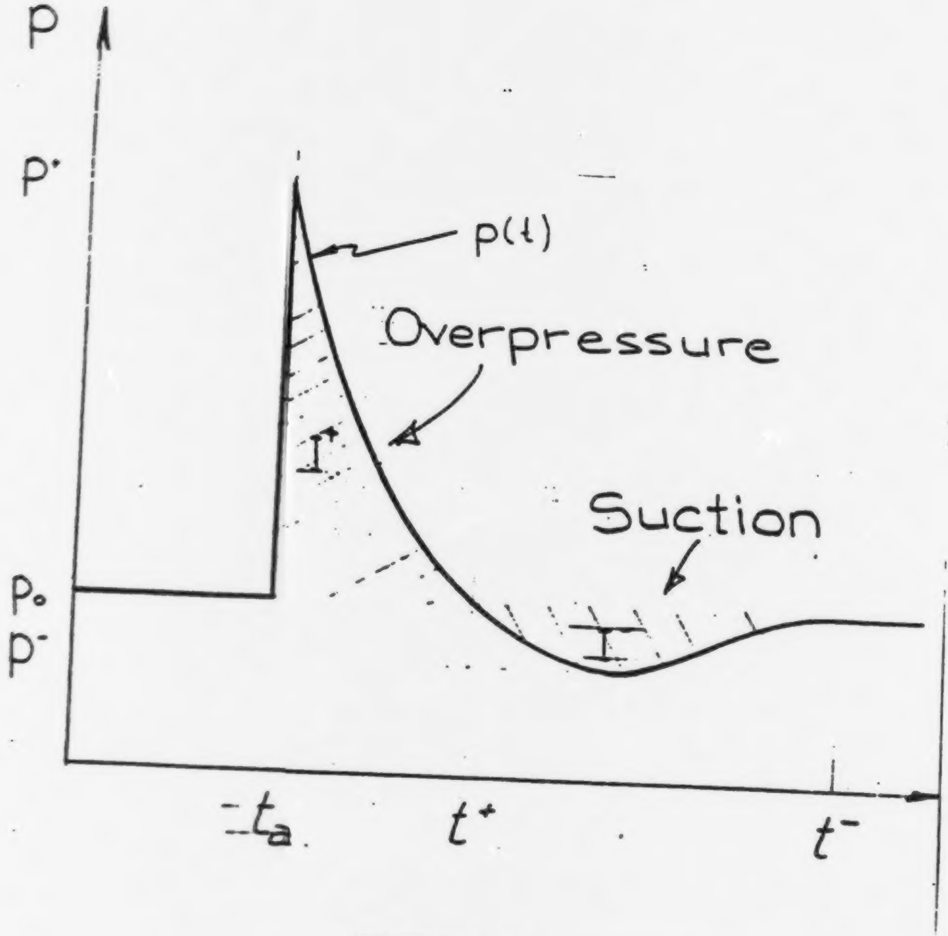

FIGURE J.1

CANONICAL BLAST WAVE CHARACTER

The local pressure is ambient until t_a, when the blast, shock front arrives. The local pressure then rises rapidly reaching p^+ for maximum absolute pressure value of $p^+ + p_o$. The positive overpressure decays to ambient over a time t^+, that is $t_a + t^+$ from initiation; to cross over the ambient pressure level: This period is called the positive phase. Next, an underpressure situation ensues, during which a partial vacuum is created. The underpressure remains for a time t^- for relaxation to the ambient pressure level. The relaxation is complete at $t_a + t^+ + t^-$ from initiation. The negative pressure period is called the suction or negative phase.

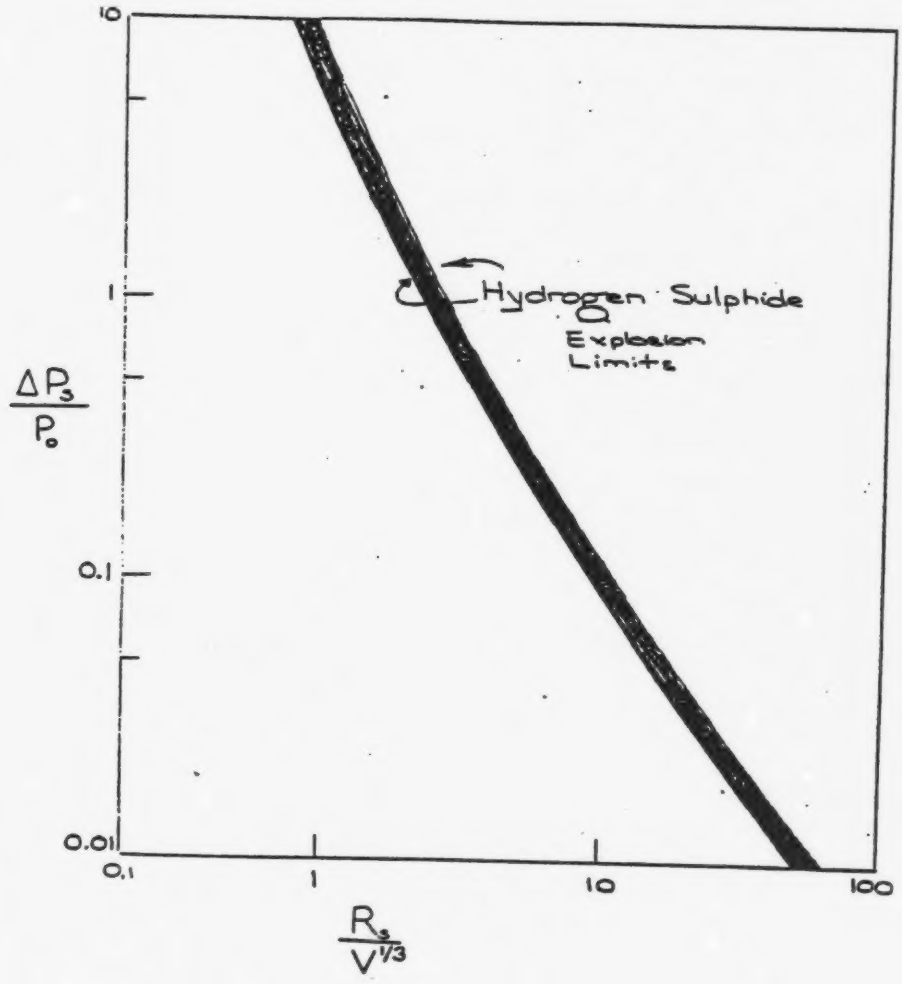

FIGURE J.2

BLAST WAVE OVERPRESSURE RATIO FOR HYDROGEN SULPHIDE DETONATION IN AIR

The scaled integrated positive pressure, the positive impulse, is shown. The illustration shows the decrease of the overpressure with distance scaled by the cube root of bag radius. The results lie in a narrow band in the region between the detonability limits of hydrogen sulphide. This shows that a single curve may be used for blast effect calculations.

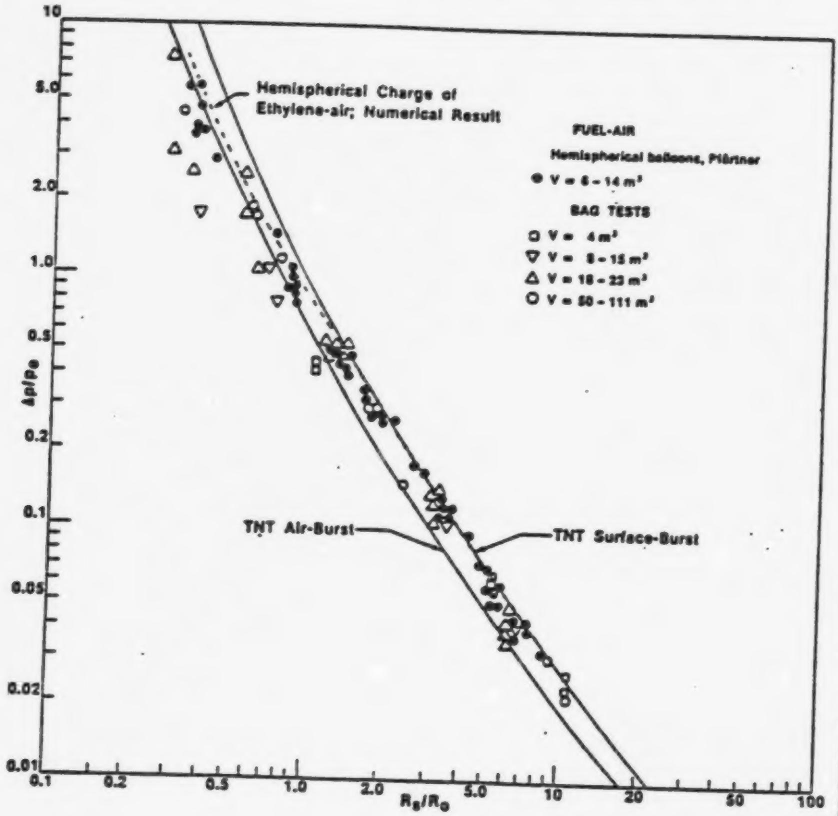

FIGURE J.3

BLAST WAVE OVERPRESSURE RATIO FOR
ETHYLENE DETONATION IN AIR

The results are similar to those for hydrogen sulphide in air. Blast effects are shown for the mixtures at grade and elevated above it.

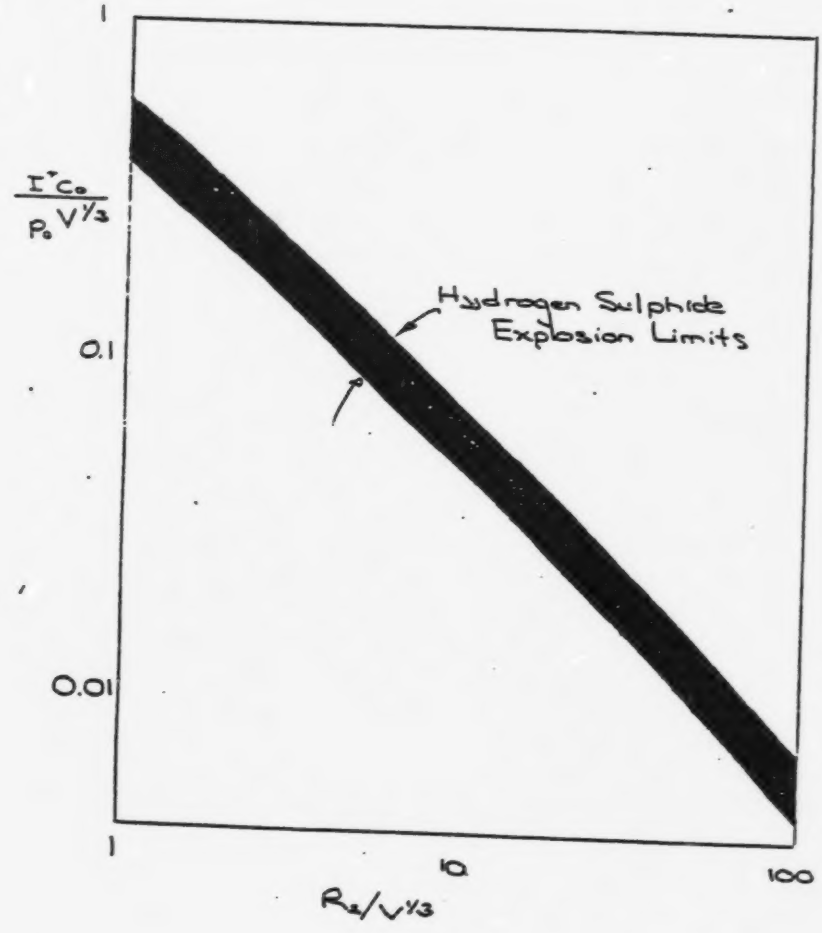

FIGURE J.4

SCALED POSITIVE IMPULSE FOR
HYDROGEN SULPHIDE DETONATION IN AIR

The positive impulse I^+ has been calculated and scaled for hydrogen sulphide combustion. The hydrogen sulphide explosion limits are shown to lie in the detonability band. The results can be compared with those for ethylene in air [see Figure J.5].

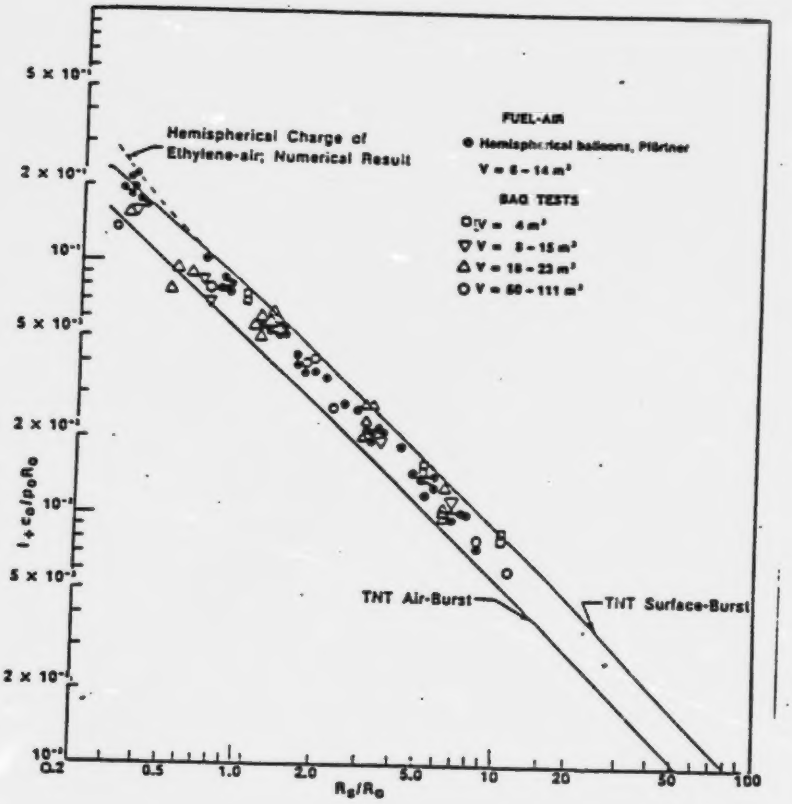

FIGURE J.5

SCALED POSITIVE IMPULSE FOR
ETHYLENE DETONATION IN AIR

The positive impulse I^+ for ethylene detonation in air compares with that for hydrogen sulphide detonation [see Figure J.4].

APPENDIX B

Detonations in Hydrogen Sulphide-Air Cloud

by

A. Sulmistras, I.O. Moen and A.J. Saber.

UNCLASSIFIED

DEFENCE RESEARCH ESTABLISHMENT SUFFIELD
RALSTON, ALBERTA

SUFFIELD MEMORANDUM NO. 1140

DETONATIONS IN HYDROGEN SULPHIDE-AIR CLOUDS

by

A. Sulmistras*
I. O. Moen
and
A. J. Saber*

PCN No. 27C50

February 1985

---

*Mechanical Engineering Department, Concordia University, Montreal, Quebec.

UNCLASSIFIED

DEFENCE RESEARCH ESTABLISHMENT SUFFIELD
RALSTON, ALBERTA

SUFFIELD MEMORANDUM NO. 1140

DETONATIONS IN HYDROGEN SULPHIDE-AIR CLOUDS

by

A. Sulmistras
I. O. Moen
and
A.J. Saber

ABSTRACT

This paper reports on an investigation to determine the detonation hazards of hydrogen sulphide/air mixtures in relation to the detonation hazards of other more common fuel-air mixtures. Parameters which characterize the sensitivity of fuel-air mixtures to detonation are discussed. Theoretical and empirical relations between the various detonation parameters are also described, and the current status of detonation hazard evaluation is summarized. Finally, the results from a series of hydrogen sulphide/air field trials are used together with previous results and numerical calculations to determine the sensitivity of this mixture to detonation. It is found that hydrogen sulphide forms a mixture with air that is less sensitive to detonation than most common gaseous hydrocarbon fuels except methane.

SPONSORSHIP

The investigation described in this report is part of a project to characterize the explosion hazards of hydrogen sulphide, which is sponsored by the Atomic Energy Control Board of Canada. The present report is the second report on this project. A previous report entitled "Investigation of The Explosion Hazards of Hydrogen Sulphide" was prepared under contract by A.J. Saber of Concordia University.

ACKNOWLEDGEMENTS

Several colleagues and organizations contributed to the work described in this paper. We would particularly like to thank Dr. Joseph Shepherd of Sandia National Laboratories for performing the calculations which allowed us to tie all the results together, and professors John Lee and Rom Knystautas for giving us access to some of the unpublished results from McGill University.

The assistance of Mr. Gayle Hall and Mr. Stephen Ward in planning and carrying out some of the field trials is gratefully acknowledged. We would also like to thank the personnel of the Field Operations Section, the Electronic Design and Instrumentation Group, and the Photo Group at DRES for their valuable assistance during the field trials. The excellent safety course and advice given by Bryne Emeneau of AECL was instrumental in planning the safety procedures required for the field tests. We would also like to thank Mr. Stan Mellsen for performing the dispersion calculations which helped us establish safety distances for the trials.

Finally we would like to thank Dr. Paul Thibault and Professor Rom Knystautas for their input through enlightening scientific and technical discussions.

TABLE OF CONTENTS

Page

ABSTRACT i

SPONSORSHIP ii

ACKNOWLEDGEMENTS iii

TABLE OF CONTENTS iv

LIST OF FIGURES v

LIST OF TABLES vi

1. INTRODUCTION .... 1.

2. DETONATION PARAMETERS .... 3.

   2.1 Equilibrium Properties .... 4.
   2.2 Minimum Initiation Energy .... 5.
   2.3 Critical Tube Diameter .... 6.
   2.4 Detonation Structure .... 7.
   2.5 Detonability Limits .... 9.

3. EXPERIMENTAL DETAILS .... 11.

4. RESULTS AND DISCUSSION .... 12.

   4.1 Equilibrium Detonation Properties .... 13.
   4.2 Cell Size and Critical Tube Diameter .... 14.
   4.3 Minimum Initiation Energy .... 16.

5. CONCLUSION .... 17.

REFERENCES
TABLES
FIGURES

APPENDIX A - Safety Procedures for Hydrogen Sulphide Trials

APPENDIX B - Cell Structure Records

LIST OF FIGURES

FIGURE 1 CHAPMAN-JOUGUET (C-J) DETONATION PARAMETERS FOR VARIOUS FUEL-AIR MIXTURES
1a C-J VELOCITY vs. EQUIVALENCE RATIO
1b C-J PRESSURE RATIO vs. EQUIVALENCE RATIO
1c C-J TEMPERATURE RATIO vs. EQUIVALENCE RATIO
1d DETONATION ENERGY (Q) vs. EQUIVALENCE RATIO

FIGURE 2 TYPICAL CELLULAR STRUCTURE OF DETONATIONS IN FUEL-AIR MIXTURES
2a TRANSVERSE WAVE STRUCTURE OF DETONATION
2b SMOKED FOIL RECORD
2c INTERPRETATION OF SMOKED FOIL RECORD

FIGURE 3a AERIAL VIEW OF TEST SITE
3b EXPERIMENTAL LAYOUT
3c SCHEMATIC OF EXPERIMENTAL LAYOUT

FIGURE 4 H_2S TRIALS INSTRUMENTATION LAYOUT

FIGURE 5 CRITICAL TUBE PRESSURE RECORDS (DETONATION FAILURE)

FIGURE 6 C-J VELOCITY vs. % HYDROGEN SULPHIDE

FIGURE 7 C-J PRESSURE vs. % HYDROGEN SULPHIDE

FIGURE 8 COMPARISON OF CELL STRUCTURES

FIGURE 9 TEMPERATURE PROFILE IN THE ZND MODEL OF A DETONATION

FIGURE 10 INDUCTION ZONE LENGTH vs. % H_2S

FIGURE 11 COMPARISON OF CELL DIAMETERS WITH SCALED INDUCTION LENGTH

FIGURE 11 CRITICAL TUBE DIAMETER COMPARISONS FOR VARIOUS FUELS

FIGURE 13 CRITICAL INITIATION ENERGY vs. CRITICAL TUBE DIAMETER

LIST OF TABLES

TABLE I - Detonation Parameters for Fuel-Air Mixtures

TABLE II - Field Trials Summary

TABLE III - Measured Detonation Parameters

DEFENCE RESEARCH ESTABLISHMENT SUFFIELD
RALSTON, ALBERTA

SUFFIELD MEMORANDUM 1140

DETONATIONS IN HYDROGEN SULPHIDE-AIR CLOUDS

by
A. Sulmistras
I. O. Moen
and
A.J. Saber

1. INTRODUCTION

Many manufacturing and industrial plants store and use large quantities of flammable gases. For personnel and plant safety, it is therefore necessary to realistically assess the potential hazards from an accidental spill of these fuels. Of particular importance are the consequences if the spilled gases are ignited. If ignition occurs immediately, a diffusion flame will result and the rate of burning will be controlled by the mixing of the fuel with air. In this case, the hazards due to thermal radiation from the burning fireball are more important than blast effects. However, if immediate ignition does not occur, a potentially explosive fuel-air cloud will develop. This cloud will be fuel lean at the outer perimeter and fuel rich near the source. Depending on the nature of the ignition source and reactivity of the fuel-air mixture, such a cloud can either detonate or burn. Detonations are the most devastating explosions possible and are characterized by high velocities and high pressures. Flame velocities and flame pressures, on the other hand, depend on the obstacle configuration and flow field into which the flame propagates. An initially laminar flame in the presence of obstacles, for example, will accelerate and become turbulent with a corresponding increase in its velocity and pressure.[1,2] Also, depending on the scale of turbulence and the flame speed, transition to detonation could occur.[3,4] In order to assess the explosion hazards associated with a spill of a given fuel, one must first quantify the sensitivity of a given fuel-air mixture to detonation and transition to detonation.

Two key properties which characterize the detonability of an explosive mixture are; i) the critical energy, E_c, required to initiate detonation in the mixture, and ii) the critical tube diameter, d_c, required for a planar detonation emerging from a tube to transmit to an unconfined spherical detonation. These properties are intimately related to the chemical processes within the detonation wave. Due to the complexity of the detonation structure, these detonation parameters cannot yet be calculated from first principles. Experimental input is therefore required in order to characterize the detonability of an explosive mixture. Fortunately, theoretical and empirical relationships between various detonation parameters have recently been established, so that a number of experimental methods can now be used to determine the detonation sensitivity of a given mixture. A more complete discussion of detonation parameters and their inter-relationships is given in Section 2.

Once it is assumed that the threat of detonation does exist, it is important to determine the blast effects. Detonation parameters, such as detonation velocity, pressure and temperature, can be calculated from equilibrium thermodynamic chemistry alone. Computer codes are readily available for this purpose.[5] These equilibrium parameters provide the initial conditions for calculation of the complete blast field both inside and outside the detonation cloud. Considerable theoretical and numerical work in this area has been done for the Defence Research Establishment Suffield (DRES) by Thibault. This work is now at the point where accurate flow field predictions from fuel-air detonations can be made.[6,7] Thus, once the potential for detonation and transition to detonation have been determined, a realistic estimate of the subsequent blast waves can be made.

The present paper reports on an experimental investigation to determine the sensitivity of hydrogen sulphide/air (H_2S/air) mixtures to detonation in relation to the sensitivity of other more common fuel-air mixtures. Hydrogen sulphide is a gaseous fuel at standard atmospheric conditions and is used in large quantities in the Girdler-Sulphide process for production of heavy water (deuterium oxide), which is an essential material for the operation of CANDU nuclear reactors.

Previous studies on detonations in H_2S/air were limited to confined detonation tubes[8] and the influence of confinement was not accounted for. However, some of the data from these tests do provide useful input to the assessment of the detonability when interpreted in the light of more recent developments.[9]

A brief review of detonation parameters, their inter-relationship and physical significance is given in Section 2. This is followed in Section 3 by a description of the experimental apparatus and diagnostic techniques used in the present experiments. The experimental results are presented and discussed in Section 4, and Section 5 contains the conclusion to this investigation.

2. DETONATION PARAMETERS

A detonation can be simply described as a coupled reaction zone-shock wave complex which propagates through a uniform combustible mixture at a constant velocity. The shock wave heats up the mixure to a temperature above the ignition temperature, thus providing the ignition source for combustion to begin, and the chemical energy released in the reaction zone provides the energy required to maintain the shock wave.

A one-dimensional model of the detonation wave, usually called the Zeldovich-von Neumann-Doring or ZND model, includes an induction zone separating the leading shock wave and the onset of chemical reaction.[10] It is now known that the structure of detonations is in fact three-dimensional and includes waves moving transverse to the direction of detonation propagation. Nevertheless, the ZND model provides a useful first approximation to the detonation structure. In fact, many detailed chemical-kinetic models of detonations use the hypothetical ZND induction zone length to characterize the relative detonability of different explosive mixtures.

The parameters which are used to characterize a detonation include: i) the equilibrium properties (i.e., detonation velocity, pressure and temperature), ii) the minimum energy, E_c, required to establish a detonation, iii) the critical tube diameter, d_c, which characterizes the minimum size of a detonable cloud, and iv) parameters which characterize the structure of the detonation (i.e., the transverse wave spacing, S, or the ZND induction length, Δ). Detonation parameters for some common fuel-air mixtures at stoichiometric composition are given in Table I. Results for hydrogen sulphide/air mixtures which were obtained in the present study are also included in this table.

2.1 Equilibrium Properties

The velocity of a detonation can be calculated based on the total chemical energy released in the reaction zone without regard to how this energy is deposited. The corresponding pressure and temperature at the end of the reaction zone, or the so-called Chapman-Jouguet (C-J) point, can also be calculated from equilibrium chemistry alone. Standard numerical codes which combine chemical equilibrium calculations with the gasdynamic C-J conditions are available for this purpose.[5]

Detonation pressure ratios and velocities for some fuel-air mixtures at stoichiometric composition are given in Table I, and the variation of C-J detonation velocity, pressure ratio and temperature ratio with fuel-air composition are shown in Figures 1a), b) and c), respectively. The fuel-air composition is denoted by the equivalence ratio, which is defined as the fuel to air ratio divided by the fuel to air ratio at stoichiometric composition. Also included in Table I and plotted in Figure 1d, is the chemical energy, Q, released in the detonation wave. This parameter can be used to estimate the far-field blast wave from a detonating cloud by comparing with the blast from an equivalent energy TNT solid-explosive charge.[6] The energy content of TNT is about 4.2 MJ/kg, which can be compared with 2.0 MJ/kg of mixture for a stoichiometric H_2S/air cloud. Since stoichiometric H_2S/air contains only 8% H_2S by mass, this corresponds to 22 MJ/kg of H_2S. It must be emphasized that blast estimates based on TNT equivalent energy are reliable only in the far-field and should not be used for locations close to the fuel-air cloud (i.e., closer than twice the maximum dimension of the cloud).

2.2 Minimum Initiation Energy

A minimum quantity of energy is required in order to establish a detonation in a given explosive mixture. This energy depends on the geometry of the cloud, the boundary conditions and the source of the energy. For fuel-air mixtures, the critical initiation energy is usually characterized by the minimum mass of tetryl high-explosive required to initiate a spherical detonation in an unconfined cloud. The equivalent energy of tetryl is approximately 4.2 KJ/kg. The minimum tetryl initiation masses for several fuel-air mixtures are given in Table I. These range from about 1 g for acetylene and hydrogen to an estimated 22 kg for methane. Further data, including data for off stoichiometric compositions can be found in the reviews by Bull[11] and by Lee[12]. The dependence of the critical energy on composition is typically in the form of a U-shaped curve with the minimum near stoichiometric composition. Matsui and Lee[13] proposed that this minimum energy be used as a relative measure of the detonation hazard of the gas mixture.

Unfortunately, the critical initiation energy is relatively difficult to measure experimentally. It is usually determined by a GO NO-GO procedure based on the variation of high-explosive charge detonated in a cloud of the mixture. For insensitive fuel-air mixtures, 100 g or more of explosives are required to initate detonation and large clouds are necessary to ensure that a stable detonation has been established. Furthermore, the explosive charges must be carefully prepared and positioned away from cloud boundaries in order to ensure consistent results. Due to these experimental difficulties, critical tube diameter tests have to a large extent replaced critical energy tests for determining the detonation sensitivity of fuel-air mixtures.

2.3 Critical Tube Diameter

The critical tube diameter, d_c, is the minimum diameter of a round tube for which a detonation wave emerging from the tube will successfully re-establish itself in a surrounding unconfined cloud. With a smaller tube and the same explosive mixture, the expansion as the detonation wave diffracts from the tube causes the shock wave and combustion zone to separate to such an extent that the detonation is quenched. The critical tube diameter is therefore a measure of the minimum frontal size of detonation required for stable propagation in an unconfined cloud. In other words, an unconfined cloud with one dimension less than d_c could not support a detonation.

The critical tube diameter is as characteristic of an explosive mixture as the critical initiation energy and provides an alternative measure of detonation sensitivity. Based on a simple work-done model, Matsui and Lee[13] obtain a relationship between these two detonation parameters of the form, $E_c \propto d_c^3$. Although such a relationship provides a reasonable correlation for many fuels, the proportionality factor depends on the fuel.[14]

Critical tube diameters for some common fuel-air mixtures at stoichiometric composition are included in Table I. Notice that these mixtures span a large range of critical tube diameters, from a minimum of 0.115 m for acetylene-air up to an estimated value of about 3.6 m for methane-air. These data, as well as data for off-stoichiometric compositions are summarized in References 12 and 14.

The variation with composition is again represented by a U-shaped curve with a minimum critical tube diameter, corresponding to maximum sensitivity, near stoichiometric composition.

Both the critical tube diameter and the critical initiation energy are intimately related to the cellular detonation structure and the detailed chemical kinetic processes within the cellular detonation front. In fact, empirical relations between these parameters and the parameters which characterize the detonation structure have been established. These relations are now being used to determine the detonation sensitivity of an explosive mixture based solely on the scale of the detonation structure.

2.4 Detonation Structure

A detonation wave consists of a three-dimensional shock structure which includes transverse waves moving perpendicular to the detonation front as illustrated in Figure 2a.[10,15] A "footprint" of this structure can be recorded by placing a soot-coated foil parallel to the direction of propagation. As the detonation passes the soot-foil, the slipstreams behind the triple-point shock interactions trace out a diamond shape structure as seen in Figure 2b. It is the width of the diamonds in this structure, corresponding to the maximum separation of the transverse waves, which is measured as indicated in Figure 2c.[16] The cell width, S, is also commonly referred to as the detonation cell size or cell diameter. The cell length is approximately 1.6 times the cell width.[17]

The detonation cell size is another fundamental length scale which can be used to characterize the sensitivity of an explosive mixture, with larger cells corresponding to less sensitive mixtures. For a given mixture, the cell is usually smallest close to stoichiometric composition and increases in size away from stoichiometry as the mixture becomes less sensitive. The cell sizes for some common fuel-air mixtures at stoichiometric composition are included in Table I.[12,14,16-18]

The regularity of the cellular structure depends on the explosive mixture. For less sensitive mixtures with large cells, the structure can become highly irregular with many modes of cellular patterns. Identification of the dominant mode is therefore subject to some interpretation.[14] There is now considerable experimental evidence that the cell size, properly interpreted, is related to the critical tube diameter through the simple relation, $d_c = 13\ S$.[12,18,19] For the fuel-air mixtures included in Table I, the ratios of critical tube diameter to cell size are between 11.7 (for acetylene) and 15.4 (for ethylene), in good agreement with the emipirical d_c=13 S relation. The sensitivity of an explosive mixture can therefore be determined by simply monitoring the structure of detonations in the mixture. This method is now widely used, particularly for the less sensitive fuel-air mixtures and for other systems which are not amenable to large scale critical tube diameter testing. Cell size measurements are being used, for example, to determine the detonation sensitivity of hydrogen/air/steam at elevated temperatures for nuclear reactor safety studies.[20,21]

The modelling of the coupled chemical kinetic-gasdynamic processes within a cellular detonation front is still in the early development stages,[22,23] so that predictions of the cell size for a given mixture cannot yet be made in a reliable manner. However, comprehensive chemical kinetic models have been used to calculate the one-dimensional ZND induction zone length, Δ. It is then assumed that the cell size is proportional to this length (i.e., $S = A\ \Delta$). Based on this assumption, extensive induction length calculations have been performed by Westbrook[24-26] in order to predict cell sizes for various hydrocarbon and hydrogen systems. Roller and Shepherd[27] have also used this approach to predict the detonability of hydrogen/air/steam and hydrogen/air/carbon dioxide mixtures. In general, agreement with experiments is good, although deviations from a linear relationship are observed, particularly for very lean and rich mixture compositions. Furthermore, the proportionality factor, A, depends on the fuel-air system so that some cell size and/or critical tube diameter data are required to determine this factor.

2.5 Detonability Limits

From the practical point of view it is important to know for what fuel-air compositions a mixture is detonable. For an unconfined cloud, the minimum dimension of the cloud must be larger than the critical tube diameter in order for the cloud to support a detonation. Detonability limits could therefore be defined based on the size of the cloud. This does not take into account the energy required to establish a detonation in the cloud. For large unconfined clouds, composition limits based on initiation energy are probably more meaningful than those based on cloud size. In other words, the compositional limits are determined by specifying the maximum amount of energy or mass of solid explosive available to initiate a detonation. Mixtures which require less energy than this specified maximum are called detonable and those which require more are called non-detonable. The compositional limits therefore depend on the specified maximum energy.[12]

Composition limits based on a specified maximum energy become meaningless in a realistic accidental spill scenerio where there are obstacles and partially confined spaces to accelerate the flame and cause localized explosions. In such situations the energy required to establish a detonation can be supplied by combustion of the mixture itself and need not be supplied externally. Recent studies of transition to detonation show that explosions of pockets with dimensions of the order of the critical tube diameter can cause onset of detonation in a surrounding cloud.[4] This is not the only possible mechanism for transition to detonation, but all mechanisms do rely on achieving fast enough combustion to produce shock waves of sufficient strength and duration to cause onset of detonation.[3] Reliable criteria for transition to detonation in terms of minimum flame speed, rate of burning and energy release are not yet available. Such criteria will depend on the reaction chemistry which is characterized, at least globally, by the detonability parameters previously described.

The critical tube diameter, or equivalently the cell size, also determines the size of opening required for a confined detonation to transmit into a surrounding cloud. Since transition to detonation is much more likely in confined spaces, such transmissions can be important for explosion hazards evaluation.

Specifications of detonability limits for realistic accidental spill scenarios must therefore take into account not only the initial conditions (i.e., the ignition source) but also the boundary conditions (i.e., the presence of obstacles and partial confinement). For accidental spill situations, it is therefore more meaningful to base limits on the dimensions of the cloud in relation to the critical tube diameter. If these dimensions are smaller than the critical tube diameter, the unconfined parts of the cloud cannot support a detonation. Even in highly confined geometries, a minimum size of cloud is required in order for a stable detonation to propagate. The limiting condition in a confined tube, for example, occurs when only one transverse wave is present. This mode of propagation is called "single-head spin" propagation.[9,15]

The cell size at the onset of single-head spin in a tube of diameter D can be calculated by assuming a purely acoustic transverse wave. This gives a spin pitch (or cell length) to tube diameter ratio, $P/D = \pi V/k_1 c$, where V is the detonation velocity, c is the local speed of sound and k_1 is the first root of the derivative of the Bessel function of order one ($k_1 = 1.841$). The corresponding cell width is then given by, $S = 0.6\ P$. Moen et al.[9] used the onset of "single-head spin" in different diameter tubes to determine the cell size for several ethylene-air mixtures. The cell sizes obtained in this manner are in excellent agreement with those measured from soot foils.

From the above discussions, it is clear that there are many ways of characterizing the detonability of an explosive mixture. Fortunately, theoretical and empirical links have been established in recent years, so that the assessment of detonability can now be made in a reliable manner using a variety of methods. In the investigation of hydrogen sulphide/air mixtures, we have taken advantage of these links to minimize the number of tests required with this highly toxic material.

3. EXPERIMENTAL DETAILS

The experimental test series was performed at the DRES fuel-air facility. An aerial view of the facility showing the test pad, instrumentation and fuel-flow control trailers, and high-speed camera shelters is included as Figure 3a. The facility, which is described in detail in Reference 28, is centered around an 18.3 m x 7.6 m concrete test pad onto which the experimental apparatus can be mounted. A photograph of the test pad with a typical test section used in the present critical tube diameter tests is shown in Figure 3b. The test section consisted of a 0.89 m diameter steel tube, 7.8 m long, attached to either a 1.8 or 0.89 m diameter polyethylene bag at one end. The length of the bag was varied from 0.5 m to 5 m, depending on the test. A schematic diagram of a typical test configuration is shown in Figure 3c.

In addition to tests using hydrogen sulphide (H_2S), two tests were performed using butane (C_4H_{10}) as a fuel so that a direct comparison between detonations with H_2S and a common hydrocarbon fuel could be made. The test gases (Technical grade, 99% pure H_2S or CP grade, 99% pure C_4H_{10}) were mixed with the initial air in the test volume by a multipath recirculation system using a high-capacity centrifugal blower.

The composition and mixture homogenity in the test volume were monitored by continuously analyzing samples taken from two ports in the tube using a "Wilks Miran 1A" infrared gas analyzer. The absorption spectrum for hydrogen sulphide shows that this gas is a poor absorber in the infrared. A small absorbance peak can be found at wavelength, $\lambda = 3.70$ μm, with other peaks between $\lambda \sim 7.5$ μm to $\lambda \sim 9.5$ μm. The poor absorbtion characteristics of hydrogen sulphide required that large absorption pathlengths be used. This greatly increased the possibility of small impurities affecting the infrared readings. The concentration of H_2S during the first three trials were monitored at a wavelength of 8.0 μm. At this wavelength, impurities in the system tended to overestimate the hydrogen sulphide concentration. Subsequent trials were conducted using $\lambda = 3.70$ μm. The difficulties in assuring an accurate mixture were then significantly reduced, and the maximum uncertainty in H_2S concentration was less than ±0.25% H_2S. With butane as a fuel, this uncertainty was less than 0.05% C_4H_{10}.

Once the desired fuel-air composition had been attained in the test volume, detonation was initiated at the far end of the tube using a DM12 high-explosive charge. In one test, this charge was placed on the pad at the centre of the bag.

The arrival and pressure profile of the wave were monitored at various positions along the tube and bag using piezoelectric pressure transducers. Far-field pressure profiles were also monitored in selected tests. The positions of the pressure transducers is shown in Figure 4. High-speed photographic records of the transmission and propagation of the wave were obtained using a Photec camera (~ 12,000 half frames/sec) placed 90° to the tube axis. A Hycam camera (~ 12,000 half-frames/sec) placed at a 30° angle, as well as an end camera (~ 5,000 frames/sec) looking directly down the tube, were also used on selected trials. The positions of these cameras are illustrated in Figure 4. The detonation cell structure was recorded by placing a large steel sheet (3 m long by 1.5 m wide) around the inside walls of the tube. This sheet was carefully sooted using a rich burning acetylene-oxygen torch.

Since hydrogen sulphide and the main product of combustion, sulphur dioxide, are both highly toxic, special safety procedures were followed in carrying out the tests. These procedures are outlined in Appendix A.

4. RESULTS AND DISCUSSION

A summary of the trials performed is given in Table II. For all hydrogen-sulphide/air mixtures, the detonation failed to transmit from the tube into the bag. The critical tube diameter for H_2S/air is therefore larger than 0.89 m. For butane/air mixtures, however, the detonation successfully transmitted into the bag so that for these mixtures the critical tube diameter is less than 0.89 m.

4.1 Equilibirum Detonation Properties

The failure of the detonations to re-establish themselves in the bag for H_2S/air mixtures was confirmed from both the high-speed photographic records and the pressure records. A typical set of pressure records showing failure in the bag is included in Figure 5. The records in the tube (Positions #1, 2, 3) are characteristic of a stable detonation wave propagating at a velocity of 1660 m/s with a peak overpressure of about 15 atmospheres. The pressure fluctuations observed during the first millisecond or so after the arrival of the wave are due to pressure variations within the three-dimensional detonation structure. As the detonation wave propagates into the bag, it is quenched by the expansion and fails to re-establish itself. By the time the pressure wave reaches Position #5, 3 m from the tube exit, the peak overpressure is less than 3 atmospheres.

As discussed in the previous section, H_2S concentrations measured by the IR analyzer in Trials #10, 11 and 12 were higher than actual due to the presence of impurities. The H_2S/air compositions were therefore inferred from the detonation velocity measured in the tube. Previous tests, in the same 0.89 m tube for a variety of fuel-air mixtures, show that the measured detonation velocities are in excellent agreement with the calculated C-J values. Typically, the observed velocity is 1 - 2% less than the calculated velocity. This observed velocity deficit is due to boundary effects in the tube. Based on these previous observations, the composition in Trials 10, 11 and 12 was inferred by taking one concentration limit at the C-J velocity corresponding to the observed velocity and the other limit at a C-J velocity 2.5% larger. The reliability of this estimate was confirmed in two subsequent tests (Trial #26 and 29) with more accurate IR-analyzer readings. The measured detonation velocities are tabulated in Table III, and the observed and calculated detonation velocities for H_2S/air are compared in Figure 6. For both Trial #26 and 29 the measured velocity is within 2.5% of the calculated value. Detonation velocities observed in butane/

air are also within 2.5% of the calculated C-J value. The compositions inferred for Trials #10, 11 and 12, as indicated in Figure 6, should therefore give a reliable estimate of the H_2S/air mixture in the test section.

A further check on the composition and the stability of the detonation waves in the tube is provided by detonation pressure inferred from the pressure records. Unfortunately, these records can be difficult to interpret due to the pressure fluctuations. An estimate of the C-J pressure can be obtained by extrapolating a curve representing the average pressure over a 1 ms interval to the time of arrival. The results from such estimates are included in Table III. The pressures measured in H_2S/air mixtures are compared with the theoretical C-J pressures in Figure 7.

4.2 Cell Size and Critical Tube Diameter

The above comparisons between observed and calculated equilibrium detonation properties confirm that stable detonations in H_2S/air were established in the tube. None of these detonations successfully transmitted into the bag so that a direct measure of a critical tube diameter could not be made. Only a lower bound of 0.89 m on the critical tube diameter for H_2S/air could be established. A more quantitative assessment of the detonability was obtained from the cellular structure recorded on the sooted steel sheets. Cell structures observed for near stoichiometric butane/air and two H_2S/air mixtures are compared in Figure 8. This comparison shows that the cell size in stoichiometric H_2S/air is about twice that in stoichiometric C_4H_{10}/air. For mixtures with 10% H_2S, the cell size is more than a factor of two larger than at stoichiometric H_2S/air composition. The cell sizes measured in the present tests are given in Table III and cell structure records from all the H_2S air tests are included in Appendix B.

The two additonal cell size data for H_2S/air shown in Table III were obtained by re-examining pressure records from tests performed at McGill University in a 145 mm diameter tube.[8] These records show that single-head spin appears in this tube for H_2S concentrations between 9% - 10% and 20% - 22%.

Using the relation, $P/D = \pi V/k_1 c$, discussed in Section 2.4, this gives a spin pitch or cell length of 432 mm between 9 -10% H_2S and 440 mm between 20 - 22% H_2S. The corresponding cell widths based on $S = 0.6\ P$ are 260 mm and 264 mm, respectively.

As discussed in Section 2.4, the one-dimensional ZND induction zone length, Δ, has been used as an alternate detonation sensitivity parameter. Induction zone length correlations have been relatively successful in describing the variation in detonation parameters with composition and additives for a variety of mixtures.[24-27,29] The predictions of Roller and Shepherd for the hydrogen/air/steam system are particularly impressive.[27] At our request, Shepherd performed similar calculations for the H_2S/air system.[30] His chemical-kinetic calculations are based on 51 reactions and 17 species, and he defines an induction length as the length from the shock to the location of the point at which the local gas velocity is 0.95 of the local speed of sound (Mach No. $M = 0.95$) in a one-dimensional ZND model of the detonation wave. This point occurs at a distance slightly after the point of maximum rate of temperature increase as illustrated in Figure 9. Shepherd's results for the induction zone length are plotted as a function of H_2S/air composition in Figure 10. A comparison of the variation of the cell size with that of the induction zone length can be made by assuming a linear relationship between these two length scales as discussed in Section 2.4. For H_2S/air, the scaling factor relating the cell size and the induction zone length was determined by normalizing to a cell size of 110 mm at 14.2% H_2S. This gives a scaling factor of 17.8, which can be compared with a factor of 24.2 obtained for hydrogen/air mixtures. The comparison of measured cell size with scaled induction zone length in Figure 11, shows that this correlation is in good agreement with experiment and that the scaled induction zone length can be used to predict cell sizes for H_2S/air compositions between about 9% and 22% H_2S. Extrapolation to leaner and richer mixtures is also possible. However, previous results for other fuel-air mixtures show that such extrapolations tend to underestimate the sensitivity of very lean and rich mixtures.[14,16]

The empirical correlation $d_c = 13\ S$ can now be used to estimate the critical tube diameter for comparison with more common fuels. Critical tube diameters for a variety of fuel-air mixtures are compared with those for H_2S/air in Figure 12. The results for acetylene, hydrogen, ethylene and propane are based on the correlations of critical tube diameter results by Moen et al.[14] All the other results are based on a 13 S estimate. The minimum critical tube diameter for H_2S/air is 1.3 m at stoichiometric composition. This can be compared with minimum critical tube diameters of less than 0.9 m for common fuels such as propane and butane. Only methane/air mixtures are less sensitive to detonation with an estimated minimum critical tube diameter of almost 4 m.

4.3 Minimum Initiation Energy

A good illustration that the energy required to initiate a detonation depends on the configuration of the cloud and the cloud boundaries is obtained by comparing Trials #10 and #30. In both trials the mixture was about 10% H_2S in air. In Trial #10, a 300 g explosive charge placed at one end of the tube successfully initiated an essentially planar confined detonation in the tube. However, in Trial #30, a 500 g charge placed on the ground under the plastic bag failed to initiate an expanding hemispherical detonation in the bag. Furthermore, the 500 g charge was placed on a solid surface so that the effective energy of the charge is approximately doubled. Considerably more energy is therefore required to initiate a detonation in an unconfined cloud than in the same mixture confined in a tube.

The failure of an equivalent 1 kg mass of solid explosive to initiate an unconfined detonation in a 10% H_2S/air mixture, with an estimated critical tube diameter of 3.6 m, is consistent with the approximate $E_c \propto d_c^3$ relationship observed for other fuel-air mixtures. As shown in Figure 13, the proportionality factor depends on the mixture, but even using the factor for ethane fuel, which has the smallest factor, a minimum solid explosive mass of about 2 kg would be required to initiate a detonation in a H_2S/air mixture with the same critical tube diameter. It can therefore be concluded that the factor relating E_c and d_c^3

is not significantly smaller for H_2S/air mixtures. In other words, the minimum initiation energies estimated from Figure 13, based on the ethane curve, provides a lower bound to the energy required. For stoichiometric H_2S/air with a critical tube diameter of 1.3 m, this lower bound is 80 g of tetryl. However, as discussed above, this is for a completely unconfined cloud. The minimum energy could be significantly lower for confined clouds.

5. CONCLUSION

The relative detonation sensitivity of hydrogen sulphide air mixtures has been determined in a series of large scale experimental tests. These tests show that H_2S/air mixtures are less sensitive to detonation than propane or butane/air mixtures. Evaluations based on these common hydrocarbon fuels therefore provide a conservative estimate of the detonation hazards associated with a spill of hydrogen sulphide.

A minimum critical tube diameter of 1.3 m is obtained for stoichiometric H_2S/air mixtures. This can be compared with corresponding critical tube diameters less than 0.9 m for both propane and butane/air mixtures. Of the common hydrocarbon gases, only methane forms a less detonation sensitive mixture than hydrogen sulphide when mixed with air.

The minimum energy required to establish a detonation in an unconfined hydrogen sulphide/air cloud, is estimated to be larger than that from 80 g of solid explosives. It is therefore unlikely that detonation could accidentally occur in such a cloud. However, most accidental spills occur in environments with obstacles and partially confined spaces. In such environments, flame acceleration and localized explosions will play an important role in assessing the detonation hazards. Although considerations of transition to detonation in such situations are outside the scope of the present investigation, it can be concluded that transition to detonation is less likely with hydrogen sulphide than with most common gaseous hydrocarbon fuels except methane.

REFERENCES

1. Moen, I.O., Donato, M., Knystautas, R., Lee, J.H. and Wagner, H.Gg., "Turbulent Flame Propagation and Acceleration in the Presence of Obstacles", Progress in Astronautics and Aeronautics, 75, 33 (1981).

2. Moen, I.O., "Fuel-Air Explosions" (J.H. Lee and C.M. Guirao, Eds.), SM Study No. 16, p. 101, University of Waterloo Press, Ontario, Canada, 1982.

3. Lee, J.H.S. and Moen, I.O., "The Mechanism of Transition from Deflagration to Detonation in Vapour Cloud Explosions", Progress in Energy and Combustion Science, 6, 359 (1980).

4. Moen, I.O., Thibault, P.A., Bjerketvedt, D. and Jenssen, A., "Transition to Detonation in a Large Fuel-Air Cloud", Defence Research Establishment Suffield, Ralston, Alberta; open literature paper, submitted to Combustion and Flame, Oct. 1984.

5. Gordon, S. and McBride, B., "Computer Program for Calculation of Complex Chemical Equilibrium Compositions, Rocket Performance, Incident and Reflected Shocks, and Chapman-Jouguet Detonations", NASA Report SP-273, Washington, D.C., 1976.

6. Moen, I.O., Thibault, P.A. and Funk, J.W., "Blast Waves from Non-Spherical Fuel-Air Explosions", Proceedings of the Eight International Symposium on Military Applications of Blast Simulation, Paper No. I.7, Spiez, Switzerland, June 1983.

7. Thibault, P.A., "Blast Waves from Detonation of Fuel-Air Clouds", Defence Research Establishment Suffield, Ralston, Alberta (in draft Feb. 1985).

8. Lee, J.H.S. and Knystautas, R., McGill University. Private communication, July 1984.

9. Moen, I.O., Donato, M. Knystautas, R. and Lee, J.H., "The Influence of Confinement on the Propagation of Detonations Near the Detonability Limits", Eighteenth Symposium (International) on Combustion, p. 1615, The Combustion Institute, Pittsburgh, Pa., 1981.

10. Fickett, W. and Davies, W.C. "Detonation", University of California Press, Berkeley, California, 1979.

11. Bull, D.C., "Concentration Limits to the Initiation of Unconfined Detonation in Fuel/Air Mixtures", Trans. I. Chem Eng. 57, 219 (1979).

12. Lee, J.H.S., "Dynamic Parameters of Gaseous Detonations", Annual Review of Fluid Mechanics, 16, 311 (1984).

13. H. Matsui, J.H.S. Lee, "On the Measure of the Relative Detonation Hazards of Gaseous Fuel-Oxygen and Air Mixtures", Seventeenth Symposium (International) on Combustion p. 1269, The Combustion Institute, Pittsburgh, Pa., 1978.

14. Moen, I.O., Thibault, P.A., Funk, J.W., Ward, S.A. and Rude, G., "Detonation Length Scales for Fuel-Air Explosives". Proceedings of the 9th International Colloquium on Dynamics of Explosions and Reactive Systems, Poitiers, France, July 3 - 8, 1983. Progress in Astronautics and Aeronautics, 94, p. 55, 1984.

15. Strehlow, R.A., "Combustion Fundamentals", McGraw-Hill Inc. New York, 1984.

16. Moen, I.O., Murray, S.B., Bjerketvedt, D., Rinnan, A., Knystautas, R. and Lee, J.H., "Diffraction of Detonation from Tubes into a Large Fuel-Air Explosive Cloud", Nineteenth Symposium (International) on Combustion, p. 635, The Combustion Institute, Pittsburgh, Pa., 1982.

17. Bull, D.C., Elsworth, J.E., Shuff, P.J. and Metcalf, E., "Detonation Cell Structures in Fuel/Air Mixtures", Combustion and Flame 45, 7 (1982).

18. Knystautas, R., Guirao, C., Lee, J.H. and Sulmistras, A., "Measurement of Cell Size in Hydrocarbon-Air Mixtures and Predictions of Critical Tube Diameter, Critical Initiation Energy and Detonability Limits", Proceedings of the 9th International Colloquium on Dynmaics of Explosions and Reactive Systems, Poitiers, France, July 3-8, 1983. Progress in Astronautics and Aeronautics, 94, p. 23, 1984.

19. Knystautas, R., Lee, J.H. and Guirao, C.M., "The Critical Tube Diameter for Detonation Failure in Hydrocarbon-Air Mixtures", Combustion and Flame, 48, 63 (1982).

20. Lee, J.H.S., Knystautas, R., Guirao, C., Benedick, W.B. and Shepherd, J.E., "Hydrogen-Air Detonations", Second International Workshop on the Impact of Hydrogen on Water Reactor Safety, Albuquerque, New Mexico, Oct. 3-7, 1982.

21. Guirao, C.M., Knystautas, R., Lee, J.H.S., Benedick, W., and Berman, M., "Hydrogen-Air Detonations", Nineteenth Symposium (International) on Combustion, p. 583, The Combustion Institute, Pittsburgh, Pa., 1982.

22. Hiramatsu, K., Fujiwara, T. and Taki, S., "A Computational Study of Transmission of Gaseous Detonation to Unconfined Space", presented at Twentieth International Symposium on Combustion, Ann Arbor, Michigan, Aug. 12-17, 1984.

23. Kailasanath, K., Oran, E.S., Boris, J.P. and Young, T.R., "Numerical Simulations of the Structure and Propagation of Self-Sustained Detonations", Naval Research Laboratory, Washington, D.C., NRL Memorandum Report 5380, June, 1984.

24. Westbrook, C.K., "Fuel-Air Explosions", (J.H. Lee and C. Guiro Eds.), SM Study No. 16, p. 189, University of Waterloo Press, 1982.

25. Westbrook, C.K., "Chemical Kinetics of Hydrocarbon Oxidation in Gaseous Detonations", Combustion and Flame 46, 191 (1982).

26. Westbrook, C.K. and Urtiew, P.A., "Chemical Kinetic Prediction of Critical Parameters in Gaseous Detonations", Nineteenth Symposium (International) on Combustion, p. 615, The Combustion Institute, Pittsburgh, Pa., 1982.

27. Roller, S.F. and Shepherd, J.E., "Predictions of Detonability of Hydrogen-Air-Steam Mixtures", Proceedings of the Second International Conference on the Impact of Hydrogen on Water Reactor Safety, p. 1007, Albuquerque, New Mexico, Oct. 1982.

28. Funk, J.W., Murray, S.B., Moen, I.O. and Ward, S.A., "A Brief Description of the DRES Fuel-Air Explosives Testing Facility and Current Research Program", Proceedings of the International Conference on Fuel-Air Explosions, Nov. 4 - 6, 1981, SM Study No. 16, p. 565, University of Waterloo Press, Ontario, Canada, 1982.

29. Moen, I.O., Ward, S.A., Thibault, P.A., Lee, J.H., Knystautas, R., Dean, T. and Westbrook, C.K., "The Influence of Diluents and Inhibitors on Detonations", Proceedings of the Twentieth International Symposium on Combustion, Ann Arbor, Michigan, Aug. 12-17, 1984, to be published.

30. Shepherd, J.E., Sandia National Laboratories, Albuquerque, New Mexico, private communication, July, 1984.

TABLE I

DETONATION PARAMETERS FOR FUEL-AIR MIXTURES

(Stoichiometric Composition; Initial Pressure 1 atm; Initial Temperature 298.15K)

Fuel	% Fuel By Volume	Detonation Pressure Ratio	Velocity (m/s)	Energy Release (MJ/kg mixture)	Initiation Energy (g tetryl)	Critical Tube Diameter (m)	Cell Width (mm)
Acetylene (C_2H_2)	7.75	19.1	1864	2.44	1.25	0.115	9.8
Hydrogen (H_2)	29.6	15.6	1968	2.82	1.1	0.20	15
Ethylene (C_2H_4)	6.54	18.4	1822	2.35	10 NO GO 15 GO	0.43	28
Ethane (C_2H_6)	5.66	18.0	1825	2.31	30 NO GO 40 GO	~ 0.9	54 - 62
Propylene (C_3H_6)	4.46	18.5	1809	2.31	12.5	0.7	--
Propane (C_3H_8)	4.03	18.3	1798	2.29	50 NO GO 80 GO	0.9	69
n-Butane (C_4H_{10})	3.13	18.4	1796	2.28	50 NO GO 80 GO	~ 0.7 (13 S)	50 - 62
Methane (CH_4)	9.48	17.2	1801	2.31	22 x 10^3 (estimate)	3.6 (13 S)	280 ± 30
Hydrogen Sulphide (H_2S)	12.3	15.3	1647	1.96	>80	1.3 (13 S)	100
Hexane (C_6H_{14})	Aerosol	18.6	1795	2.28	25	--	--

TABLE II

FIELD TRIALS SUMMARY

TRIAL #	FUEL % (BAG DIAMETER x LENGTH)	TOTAL GAS VOLUME DIAGNOSITCS	INITIATION CHARGE	COMMENTS
10	H_2S 9.6% - 10.3% (1.8 m x 3.0 m)	12.5 m^3 Gas Mixture 6 Pressure Tranducers 1 Camera (90°)	300 g DM12	• Detonation failure in bag • Obtained cell structure record.
11	H_2S 10.5% - 11.4% (1.8 m x 3.0 m)	12.5 m^3 Gas Mixture 6 Pressure Transducers 1 Camera (90°)	500 g DM12	• Detonation failure in bag • Obtained cell structure record.
12	H_2S 12.0% - 13.2% (1.8 m x 3.0 m)	12.5 m^3 Gas Mixture 6 Pressure Transducers 1 Camera (90°)	500 g DM12	• Detonation failure in bag • Obtained cell structure record.
26	H_2S 13.9% - 14.5% (0.9 m x 0.5 m)	5.2 m^3 Gas Mixture 4 Pressure Transducers 1 Camera (0°)	300 g DM12	• Detonation failure in bag • Obtained cell structure record.
27	C_4H_{10} 3.1% - 3.2% (1.8 m x 3.1 m)	12.5 m^3 Gas Mixture 4 Pressure Transducers 3 Cameras (0°-30°-90°)	300 g DM12	• Successful detonation transmission into bag. • Obtained cell structure record.
28	C_4H_{10} 3.1% - 3.2% (2.0 m x 4.8 m)	19.4 m^3 Gas Mixture 6 Pressure Transducers 3 Cameras (0°-30°-90°)	300 g DM12	• Successful detonation transmission into bag. • Obtained cell structure record. • Far-field pressure results
29	H_2S 12.4% - 12.8% (0.9 m x 5 m)	8.0 m^3 Gas Mixture 6 Pressure Transducers 3 Cameras (0°-30°-90°)	300 g DM12	• Detonation failure in bag • Obtained cell structure record. • Far-field pressure results
30	H_2S 9.5% - 10.0% (2.0 m x 4.8 m)	19.4 m^3 Gas Mixture 6 Pressure Transducers 3 Cameras (0°-30°-90°)	500 g DM12 placed on ground at centre of bag	• Charge failed to initiate detonation

TABLE III

MEASURED DETONATION PARAMETERS

TEST #	% FUEL (by Volume)	AVERAGE VELOCITY (m/s) (in tube)	AVERAGE OVERPRESSURE (atm) (three readings)	CELL SIZE (mm)
10	9.6 - 10.3% H_2S	1544	13.6	265 - 290
11	10.5 - 11.4% H_2S	1587	14.3	160 - 190
12	12.0 - 13.2% H_2S	1660	15.2	100 - 130
26	13.9 - 14.5% H_2S	1633	14.8	102 - 118
27	3.1 - 3.2% C_4H_{10}	1817	16.2	50 - 60
28	3.1 - 3.2% C_4H_{10}	1784	15.6	55 - 62
29	12.4 - 12.8% H_2S	1611	15.2	85 - 120
Onset of single-head spin in 145 mm tube (McGill) Ref. 8	9 - 10% H_2S	----	----	260 mm
	20 - 22% H_2S	----	----	264 mm

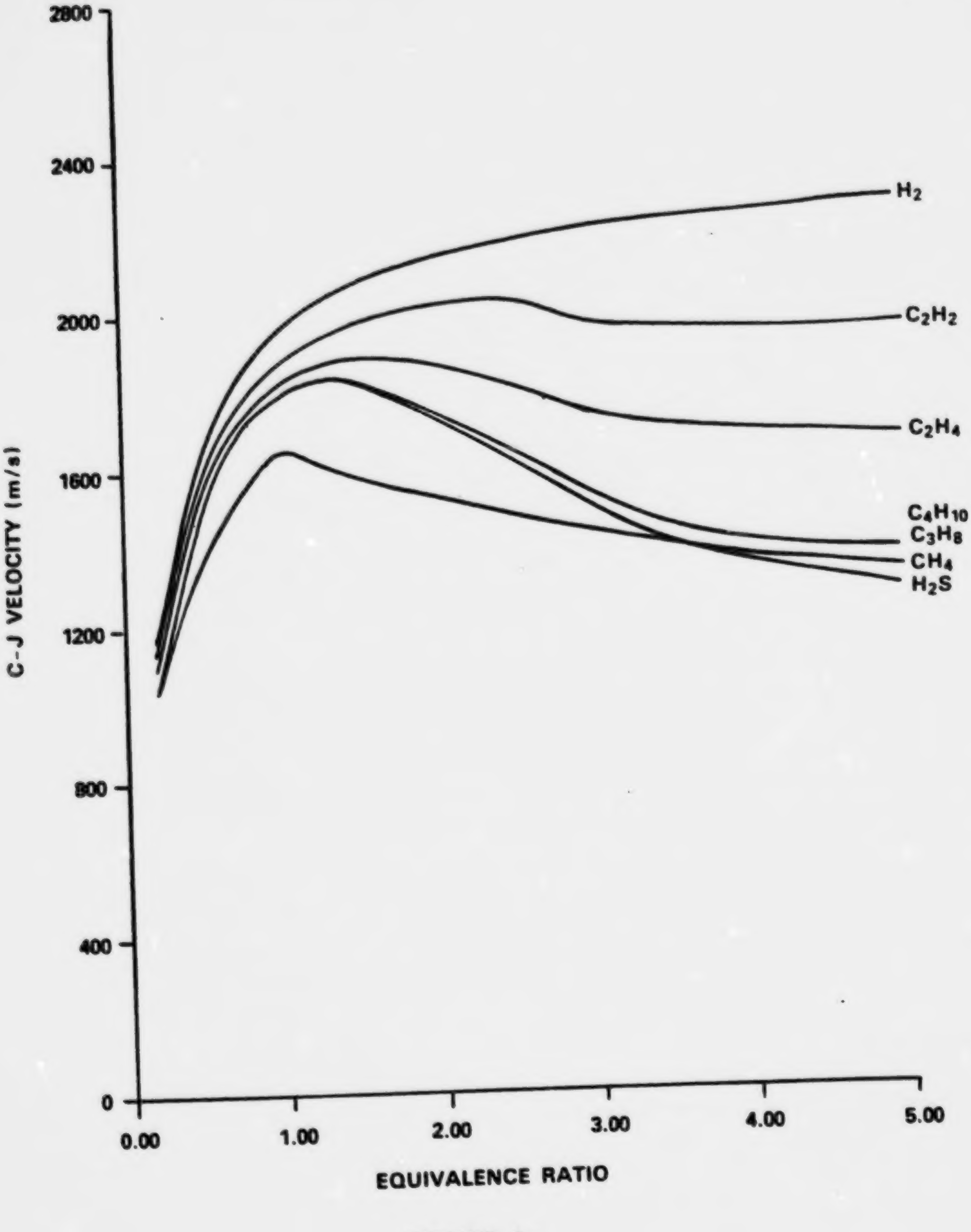
2800
2400
2000
1600
1200
800
400
0
C-J VELOCITY (m/s)
0.00
1.00
2.00
3.00
4.00
5.00
EQUIVALENCE RATIO
H_2
C_2H_2
C_2H_4
C_4H_{10}
C_3H_8
CH_4
H_2S

FIGURE 1a

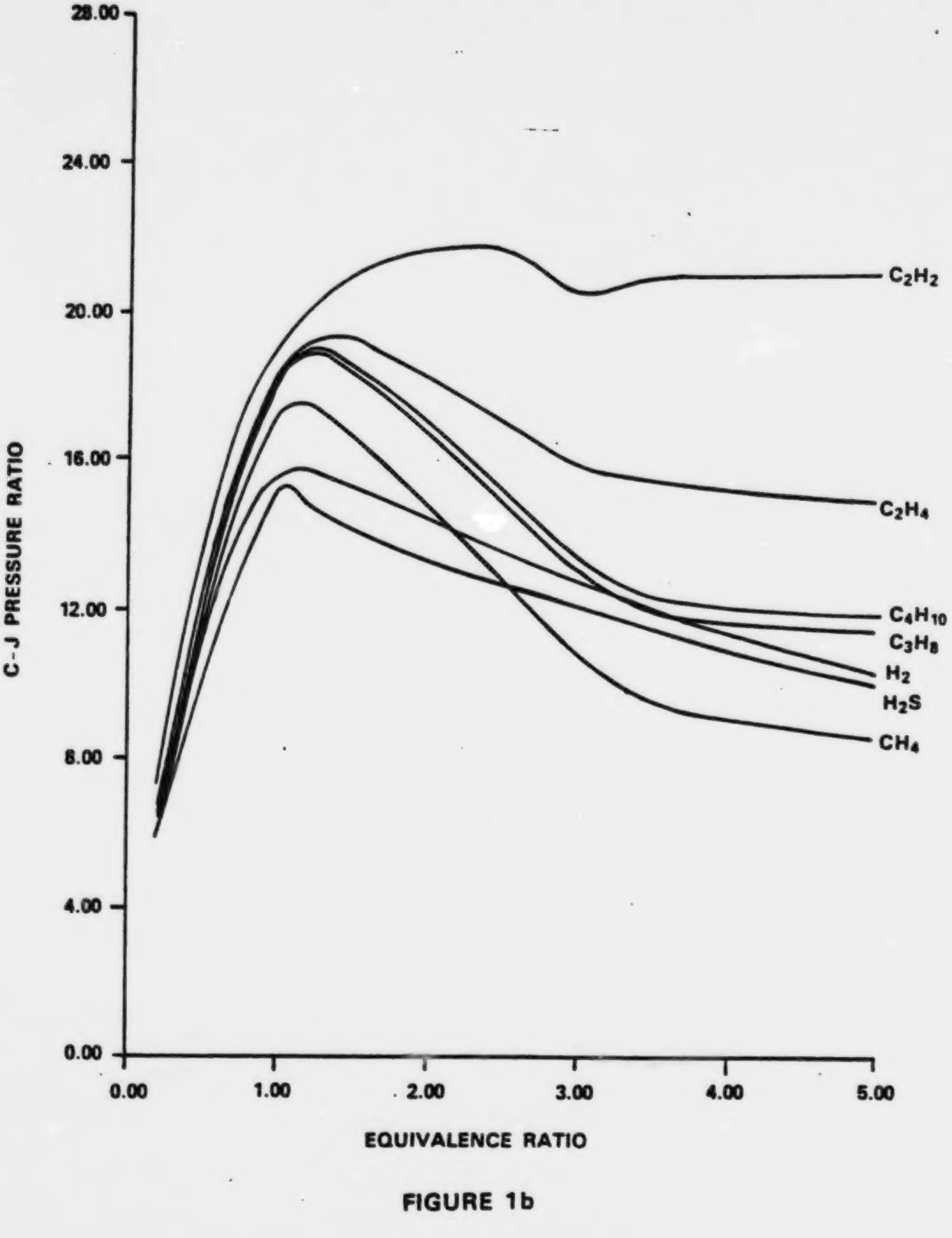
28.00
24.00
20.00
16.00
12.00
8.00
4.00
0.00
C-J PRESSURE RATIO
0.00
1.00
2.00
3.00
4.00
5.00
EQUIVALENCE RATIO
C_2H_2
C_2H_4
C_4H_{10}
C_3H_8
H_2
H_2S
CH_4

FIGURE 1b

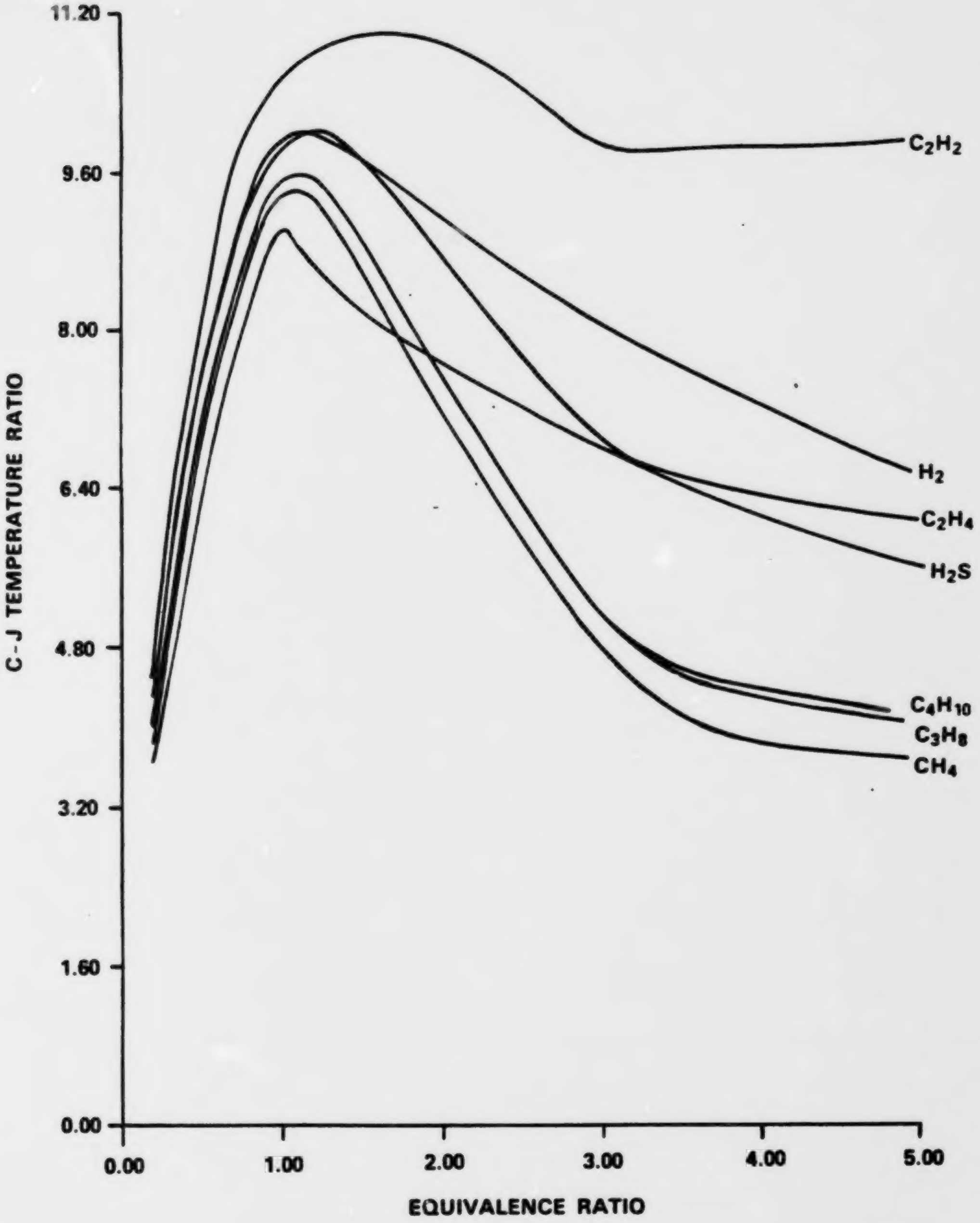
11.20
9.60
8.00
6.40
4.80
3.20
1.60
0.00
C-J TEMPERATURE RATIO
0.00
1.00
2.00
3.00
4.00
5.00
EQUIVALENCE RATIO
C_2H_2
H_2
C_2H_4
H_2S
C_4H_{10}
C_3H_8
CH_4

FIGURE 1c

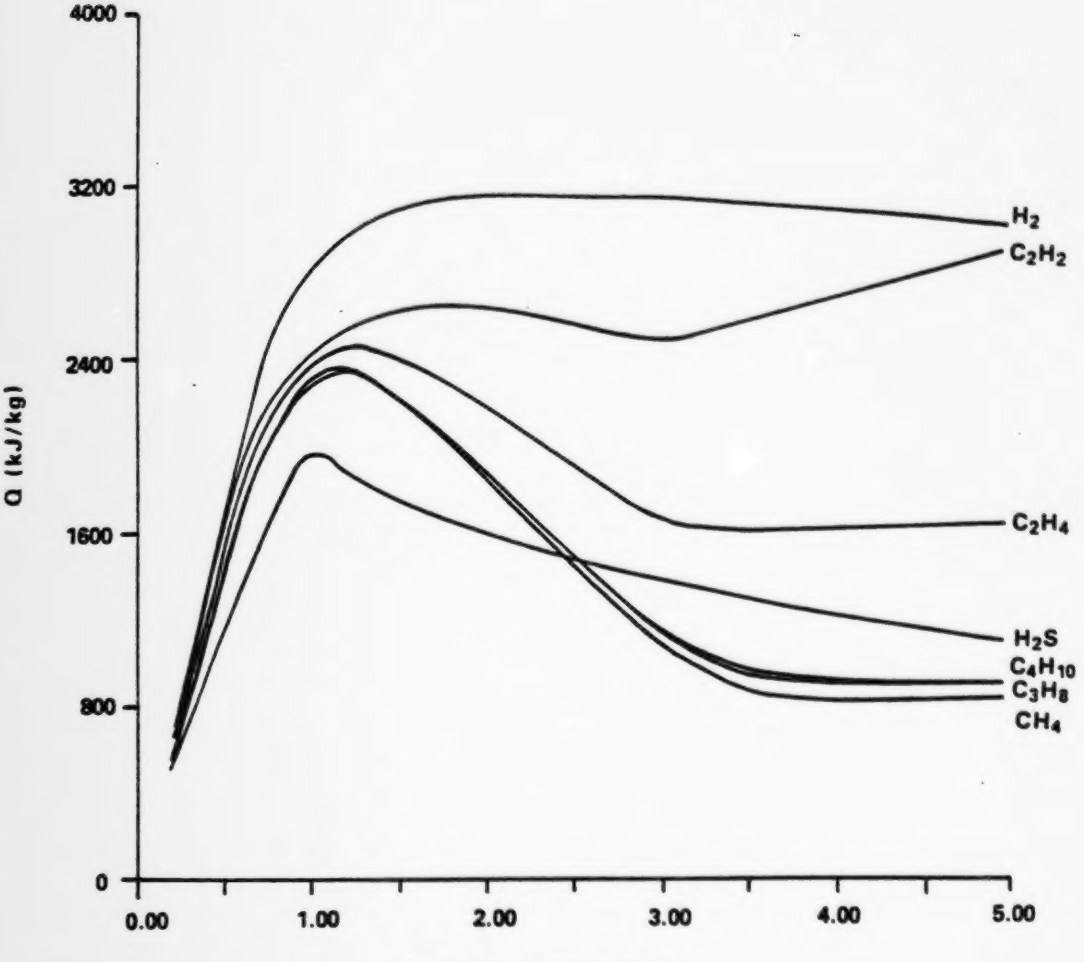
4000
3200
2400
1600
800
0
Q (kJ/kg)
0.00
1.00
2.00
3.00
4.00
5.00
EQUIVALENCE RATIO
H_2
C_2H_2
C_2H_4
H_2S
C_4H_{10}
C_3H_8
CH_4

FIGURE 1d

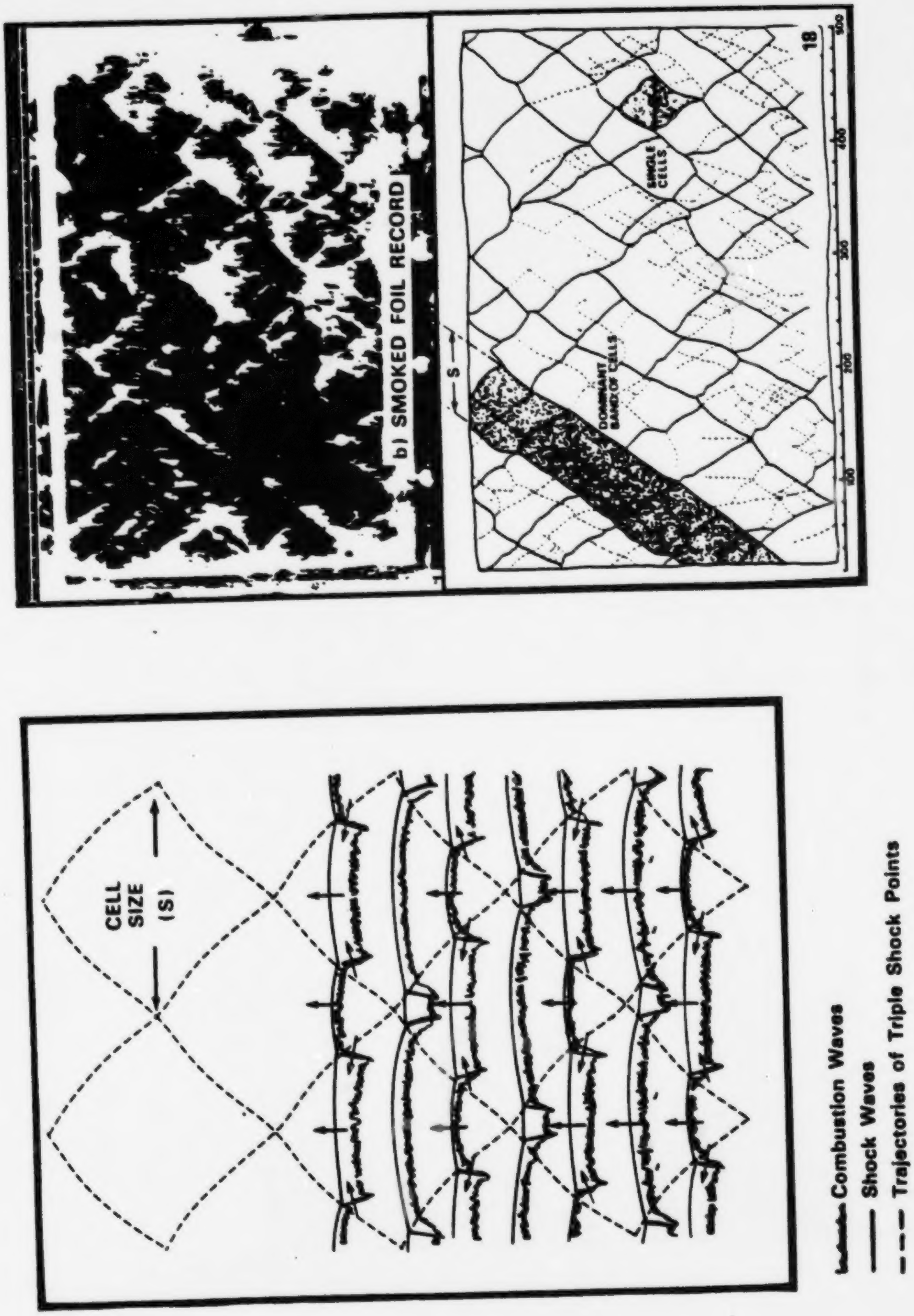

a) TRANSVERSE WAVE STRUCTURE OF GASEOUS DETONATIONS

c) INTERPRETATION OF SMOKED FOIL RECORD

Figure 2. TYPICAL CELLULAR STRUCTURE OF DETONATIONS IN FUEL-AIR MIXTURES

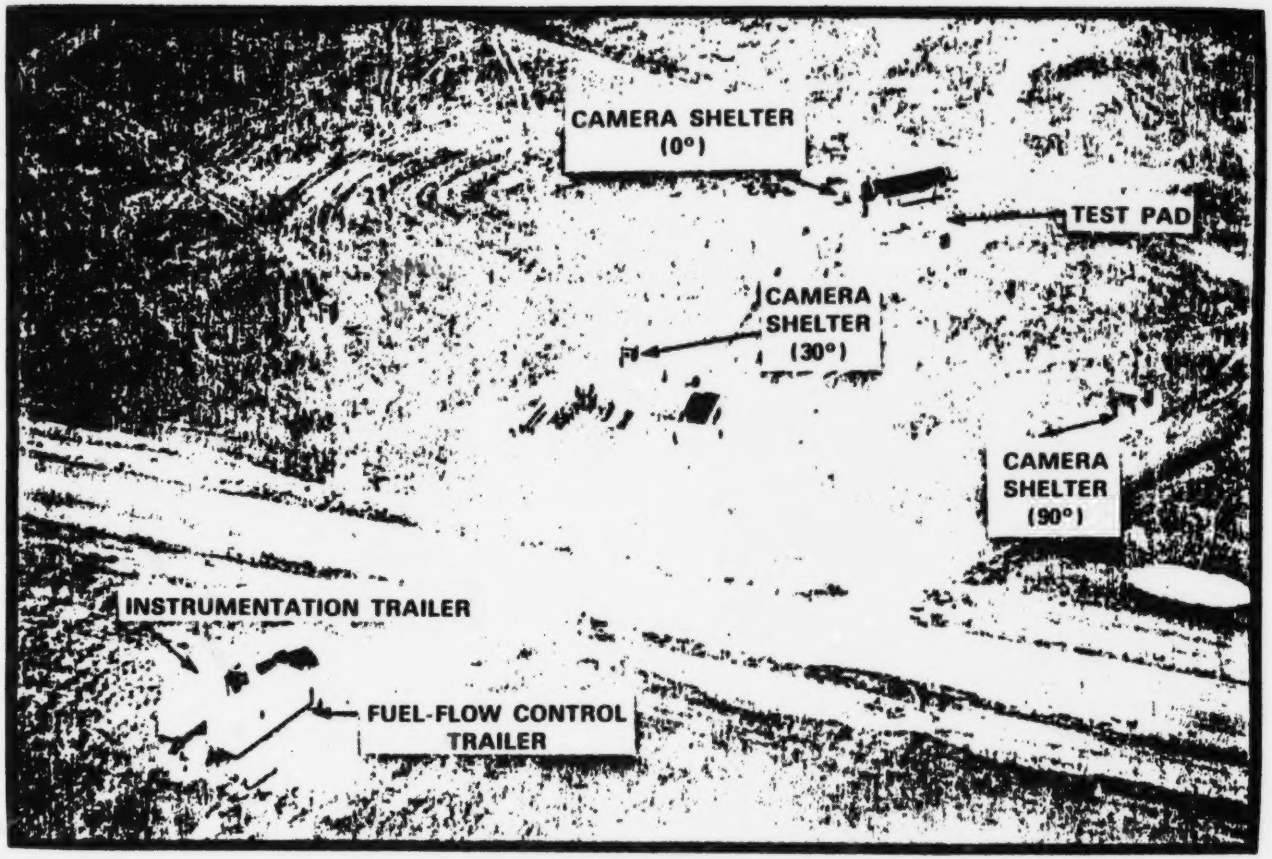

Figure 3a. AERIAL VIEW OF TEST SITE

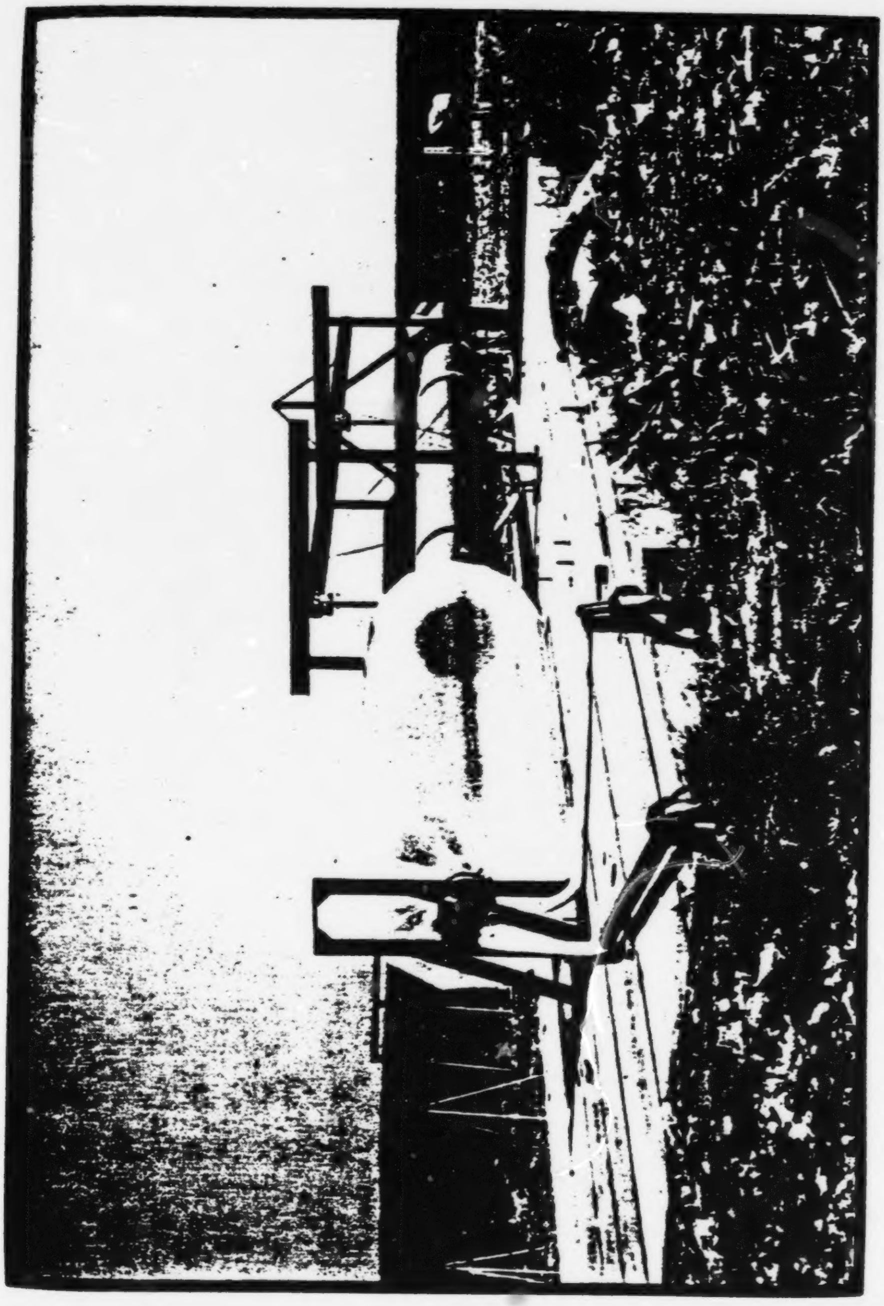

Figure 3b. EXPERIMENTAL LAYOUT

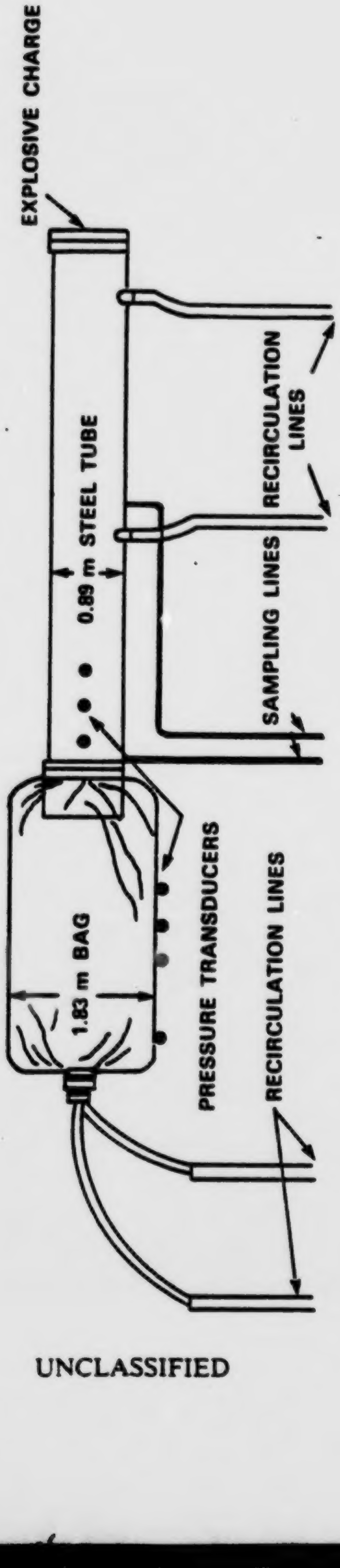

Figure 3c. SCHEMATIC OF EXPERIMENTAL LAYOUT

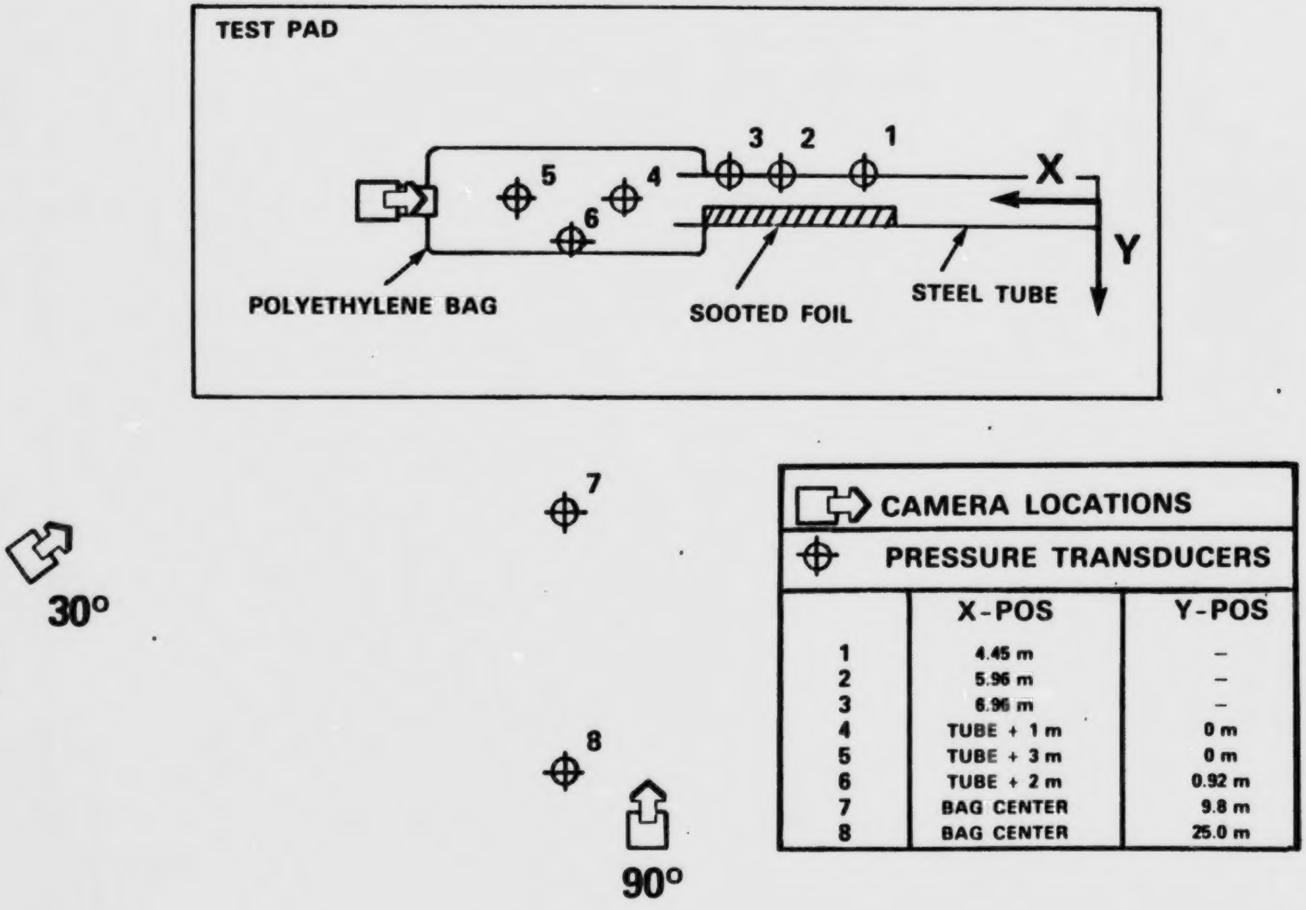

	X-POS	Y-POS
1	4.45 m	–
2	5.96 m	–
3	6.96 m	–
4	TUBE + 1 m	0 m
5	TUBE + 3 m	0 m
6	TUBE + 2 m	0.92 m
7	BAG CENTER	9.8 m
8	BAG CENTER	25.0 m

Figure 4. H_2S TRIALS: INSTRUMENTATION LAYOUT

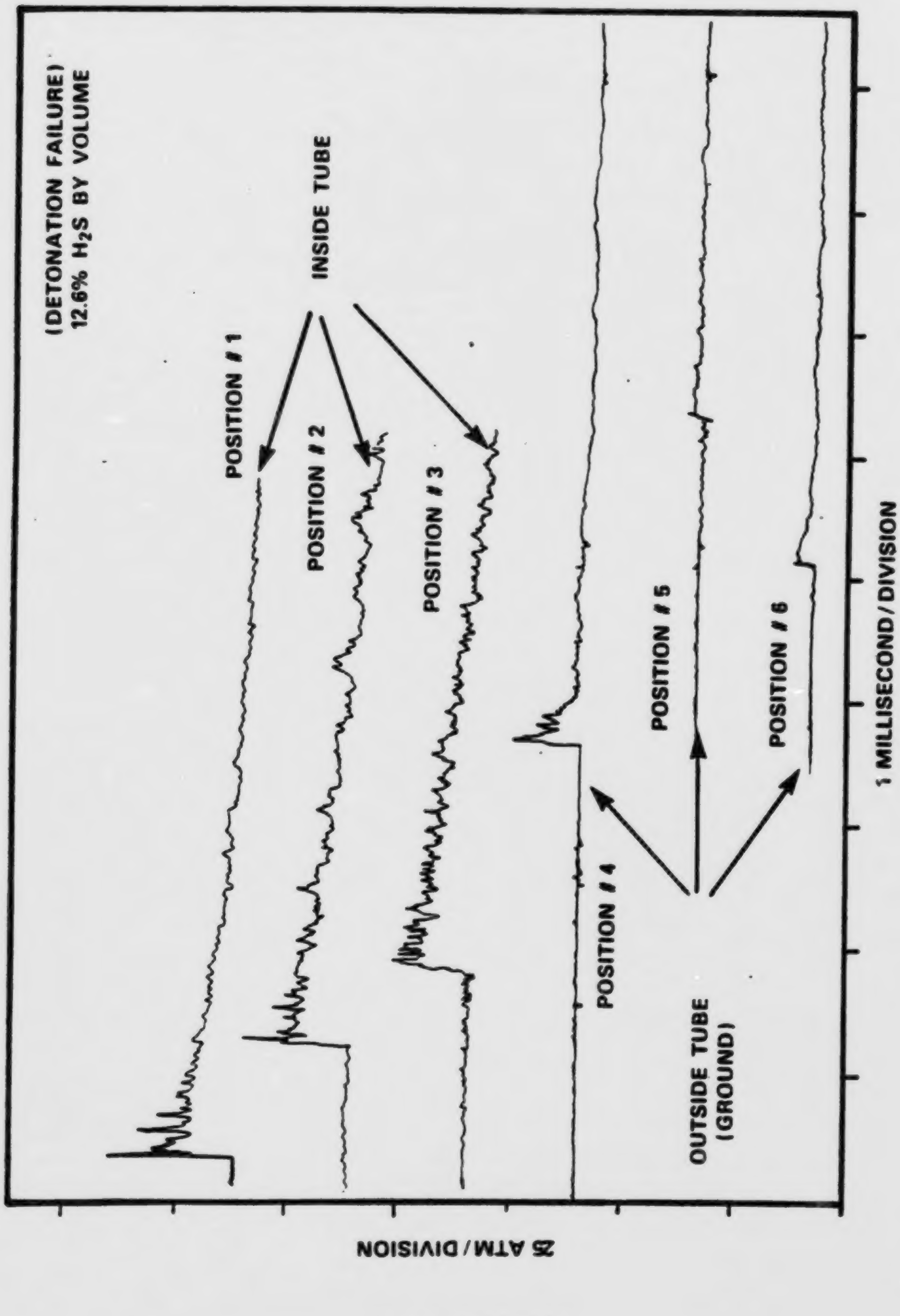

Figure 5. CRITICAL TUBE PRESSURE RECORDS

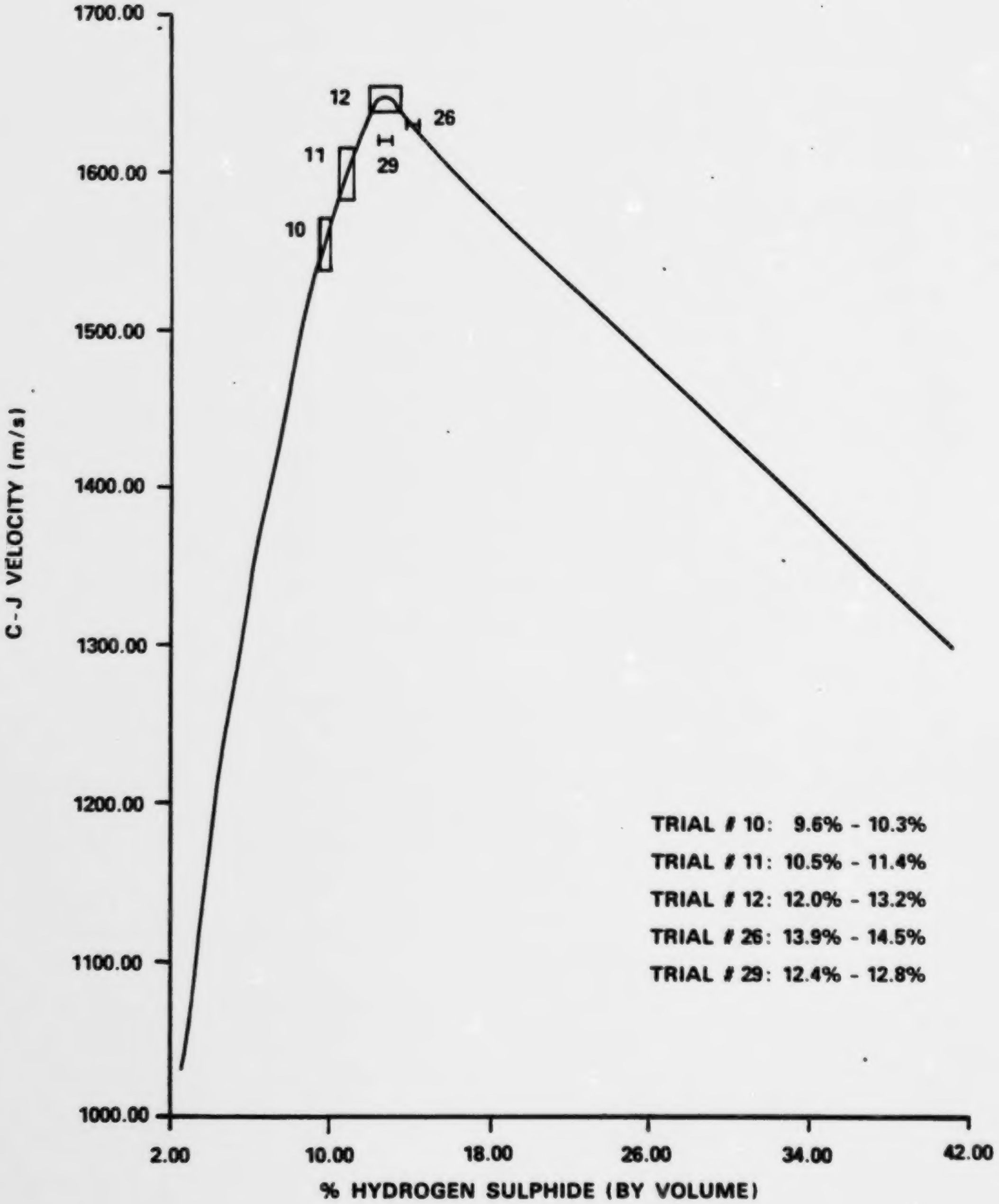

Figure 6. HYDROGEN SULPHIDE

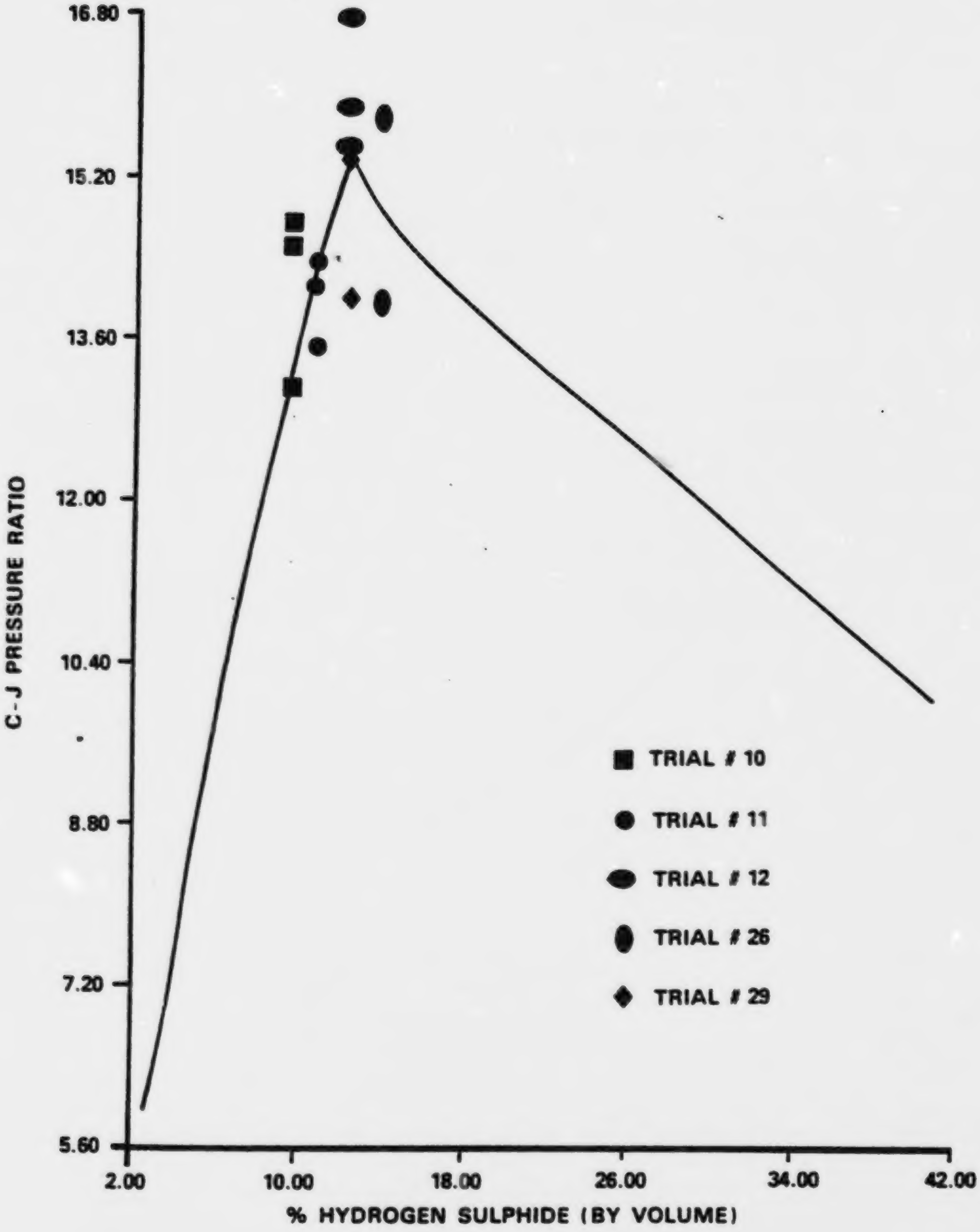

Figure 7. HYDROGEN SULPHIDE

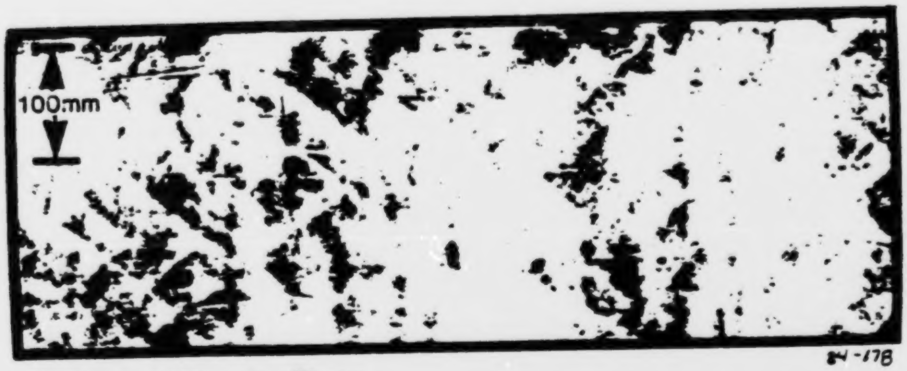

84-178

BUTANE - 3.16% S ~ 55 mm

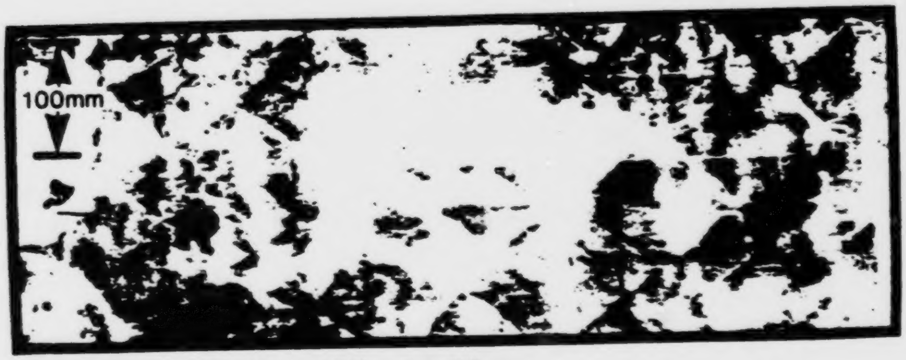

HYDROGEN SULPHIDE - 14.2% S ~ 110 mm

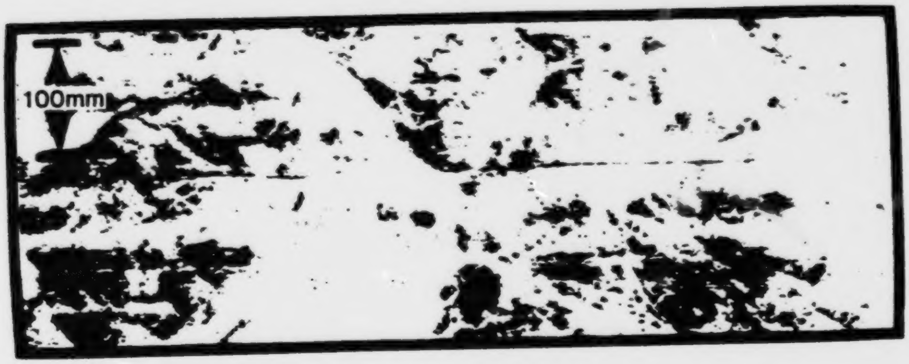

HYDROGEN SULPHIDE - 10.0% S ~ 275 mm

Figure 8. COMPARISON OF CELL STRUCTURES

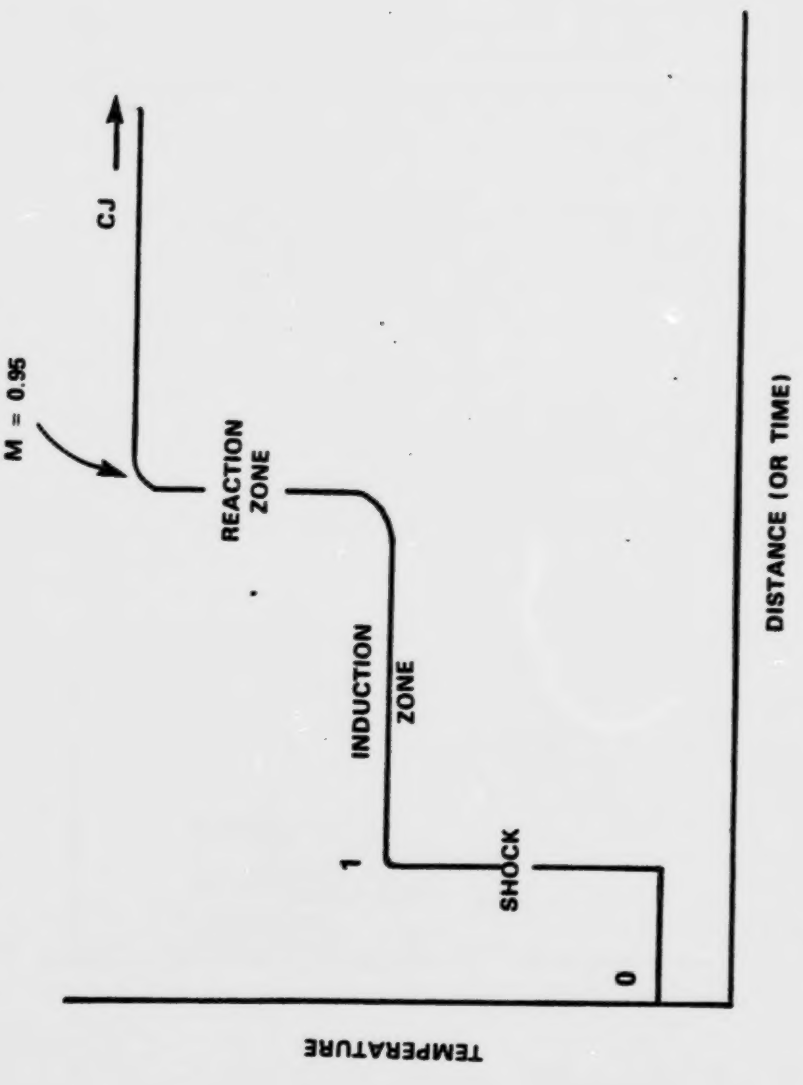

Figure 9. TEMPERATURE PROFILE IN THE ZND MODEL OF A DETONATION

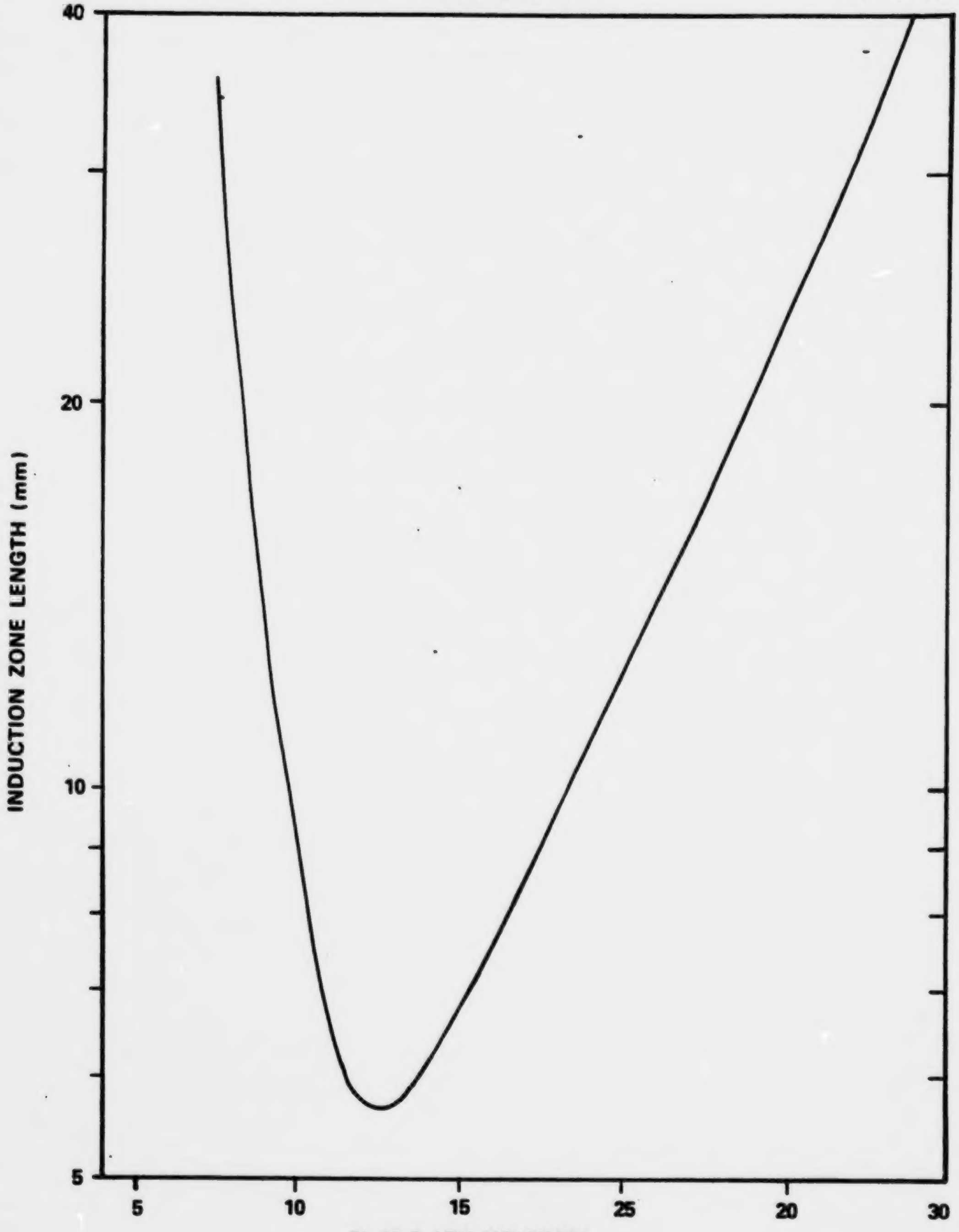
40
20
10
5
INDUCTION ZONE LENGTH (mm)
5
10
15
25
20
30
% H₂S (BY VOLUME)

FIGURE 10

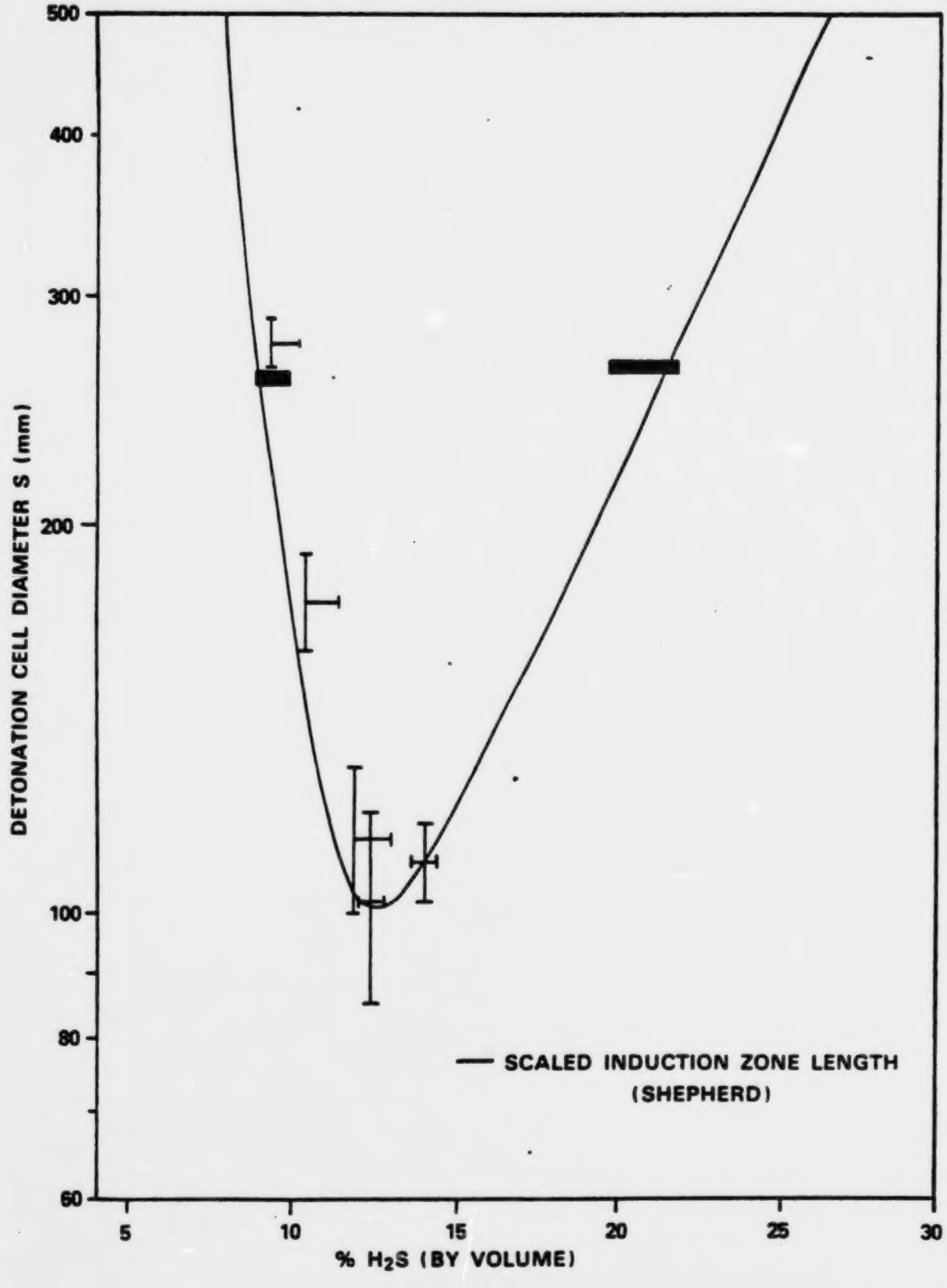
500
400
300
200
100
80
60
DETONATION CELL DIAMETER S (mm)
5
10
15
20
25
30
% H_2S (BY VOLUME)
— SCALED INDUCTION ZONE LENGTH (SHEPHERD)

FIGURE 11

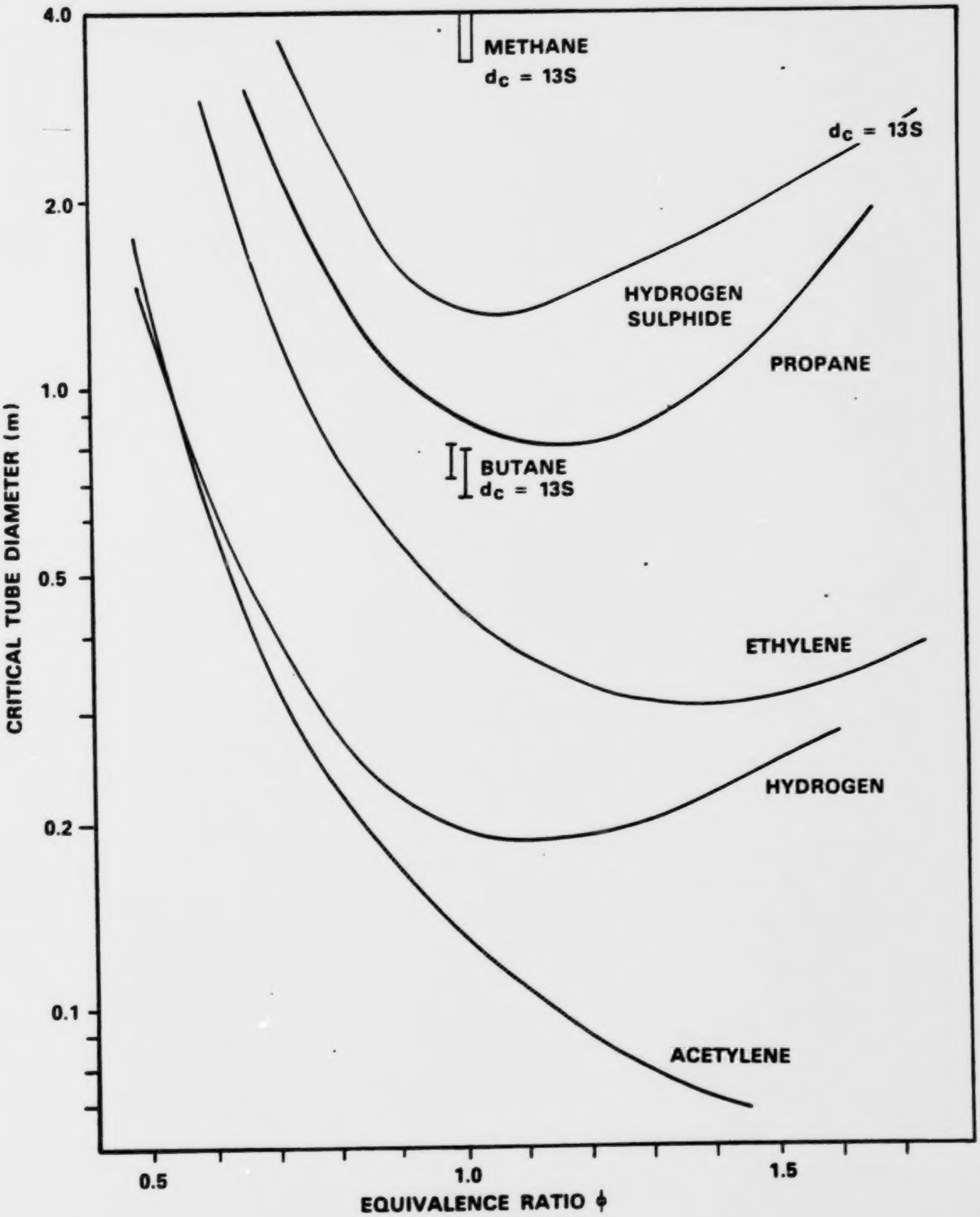
4.0
2.0
1.0
0.5
0.2
0.1
CRITICAL TUBE DIAMETER (m)
METHANE
d_c = 13S
d_c = 13S
HYDROGEN SULPHIDE
PROPANE
BUTANE
d_c = 13S
ETHYLENE
HYDROGEN
ACETYLENE
0.5
1.0
1.5
EQUIVALENCE RATIO ϕ

FIGURE 12

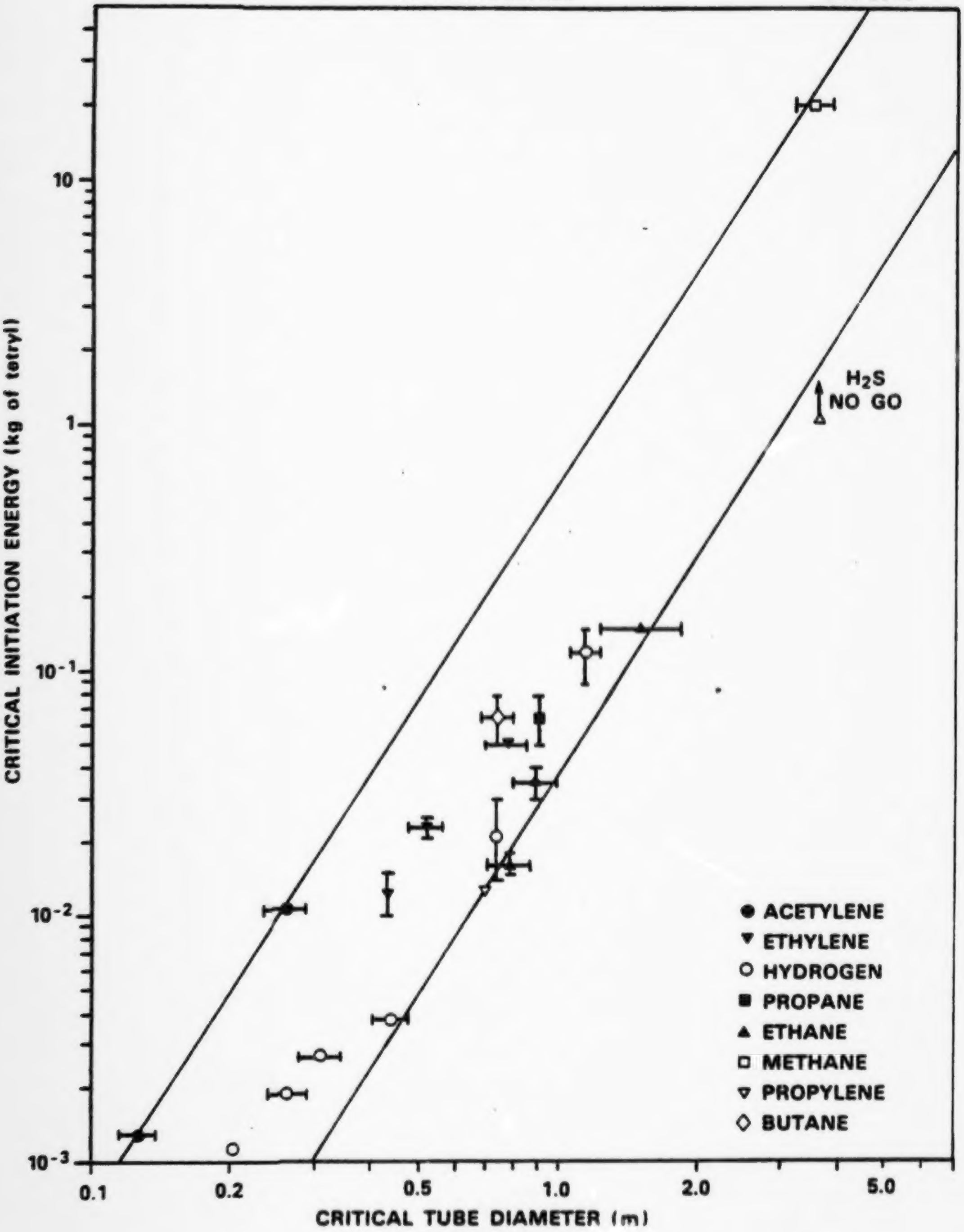
CRITICAL INITIATION ENERGY (kg of tetryl)
10
1
10^{-1}
10^{-2}
10^{-3}
0.1
0.2
0.5
1.0
2.0
5.0
CRITICAL TUBE DIAMETER (m)
H_2S
NO GO
● ACETYLENE
▼ ETHYLENE
○ HYDROGEN
■ PROPANE
▲ ETHANE
□ METHANE
▽ PROPYLENE
◇ BUTANE

FIGURE 13

APPENDIX A

SAFETY PROCEDURES FOR HYDROGEN SULPHIDE TRIALS

Hydrogen sulphide and the product of combustion, sulphur dioxide, are highly toxic gases. A comprehensive safety plan was therefore necessary in order to ensure safety for all personnel.

In order that everyone involved with the trials became familiar with hydrogen sulphide, a specially tailored Hydrogen Sulphide Safe Handling Program was given. The course was prepared and taught by Bryne F. Emeneau of the A.E.C.L. Port Hawksbury Heavy Water Plant. The course material consisted of i) the physical and toxicological properties of hydrogen sulphide (Tables A-I and A-II show the exposure effects of H_2S and SO_2 respectively), ii) familiarization and proper care of related safety equipment such as self-contained breathing apparatus, resuscitators, and various H_2S concentration monitoring devices, and iii) hands-on training of various resuscitative techniques such as CPR, artificial respiration, and aid to a choking victim. Special procedures particular to the FAE trials were also formulated and discussed.

Since the effects of a leak of any toxic gas are severely compounded in an enclosed environment, the use of the fuel flow control trailer was not suitable. In its place, an outdoor control station was built. The station centered around a large tent which housed the flow control and monitoring equipment. During trials, the front and rear panels of the tent were removed in order to allow for complete and continuous ventilation of the area.

Numerous types of safety equipment were used during the hydrogen sulphide FAE tests. Available to personnel directly involved with the trials were six self-contained breathing apparatus with spare bottles and four escape masks with hydrogen sulphide cannisters. Monitoring equipment included two electronic H_2S detectors, two sampling tube detectors for both H_2S and SO_2, lead acetate tape for connector leak detection as well as lead acetate ampoules which were worn by all trial personnel. A medical officer equipped with resuscitative equipment was also present for each trial involving hydrogen sulphide.

In order to determine the possible downwind concentrations of H_2S if a substantial leak in the setup was to occur, dispersion calculations of H_2S as well as SO_2 were performed. The results of these calculations are summarized in Tables A-III and A-IV. Based on these calculations, a safety zone of 5 km radius was established. Only personnel aware of procedures during an emergency were allowed inside the safety zone during trials involving H_2S. Also, due to the close proximity of several other test sites (<1 km), H_2S trials could only be conducted when wind direction and speed were within strict limits. As an added safety feature, a large air-horn was installed in order to warn personnel within the safety zone that a hazardous wind change coupled with an H_2S leak had occurred.

Procedures and guidelines were developed for specific phases of the trials. These included post-trial procedures, abort procedures and emergency procedures. Also, prior to each trial, equipment checks (including checks of self-contained breathing apparatus, monitoring equipment, flow lines, etc.) were performed to ensure everything was in proper working order. Finally, all personnel were informed over open radio when flow of H_2S began and also when the area was deemed clear after a trial.

TABLE A-I

TOXICITY TABLE
FOR HYDROGEN SULPHIDE (H_2S)

1 PPM = 0.0001% (1/10,000 of 1%)	CAN SMELL
10 PPM = 0.001% (1/1,000 of 1%)	ALLOWABLE FOR 8 HOURS EXPOSURE THRESHOLD LIMIT VALUE (T.L.V.)

IF THE LEVEL IS ABOVE 10 PPM, THEN PROTECTIVE EQUIPMENT MUST BE WORN

100 PPM = 0.01% (1/100 OF 1%)	KILLS SMELL IN 3 TO 15 MINUTES IRRITATION OF EYES AND THROAT
200 PPM = 0.02% (2/100 OF 1%)	KILLS SMELL RAPIDLY BURNS EYES AND THROAT
500 PPM = 0.05% (5/100 OF 1%)	LOSES SENSE OF REASONING AND BALANCE STOPPAGE OF BREATHING IN 2 TO 15 MINUTES VICTIM NEEDS ARTIFICIAL RESPIRATION
700 PPM = 0.07% (7/100 OF 1%)	UNCONSCIOUS QUICKLY BREATHING WILL STOP AND DEATH RESULTS UNLESS RESCUED IMMEDIATELY
1000 PPM = 0.1% (1/10 OF 1%)	UNCONSCIOUS AT ONCE BRAIN DAMAGE UNLESS RESCUED PROMPTLY

1% = 10,000 PPM

PPM - PARTS OF GAS PER MILLION PART OF AIR BY VOLUME

TABLE A-II

TOXICITY TABLE
FOR SULPHUR DIOXIDE (SO_2)

3 - 5 PPM = 0.0003 - 0.0005%	CAN SMELL (ROTTEN EGGS)
5 PPM = 0.0005%	ALLOWABLE FOR 8 HOURS EXPOSURE THRESHOLD LIMIT VALUE (T.L.V)

IF THE LEVEL IS ABOVE 5 PPM, THEN PROTECTIVE EQUIPMENT MUST BE WORN.

20 PPM = 0.002%	COUGHING AND IRRITATION OF EYES
1000 PPM = 0.1%	LETHAL CONCENTRATION CONCENTRATION THAT WILL CAUSE DEATH WITH SHORT-TERM EXPOSURE

1% = 10,000 PPM

PPM - PARTS OF GAS PER MILLION PARTS OF AIR BY VOLUME

TABLE A-III

DOWNWIND CONCENTRATION OF H_2S

CONDITIONS:

12% H_2S IN 20 m^3 (~ 3 kg)

15 kph Wind

DISTANCE	CONCENTRATION	
	Neutral Atmosphere Stability	Mild Inversion
150 m	3500 mg/m^3 or 2300 ppm	7358 mg/m^3 or 4900 ppm
1 km	123 mg/m^3 or 80 ppm	193 mg/m^3 or 130 ppm
5 km	9.3 mg/m^3 or 6 ppm	20 mg/m^3 or 13 ppm

CALCULATIONS WERE DONE BY S.B. MELLSEN, CHEM. SECTION;
DRES 3613E-1 (CHEM), MEMORANDUM DATED 21 March, 1984.
CONCENTRATIONS SHOWN REPRESENT UPPER LIMITS.

TABLE A-IV

DOWNWIND CONCENTRATION OF SO_2

CONDITIONS: COMBUSTION PRODUCT FROM 3 kg H_2S IN AIR.

$$H_2S + \frac{3}{2}(O_2 + 3.76\ N_2) \rightarrow H_2O + SO_2 + 5.64\ N_2$$

REACTION OF 3 kg H_2S PRODUCES ABOUT 6 kg SO_2

15 kph WIND

DISTANCE	CONCENTRATION	
	NEUTRAL ATMOSHPERIC STABILITY	MILD INVERSION
150 m	5800 mg/m^3 or 2300 PPM	12200 mg/m^3 or 4900 PPM
1 km	190 mg/m^3 or 80 PPM	320 mg/m^3 or 130 PPM
5 km	16 mg/m^3 or 6 PPM	33 mg/m^3 or 13 PPM

CALCULATIONS WERE DONE BY S.B. MELLSEN, CHEM. SECTION;
DRES 3613E-1 (CHEM), MEMORANDUM DATED 19 APRIL 1984.
CONCENTRATIONS SHOWN REPRESENT UPPER LIMITS.

UNCLASSIFIED

APPENDIX B

CELL STRUCTURE RECORDS

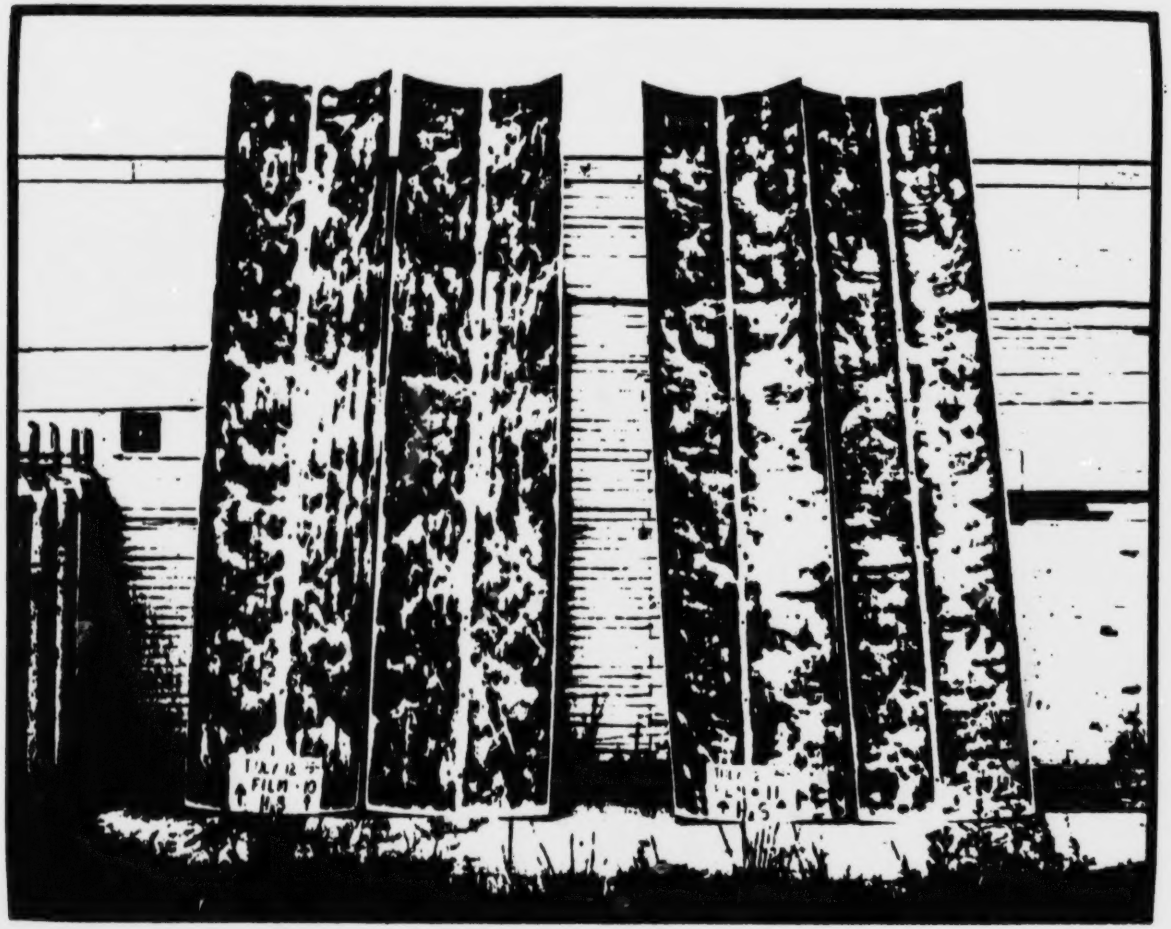

84-178

TRIALS # 10 AND # 11: SMOKED FOIL RECORDS
9.6% – 10.3% H_2S 10.5% – 11.4% H_2S

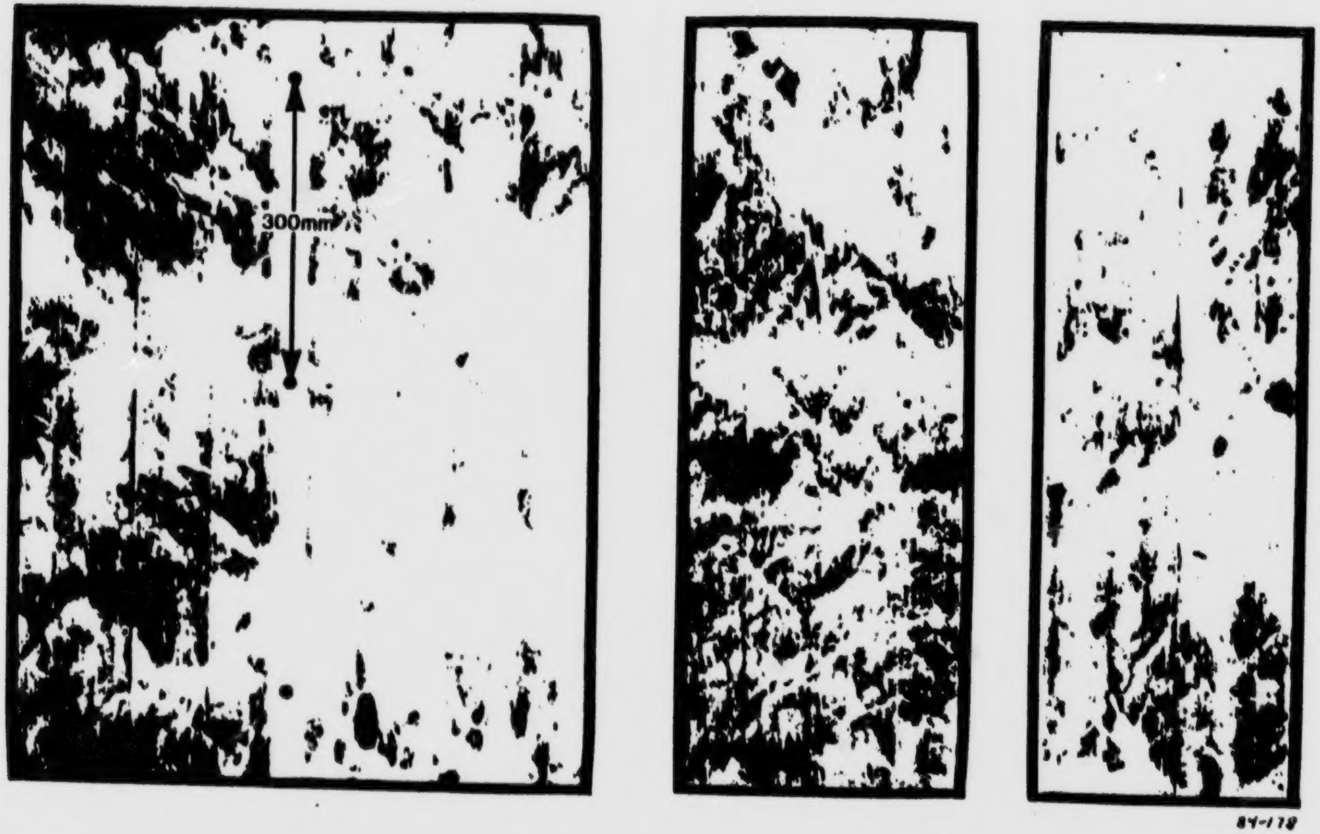

TRIAL # 10: CELL STRUCTURE
9.6% – 10.3% H_2S S ~ 275 mm

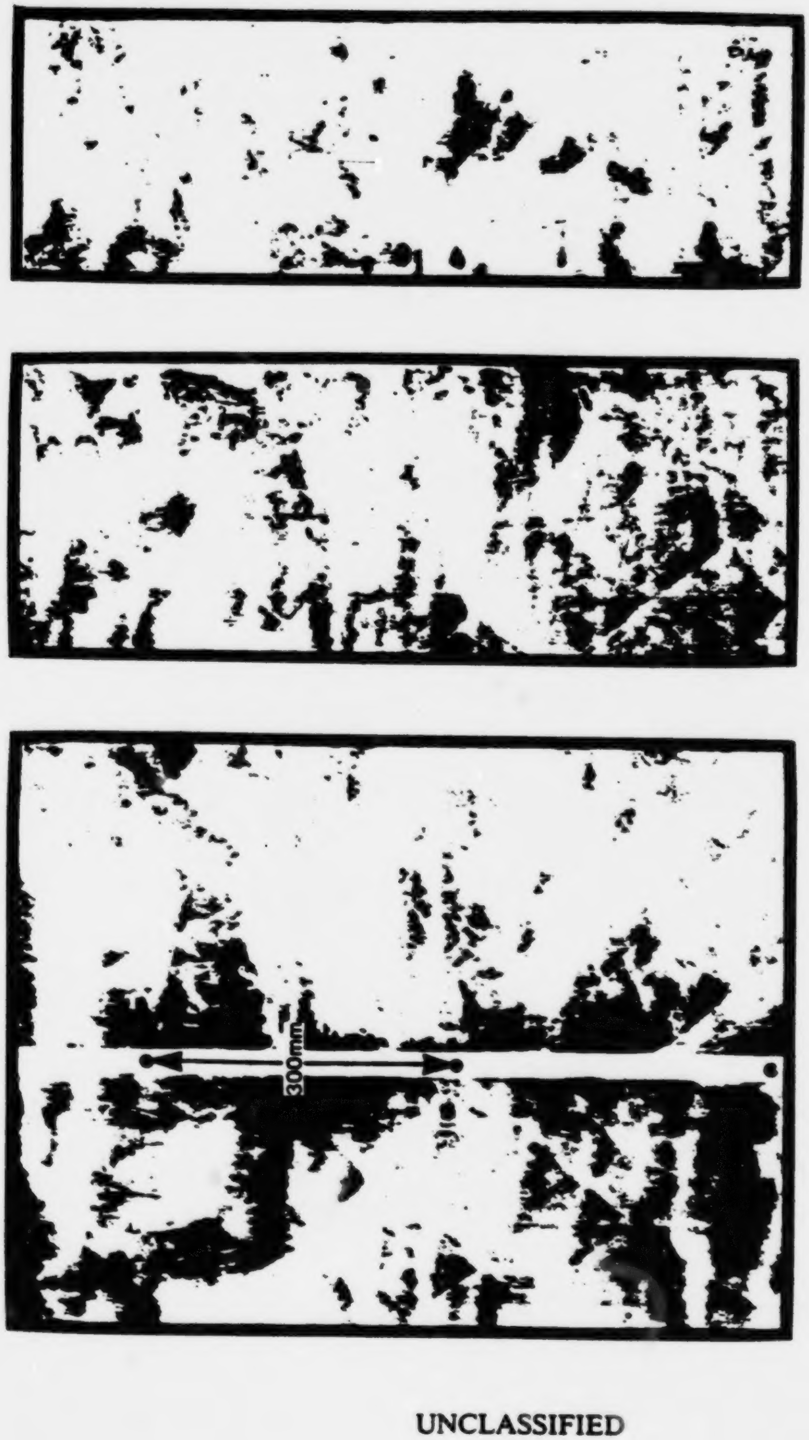

TRIAL # 11: CELL STRUCTURE
10.5% — 11.4% H_2S S ~ 175 mm

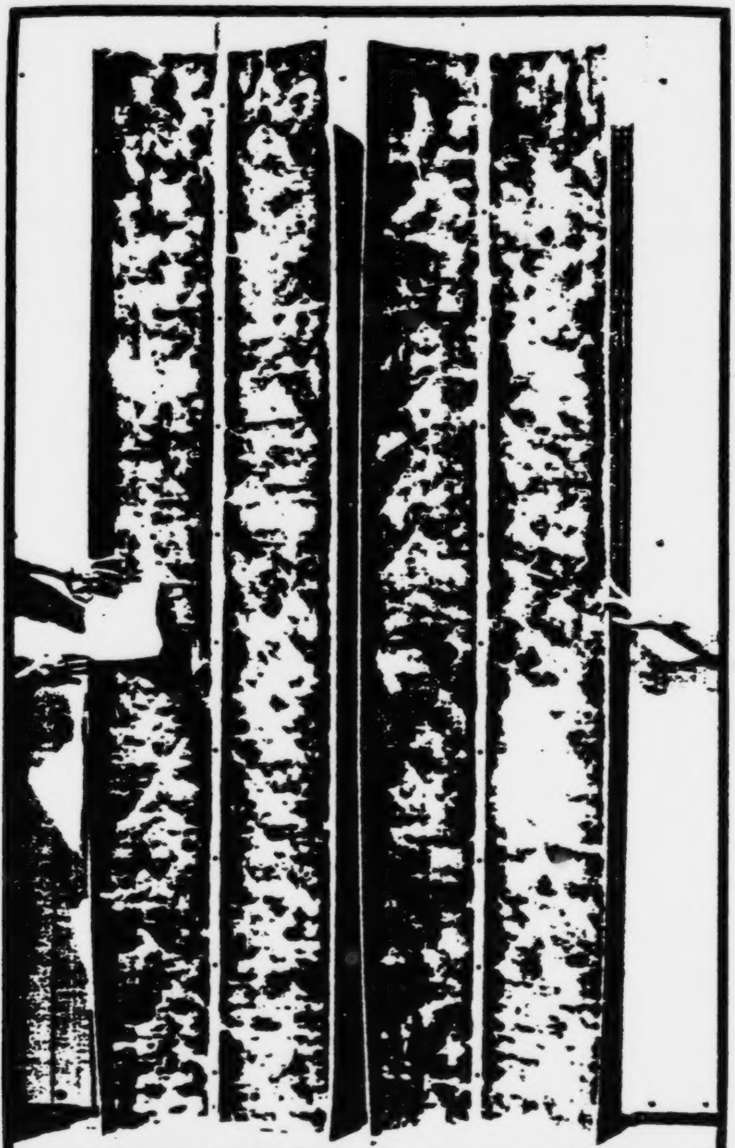

TRIAL # 12: SMOKED FOIL RECORD
12.0% — 13.2% H_2S

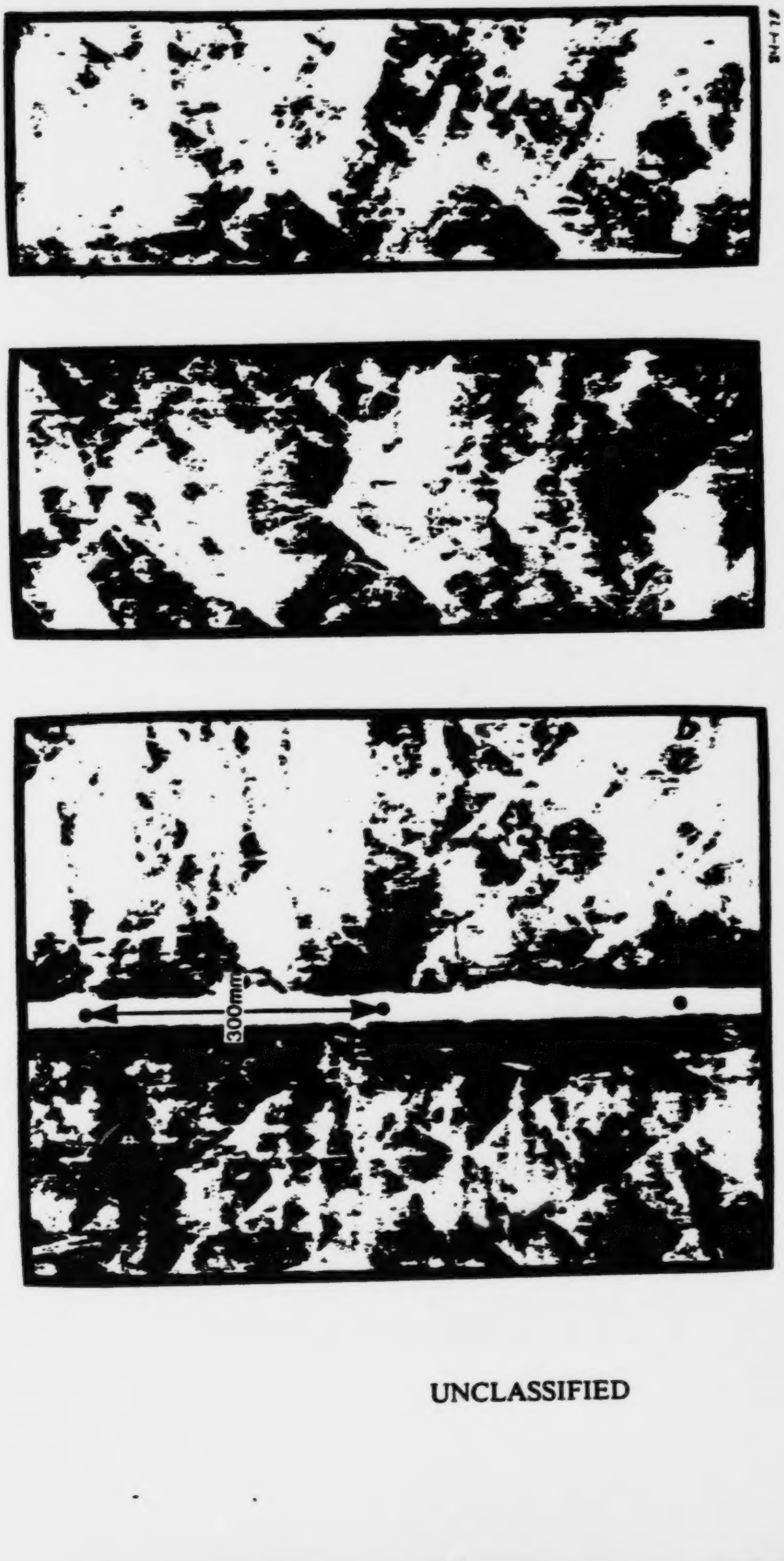

TRIAL # 12: CELL STRUCTURE

12.0% — 13.2% H_2S S ~ 115 mm

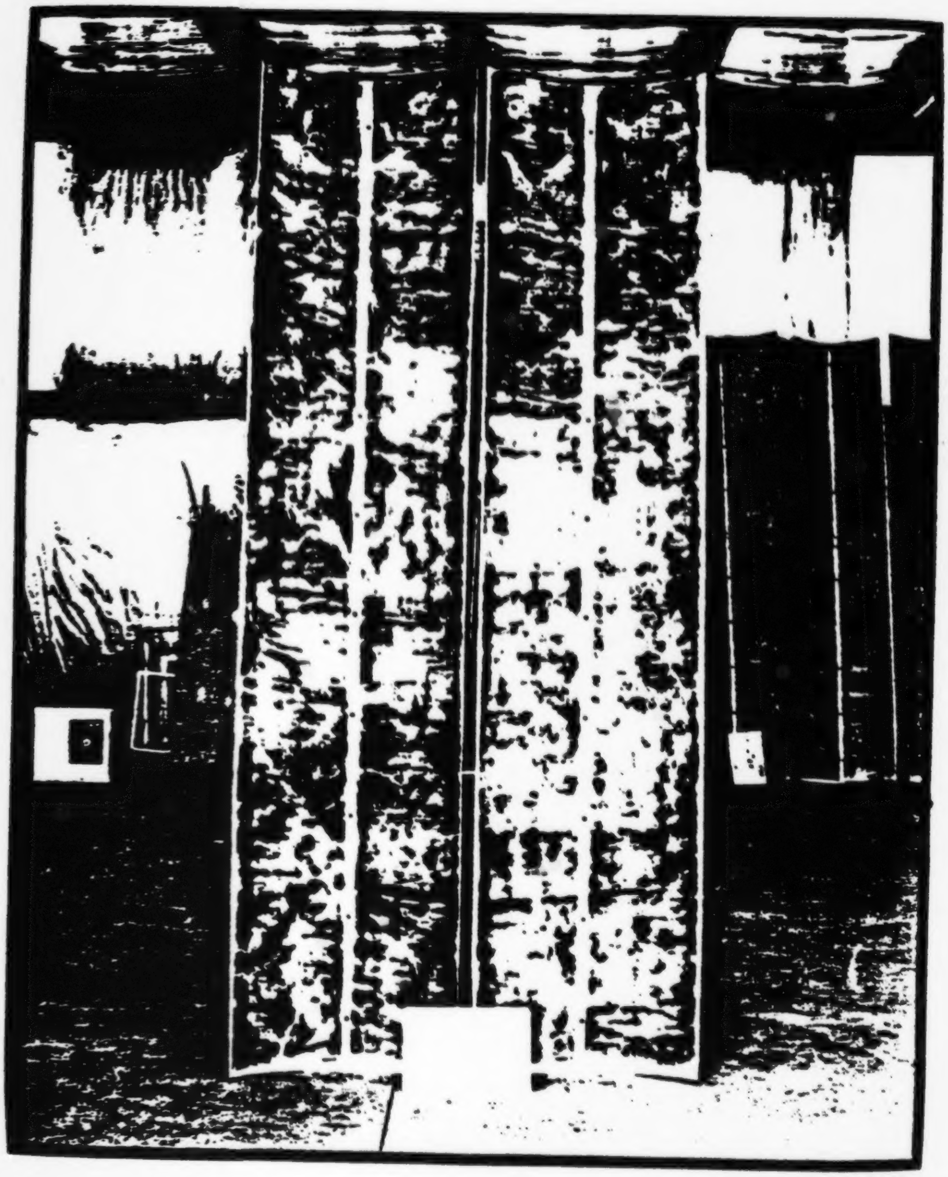

TRIAL # 26: SMOKED FOIL RECORD
13.9% — 14.5% H_2S

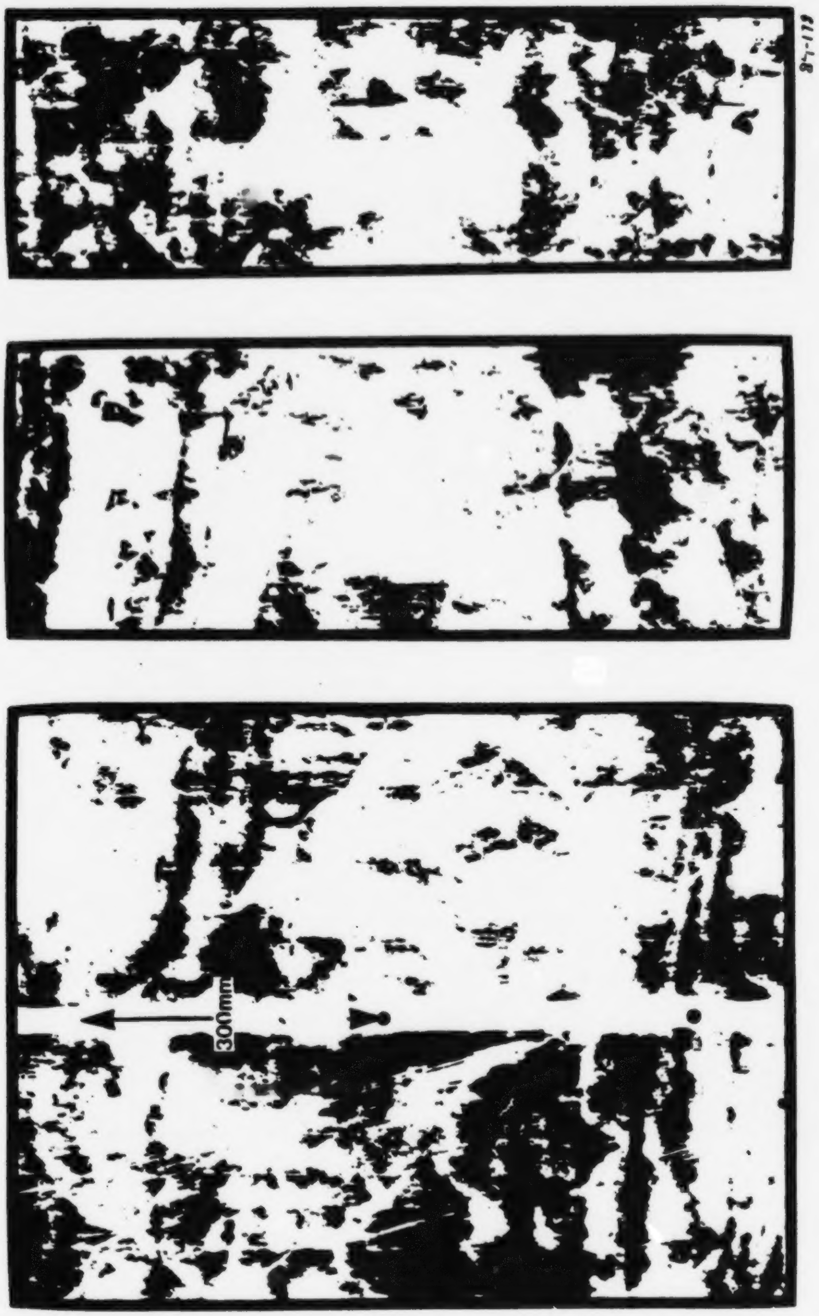

TRIAL # 26: CELL STRUCTURE
13.9% — 14.5% H_2S S ~ 110 mm

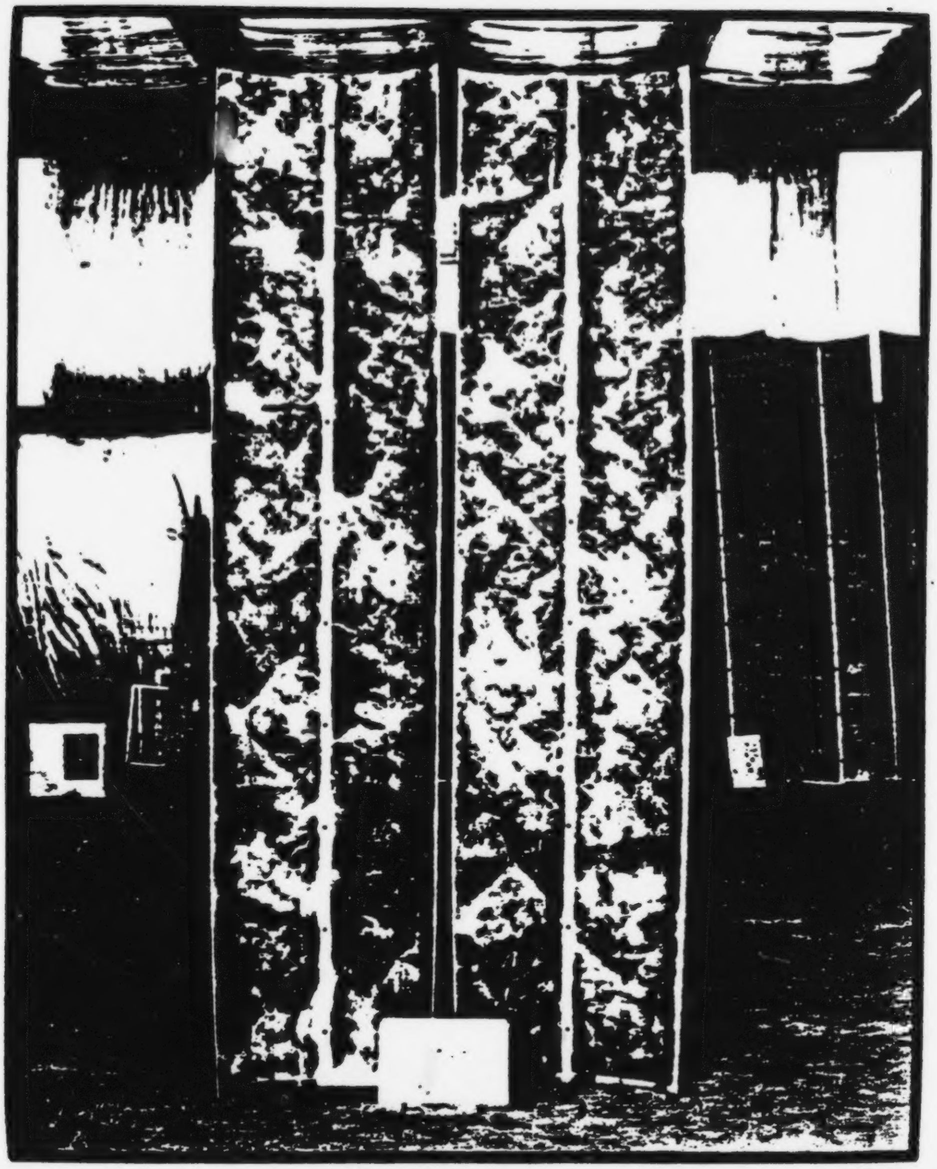

84-178

TRIAL # 29: SMOKED FOIL RECORD
$12.4\% - 12.8\%$ H_2S

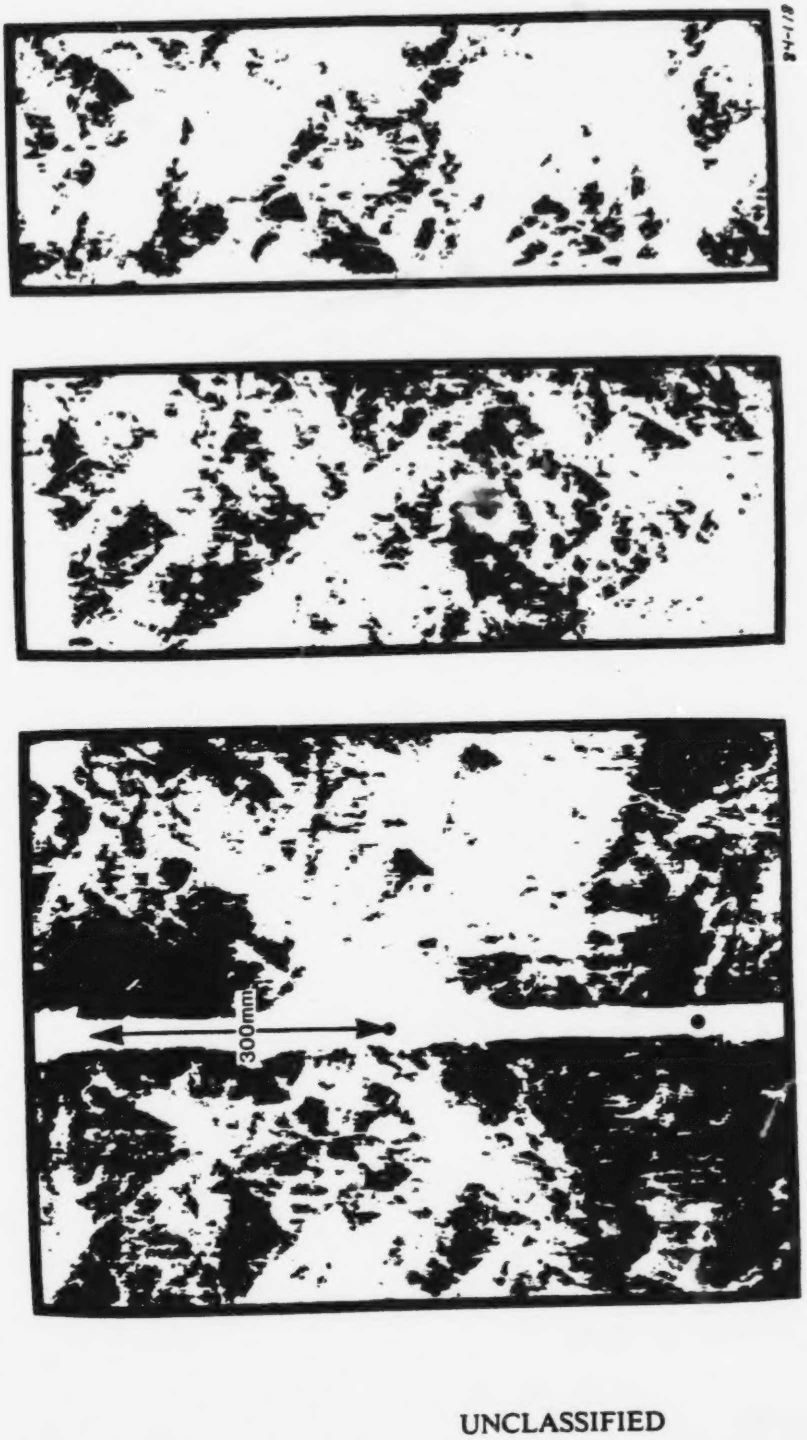

TRIAL # 29: CELL STRUCTURE
12.4% — 12.8% H_2S S ~ 100 mm

Chemical Kinetics and Cellular Structure *of* Detonations in Hydrogen Sulphide and Air

J. E. Shepherd
Member of the Technical Staff
Fluid and Thermal Sciences Dept.
Sandia National Laboratories
Albuquerque, NM, USA

A. Sulmistras
Research Assistant
Dept. of Mechanical Engineering
Concordia University
Montreal, Quebec, Canada

A. J. Saber
Professor
Dept. of Mechanical Engineering
Concordia University
Montreal, Quebec, Canada

I. O. Moen
Defence Scientist
Military Engineering Section
Defence Research Establishment Suffield
Ralston, Alberta, Canada

Abstract

Detailed analyses of hydrogen sulphide oxidation have been used to characterize the reaction zone structure at temperatures and pressures typical of detonations in mixtures of hydrogen sulphide and air. Detonation reaction zone lengths are calculated for a wide range of compositions, and the variation of these lengths with initial pressure and water vapor dilution are calculated. Estimates of detonation cell size λ are made based on scaling factors established for other fuel-air systems. These estimates are compared with results obtained in an experimental investigation of the detonability of mixtures of hydrogen sulphide and air. The predicted cell size of 10 cm at stoichiometric composition and standard initial conditions is in excellent agreement with the experimental results. The predicted variation of cell size also agrees well with the experimental observations over a concentration range of 10 to 20% (by volume) hydrogen sulphide. Based on the $d_c = 13\lambda$ estimate of critical tube diameter d_c, the minimum critical tube diameter (for a stoichiometric mixture) is 1.3 m. Mixtures of hydrogen sulphide and air are therefore slightly less sensitive to detonation than propane-air mixtures, which have a minimum critical tube diameter of 0.9 m.

Introduction

Hydrogen sulphide (H_2S) is a flammable gas which is used in large quantities in the Girdler-Sulphide process for the production of heavy water (deuterium oxide), an essential material for the operation of the CANDU nuclear reactors. In the oil and gas industry, H_2S is the main constituent of "sour gas" gas wells. Despite this common occurence of H_2S in industry, very little is known about its susceptibility to detonation and the potential for transition to detonation from flames propagating around obstacles, *i.e.*, chemical plant piping. Due to the toxicity and corrosiveness of H_2S, there have been very few studies of this problem.

Two key parameters have been used to characterize the sensitivity of combustible mixtures to detonation. These are: i) the critical energy E_c required to directly initiate detonation, and ii) the critical tube diameter d_c required for successful transition from a planar detonation in a tube to an unconfined spherical detonation. Due to the nature of these parameters, several experimental trials must be carried out to obtain a single reliable datum. For fuel-air mixtures, these trials must be carrried out in large-scale field tests, an expensive and time-consuming procedure.

Recent developments (Lee 1984) in gaseous detonations have led to the identification of the detonation cell size as an alternative measure of detonability. Furthermore, detailed chemical kinetic models have been used* to calculate the variation in cell size, as well as E_C and d_c, with composition, pressure and gaseous additives. These developments have been used to minimize the scale and number of tests required to assess the detonability of gaseous explosive systems.

Previous correlations and models have focussed on systems based on either hydrogen or hydrocarbon fuels. In this paper, these correlations and models are assessed and used for the H_2S-air system. The paper is divided into two parts. In the first part, the oxidation kinetics and reaction zone modeling are discussed. Detonation reaction zone lengths are calculated and estimates of cell size are made using analogies to other

---

*see Lee *et al.* (1982), Shepherd and Roller (1982), Westbrook and Urtiew (1982), and Moen *et al.* (1984a).

fuel-air systems. In the second part, these estimates are compared with the results obtained in an experimental investigation of H_2S-air detonability.

Kinetics

Hydrogen sulphide oxidation is both a challenging and interesting topic. The mechanisms have not been studied as extensively as hydrocarbon oxidation, but should be similar and simpler. It is the analogue of a single-carbon, hydrocarbon-like fuel. If not for the toxicity of this substance, it would be an ideal experimental fuel for testing various reaction mechanism hypotheses.

The principle elements of the reaction mechanism which resemble hydrocarbon oxidation are: there is a pyrolysis or thermal decomposition stage; the sulfur- and hydrogen-containing radicals compete for the available oxygen; and, the species SO and SO_2 play an analogous role to CO and CO_2. Almost all processes involving carbon-containing species have an analogue with a sulfur-containing species. The hydrogen oxidation portions of both mechanisms are identical.

The H_2S-air reaction mechanisms and rate constants used in the present work are given in Table 1 (hydrogen oxidation only) and Table 2 (sulfur oxidation only). Mechanisms and constants were obtained from previously published data or estimates. A brief discussion of the literature is given below.

The last complete review of gaseous sulphur chemistry was by Cullis and Mulcahy (1972); while giving a good overview, few data on high-temperature rates were given. More recent discussions and experimental data for flames can be found in Muller *et al.* (1979) and Bernez-Cambot *et al.* (1981). Extensive reaction mechanisms with rate constant values are given in Frenklach *et al.* (1981) and Wendt *et al.* (1983); our mechanism is drawn primarily from these two works. Especially valuable is the work of Frenklach *et al.* (1981), a combined experimental and modeling study of the reaction rates behind reflected shock waves. Conditions in those tests were similar to those found behind detonation waves, although the shock strength was lower (Mach number ~ 2.7) than that typical of detonations (Mach number ~ 4). Finally, we mention two studies of the thermal decomposition mechanisms of H_2S, Bowman and Dodge (1976) and Roth *et al.* (1982).

The elementary reactions and rate constant values given in Table 1 can be divided into three categories. Hydrogen oxidation reactions (numbers 1-19) involving the species H_2, O_2, H, O, OH, H_2O, HO_2, H_2O_2, and diluents Ar, CO_2, and N_2 are taken from Miller *et al.* (1983). The mechanism is essentially identical to that used by Frenklach *et al.* (1981) and the Miller *et al.* (1983) rate constants have been used in related investigations[†] of hydrogen-air detonability. The only species considered by Frenklach *et al.* (1981) that we have omitted is O_3; calculations with and without this species indicate that it plays an insignificant role.

The bulk of the H_2S reactions, involving the species H_2S, HS, S, S_2, SO, SO_2 and others mentioned above are taken from Frenklach *et al.* (1981). All of the reactions which Frenklach *et al.* (1981) found to be most important were included. We only omitted 7 of the reactions: 4 involving the HSO species and 3 others which had very small sensitivity parameters and for which only estimated rate constants were available. Computations showed that this slightly smaller mechanism could adequately reproduce the test case results discussed in Frenklach *et al.* (1981). On the other hand, the Wendt *et al.* (1983) mechanism lacks some crucial reactions and is unable to reproduce those test case results.

Wendt *et al.* (1983) have developed a more detailed reaction mechanism for the HSO species than Frenklach *et al.* (1981) so we have chosen to use that portion of their mechanism. However, all rates are estimated and there are no experimental data to support either the mechanism or rates. The thermochemical properties of HSO are those determined by White and Gardiner (1979). The HSO species was included to test the conjecture (Frenklach *et al.* 1981) of its importance in improving the predictions of the reaction mechanism.

[†] see Shepherd and Roller (1982), Lee *et al.* (1982) and Shepherd (1985).

Detonation Reaction Zone Structure

The idealized, one-dimensional Zeldovich, von Neumann and Doring (ZND) model of detonation structure was used to calculate the characteristic reaction zone length. As discussed later, this reaction zone length is then used in a simple empirical correlation to predict detonation cell sizes. A complete description of this method and its application to hydrogen-air-diluent systems can be found in Lee *et al.* (1982) and Shepherd and Roller (1982). A brief outline of the method is given below.

First, the Chapman-Jouguet (CJ) detonation velocity is calculated with the equilibrium code of Gordon and McBride (1971). Using nominal initial conditions of 1 atm and 300 K, CJ conditions were calculated for H_2S-air mixtures with H_2S volume fractions between 5 and 45% of the total mixture. Results are given in Fig. 1. Air composition was approximated as 0.21 mole fraction O_2 and 0.79 N_2. Using the calculated CJ detonation velocities and the reaction mechanism shown in Tables 1 and 2, the structure of the reaction zone was calculated by integrating the governing equations along the Rayleigh line from the von Neumann point towards the CJ condition.

Results of a calculation for a near-stoichiometric mixture (13% H_2S in mixture; 12.3% is stoichiometric) are shown in Figs. 2-5. The temperature profile is shown in Fig. 2 and the species in Figs. 3-5. The temperature profile shows that the "induction" period is strongly exothermic, indicating that a thermal explosion mechanism is operating. However, as pointed out in Frenklach *et al.* (1981), this conclusion is strongly dependent on the rate constants used and, in particular, is quite sensitive to the values for reaction (22),

$$H_2S + O \rightleftharpoons SO + H_2 .$$

We have shown these profiles to indicate the sort of reaction zone structure produced with our particular mechanism and constants. A similar temperature rise during the "induction" period is found for both richer and leaner mixtures.

There is a strong interaction between hydrogen and sulphur oxidation, but as seen in Figs. 4 and 5, the sulphur-containing species SO_3, SO, and SH are the dominant minor species produced within the 0.1 to 0.5 cm zone. The major hydrogen-containing species, H_2 and H_2O, are present in about the same amount as the dominant sulphur species, SO_2. The minor hydrogen-containing species, OH, H, O, HO_2 and H_2O_2, are present in amounts that are 1 to 2 orders-of-magnitude less than the minor sulphur species (except for S_2, S, and HSO) in this zone.

The relative magnitudes of the minor hydrogen species are similar to those observed in lean hydrogen-air mixtures. The species HO_2 and H_2O_2 are more abundant in the first portion of the reaction zone than OH, H or O. This is due to the well-known competition between the three-body reactions (5-7),

$$H + O_2 + M \rightleftharpoons HO_2 + M ;$$

and the chain-branching reaction (3),

$$H + O_2 \rightleftharpoons OH + O.$$

In the latter portion of the reaction zone, the chain-branching mechanism overtakes the slower oxidation path of reaction (8) and the OH, H and O species dominate. The peroxides produced earlier are rapidly consumed in the chain-branching explosion.

In general, the species HSO is present in the smallest quantities. Near the end of the reaction zone, it has a concentration comparable those of HO_2 and H_2O_2. Otherwise, it is present in negligible amounts. Omitting this species entirely did not noticeably affect any of the results. However, since most of the reaction rates are speculative for reactions involving this species, the present results do not rule out its importance. As pointed out by Frenklach *et al.* (1981), the present set of reactions appears to be fundamentally incomplete. Basic experimental observations, such as the acceleration of reaction by H_2O, cannot be predicted by merely adjusting the rate constants. Perhaps some insight into these difficulties can be obtained by examining the reaction set for methylene (CH_2) oxidation.

The species S_2 and S are present in the next smallest quantities. As expected, these species are present in much larger concentrations in rich mixtures than in lean. For lean mixtures, these species are present in concentrations comparable to those of HO_2 and H_2O_2.

Reaction Zone Length Scale

The length of the reaction zone as a function of equivalence ratio is the main result of our calculations. We have used several measures of the reaction zone length in our previous studies and have obtained a reasonable correlation with measured detonation cell sizes. Three reaction zone lengths for dry H_2S-air mixtures are shown in Fig. 6 for H_2S concentrations between 5 and 45%. The first length ℓ_1 is computed from the ZND detonation structure and corresponds to the location of the maximum temperature gradient dT/dx. The second length ℓ_2 is derived from the approximate induction time formula given in Frenklach *et al.* (1981) for the data of Bradley and Dobson (1967). The third length ℓ_3 is based on a sensitivity parameter which can be approximated as $-T_{vn}\partial\ell_1/\partial T_{vn}$ where T_{vn} is the von Neumann spike temperature. These lengths and the basic CJ detonation parameters are also given in Table 3.

The first measure of reaction zone length has been used in many previous studies of this type. The distance ℓ_1 is usually the length of the thermally neutral portion of the reaction zone, or induction zone length. This is equivalent to the length used by Westbrook and Urtiew (1982), however, they used a constant-volume approximation to the Rayleigh line process. Using ℓ_1 alone to characterize the detonation reaction zone structure, Westbrook and Urtiew have demonstrated that semiquantitative predictions can be made for cell size, critical tube diameter and initiation energy in many different fuel-air and fuel-oxygen detonations.

We have used the present computational scheme to sucessfully model the effect of carbon dioxide (Lee *et al.* 1982) and water dilution (Shepherd and Roller 1982) on hydrogen-air detonations. In those studies, a length scale characteristic of the total extent of the reaction zone, induction zone plus recombination zone, was used. In hydrogen oxidation, the induction zone is essentially thermally neutral, so that the total reaction zone length can be substantially larger (at least for mixtures with 20 -

40% H_2) than the induction zone alone. However, the present kinetic scheme results in an exothermic induction zone for hydrogen sulphide and the distinction between total and induction length is not as useful.

The second induction length is derived from the approximate induction time formula given in Frenklach *et al.* (1981),

$$t_{ind} = 5 \times 10^{-13}[O_2]^{-0.45}[H_2S]^{-0.33} \exp(26,200/RT)$$

where $[O_2]$ and $[H_2S]$ are the postshock concentrations in moles/cm^3, T is the temperature in Kelvins, and t_{ind} is in seconds. The effective activation energy is in calories/mole. The length ℓ_2 is calculated by multiplying this time by the postshock fluid velocity relative to the shock wave. While approximate, this method is very useful for rapid estimates. As shown in Fig. 6, this simple technique yields results that are very similar to those of the much more complex technique used to derive ℓ_1. That similarity is no fluke, the reaction mechanism was adjusted by Frenklach *et al.* (1981) to reproduce the data from which the induction time fit was derived.

Curve ℓ_2 is lower than ℓ_1 because the approximate induction time formula was derived to describe the first appearance of OH and SO_2. That point occurs much earlier in the reaction zone than the location of the maximum temperature derivative, ℓ_1. The approximate formula we have chosen is not the one Frenklach *et al.* (1981) developed from their data but rather a refit of Bradley and Dobson's. We prefer this fit because it more closely follows the pressure dependence predicted by detailed simulations. We have calculated ℓ_1 for detonations of 8, 13 and 18% H_2S in mixtures at initial pressures of 0.1-1.0 atm. The results are shown in Fig. 7.

The pressure dependence shown in Fig. 7 can be approximated as a power law, $\ell \sim p^n$. The exponent n is $\approx$ -0.72 for the 13 and 18% cases; it is $\approx$ -0.48 for the 8% case. For a fixed composition and initial temperature, the detonation velocity, postshock temperature and fluid velocity are all approximately independent of the initial pressure. This means that the pressure exponent predicted by the simple induction time formula is approximately equal to the sum of the concentration powers, which is -0.78. This has the same sign as that predicted by the detailed simulation and is in good quantitative agreement with the 13 and 18% cases. The induction time correlation developed by Frenklach *et al.* (1981) for their data would predict an exponent of +0.31. Since the correlation of Bradley and Dobson's data also predicts the Frenklach *et al.* (1981) data with reasonable accuracy, we believe that it is a better all-around correlation for estimation of induction time.

The third distance ℓ_3 is a more recent development (Shepherd 1985) that is found to correlate better, for hydrogen-air detonations, with detonation cell size than the other two lengths. Briefly, the constant-volume model of the Rayleigh line is used to obtain the length ℓ_1 as a function of von Neumann spike temperature. The derivative $\partial\ell_1/\partial T_{vn}$ is then approximated numerically from these results.

Physically, this derivative can be related to the effective activation energy E for a global (single-step) model of the reaction kinetics. This is one of the most important parameters in determining the stability of the detonation to both longitudinal (one-dimensional) and transverse (multidimensional) perturbations. If the induction time can be represented by a simple formula of the type discussed above,

$$t_{ind} = C[\text{fuel}]^{\alpha}[\text{O}_2]^{\beta}\exp(E/RT),$$

then by calculating the induction time at different temperatures, but fixed composition and pressure, E can be determined from the slope of a plot of $\log t_{ind}$ *vs* $1/T$. Deviations from a constant slope indicate a change in the dominating processes with temperature or that a multistep approximation may be more appropriate.

An example of such a plot is shown in Fig. 8. The abscissa is actually T_{vn}/T rather than just $1/T$; this means that the slope of the curve is the reduced activation energy $E^{*} = E/RT_{vn}$. Despite the complexity of the reaction mechanism, the plot is quite linear, indicating that the global approximation is very good over the range shown. The temperature range covered in Fig. 8 represents a variation of shock velocities from $0.5 \times U_{CJ}$ to $1.5 \times U_{CJ}$; this is the typical oscillation range observed in unstable detonations. Due to the linearity of the plots, the effective activation energy calculated by examining small variations of T ($\pm 1\%$ of T_{vn}) is approximately the same as that determined by fitting a line to a plot like Fig. 8. For other fuels, that is typically not the case; the induction time curve tends to flatten out since endothermic processes like dissociation become important when the detonation is strongly overdriven.

Using small temperature variations, calculations over the range of 5 to 30% H_2S give similar results and the effective activation energy is remarkably constant, the average value being 25.3 ±0.3 kcal/mole. Comparisons with the large amplitude results for selected cases indicate that this value is also appropriate for large temperature variations. This value is slightly lower than the value of 26.2 kcal/mole used in the approximate formula developed by Frenklach *et al.* (1981) and well within their quoted standard deviation.

The length scale ℓ_3 can be related to the effective activation energy by substituting the global expression for induction time into the derivative (using $\ell = u \times t_{ind}$):

$$-\frac{T_{vn}}{\ell}\frac{\partial \ell}{\partial T} = \frac{E}{RT_{vn}} = E^{*}.$$

In other words,

$$\ell_3 \sim E^{*}\ell\,;$$

the reduced activation energy lies in the range $8.5 \leq E^{*} \leq 13$ for all mixtures and $\ell \sim \ell_1$. The reaction zone length ℓ calculated in these sensitivity studies is not exactly the same as ℓ_1 since a constant-volume approximation to the Rayleigh line is used rather than the true ZND model.

Since water vapor is expected to be present in most industrial situations where H_2S is a detonation hazard, we have performed some sensitivity calculations of its effect on the reaction zone length. The effect of 1, 5, and 10% water vapor on ℓ_1 for selected mixtures (ϕ = 0.375, 0.795, 1.26, 1.78, 2.38, 3.06) is shown together with the dry mixture results in Fig. 9. Strictly speaking, it is not possible to have an equilibrium water vapor pressure above 3.5% at 300 K but we assumed this state in order to compare these results to the previous dry cases.

Water vapor has a retarding effect on the reaction, increasing water vapor concentration increases the reaction zone length. Away from the limits, *i.e.*, between 10 and 30% H_2S in the dry mixture, the ratio of diluted to undiluted reaction zone length is independent of the equivalence ratio. The value of this ratio is 1.1, 1.4, and 2.1 for 1, 5, and 10% water vapor dilution at a fixed total pressure (1 atm) and initial temperature (300K).

These results are similar to those both calculated and observed for water vapor addition to hydrogen-air mixtures. The mechanism in H_2-air-H_2O and the present case appears to be primarily thermodynamic rather than a shift in the kinetic mechanism. Adding an inert diluent to a fuel-air mixture effectively reduces the heat of reaction, lowering the detonation velocity and postshock temperature. Using the approximate induction time formula and the calculated postshock temperatures, it is possible to account for 90% of the increase in ℓ_1; the other 10% can be accounted for by the decrease in partial pressure of reactants. This is true away from the limits; an additional increase possibly due to kinetic effects is observed at both the rich and lean limits.

The effect shown in Fig. 9 is contrary to the experimental observations of Frenklach *et al.* (1981) but in agreement with their computations. As mentioned above, this discrepancy is probably due to omitting a path in the reaction mechanism. Unfortunately, there is a large amount of scatter in the data of Frenklach *et al.* (1981), which will make determining this mechanism difficult without further experimentation.

Estimation of Detonation Cell Sizes

The application of the kinetic models to predicting cell size λ is severely limited by the lack of a quantitative, two-dimensional detonation instability theory. Without such a theory, the most productive approach is to empirically correlate the measured cell sizes with the calculated reaction zone lengths, described above. The simplest approach is to use a linear scaling $\lambda = \mathcal{A}_i \ell_i$. Experimentally, $\mathcal{A}$ is found to be a strong function of equivalence ratio for many methods of calculating ℓ. For example, in H_2-air mixtures, $\mathcal{A}_1$ can vary from 10-80 with a rather peculiar dependence on ϕ (Shepherd 1985). On the other hand, $\mathcal{A}_3$ is much smaller, on the order of 2 to 10 for the hydrogen-air system.

The "constant" $\mathcal{A}$ also strongly depends both on the fuel-oxidizer system and the initial conditions. The only general statement that can be made is that for a given fuel-oxidizer combination, the experimentally determined $A(\phi)$ appears to be valid for diluted mixtures as long as the diluent is relatively inert (Shepherd 1985). Westbrook and Urtiew (1982) state that a value of $A = 20$ is appropriate for many stoichiometric fuel-air mixtures initially at atmospheric pressure and room temperature. For stoichiometric mixtures of H_2S-air, $\ell_1 = 0.5$ cm, implying a value of $\lambda = 10$ cm. Of course, this only applies to the "standard" length scale ℓ_1 and should be taken as an approximate guideline. This is especially true in the present case since the reaction zone structure is rather atypical, most previously investigated fuel-air detonations show much less exothermicity in the induction zone than the present calculations indicate. Investigations (Frey *et al.*, 1976) of the longitudinal instability of one-dimensional detonations have shown that the structure (temperature profile) of the reaction zone can have a strong influence on the instability characteristics.

The value of A_1 for H_2S-air mixtures can be estimated from corresponding values for hydrocarbon-air mixtures with similar sensitivities. From the data of Moen *et al.* (1984b) and both past and present work on H_2S, it appears that the H_2S-air system is very similar in sensitivity to ethane (C_2H_6), which for stoichiometric mixtures in air has $\ell_1 = 0.45$ cm. The data for ethane imply that for stoichiometric mixtures $10 \leq A_1 \leq 20$. This is consistent with the other values mentioned above. In order to use the approximate values given by ℓ_2, an additional multiplicative factor of 1.5 should be used.

Investigations (Shepherd 1985) with other fuels show that values of A_3 are much smaller than A_1, and are less sensitive to changes in ϕ. For example, away from the rich and lean limits, A_3 for hydrogen-air mixtures only varies between 4 and 10. However, since we have less experience with ℓ_3, the extrapolation between substances is more uncertain. A tentative guideline for the present application might be a lower bound of $A_3 = 4$ and an upper bound of $A_3 = 10$. The predictions for cell size and comparison with the experimental data are given in the next section.

Experimental Results

Facility and Procedures

Critical tube experiments were performed at the DRES fuel-air test site. These experiments are described in detail by Sulmistras *et al.* (1985). The experimental facility is centered around an 0.89 m diameter by 7.8 m long steel test section. To simulate an unconfined cloud for the critical tube diameter tests, 1.8 m diameter polyethylene bags measuring up to 5 m in length were attached to one end of the steel tube. At the opposite end, a solid explosive charge was used to initiate the detonation. Hydrogen sulphide gas (99% pure) was mixed with the initial air in the test volume and recirculated using a high capacity centrifugal blower. The composition and homogeneity of the mixture in the test volume were monitored with an infared gas analyzer by continuously analyzing samples taken from several ports in the tube.

The detonation travel was monitored with piezo-electric pressure transducers at up to seven positions along the tube. The fate of the detonation as it emerged from the tube was also monitored by high-speed photography taken from three positions. The detonation cell size was determined in two ways. First, prior to the detonation, a carefully "sooted" sheet (3 m × 1.5 m) was placed around the inside periphery of the tube to record the detonation cellular structure for each trial. Second, in tests used only to determine cell size, polyethylene bags the same size as the steel tube were used in order to obtain "bag strips." As discussed by Moen *et al.* (1982) these strips are produced by the cutting action of the shock triple points and the width of these strips is equal to the cell width.

Results and Discussion

For all the mixtures tested, ranging from ~ 10 to 14% H_2S by volume, the detonation failed to transit from the tube into a spherical wave in the plastic bag. The critical tube diameter for the most sensitive compositions is therefore greater than 0.89 m.

A more quantitative assessment of the detonability of H_2S-air mixtures was obtained from the cellular structure recorded on the sooted steel sheets. A typical smoked foil record for 14.2% H_2S is shown in Fig. 10. The minimum cell size λ of 10 cm was obtained at stoichiometric composition. On either side of stoichiometric composition, cell size increased. Values ranged from 27.5 cm at 10% H_2S to 11.0 cm at 14.2% H_2S.

Additional information was extracted from "single-head spin" tests conducted at McGill University (Lee and Knystautas 1984) in a 14.5 cm diameter tube. Moen *et al.* (1981) have proposed that the cell size at the onset of single-head spin in a tube of diameter D can be calculated by assuming a purely acoustic transverse wave. This gives a spin pitch P (or cell length) to tube diameter ratio of $P/D = \pi U/k_1 c$, where U is the detonation velocity, c is the local speed of sound, and k_1 is the first root of the derivative of the Bessel function of order one, $k_1 = 1.841$.

The McGill records show that single-head spin appears in a 14.5 cm diameter tube for H_2S concentrations between 9-10 and 20-22%. The acoustic model yields cell lengths of 43.2 cm and 44.0 cm, respectively. Corresponding cell widths based on $\lambda = 0.6P$ are 26.0 cm and 26.4 cm, respectively. Another frequently used estimate (Lee 1984) of cell size at the onset of single-head spin is $\lambda = \pi D$. This would give a value of $\lambda = 45.5$ cm in both cases.

All of the cell size data are summarized in Table 4, together with the detonation pressures and velocities observed in the steel tube. The velocities are in good agreement with the theoretical CJ values given in Table 3 and Fig. 1, indicating that stable detonations had been established inside the tube.

The experimentally determined cell sizes are compared with those predicted by $20\ell_1$ in Fig. 11. The predicted values are in good agreement with the observations. The approximate guideline proposed by Westbrook and Urtiew (1982) is therefore applicable to H_2S-air in spite of the atypical reaction zone structure associated with this system. Also shown in Fig. 11 is 4 times the characteristic length ℓ_3. The factor relating ℓ_3 to the cell size ranges from about 3.5 at stoichiometric to about 5.5 at 10% H_2S. This is slightly smaller than the values found for hydrogen-air detonations over a similar range of equivalence ratios.

These estimates, derived from results for hydrogen- and hydrocarbon-air detonations, are surprisingly reliable for a system with an atypical reaction zone structure such as H_2S-air. In fact, correlations based on either $20\ell_1$ or $4\bar{\ell}_3$ predict the cell size within a factor of two over a fairly wide range of compositions. The success of these correlations indicates that the characteristic cell size is relatively insensitive to the differences in the reaction zone structure between common hydrocarbon-air and H_2S-air systems.

These differences appear to be reflected more in the details of the cellular structure. The structure in H_2S-air shown in Fig. 10 is more regular than that typically observed in propane and ethylene systems by Moen *et al.* (1984b). There are certainly indications of substructure, but the cells themselves are more clearly defined in H_2S-air. This observation may be related to the apparent stability of the chemical processes to variations in the gasdynamic conditions, as discussed above. It is interesting that Bull *et al.* (1982) and Strehlow (1969) noted that the cellular structure of H_2-air and H_2-O_2 detonations was also more regular than those of hydrocarbon-air or hydrocarbon-O_2 detonations. A common link is that both H_2S-air and H_2-air detonations have smaller values of reduced activation energy E^* than most other fuel-air detonations. Approximate theories of detonation stability indicate that decreasing E^* has a stabilizing effect.

The Critical Tube Diameter

Detonation transmission was not observed in any of the critical tube experiments, indicating that the critical tube diameter is greater than 0.89 m at a stoichiometric composition. Lacking any data, estimates of the critical tube diameter for H_2S-air can be made using the empirical relation $d_c = 13\lambda$. This relation has been established for many fuel-oxidizer systems with similar cellular structure by Knystautas *et al.* (1982). At stoichiometric conditions, the measured cell size of 10 cm implies a critical tube diameter of 1.3 m, consistent with the observations of transmission failure at 0.89 m.

Critical tube diameters for a variety of fuel-air mixtures, including H_2S-air are shown in Fig. 12. The results for acetylene, hydrogen, ethylene and propane are based on the correlations of experimental critical tube diameter results by Moen *et al.* (1984b). The methane and H_2S results are calculated from $d_c = 13\lambda$. For these common fuels, H_2S lies between methane (less sensitive) and propane (more sensitive) on the relative detonation hazard scale proposed by Matsui and Lee (1978).

Summary

A detailed kinetic model for hydrogen sulphide oxidation is used to calculate reaction zone length scales for detonations of H_2S-air mixtures at standard conditions. The conventional induction length at stoichiometric conditions is found to be 0.5 cm; the detonation cell size is estimated to be $\sim$ 10 cm. Results of model calculations can be represented fairly accurately by a single-step (global) reaction mechanism with an effective activation energy of 25.3 kcal/mole. The pressure dependence of the reaction zone length can be approximately represented by p^n, with $-0.75 \leq n \leq -0.48$. Water vapor dilution increases the reaction zone length: the ratio of diluted to undiluted lengths is 1.1, 1.4, and 2.1 for 1, 5, and 10% dilution of stoichiometric mixtures.

The predicted cell sizes are in good agreement with those measured experimentally in a series of tests performed to determine the relative detonation hazard of H_2S-air mixtures. The measured minimum cell size of about 10 cm at stoichiometric composition and standard initial conditions is in exact agreement with the estimate based on the conventional induction length with the same scaling factor of 20 as found for other more common fuel-air mixtures. The variation in cell size with composition, based on this scaling factor, is also in good agreement with experimental cell sizes measured for compositions between 10 and 20% H_2S. Based on the $d_c = 13\lambda$ estimate, the critical tube diameter at stoichimetric composition is 1.3 m. H_2S-air therefore lies between methane-air ($d_c \simeq 3.6$ m) and propane-air ($d_c \simeq 0.9$ m) in terms of relative detonation hazard.

Acknowledgments

The experiments were partially funded by the Atomic Energy Control Board of Canada and the Canadian Department of National Defence. The modeling was supported by the U. S. Department of Energy and performed at Sandia National Laboratories.

References

Bernez-Cambot, J., Vovelle, C. and Delbourgo, R. (1981) Flame Structures of H_2S-Air Diffusion Flames. *18th Symposium (Intl.) on Combustion*, pp. 777–783, The Combustion Institute, Pittsburgh, Pa.

Bowman, C. T. and Dodge, L. G. (1976) Kinetics of the Thermal Decomposition of Hydrogen Sulfide Behind Shock Waves. *16th Symposium (Intl.) on Combustion*, pp. 971–982, The Combustion Institute, Pittsburgh, Pa.

Bradley, J. N. and Dobson, D. C. (1967) Oxidation of Hydrogen Sulfide in Shock Waves. I. Absorption Studies of OH and SO_2 in H_2S-O_2-Ar mixtures. *J. Chem. Phys.* **46**(8), 2865–2871.

Bull, D. C., Ellsworth, J. E., and Schuff, P. J. (1982) Detonation Cell Structure in Fuel/Air Mixtures. *Combustion and Flame* **45**, 7–22.

Cullis, C. F. and Mulcahy, M. F. R. (1972) The Kinetics of Combustion of Gaseous Sulfur Compounds. *Combustion and Flame* **18**, 225–292.

Frenklach, M., Lee, J. H., White, J. N., and Gardiner, W. C., Jr. (1981) Oxidation of Hydrogen Sulphide. *Combustion and Flame* **41**, 1–16.

Gordon, S. and McBride, B. J. (1971) Computer Program for the Calculation of Complex Chemical Equilibrium Compositions, Rocket Performance, Incident and Reflected Shocks and Chapman-Jouguet Detonations. NASA SP-273.

Howe, P., Frey, R., and Melani, G. (1976) Observations Concerning Transverse Waves in Solid Explosives. *Combustion Sci. Technol.* **14**, 63-74.

Knystautas, R., Lee, J. H., and Guirao, C. (1982) The Critical Tube Diameter for Detonation Failure in Hydrocarbon-Air Mixtures. *Combustion and Flame* **48**, 63–83.

Lee, J. H. (1984), Parameters of Gaseous Detonation, *Ann. Rev. of Fluid Mech.* **16**, 311–336.

Lee, J. H. and Knystautas, R. (1984) McGill University (private communication).

Lee, J. H., Knystautas, R. M., Guirao, C., Benedick, W. B. and Shepherd, J. E. (1982) Hydrogen-Air Detonations. *Proc. 2nd Intl. Workshop on Hydrogen Behavior in Light Water Reactors*, pp. 961–1006, (Eds. M. Berman and L. Thompson) available as Sandia National Laboratories Report SAND82-2456.

Matsui, H. and Lee, J. H. (1978) On the Measure of Relative Detonation Hazards of Explosive Gases. *17th Symposium (Intl.) on Combustion*, pp. 1153–1164, The Combustion Institute, Pittsburgh, Pa.

Miller, J. A., Mitchell, R. E., Smooke, M. D., and Kee, R. J. (1982) Towards a Comprehensive Kinetic Mechanism for Oxidation of Acetylene. *19th Symposium (Intl.) on Combustion*, pp. 181–196, The Combustion Institute, Pittsburgh, Pa.

Moen, I. O., Donato, M., Knystautas, R. and Lee, J. H. (1981) The Influence of Confinement on the Propagation of Detonations near the Detonability Limits. *18th Symposium (Intl.) on Combustion*, pp. 1615–1622, The Combustion Institute, Pittsburgh, Pa.

Moen, I. O., Murray, S. B., Bjerketvedt, D., Rinnan, A., Knystautas, R., and Lee, J. H. (1982) Diffraction of Detonation from Tubes into a Large Fuel-Air Explosive Cloud. *19th Symposium (Intl.) on Combustion*, pp. 635–644, The Combustion Institute, Pittsburgh, Pa.

Moen, I. O., Ward, S. A., Thibault, P. A., Lee, J. H., Knystautas, R., Dean, T., and Westbrook, C. K. (1984a) The Influence of Diluents and Inhibitors on Detonations. *20th Symposium (Intl.) on Combustion*, to be published.

Moen, I. O., Funk, J. W., Ward, S. A., Rude, G. M. and Thibault, P. A. (1984b) Detonation Length Scales for Fuel-Air Explosives. *AIAA Progress in Astronuatics and Aeronautics* **94**, 55–79.

Muller, C. H., III, Schofield, K., Steinberg, M., and Broida, H. P. (1979) Sulfur Chemistry in Flames. *17th Symposium (Intl.) on Combustion*, pp. 867–879, The Combustion Institute, Pittsburgh, Pa.

Roth, P., Lohr, R., and Barnes, V. (1982) Thermal Decomposition of Hydrogen Sulfide at Low Concentrations. *Combustion and Flame* **45**, 273-285.

Shepherd, J. E. and Roller, S. F. (1982) Effect of Steam on the Detonability of Hydrogen-Air Mixtures. *Proc. 2nd Intl. Workshop on Hydrogen Behavior in Light Water Reactors*, pp. 1007–1026, (Eds. M. Berman and L. Thompson) available as Sandia National Laboratories Report SAND82-2456.

Shepherd, J. E. (1985) Detonation Modeling and Reaction Kinetics in Hydrogen-Air-Diluent Mixtures. Submitted for publication at the 10th International Colloquium on Dynamics of Explosions and Reactive Systems.

Strehlow, R. A. (1969) The Nature of Transverse Waves in Detonations. Astronautica Acta 14, 539–548.

Sulmistras, A., Moen, I. O., and Saber, A. J. (1985) Detonations in Hydrogen Sulphide-Air Clouds. Suffield Memorandum No. 1140, Defence Research Establishment Suffield, Ralston, Alberta, Canada.

Wendt, J. O. L., Wootan, E. C., and Corley, T. L. (1983) Postflame Behavior of Nitrogenous Species in the Presence of Fuel Sulfur I. Rich, Moist CO/Ar/O_2 Flames. *Combustion and Flame* 49, 261-274.

Westbrook, C. K. and Urtiew, P. A. (1982) Chemical Kinetic Prediction of Critical Parameters in Gaseous Detonations. *19th Symposium (Intl.) on Combustion*, pp. 615–623, The Combustion Institute, Pittsburgh, Pa.

White, J. N. and Gardiner, W. C., Jr. (1978) Thermochemical Properties of the HSO Radical. *Chem. Phys. Lett.* 58(3), 470-472.

Figure Captions

1. Chapman-Jouguet detonation velocities for H_2S-air mixtures initially at 1 atm pressure and 300 K temperature.

2. Variation of temperature through the reaction zone of a near-stoichiometric (13% H_2S in mixture) H_2S-air detonation. Initial pressure, 1 atm; initial temperature 300 K.

3. Variation of N_2, H_2O, H_2, O_2, and H_2 mole fractions through the reaction zone. Conditions given in Fig. 2.

4. Variation of OH, H, O, HO_2, and H_2O_2 mole fractions through the reaction zone. Conditions given in Fig. 2.

5. Variation of SO_3, SO_2, SO, S, S_2, SH, and HSO mole fractions through the reaction zone. Conditions given in Fig. 2.

6. Reaction zone lengths *vs* the concentration of hydrogen sulphide (volume percent in mixture). ℓ_1 is the distance to the maximum temperature derivative; ℓ_2 is based on the approximate induction time formula; ℓ_3 is the characteristic length derived from the sensitivity analysis.

7. Pressure dependence of detonations with 8, 13 and 18% H_2S in air, initial temperature of 300 K.

8. Temperature dependence of 15% H_2S detonation induction time; initial pressure of 1 atm. Induction time corresponds to the length ℓ_1 as calculated by the constant-volume approximation to the Rayleigh line.

9. Effect of 1, 5 and 10% H_2O dilution on the reaction zone length ℓ_1 for various mixtures. Initial pressure 1 atm, initial temperature 300 K. The solid line is ℓ_1 for dry mixtures.

10. Cell structure recorded on the smoked foil for 14.2% H_2S.

11. Comparison of measured cell size λ with $20\ell_1$ and $4\ell_3$.

12. Critical tube diameter *vs* equivalence ratio for selected fuel air systems. Acetylene, hydrogen and propane results are from the correlations of Moen *et al.* (1984b) based on direct measurement. Methane and hydrogen sulphide are based on cell size and the 13λ estimate.

Table Captions

1. Hydrogen Oxidation Mechanism and Rate Constants

2. Hydrogen Sulphide Oxidation Mechanism and Rate Constants

3. Detonation Calculation Summary

4. Measured Detonation Parameters

Table 1

REACTION	A	β	E
1. $H_2 + O_2 \rightleftharpoons OH + OH$	1.70×10^{13}	0.00	47780.
2. $OH + H_2 \rightleftharpoons H_2O + H$	1.17×10^{9}	1.30	3626.
3. $H + O_2 \rightleftharpoons OH + O$	5.13×10^{16}	-0.82	16507.
4. $O + H_2 \rightleftharpoons OH + H$	1.80×10^{10}	1.00	8826.
5. $H + O_2 + M \rightleftharpoons HO_2 + M$	2.10×10^{18}	-1.00	0.
6. $H + O_2 + O_2 \rightleftharpoons HO_2 + O_2$	6.70×10^{19}	-1.42	0.
7. $H + O_2 + N_2 \rightleftharpoons HO_2 + N_2$	6.70×10^{19}	-1.42	0.
8. $OH + HO_2 \rightleftharpoons H_2O + O_2$	5.00×10^{13}	0.00	1000.
9. $H + HO_2 \rightleftharpoons OH + OH$	2.50×10^{14}	0.00	1900.
10. $O + HO_2 \rightleftharpoons O_2 + OH$	4.80×10^{13}	0.00	1000.
11. $OH + OH \rightleftharpoons O + H_2O$	6.00×10^{8}	1.30	0.
12. $H_2 + M \rightleftharpoons H + H + M$	2.23×10^{12}	0.50	92600.
13. $O_2 + M \rightleftharpoons O + O + M$	1.85×10^{11}	0.50	95560.
14. $H + OH + M \rightleftharpoons H_2O + M$	7.50×10^{23}	-2.60	0.
15. $H + HO_2 \rightleftharpoons H_2 + O_2$	2.50×10^{13}	0.00	700.
16. $HO_2 + HO_2 \rightleftharpoons H_2O_2 + O_2$	2.00×10^{12}	0.00	0.
17. $H_2O_2 + M \rightleftharpoons OH + OH + M$	1.30×10^{17}	0.00	45500.
18. $H_2O_2 + H \rightleftharpoons HO_2 + H_2$	1.60×10^{12}	0.00	3800.
19. $H_2O_2 + OH \rightleftharpoons H_2O + HO_2$	1.00×10^{13}	0.00	1800.

Reaction rate coefficients are in the form $k_f = AT^{\beta} \exp -E/RT$. Units are moles, cubic centimeters, seconds, Kelvins and calories/mole. Third body efficiencies: $k_5(H_2O) = 21k_5(Ar)$; $k_5(H_2) = 3.3k_5(Ar)$; $k_{12}(H_2O) = 6k_{12}(Ar)$; $k_{12}(H) = 2k_{12}(Ar)$; $k_{12}(H_2) = 3k_{12}(Ar)$; $k_{14}(H_2O) = 20k_{14}(Ar)$.

Table 2

REACTION	A	β	E
20. $H_2S + M \rightleftharpoons SH + H + M$	2.00×10^{14}	0.0	74080.
21. $H_2S + H \rightleftharpoons SH + H_2$	9.03×10^{12}	0.0	1698.
22. $H_2S + O \rightleftharpoons SO + H_2$	1.00×10^{13}	0.0	10000.
23. $H_2S + O \rightleftharpoons SH + OH$	4.36×10^{12}	0.0	3297.
24. $H_2S + OH \rightleftharpoons SH + H_2O$	1.40×10^{13}	0.0	860.
25. $SH + SH \rightleftharpoons H_2S + S$	1.00×10^{14}	0.0	1420.
26. $SH + H \rightleftharpoons H_2 + S$	6.31×10^{11}	0.5	0.
27. $SH + O \rightleftharpoons SO + H$	6.31×10^{11}	0.5	0.
28. $SH + O \rightleftharpoons S + OH$	6.31×10^{11}	0.5	8004.
29. $SH + S \rightleftharpoons S_2 + H$	6.31×10^{11}	0.5	0.
30. $SH + O_2 \rightleftharpoons SO + OH$	1.00×10^{13}	0.0	20000.
31. $SH + O_2 \rightleftharpoons SO_2 + H$	5.00×10^{13}	0.0	20000.
32. $SH + HO_2 \rightleftharpoons H_2S + O_2$	1.00×10^{12}	0.0	0.
33. $S + O_2 \rightleftharpoons SO + O$	6.31×10^{11}	0.5	0.
34. $S + OH \rightleftharpoons SO + H$	6.31×10^{11}	0.5	0.
35. $S_2 + O \rightleftharpoons SO + S$	6.31×10^{11}	0.5	0.
36. $S + S + M \rightleftharpoons S_2 + M$	1.00×10^{18}	-1.0	0.
37. $SO + O_2 + M \rightleftharpoons SO_3 + M$	1.00×10^{15}	0.0	0.
38. $SO + O_2 \rightleftharpoons SO_2 + O$	1.81×10^{11}	0.0	5601.
39. $SO + OH \rightleftharpoons SO_2 + H$	6.46×10^{14}	0.0	2085.
40. $SO_3 + O \rightleftharpoons SO_2 + O_2$	2.80×10^{14}	0.0	12000.
41. $SO_2 + O + M \rightleftharpoons SO_3 + M$	4.00×10^{20}	-4.0	5260.
42. $SO + O + M \rightleftharpoons SO_2 + M$	1.20×10^{22}	-1.84	0.
43. $SO + SO \rightleftharpoons SO_2 + S$	5.00×10^{11}	0.0	3298.
44. $SO_3 + SO \rightleftharpoons SO_2 + SO_2$	1.00×10^{12}	0.0	0.
45. $SH + H_2O_2 \rightleftharpoons HO_2 + H_2S$	1.00×10^{11}	0.0	0.
46. $SH + HO_2 \rightleftharpoons H_2O_2 + S$	1.00×10^{11}	0.0	0.
47. $SH + OH \rightleftharpoons H_2O + S$	1.00×10^{12}	0.0	0.
48. $HO_2 + S \rightleftharpoons SH + O_2$	1.00×10^{12}	0.0	0.
49. $HO_2 + SO_2 \rightleftharpoons SO_3 + OH$	1.00×10^{12}	0.0	0.
50. $SO_3 + H \rightleftharpoons SO_2 + OH$	1.00×10^{12}	0.0	0.
51. $H + SO + M \rightleftharpoons HSO + M$	1.60×10^{20}	-1.5	0.
52. $HSO + H \rightleftharpoons H_2 + SO$	5.00×10^{11}	0.5	2204.
53. $HSO + H \rightleftharpoons H_2S + O$	5.00×10^{10}	0.5	4488.
54. $HSO + H \rightleftharpoons SH + OH$	5.00×10^{11}	0.5	4488.
55. $HSO + OH \rightleftharpoons H_2O + SO$	5.00×10^{13}	0.0	998.
56. $HSO + O \rightleftharpoons SO + OH$	5.00×10^{11}	0.5	2204.
57. $HSO + O \rightleftharpoons H + SO_2$	1.00×10^{14}	0.0	26016.
58. $HSO + O \rightleftharpoons SH + O_2$	5.00×10^{11}	0.5	4488.
59. $HSO + O_2 \rightleftharpoons SO + HO_2$	5.00×10^{11}	0.5	2204.

Table 3

X_{H_2S}	ϕ	U_{CJ} (m/s)	P_{VN} (atm)	T_{VN} (K)	ℓ_1 (cm)	ℓ_2 (cm)	ℓ_3 (cm)
.05000	0.376	1249.9	15.296	991.1	62.3	36.3	138.
.06000	0.456	1328.6	17.380	1076.2	17.7	11.7	71.8
.07000	0.537	1398.4	19.350	1154.7	6.70	4.81	39.4
.08000	0.621	1460.8	21.212	1227.1	3.10	2.33	16.7
.09000	0.706	1516.8	22.967	1293.9	1.67	1.28	9.00
.10000	0.793	1567.0	24.610	1355.0	1.01	.779	5.42
.11000	0.882	1610.8	26.102	1409.2	.679	.518	3.60
.12000	0.974	1643.5	27.264	1449.9	.517	.386	2.70
.13000	1.067	1648.3	27.493	1454.8	.504	.364	2.60
.14000	1.162	1632.2	27.011	1432.7	.583	.409	3.00
.15000	1.260	1616.2	26.535	1411.0	.673	.460	3.49
.16000	1.360	1602.2	26.128	1392.0	.764	.512	4.01
.17000	1.426	1588.9	25.746	1374.2	.863	.568	4.61
.18000	1.567	1576.5	25.396	1357.6	.970	.626	5.26
.19000	1.675	1564.5	25.061	1341.7	1.09	.691	6.01
.20000	1.785	1552.7	24.733	1326.2	1.23	.763	6.88
.21000	1.898	1541.1	24.412	1311.0	1.38	.843	7.88
.22000	2.014	1529.6	24.096	1296.2	1.56	.932	9.05
.23000	2.133	1518.1	23.781	1281.4	1.76	1.03	10.4
.24000	2.255	1506.7	23.471	1266.9	2.00	1.15	12.0
.25000	2.380	1495.0	23.152	1252.2	2.28	1.28	14.0
.30000	3.060	1436.2	21.567	1180.4	4.58	2.32	30.8
.35000	3.845	1376.1	19.978	1110.4	10.0	4.54	74.7
.40000	4.760	1314.3	18.381	1041.8	24.4	9.74	203.
.45000	5.842	1253.8	16.867	977.6	64.1	22.2	621.

Table 4

% H_2S (by volume)	$\overline{U}^a$ (m/s)	$\overline{P}^b$ (atm)	λ (cm)
DRES critical tube tests			
9.6 - 10.3	1544	13.6	26.5 - 29.0
10.5 - 11.4	1587	14.3	16.0 - 19.0
12.0 - 13.2	1660	15.2	10.0 - 13.0
13.9 - 14.5	1633	14.8	10.2 - 11.8
12.4 - 12.8	1611	15.2	8.5 - 12.0
McGill single-head spin tests			
9 - 10	-	-	26.0 - 45.5
20 - 22	-	-	26.4 - 45.5

[a] Average detonation velocity in tube. [b] Average detonation pressure from 3 locations.

Figure 1

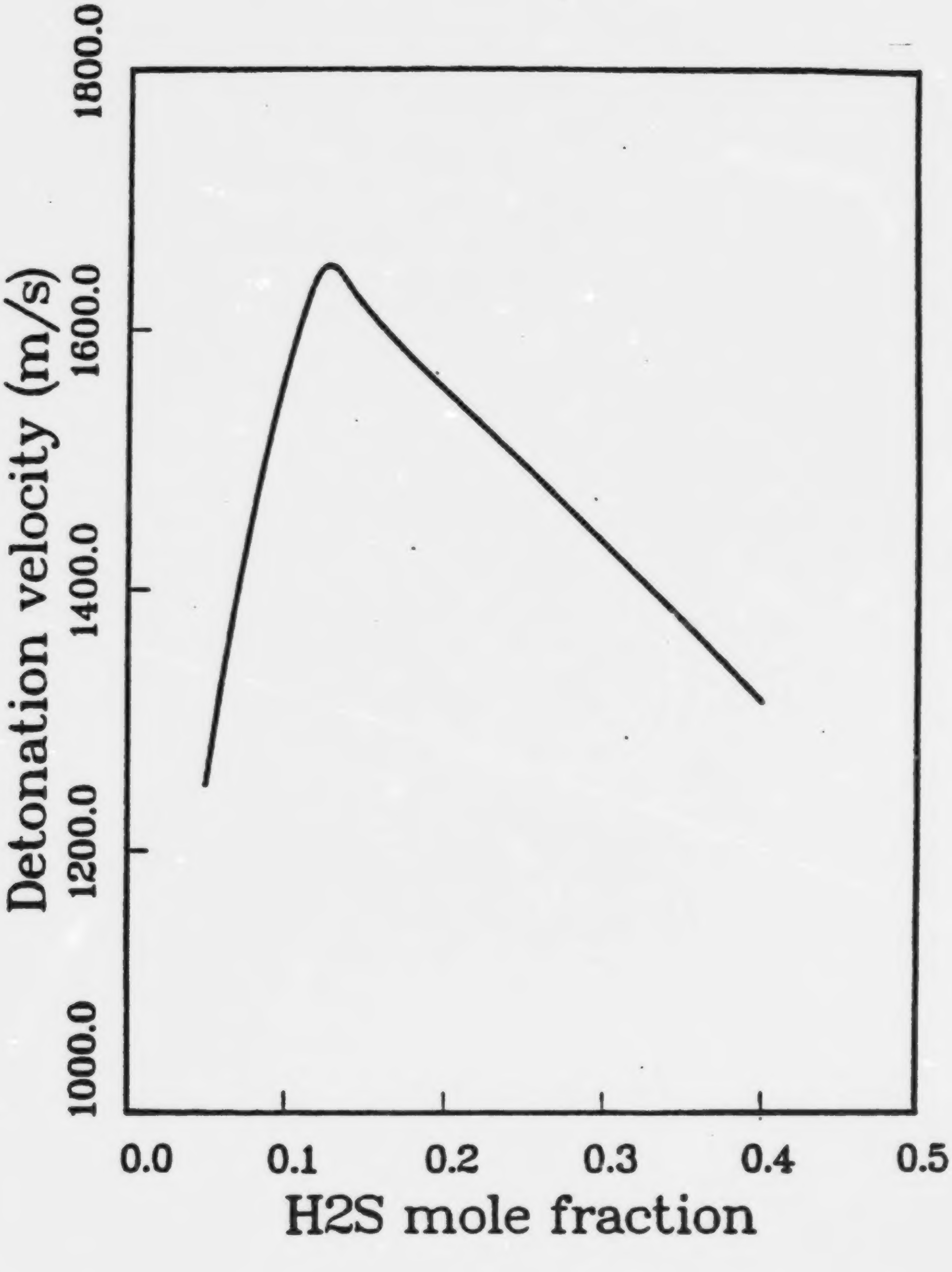
Detonation velocity (m/s)
1000.0
1200.0
1400.0
1600.0
1800.0
0.0
0.1
0.2
0.3
0.4
0.5
H2S mole fraction

Figure 2

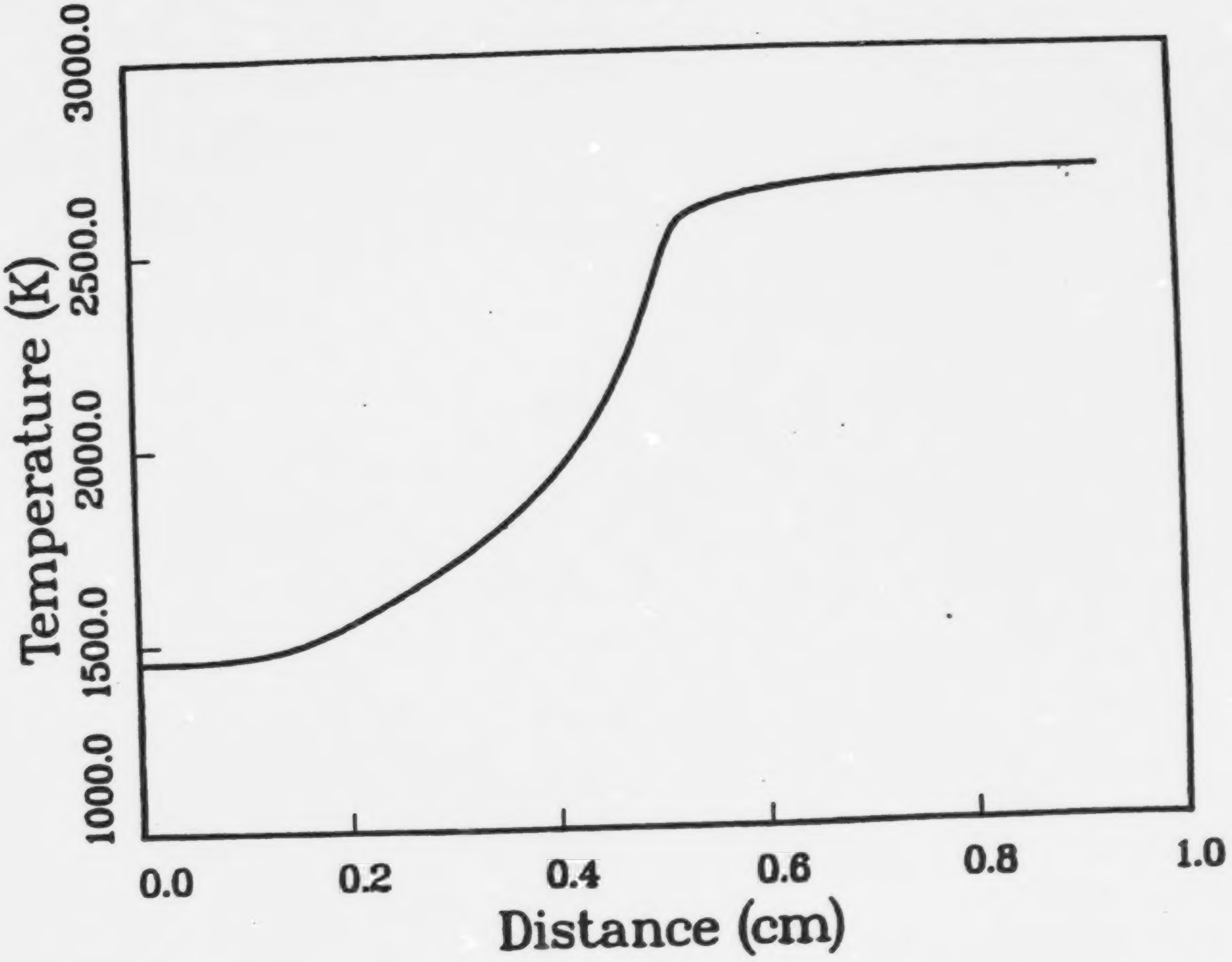

Temperature (K)
3000.0
2500.0
2000.0
1500.0
1000.0
0.0
0.2
0.4
0.6
0.8
1.0
Distance (cm)

Figure 3

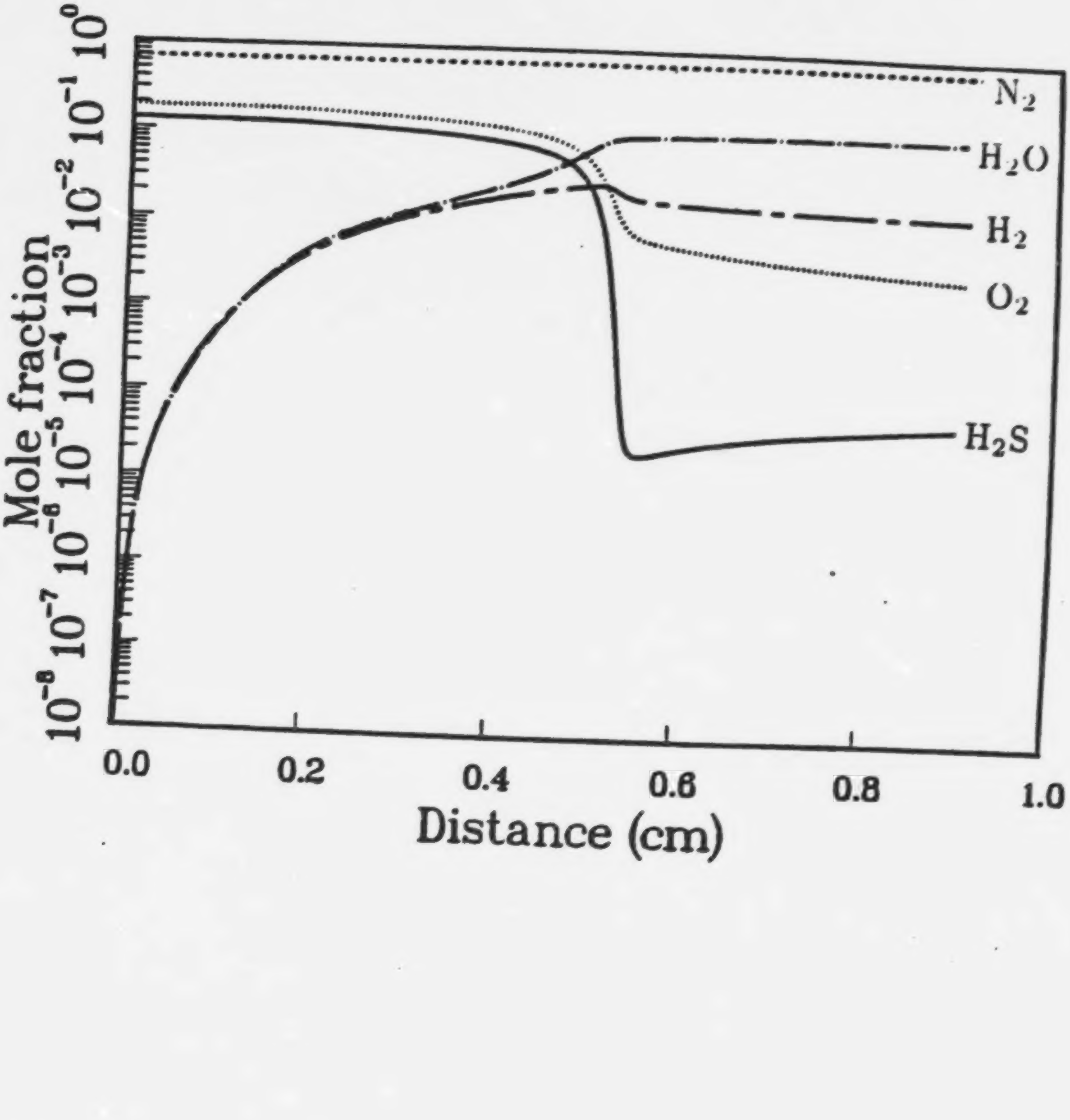
Mole fraction
10^{-8}
10^{-7}
10^{-6}
10^{-5}
10^{-4}
10^{-3}
10^{-2}
10^{-1}
10^{0}
N_2
H_2O
H_2
O_2
H_2S
0.0
0.2
0.4
0.6
0.8
1.0
Distance (cm)

Figure 4

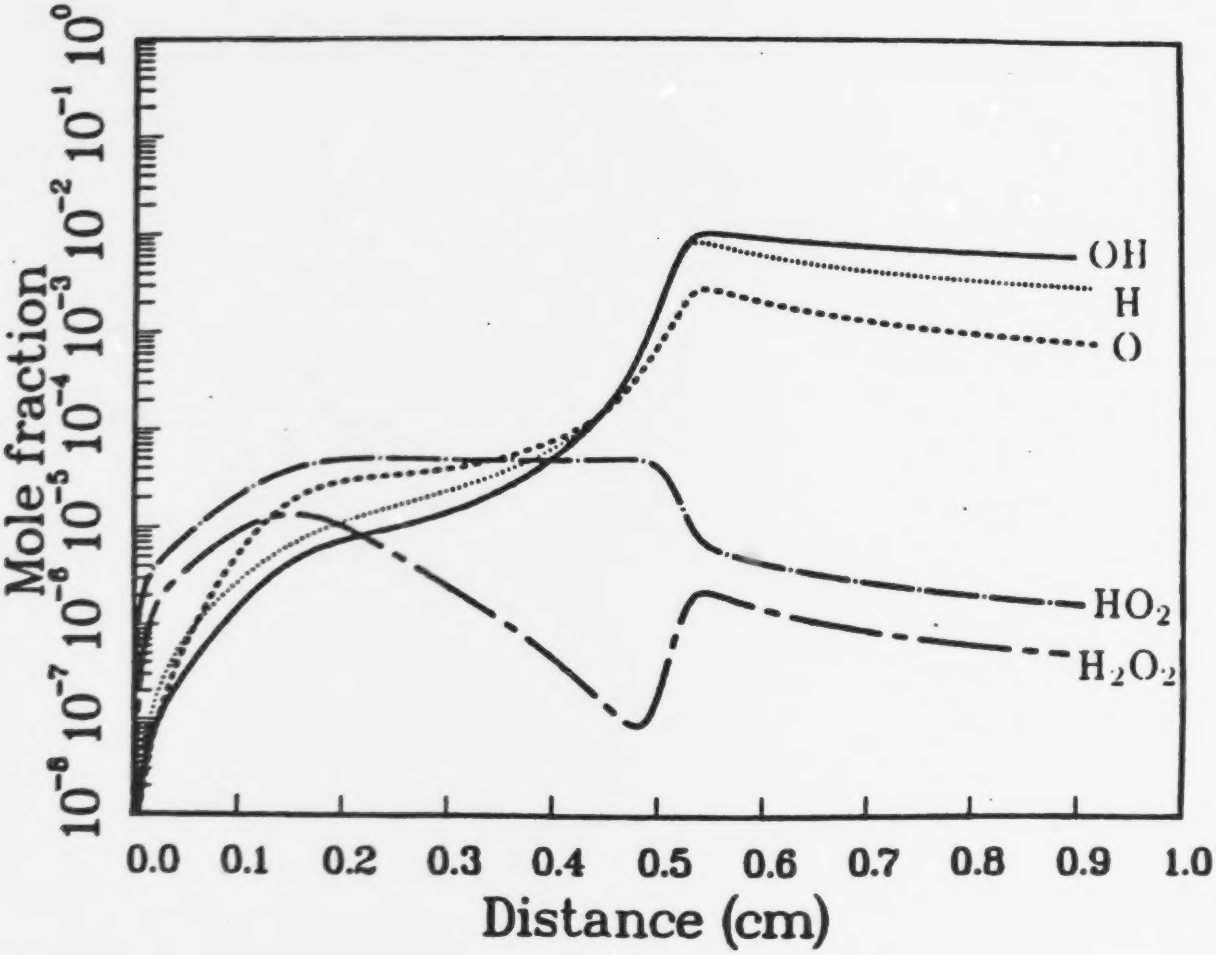

Mole fraction
10^{-8}
10^{-7}
10^{-6}
10^{-5}
10^{-4}
10^{-3}
10^{-2}
10^{-1}
10^{0}
0.0
0.1
0.2
0.3
0.4
0.5
0.6
0.7
0.8
0.9
1.0
Distance (cm)
OH
H
O
HO_2
H_2O_2

Figure 5

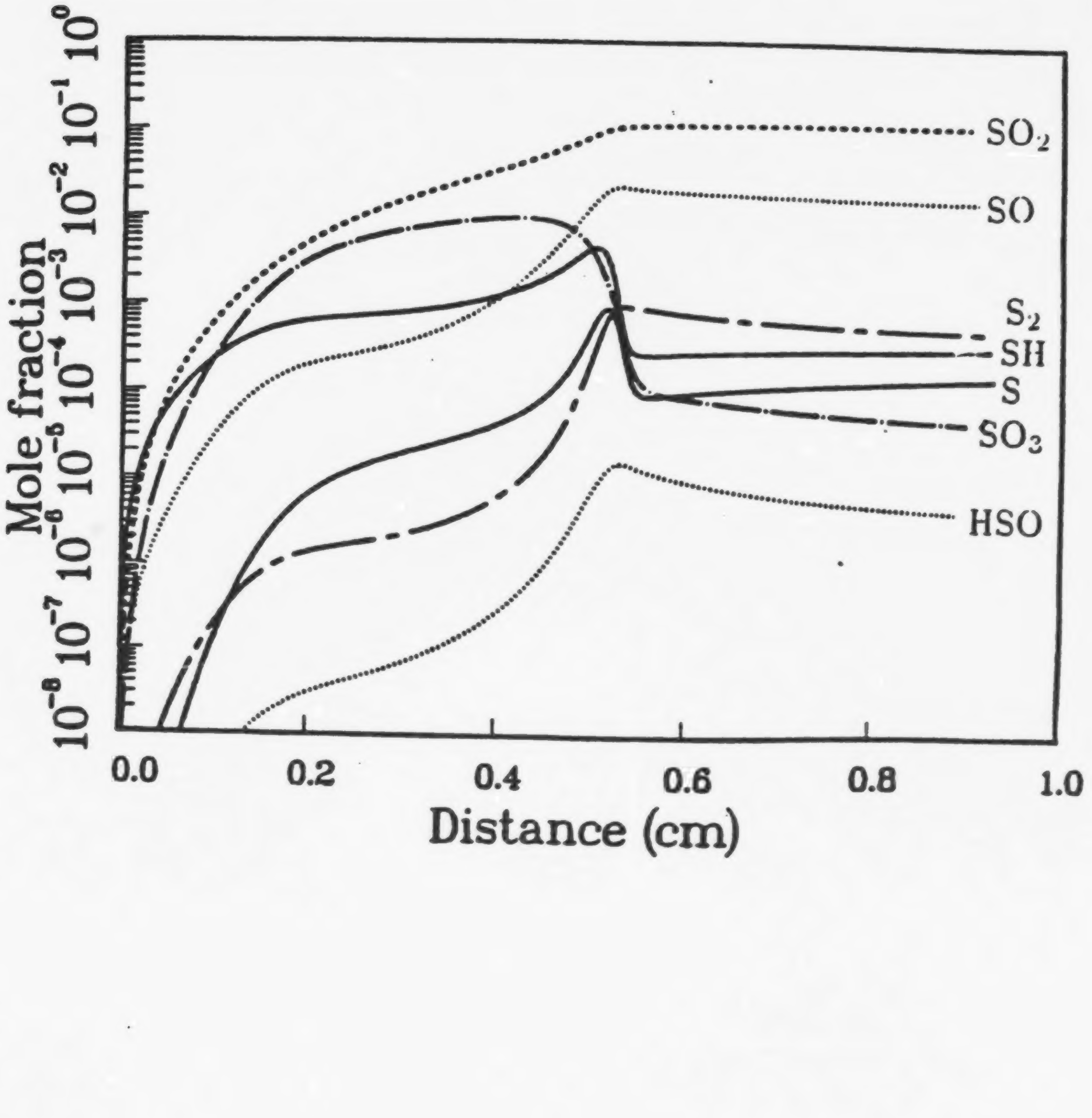

Mole fraction
10^{-8}
10^{-7}
10^{-6}
10^{-5}
10^{-4}
10^{-3}
10^{-2}
10^{-1}
10^{0}
SO_2
SO
S_2
SH
S
SO_3
HSO
0.0
0.2
0.4
0.6
0.8
1.0
Distance (cm)

Figure 6

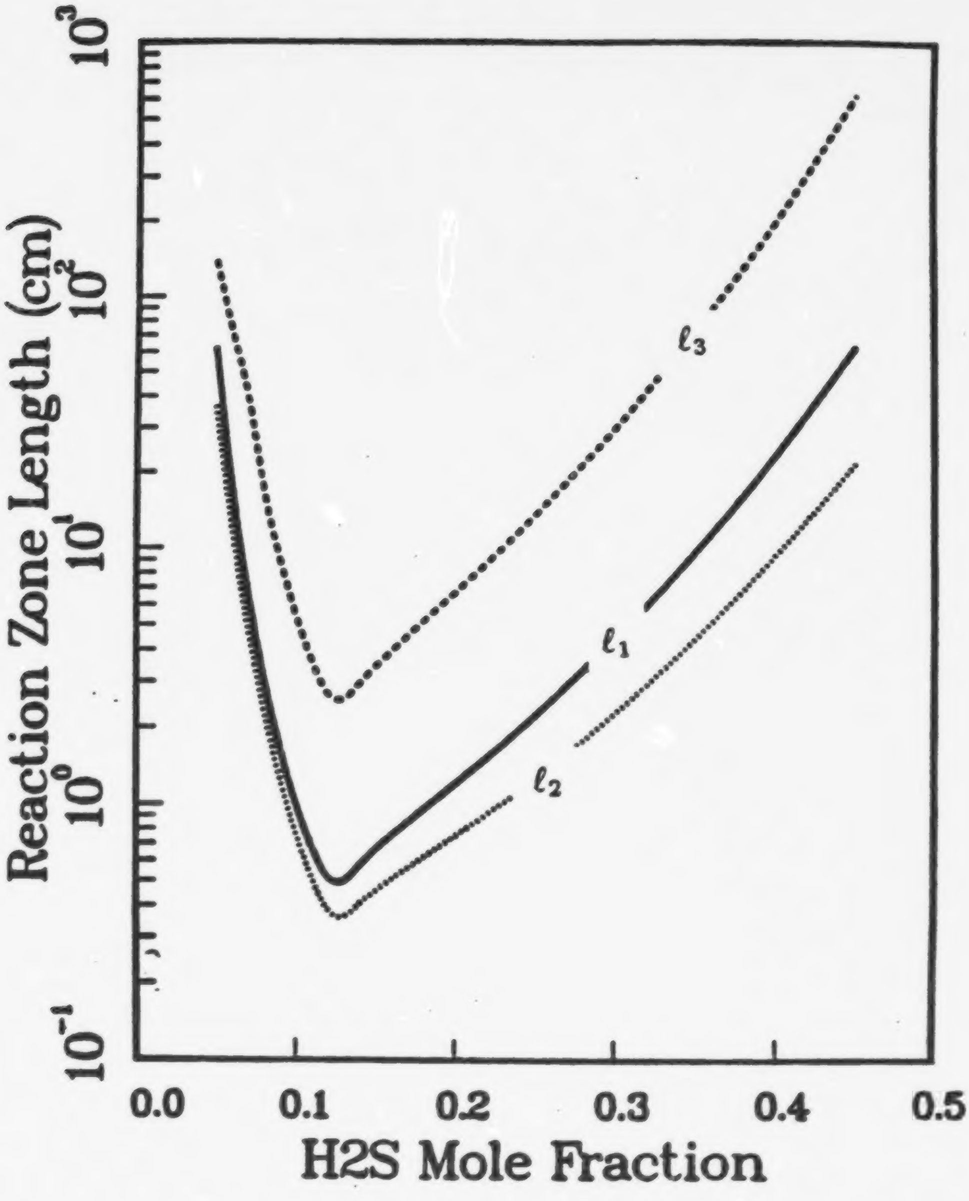
Reaction Zone Length (cm)
10^{-1}
10^{0}
10^{1}
10^{2}
10^{3}
ℓ_3
ℓ_1
ℓ_2
0.0
0.1
0.2
0.3
0.4
0.5
H2S Mole Fraction

Figure 7

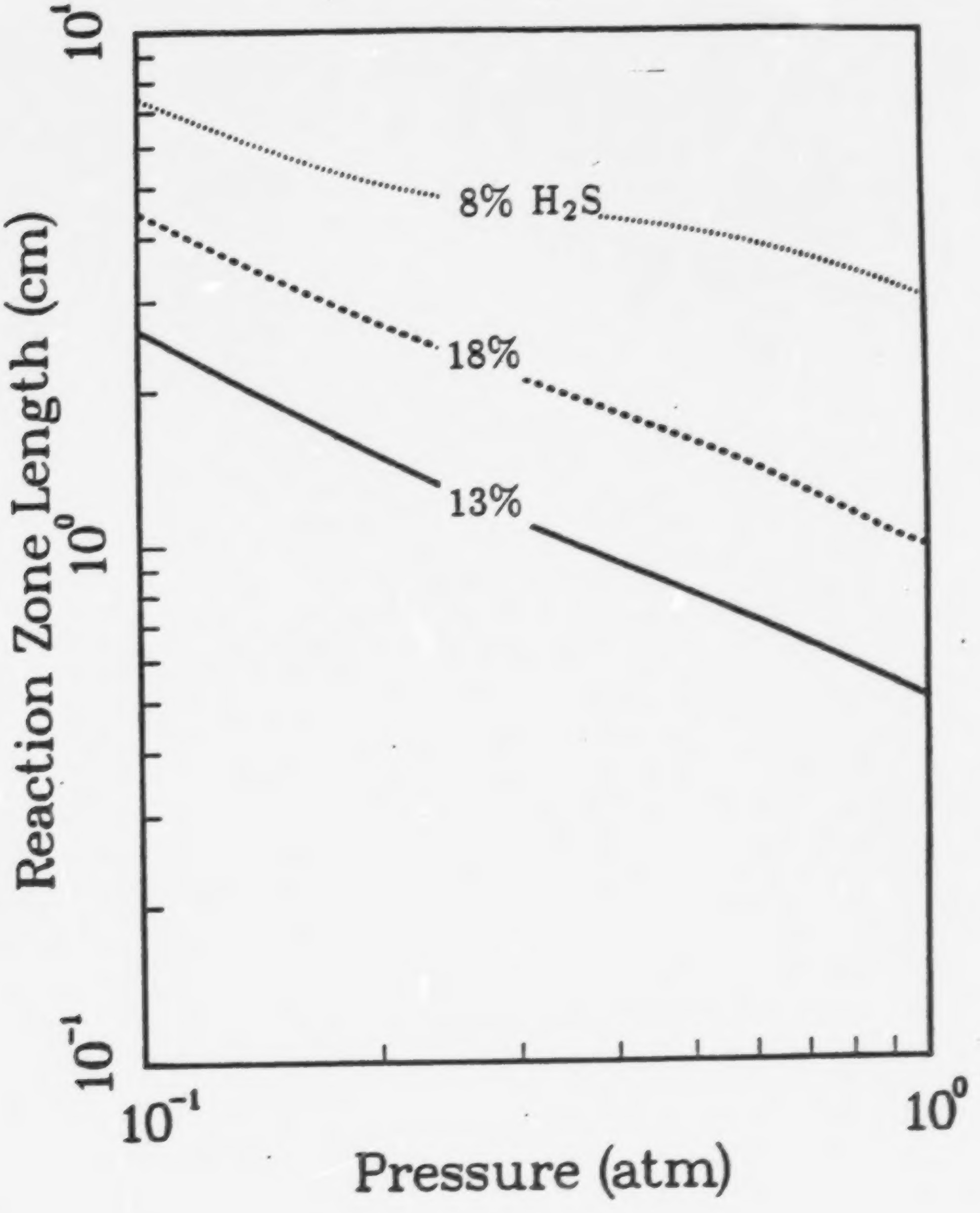
Reaction Zone Length (cm)
10^1
10^0
10^{-1}
Pressure (atm)
10^{-1}
10^0
8% H_2S
18%
13%

Figure 8

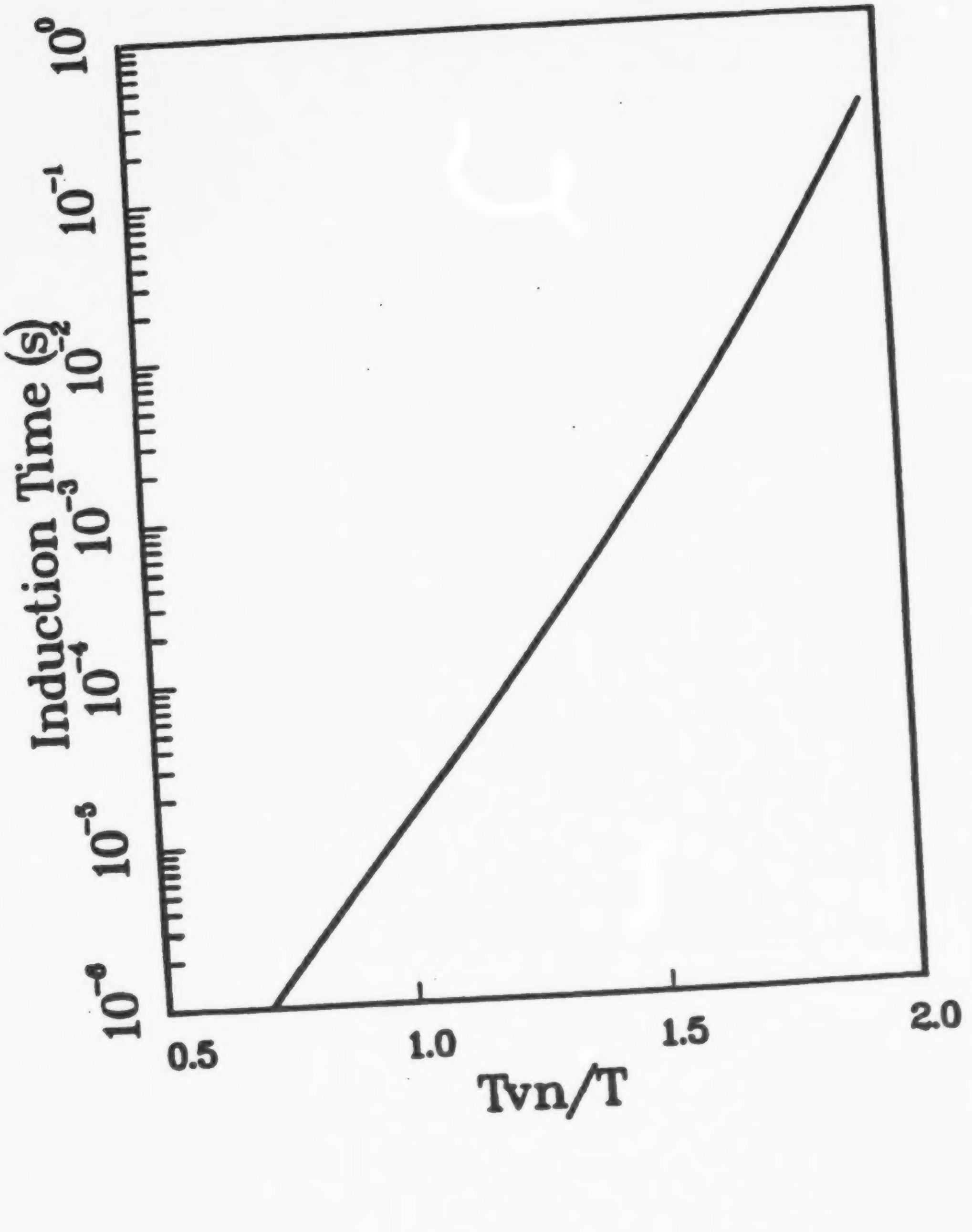

Figure 9

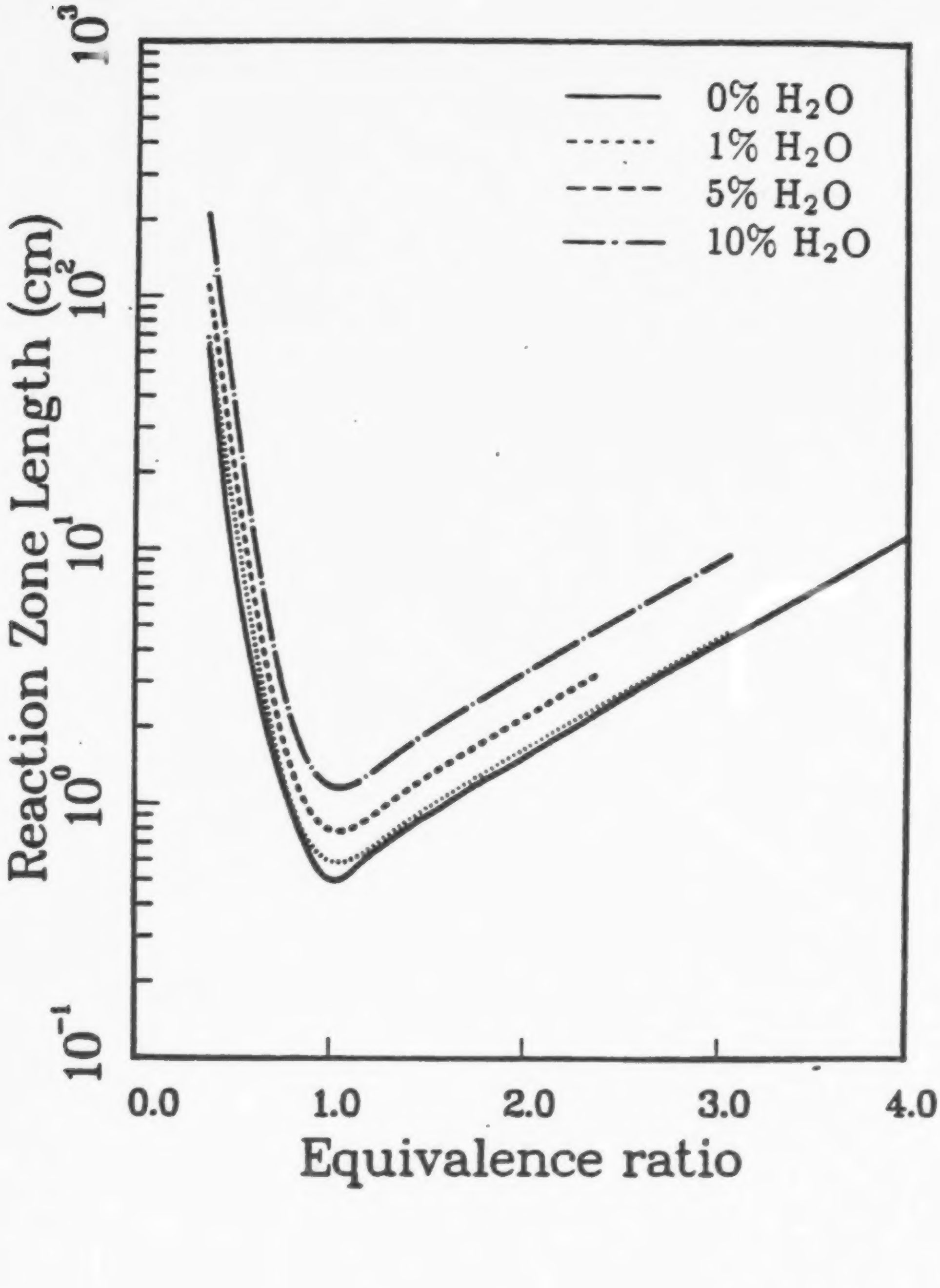

0% H_2O
1% H_2O
5% H_2O
10% H_2O
Reaction Zone Length (cm)
10^{-1}
10^{0}
10^{1}
10^{2}
10^{3}
0.0
1.0
2.0
3.0
4.0
Equivalence ratio

HYDROGEN SULPHIDE - 14.2% S ~ 110 mm

Figure 11

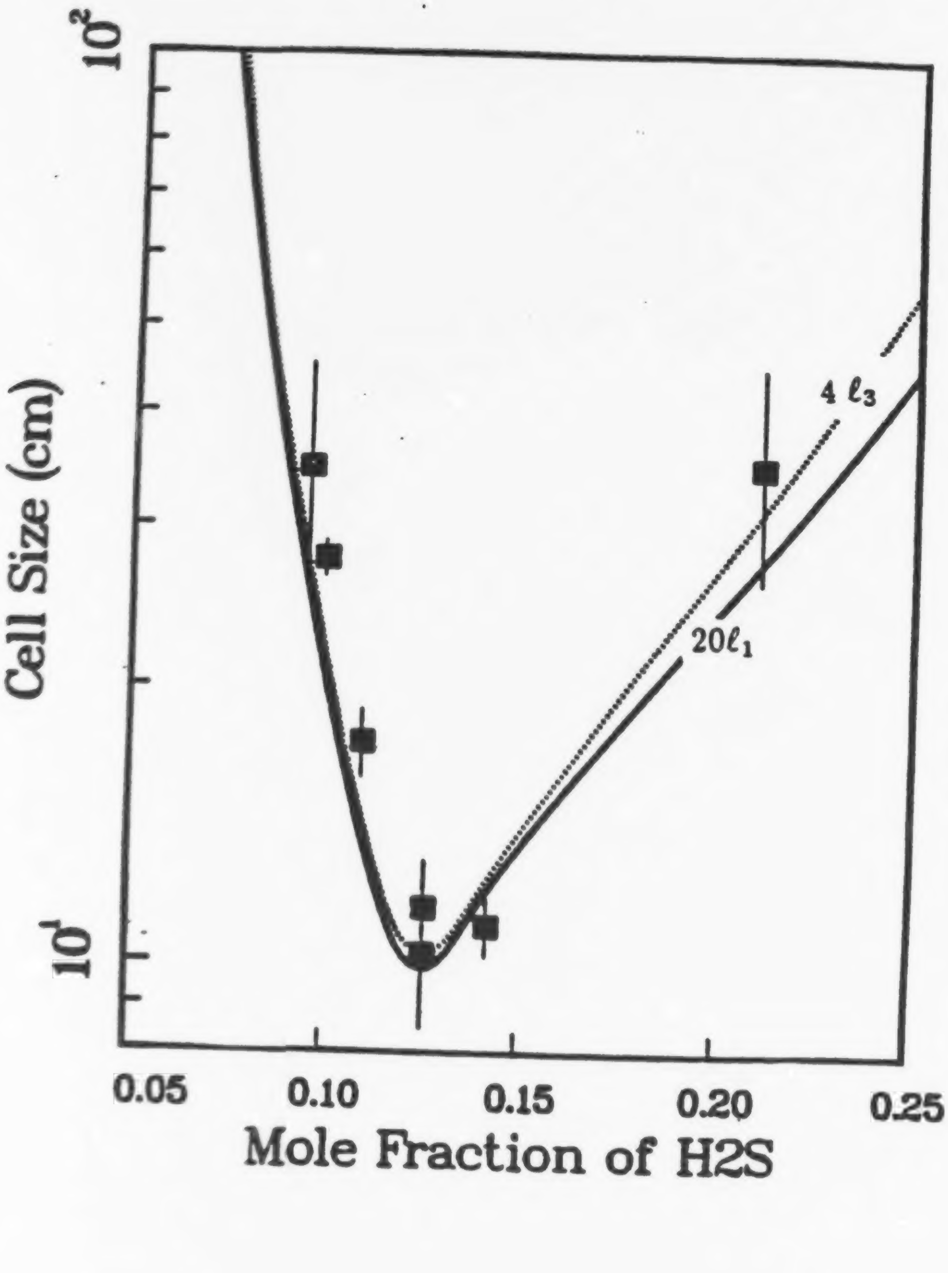

10^2
10^1
Cell Size (cm)
$4\ \ell_3$
$20\ell_1$
0.05
0.10
0.15
0.20
0.25
Mole Fraction of H2S

Figure 12

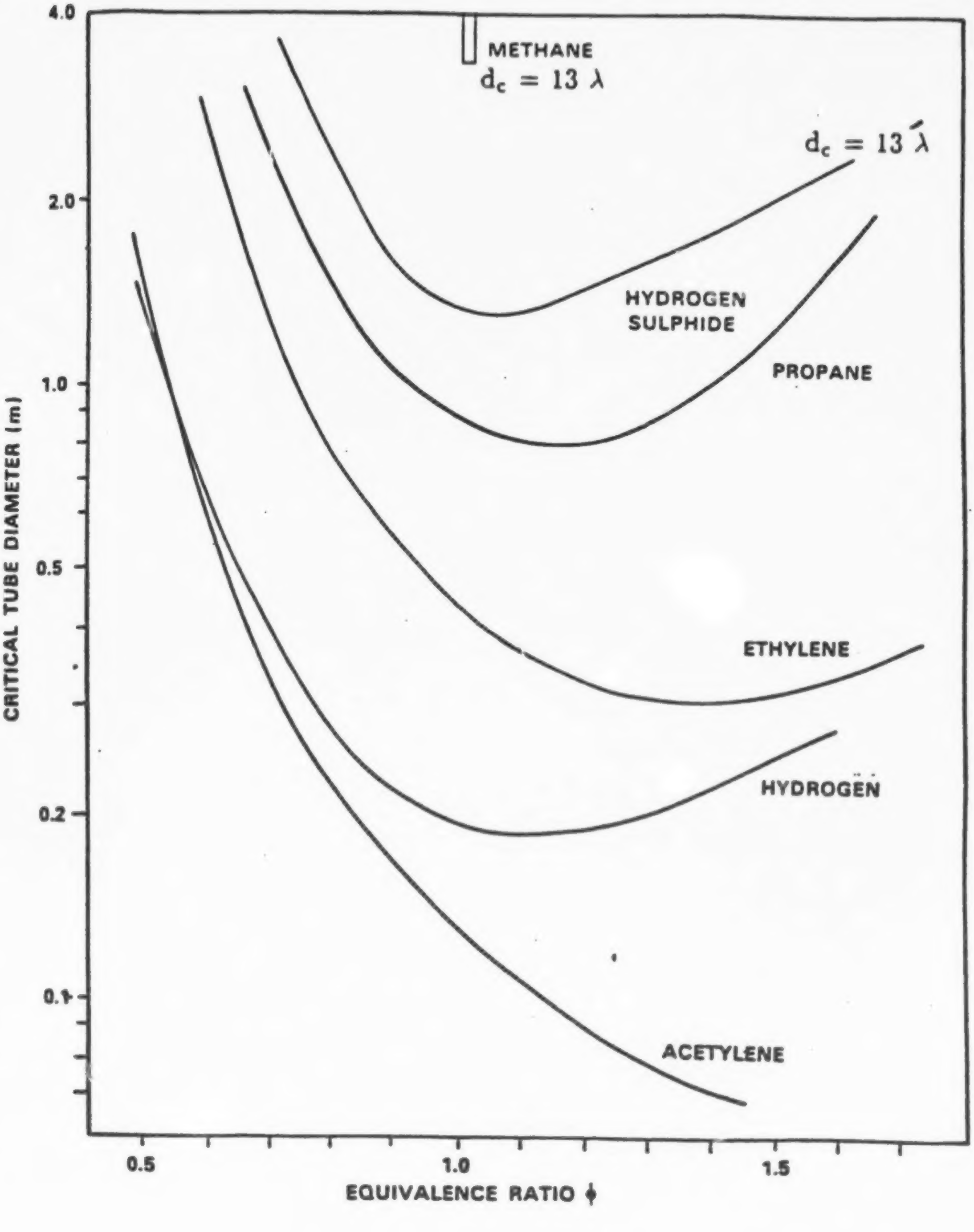
4.0
2.0
1.0
0.5
0.2
0.1
CRITICAL TUBE DIAMETER (m)
0.5
1.0
1.5
EQUIVALENCE RATIO ϕ
METHANE
$d_c = 13\lambda$
$d_c = 13\lambda$
HYDROGEN SULPHIDE
PROPANE
ETHYLENE
HYDROGEN
ACETYLENE

Figure 12

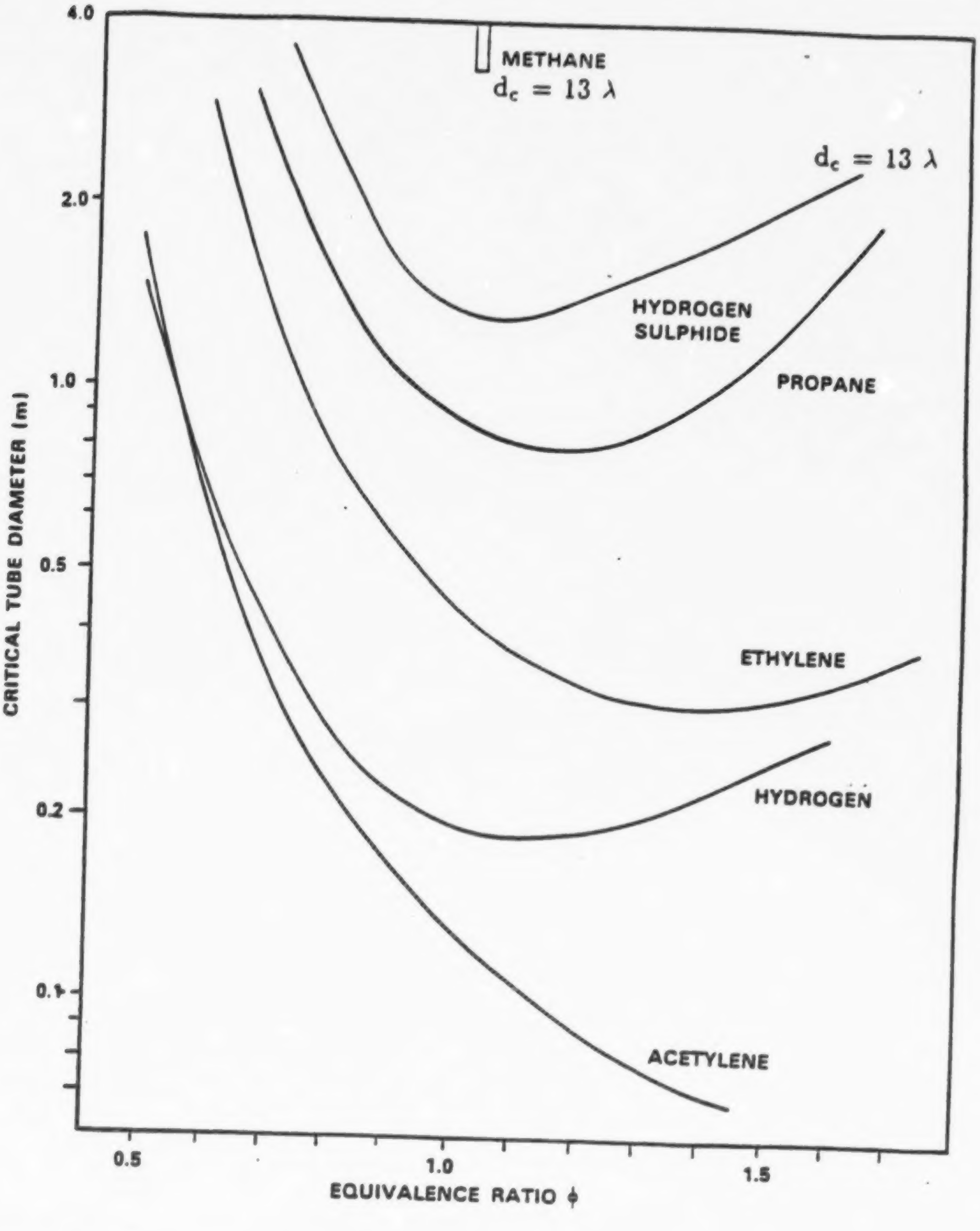
4.0
2.0
1.0
0.5
0.2
0.1
CRITICAL TUBE DIAMETER (m)
METHANE
$d_c = 13\ \lambda$
$d_c = 13\ \lambda$
HYDROGEN SULPHIDE
PROPANE
ETHYLENE
HYDROGEN
ACETYLENE
0.5
1.0
1.5
EQUIVALENCE RATIO ϕ

APPENDIX C

Chemical Kinetics and Cellular Structure of Detonations in Hydrogen Sulphide and Air

by

J.E. Shepherd, A. Sulmistras, A.J. Saber and I.O. Moen

APPENDIX D

Detonations in Hydrogen Sulphide-Air Clouds, with Comparisons to Other Fuel-Air Mixtures

by

A. Sulmistras, I.O. Moen and A.J. Saber

National Defence Défense nationale

DETONATIONS IN HYDROGEN SULPHIDE-AIR CLOUDS WITH COMPARISONS TO OTHER FUEL-AIR MIXTURES[+*]

by

A. Sulmistras[a]
I. O. Moen[b]
A. J. Saber[c]

+Presented at the Joint Technical Meeting of the Central and Western States Section of the Combustion Institute, San Antonio, Texas, April 22-23, 1985.

*The work is sponsored by the Atomic Energy Control Board of Canada and the Canadian Department of National Defence.

---

[a] Research Assistant, Dept. of Mechanical Engineering, Concordia University, Montreal, Canada.

[b] Defence Scientist, Military Engineering Section, Defence Research Establishment Suffield, Ralston, Alberta, Canada.

[c] Professor, Dept. of Mechanical Engineering, Concordia University, Montreal, Canada.

Canada

ABSTRACT

The detonability of hydrogen sulphide-air mixtures has been quantified in relation to the common hydrocarbon fuels. Critical tube diameter experiments were performed in a 0.89 m diameter tube. Detonations in all H_2S-air mixtures tested failed to transmit from planar to spherical mode as they emerged from the tube. Cell diameter data were obtained from smoked foil records as well as from onset of single-head spin tests conducted in a 145 mm diameter tube. A minimum cell diameter of 100 mm was obtained at stoichiometric conditions. Estimates of the detonation cell diameter obtained by scaling the calculated chemical kinetic induction length compare very well with experimentally measured cell diameters. Based on a d_c=13S estimate, the critical tube diameter for stoichiometric H_2S-air is 1.3 m. Comparisons with common hydrocarbons show that only methane forms a less sensitive mixture than hydrogen sulphide when mixed with air.

DETONATIONS IN HYDROGEN SULPHIDE-AIR CLOUDS WITH COMPARISONS TO OTHER FUEL-AIR MIXTURES

by

A. Sulmistras
I. O. Moen
A. J. Saber

1.0 INTRODUCTION

Many manufacturing and industrial plants store and use large quantities of flammable gases. To realistically assess potential hazards from an accidental spill, the combustion characteristics of the spilled gases must be known and quantified. In the case of a diffusion flame, the rate of mixing of the fuel with air as well as the exothermicity and emissivity of the fireball would determine the potential for equipment failure due to thermal radiation. On the other hand, in order to assess the hazards associated with the development of a fuel-air cloud, be it in an open environment, or in a confined, obstacle-filled one, a different set of combustion characteristics must be quantified. In particular, the susceptibility of the fuel-oxidizer combination to detonation must be determined.

The detonability of a fuel-oxidizer system is normally characterized by either the critical tube diameter, d_c, or the critical initiation energy, E_c. The critical initiation energy is the minimum energy required to initiate an unconfined, spherical detonation. Bull et al. (1976, 1978), and Lee and Matsui (1977) have all used the critical initiation energy to characterize the sensitivity of various explosive mixtures ranging from fuel-air to fuel-oxygen. For insensitive mixtures, measurement of this parameter becomes a rather difficult and costly exercise. A series of GO-NO GO trials, each with a variation of a high-explosive charge, must be performed for each composition. Furthermore, it has been shown that the critical energy is dependent on the nature and geometry of the initiating charge (Knystautas and Lee, 1976; Matsui and Lee, 1976) and that large clouds are necessary to ensure that a stable detonation has been established.

The critical tube diameter, d_c, is the minimum diameter of a round tube for which a detonation wave emerging from the tube will successfully overcome the sudden expansion and continue to propagate as a detonation. Experimentally, determination of the critical tube diameter still requires a GO-NO GO procedure. However, success or failure is easier to distinguish than in critical energy experiments. In addition, the results become independent of the initiating charge provided that a steady state Chapman-Jouguet detonation emerges from the tube.

The critical tube diameter and critical initiation energy represent fundamental properties of a detonative system. The two have been intimately linked through the work-done model by Lee and Matsui (1977). Also, Elsworth and Eyre (1984a) claim that indirect initiation of a fuel cloud via the critical tube or by direct means through direct initiation, are an equivalent means of characterizing the relative detonability of fuel-air mixtures.

In addition to the critical tube diameter and the critical initiation energy, the size of the detonation cell, S, as well as the detonation induction length, Δ, have been used to characterize the sensitivity of fuel-oxidizer combinations to detonation. The detonation cellular structure has been studied in detail by several authors (Strehlow, 1984; Fickett and Davis, 1979). As a detonation passes over a soot-coated plate, the trajectories of shock interactions in the detonation front trace out their familiar diamond-shaped pattern. It is sufficient to say here that it is the width of the "diamond", or the detonation cell size, which is the relevant detonation length scale. In a similar fashion, the detonation induction zone length is also a characteristic dimension of a fuel-oxidizer combination. A one-dimensional model of the detonation wave, referred to as the Zeldovich-Von Neumann-Doring (ZND) model, is used to calculate the induction zone thickness using comprehensive kinetic models. By assuming that the cell width and the induction zone length are linearly related to the critical tube diameter, the detonability of fuel mixtures can be assessed without performing GO-NO GO tests.

The present paper reports on a series of critical tube diameter trials which were performed in order to determine the detonation behavior in hydrogen sulphide-air mixtures. Trials involving butane-air mixtures were also performed in order to directly compare hydrogen sulphide with a common hydrocarbon fuel.

Hydrogen sulphide is a flammable, toxic gas. It is used in large quantities in the Girdler-Sulphide process for the production of heavy water (deuterium oxide), an essential material for the operation of CANDU nuclear reactors. In the petroleum industry, H_2S is the main constituent of "sour gas" wells. Despite its common occurrence, the susceptibility of H_2S-air mixtures to detonation has not been determined due to the toxic nature of hydrogen sulphide.

Recent developments in gaseous detonations have linked the critical tube diameter, the critical initiation energy, the detonation cell size and the one-dimensional induction zone thickness calculated from detailed chemical kinetics. The use of these empirical and theoretical correlations enables one to characterize the detonation susceptibility of hydrogen sulphide-air mixtures while keeping the number of trials with this toxic gas to a minimum.

2.0 EXPERIMENTAL DETAILS

The experimental test series was performed at the DRES fuel-air facility. The facility, which is described in detail by Funk et al. (1982), is centered around an 18.3 m x 7.6 m concrete test pad onto which a 7.8 m long by 0.89 m diameter steel tube is mounted (Figure 1). In order to simulate an unconfined cloud for the critical tube diameter tests, a 1.8 m diameter polyethylene bag, at least 3 m long was attached at one end of the tube. The ignition source, a DM12 solid explosive charge, was used to directly initiate detonation at the opposite end of the tube.

Hydrogen sulphide (Technical grade, 99% pure H_2S) was introduced and mixed with the initial air in the test volume with a multipath recirculation system using a high capacity centrifugal blower. The composition and mixture homogeneity were monitored by continuously analyzing samples taken from two ports in the tube using a "Wilks Miran 1A" infrared gas analyzer. Infrared absorbance of hydrogen sulphide was monitored at a wavelength $\lambda = 3.70\ \mu m$. Due to the poor IR response of H_2S, the maximum pathlength of 20.25 m was used.

Once the detonation was initiated, the arrival and pressure profile of the wave were monitored at various positions along the tube and bag using piezoelectric pressure transducers. High-speed photographic records of the transmission and propagation of the wave were obtained using a Photec camera (~ 12000 half frames/sec) placed at 90° to the tube axis. On selected trials a Hycam camera (~ 12000 half frames/sec) placed at a 30° angle, as well as an end camera (~ 5000 frames/sec) looking directly down the tube, were also used (Figure 2).

In order to record the detonation cellular structure, a large steel sheet measuring 3 m long by 1.5 m wide was first carefully "sooted" with a rich acetylene flame and then placed around the inside periphery of the tube near the tube exit. At the passage of the detonation wave, the familiar diamond shaped pattern, corresponding to the detonation triple point trajectories, was permanently recorded (Figure 3).

3.0 DISCUSSION

3.1 Experimental Results

Detonations of hydrogen sulphide with concentrations in air ranging from ~ 10% H_2S to ~ 14.2% H_2S (12.3% being stoichiometric) failed to transmit from a 0.89 m diameter tube into the bag which simulates an unconfined cloud. The critical tube diameter for hydrogen sulphide is therefore greater than 0.89 m. In a similar test with stoichiometric butane-air, the detonation successfully transmitted from a planar wave in the tube to a spherical wave in the bag.

Direct comparisons of critical tube diameters for stoichiometric fuel-air mixtures are made in Table I. From this table it is seen that the relative detonation hazard associated with hydrogen sulphide-air mixtures lies between propane and n-butane, which are more sensitive, and methane, which is less sensitive.

The cellular structure of H_2S-air detonations were recorded during the present trials. Qualitatively, the cellular pattern seemed more regular than those observed for hydrocarbon-air systems, although the "high frequency" substructure is still clearly visible. Quantitatively, the stoichiometric H_2S-air cell size was measured as 100 mm. This was the minimum value obtained over the concentration range explored. This compares with about 300 mm for methane, and 69 mm and 56 mm for propane and n-butane respectively. This again shows that of the common hydrocarbons, only methane forms a less detonable mixture. A direct comparison of smoke foil records for two H_2S-air mixtures with stoichiometric butane-air is shown in Figure 4.

The detonation cell size has been linked to the critical tube diameter through the emperical relation $d_c = 13S$. Knystautas et al. (1982) have shown this relation is valid over a large range of fuel-oxygen-nitrogen mixtures at atmospheric pressure. Recent evidence by Moen et al. (1984a) and Elsworth and Eyre (1984b) show that the correlation is not universal, although the latter authors show that the $d_c = 13S$ estimate provides a lower limit to the measured critical tube diameter. In other words, $d_c = 13S$ overestimates the critical tube diameter of the fuel-air mixture.

Using the $d_c = 13S$ correlation, a critical tube diameter of 1.3 m is estimated for the most detonable H_2S-air mixture. The critical tube diameter for methane is estimated at just under 4 m. The measured critical tube diameter for stoichiometric propane is 0.9 m, a value equivalent to the estimate based on 13S.

Present cell size data for stoichiometric n-butane-air yield an estimate for d_c of 0.73 m. This is consistent with the fact that detonations in this mixture were able to transmit into the plastic bag from a 0.89 m diameter tube.

Further cell diameter measurements indicate that at 10% H_2S ($\varphi \sim 0.8$) the cell size increases by almost a factor of three to 275 mm. This is confirmed by tests performed at McGill University (Knystautas and Lee, 1984a) in a 145 mm diameter tube. Records show that single-head spin appears in this tube for H_2S concentrations between 9%-10% and 20%-22%. Using the relation $P/D = \pi V/kc$ proposed by Moen et al. (1981) for onset of single-head spin in a tube, where P is the pitch or cell length, D the tube diameter, V the detonation velocity, c the local speed of sound, and k the first root of the derivative of the Bessel function of order one ($k_1 = 1.841$), the cell lengths for these concentrations are 432 mm and 440 mm, respectively. The estimated cell sizes, based on 0.6 P, are therefore 260 mm and 264 mm at 9.5% H_2S and 21% H_2S, respectively. A plot of measured detonation cell sizes for H_2S-air mixtures is shown in Figure 5.

Over the past few years, chemical kinetic modelling of gaseous detonative systems has progressed to the point where reliable induction and reaction zone lengths based on the one-dimensional ZND model can be calculated. Detonation induction zone length calculations for H_2S-air mixtures have been performed by Shepherd et al. (1985) with a chemical kinetics code using 51 reactions and 19 species. By assuming a linear relationship (i.e., $S = A\Delta$), between the induction length, Δ, and cell size, S, and by normalizing at one experimentally determined cell size to determine the proportionality factor A, predictions of cell sizes for other compositions have been made. The induction zone length normalized to a cell size of 110 mm at 14.2% H_2S gives the proportionality factor A a value of 18. A comparison of this scaled induction zone length with experimentally measured cell size is given in Figure 5. Between 9% and 22%, cell size predictions are in good agreement with experimental results. Previous results for other fuel-air systems (Moen et al. 1984a) show that further extrapolations to the lean and rich limits tend to underestimate the sensitivity of these fuel-air systems.

3.2 Practical Considerations

The critical initiation energy is an important parameter which characterizes the sensitivity of a combustible system to detonation. Based on the relative amounts of energy required to initiate detonation in various fuel-air mixtures, the detonation hazard of a given fuel can be assessed in a relative manner (Matsui and Lee, 1978).

For industrial hazards evaluations, the critical initiation energy gives an upper bound, such that any source with equal or higher energy (a minimum power is also required, Lee et al., 1974), detonation is assured. On the other hand, an ignition source with energy less than E_c, may still be capable of initiating a detonation under certain circumstances. For example, in a confined situation where a full three-dimensional expansion is restricted, less energy is required for detonation initiation.

Another method of detonation initiation is through the mechanism of flame acceleration. In this case, burning rate and flame area increases caused by upstream disturbances in the flow field (vortex generation, turbulence, etc.), can create sufficient "hot spots" to initiate detonation. A recent test by Moen et al. (1984b) showed that transition to detonation can occur for a relatively insensitive fuel-air mixture contained in an obstacle free plastic bag. Evidence of transition to detonation in other fuel-air mixtures is summarized by Berman (1985). Therefore, in a realistic sense, the critical energy should only be used as a measure of the relative detonation hazard of gas mixtures, as opposed to a quantitative one. In the same manner, the critical tube diameter gives a comparison of the relative hazards associated with different fuel-oxidizer combinations. The relative sensitivities of common fuel-air mixtures, including H_2S-air, are plotted in terms of d_c in Figure 6. Acetylene and hydrogen form the most sensitive mixtures with air. Hydrogen sulphide is relatively insensitive with only methane forming a less detonable mixture.

Besides being a measure of the relative detonation hazard associated with a given mixture, the critical tube diameter is also a direct measure of the minimum dimension for cloud in which a detonation is able to propagate in an unconfined geometry. In an unconfined cloud with a minimum dimension less than d_c the detonation would suffer an expansion great enough to separate the shock and combustion zone. The detonation would thus degenerate into a deflagration wave.

In studies to determine possibility of detonation transfer from one chamber to another, care must be exercised in using critical tube diameter data. Although d_c is a direct measure of the transmission through a circular opening, Liu et al. (1984), in a study of other opening configurations, have shown that the circular orifice is the most inefficient means to transfer detonations from one chamber to another. Furthermore, Thibault et al. (1985), using a circular orifice with circular central blockage, show that the transmission efficiency increases by a factor of more than two based on the outer diameter, and by a factor of ~ 35 based on the transmitted energy. These transmission efficiency values depend on the diameter of the central blockage, and also on the regularity of the detonation cellular structure, with increasing efficiency as the cellular structure becomes more irregular (Moen et al., 1985).

Another important area for practical consideration is the ability of a detonation to travel in a confined tube. Moen et al. (1985) have recently shown that the ability of a detonation to propagate in a smooth tube beyond "single-head spin" is dependent on the regularity of the detonation structure. For systems with "clean" or regular cellular structures (i.e., highly argon diluted acetylene-oxygen mixtures) detonation propagation failure occurs at $d_c/D \sim 14$ (D is the tube diameter; d_c, the critical tube diameter). However, for irregular cell systems such as C_2H_4-air and C_2H_2-air detonation failure is not observed at $d_c/D = 74$ and $d_c/D = 314$, respectively. All fuel-air systems tested to date, including H_2S-air, can be classed as having irregular detonation cell structure. A practical implication of these results is that the minimum dimensions required for detonation propagation in a confined situation are less, and can be much less, than the cloud height required for detonation propagation in unconfined situations for the same mixture sensitivity. It must be cautioned that these results apply to smooth tubes only. Donato (1982) has shown that with a finite disturbance, detonations beyond single-head spin are quenched. It is clear that the phenomena of detonation propagation in confined configurations needs further study.

The transition from experimental studies to practical hazards evaluations requires a great deal of caution. Both initial and boundary conditions must be specified as clearly as possible in order for realistic hazard assessments to be made.

4. CONCLUSION

The relative detonation sensitivity of hydrogen sulphide-air mixtures has been determined in a series of large scale experimental tests. Stoichiometric hydrogen sulphide-air failed to transmit into a large plastic bag from a 0.89 m diameter tube. At this mixture composition, the cell size is about 100 mm. The cell size increases to 275 mm at an equivalence ratio of ~ 0.8. Using the emperical relation $d_c = 13S$, the critical tube diameter for stoichiometric H_2S-air mixtures is estimated to be 1.3 m.

In comparison with more common hydrocarbon-air mixtures, both propane and n-butane were able to transmit into the bag from the 0.89 m diameter tube. Methane was unable to do so from a 1.8 m diameter tube. Thus, of the common hydrocarbons, only methane forms a less sensitive mixture than hydrogen-sulphide.

Detonation cell diameter measurements in hydrogen sulphide mixtures were confirmed from onset of single-head spin tests in a 145 m diameter tube. Single-head spin is observed between 9% - 10% and 20% - 22% H_2S, with corresponding cell widths of 260 mm and 264 mm, respectively.

Chemical kinetic calculations of the detonation induction length (Δ) based on the one-dimensional ZND model have been used to correlate the cell size (s) data. Accurate estimates of the cell size were obtained over the concentration range investigated, once the induction length was normalized to one experimental data point. The constant of proportionality, A, in the expression $S = A\Delta$ was found to be equal to 18.

REFERENCES

Berman, M. (1985), "The Effects of Scale and Geometry on Hydrogen-Air Detonations". Submitted to the 23rd ASME/AIChE/ANS National Heat Transfer Conference, Denver, Colorado, August 6-9.

Bull, D.C., Elsworth, J.E., Hooper, G. and Quinn, C.P. (1976), "A Study of Spherical Detonation in Mixtures of Methane and Oxygen Diluted by Nitrogen". J. Phys. D: Appl. Phys., 9, 1991.

Bull, D.C., Elsworth, J.E. and Hooper, G. (1978), "Initiation of Spherical Detonation in Hydrocarbon/Air Mixtures". Acta Astronautica, 5, 997.

Bull, D.C., Elsworth, J.E., Shuff, P.J. and Metcalfe, E. (1982), "Detonation Cell Structures in Fuel/Air Mixtures", Combustion and Flame, 45, 7.

Donato, M. (1982), "The Influence of Confinement on the Propagation of Near-Limit Detonation Waves". Ph.D. Thesis, McGill University, Montreal.

Elsworth, J.E., Eyre, J.A. (1984a), "Equality of Energy Requirements for Indirect and Direct Initiation of Gaseous Detonation". Submitted to Combustion and Flame.

Elsworth, J.E. and Eyre, J.A. (1984b), "Indirect Initiation of Spherical Detonation in Fuel/Air Mixtures by a Transition Process". Paper presented at Symposium on Heavy Gases and Risk Analysis, Bonn, W. Germany, November 1984. Proceedings to be published by Reidel Publishing Company.

Elsworth, J.E. and Eyre, J.A. (1984c), "The Susceptibility of Propene-Propane/Air Mixtures to Detonation". Combustion and Flame 55, 237.

Fickett, W. and Davis, W.C. (1979), "Detonation". University of California Press, Berkeley, California.

Funk, J.W., Murray, S.B., Moen, I.O. and Ward, S.A. (1982), "A Brief Description of the DRES Fuel-Air Explosives Testing Facility and Current Research Program". Proceedings of the International Conference on Fuel-Air Explosions, Nov. 4-6, 1981, SM Study No. 16, p. 565, University of Waterloo Press, Ontario, Canada, 1982.

Knystautas, R. and Lee, J.H.S. (1976), "On the Effective Energy for Direct Initiation of Gaseous Detonation". Combustion and Flame 27, 221.

Knystautas, R., Lee, J.H.S. and Guirao, C.M. (1982), "The Critical Tube Diameter for Detonation Failure in Hydrocarbon-Air Mixtures". Combustion and Flame, 48, 63.

Knystautas, R. and Lee, J.H.S. (1984a), McGill University. Private Communication.

Knystautas, R., Guirao, C., Lee, J.H.S. and Sulmistras, A. (1984b), "Measurements of Cell Size in Hydrocarbon-Air Mixtures and Predictions of Critical Tube Diameter, Critical Initiation Energy, and Detonability Limits". Dynamics of Shock Waves, Explosions, and Detonations: AIAA Progress in Astronautics and Aeronautics, Vol. 94, 23, AIAA, New York.

Lee, J.H.S., Knystautas, R. and Guirao, C.M. (1974), "Critical Power Density for Direct Initiation of Unconfined Gaseous Detonations". Proceedings of the Fifteenth Symposium (International) on Combustion, p. 53, The Combustion Institute.

Lee, J.H. and Matsui, H. (1977), "A Comparison of the Critical Energies for Direct Initiation of Spherical Detonations in Acetylene-Oxygen Mixtures". Combustion and Flame, 28, 61.

Liu, Y.K., Lee, J.H. and Knystautas, R. (1984), "Effect of Geometry on the Transmission of Detonation Through an Orifice". Combustion and Flame, 56, 215.

Matsui, H. and Lee, J.H.S. (1976), "Influence of Electrode Geometry and spacing on the Critical Energy for Direct Initiation of Spherical Gaseous Detonations". Combustion and Flame 27, 217.

Matsui, H. and Lee, J.H.S. (1978), "On the Measure of Relative Detonation Hazards of Gaseous Fuel-Oxygen and Air Mixtures". Seventeenth Symposium (International) on Combustion, p. 1269, The Combustion Institute, Pittsburgh, Pa.

Moen, I.O., Donato, M., Knystautas, R. and Lee, J.H. (1981), "The Influence of Confinement on the Propagation of Detonations Near the Detonability Limits". Eighteenth Symposium (International) on Combustion, p. 1615, The Combustion Institute, Pittsburgh, Pa.

Moen, I.O., Funk, J.W., Ward, S.A., Rude, G.M. and Thibault, P.A. (1984a), "Detonation Length Scales for Fuel-Air Explosives". Dynamics of Shock Waves, Explosions and Detonations: AIAA Progress in Astronautics and Aeronautics Vol. 94, 55, AIAA, New York.

Moen, I.O., Bjerketvedt, D., Jenssen, A. and Thibault, P.A. (1984b), "Transition to Detonation in a Large Fuel-Air Cloud". Combustion and Flame, to be published.

Moen, I.O., Sulmistras, A., Thomas, G.O., Bjerketvedt, D. and Thibault, P.A. (1985), "The Influence of Cellular Regularity on the Behavior of Gaseous Detonations." Submitted for presentation at 10th International Colloquium On Dynamics of Explosions and Reactive Systems, Berkeley, California, August 4-9.

Shepherd, J.E., Sulmistras, A., Saber, A.J. and Moen, I.O. (1985), "Chemical Kinetics and Cellular Structure of Detonation in Hydrogen Sulphide-Air". Submitted to 10th International Colloquium On Dynamics of Explosions and Reactive Systems, Berkeley, California, August 4-9.

Strehlow, R.A. (1984), "Combustion Fundamentals". McGraw-Hill Series in Energy, Combustion and Environment.

Sulmistras, A. (1983), "Detonation Cell Diameter Measurements of Hydrocarbon-Air and H_2-CO_2-Air Systems". Undergraduate Mechanical Laboratory II Report, McGill University.

Thibault, P.A., Bjerketvedt, D., Thomas, G.O., Sulmistras, A., Jenssen, A. and Moen, I.O. (1985), "The Role of Energy Distribution on the Transmission of Gaseous Detonations into the Unconfined". Submitted for presentation at the 10th International Colloquium on Dynamics of Explosions and Reactive Systems, Berkeley, California, August 4-9.

TABLE I

DETONATION LENGTH SCALES OF FUEL-AIR MIXTURES AT STOICHIOMETRIC CONDITIONS

FUEL	DETONATION CELL WIDTH S (mm)			CRITICAL TUBE DIAMETER d_c (m)		
	DRES[a]	McGill[b]	Thornton[k]	DRES[a]	McGill[d]	Thornton[c]
ACETYLENE C_2H_2	----	5.7 10.0	9.2	----	0.115	----
HYDROGEN H_2	----	15.0 15.5	10.8 14.2[c]	----	0.200	0.200-0.225
ETHYLENE C_2H_4	28	26.0 29.0	26.2	0.43	0.38[i]	0.475-0.550
ETHANE C_2H_6	54-62	53.5 ----	58.5	~0.9	0.67[i]	0.8-0.9
PROPYLENE C_3H_6	----	---- ----	52.0[g]	----	0.70[i]	----
PROPANE C_3H_8	69	53.5 ----	46.0 62[g]	0.9	0.70[i]	0.8-0.9
n-BUTANE C_4H_{10}	50-62[e]	53.5 ----	54[c]	<0.89[e] (0.73)[h]	0.64[i]	>1.05
ISOBUTANE C_4H_{10}	----	---- ----	----	----	----	>1.05
HYDROGEN SULPHIDE H_2S	100[e]	---- ----	----	>0.89[e] (1.3)[h]	----	----
METHANE CH_4	280± 30	300[f]	310±50[c]	>>1.8 (4.0)[h]	----	----

a. Reference Moen et al. (1984a)
b. First Value - Reference Knystautas et al. (1984b)
Second Value - Reference Knystautas et al. (1982)
c. Reference Elsworth and Eyre (1984b)
d. Reference Knystautas et al. (1982)
e. Present Results
f. Reference Sulmistras (1983)
g. Reference Elsworth and Eyre (1984c)
h. Estimate from d_c = 13S
i. Extrapolated Values
k. Reference Bull et al. (1982)

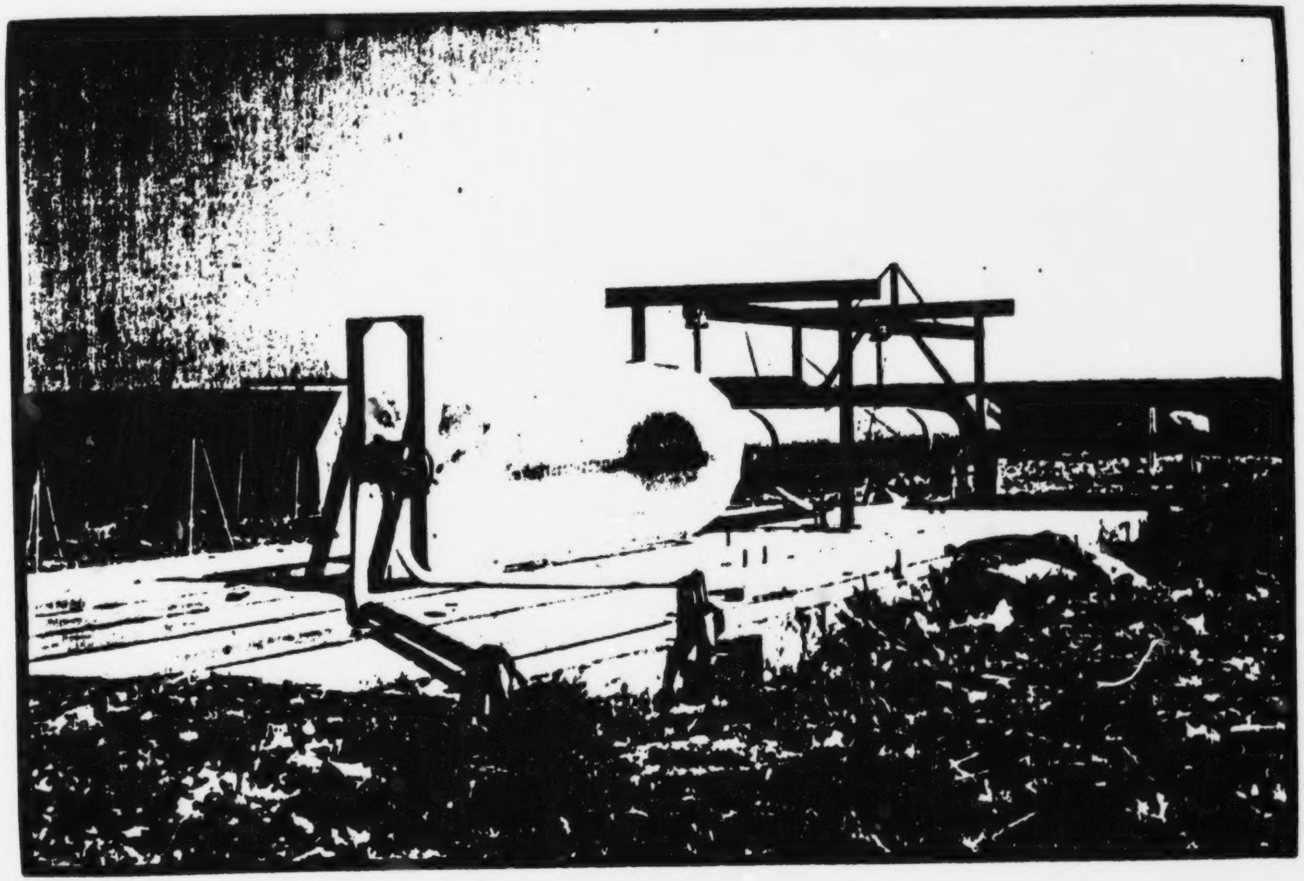

FIGURE 1. EXPERIMENTAL LAYOUT

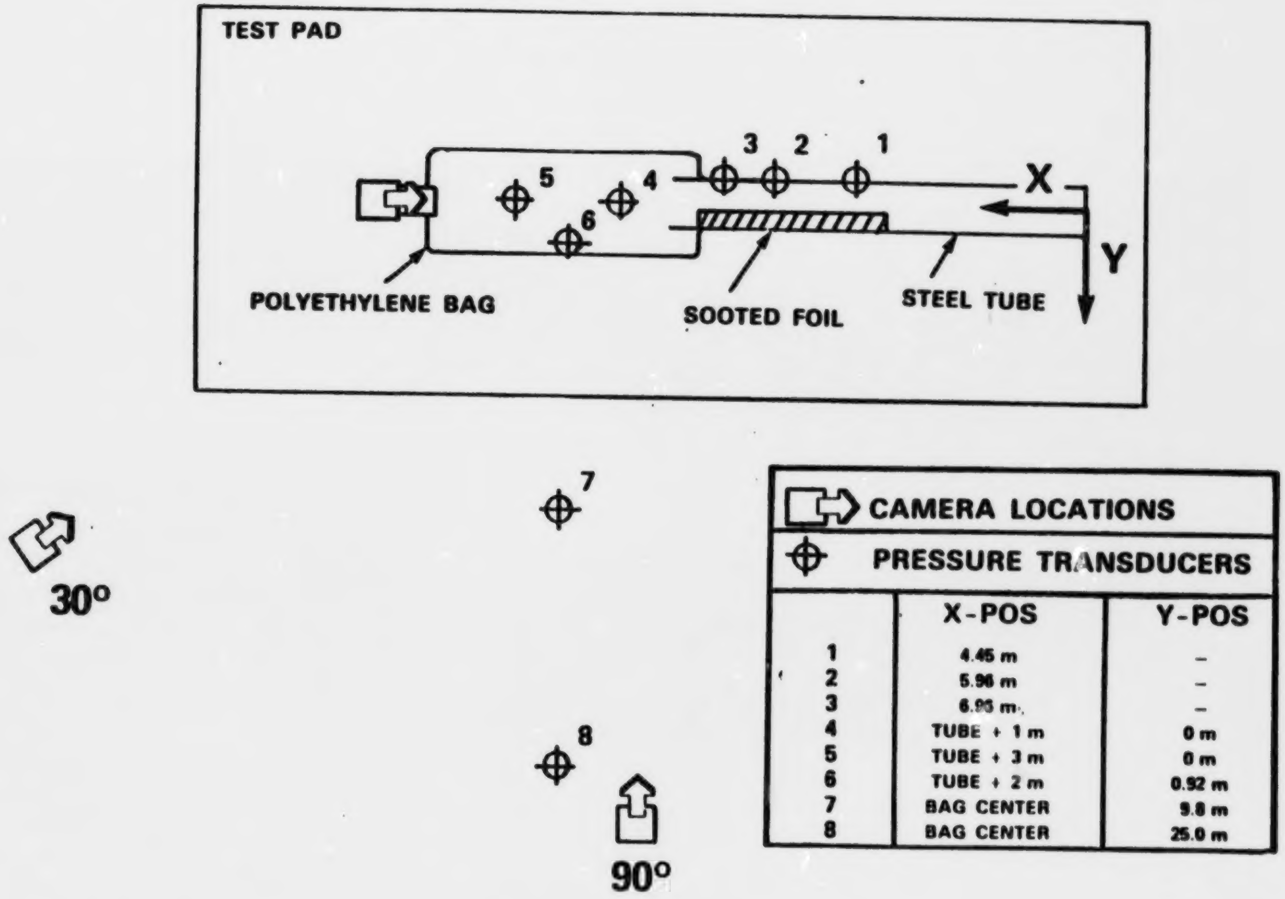

	X-POS	Y-POS
1	4.45 m	–
2	5.96 m	–
3	6.95 m	–
4	TUBE + 1 m	0 m
5	TUBE + 3 m	0 m
6	TUBE + 2 m	0.92 m
7	BAG CENTER	9.8 m
8	BAG CENTER	25.0 m

FIGURE 2. H_2S TRIALS: INSTRUMENTATION LAYOUT

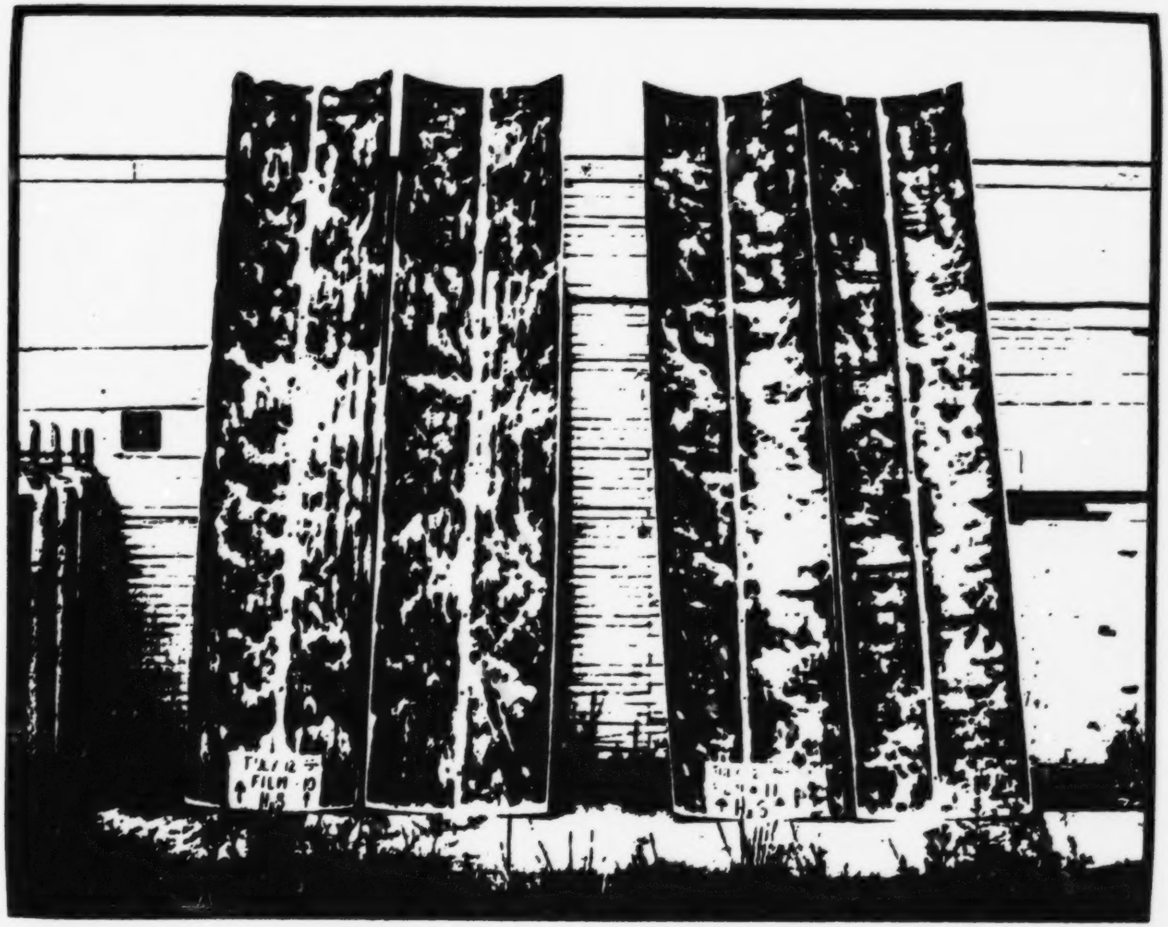

FIGURE 3. SMOKED FOIL RECORDS

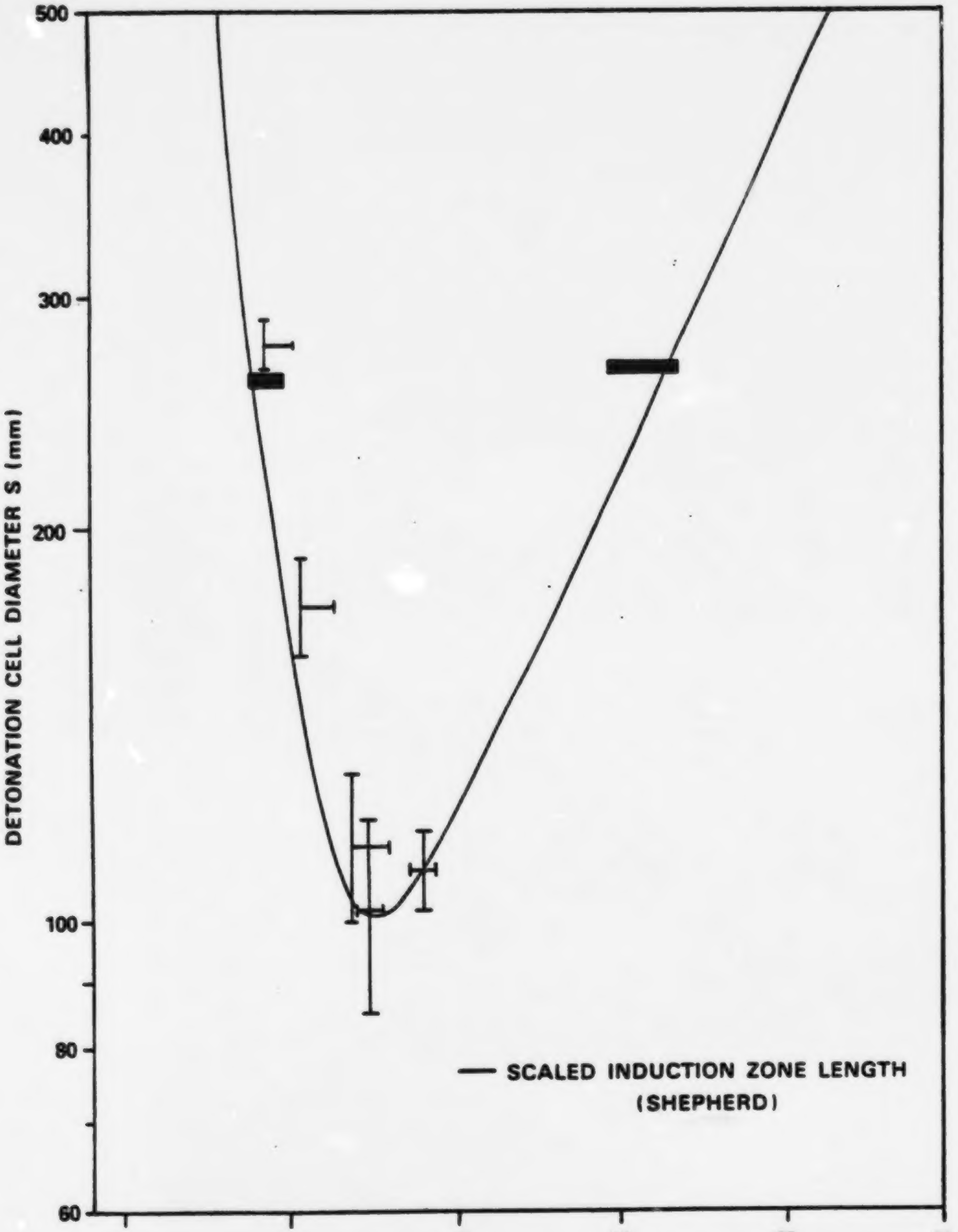
DETONATION CELL DIAMETER S (mm)
500
400
300
200
100
80
60
5
10
15
20
25
30
% H_2S (BY VOLUME)
— SCALED INDUCTION ZONE LENGTH (SHEPHERD)

FIGURE 5

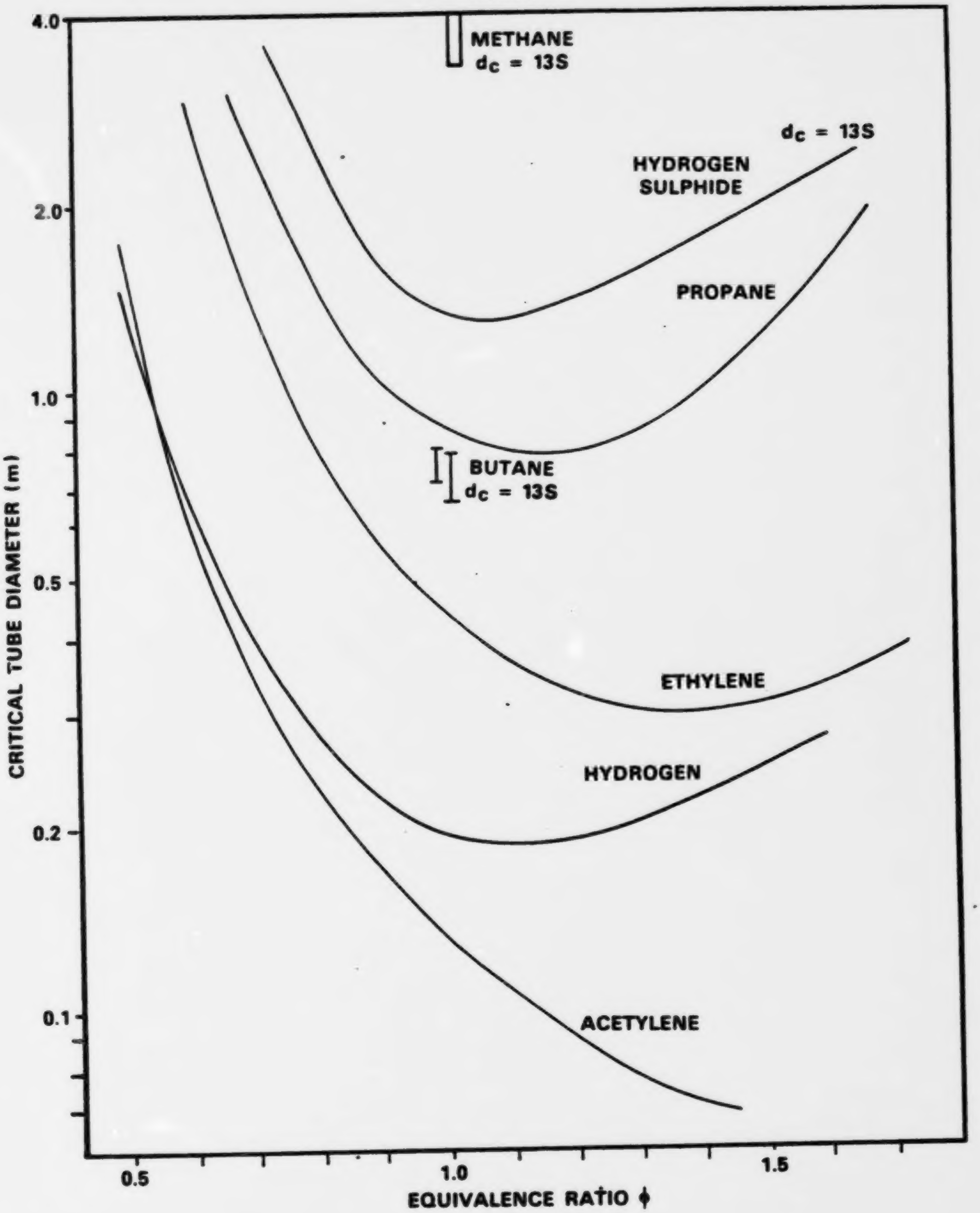

Figure 6

CRITICAL TUBE DIAMETERS FOR DETONATIONS IN VARIOUS FUEL-AIR MIXTURES

APPENDIX E

Blast Properties of H_2S-Air Detonations

by

Paul Thibault

BLAST PROPERTIES OF H_2S-AIR DETONATIONS

by

Paul Thibault

Combustion Dynamics Ltd.
Ralston, Alberta

1. INTRODUCTION

Any industrial plant which processes or stores combustible gases and liquids must contend with the possibility of an accidental spill and the resulting hazards of a fuel-air explosion. Unfortunately, a systematic risk analysis involving accidental explosions remains extremely difficult to carry out due to the problems involved in:

1) determining the most relevant spill scenarios

2) predicting the subsequent dispersion of the fuel-air cloud

3) locating the most probable ignition sources

4) determining the mode of combustion after ignition (i.e., stabilized flame, accelerating flame or detonation)

and finally

5) estimating the strength of the resulting blast and predicting the damages inflicted on the plant and personnel.

Due to these difficulties, the vulnerability of a plant to an accidental explosion must often be assessed on the basis of a so-called 'worst case' scenario. In terms of its blast damage potential, the detonation combustion mode is by far the most dangerous due to the high overpressures involved. It is fair to say that the probability of a H_2S-air detonation in a heavy water plant is virtually impossible to determine at the present time. All that can be stated with any certainty is that if it did occur, it would probably do so via Deflagration to Detonation Transition (DDT). Although our present understanding of the DDT phenomenon is extremely limited, recent research would suggest that the probability of DDT usually increases with

1) the sensitivity of the mixture to direct initiation
2) the level of confinement
3) the size of the fuel-air cloud
4) the level of turbulence.

The sensitivity of H_2S-air to the onset of detonation is relatively low (somewhere between that of methane-air and propane-air [1]). However, this insensitivity could be easily compensated by the potential size of H_2S-air clouds following an accidental spill in a heavy water plant and the level of turbulence which the numerous obstacles in the plant (i.e., pipes, towers, etc.) could generate during flame propagation. Experimentally, transition to detonations have been observed in relatively unconfined situations with lean acetylene-air [2] and hydrogen-air mixtures [3,4,5]. Ironically, in most of these cases DDT was not planned but occurred as a complete surprise to the researchers involved. This further confirms not only our precarious understanding of the DDT process but also our tendency to underestimate its likelihood. Consequently, although the probability of a detonation in a heavy water plant cannot be properly estimated for the purpose of risk analysis, the possibility of DDT should not be ruled out, a priori, in the selection of a worst case scenario.

The aim of the present report is to provide AECB with useful background information concerning the blast waves generated from H_2S-air detonations. For this purpose, one-dimensional calculations have been performed for the simple case of a uniform hemi-spherical cloud of stoichiometric H_2S-air. This particular case has been selected for its simplicity and is of course not meant to represent the outcome of a realistic spill scenario in which the H_2S-air cloud would be expected to be highly non-uniform and multi-dimensional. The intention here is simply to provide reference data which may assist AECB in evaluating the implications of a H_2S-air detonation in a heavy water plant.

2. DESCRIPTION OF CALCULATIONS

We consider a hemi-spherical cloud in which detonation is initiated at the center. As illustrated in Figure 1, the detonation is assumed to propagate spherically until it reaches the edge of the cloud. At this point a shock wave is transmitted to the ambient air which propagates outwards while decaying in strength due to expansion. The complete flow field may be computed for any given time by solving the one-dimensional equations for mass, momentum and energy which, for the spherical geometry, may be written in the following form:

$$\frac{\partial \rho}{\partial t} + \frac{1}{R^2} \frac{\partial}{\partial R}(R^2 \rho u) = 0 \qquad (1)$$

$$\frac{\partial \rho u}{\partial t} + \frac{1}{R^2} \frac{\partial}{\partial R}(R^2 \rho u^2) + \frac{\partial P}{\partial R} = 0 \qquad (2)$$

$$\frac{\partial E}{\partial t} + \frac{1}{R^2} \frac{\partial}{\partial R}(R^2 E u) + \frac{1}{R^2} \frac{\partial}{\partial R}(R^2 P u) = 0 \qquad (3)$$

where:

t = time
R = radius
ρ = mass density
u = gas velocity
E = energy density

For an ideal gas with constant heat capacity, the energy density may be expressed as

$$E = \frac{P}{(\gamma-1)} + \frac{1}{2} \rho u^2$$

and $$P = \rho R_G T$$

where P = absolute pressure

T = absolute temperature

and R_G = gas constant.

The above equations have been solved numerically using the finite difference Flux Corrected Transport (FCT) algorithm of Boris [6]. This code has been selected for its low numerical diffusion and its ability to accurately resolve shock waves using a relatively small number of grid points. The grid resolution used for the present calculation corresponds to 100 grid points per cloud radius.

During the initial stage of detonation propagation inside the H_2S-air cloud, the energy release due to combustion was incorporated into the calculation by imposing Chapman-Jouguet (C-J) conditions at the detonation front which in turn was forced to propagate at the prescribed C-J velocity V_{CJ}. These conditions were computed using the Gordon-McBride chemical equilibrium code [7]. For stoichiometric H_2S-air mixture at an initial pressure P_0 = 1 atm. and temperature T_0 = 298.15 K, the C-J conditions are:

P_{CJ} = 15.3 atm (absolute)

$\rho_{CJ} = 2.16 \times 10^{-3}$ g/cc

T_{CJ} = 2688 K

u_{CJ} = 725.6 m/sec

$\gamma_{CJ} = 1.187$

V_{CJ} = detonation velocity
= 1647 m/sec

The detailed calculations presented in this report for stoichiometric H_2S-air mixtures are very similar to those previously reported by the present author (see Moen et al. [8]) for stoichiometric ethylene-air mixtures and by Guirao et al. [9] for stoichiometric propane-air mixtures. The results presented here are however somewhat more complete since they include time histories of the dynamic pressure which have not been previously reported and may be relevant to the loading of certain structures in a heavy water plant.

3. SIDE-ON AND DYNAMIC PRESSURE TRACES

The numerical calculations were performed using a non-dimensional version of equations 1-3. In this manner only one computer run was required to obtain pressure traces for all cloud radii. For the sake of illustration, however, the results will be presented here in dimensional form for a cloud radius R_c = 10 meters. This particular choice is of course totally arbitrary and is not made with any particular spill scenario in mind.

The side-on overpressure and dynamic pressure traces for 20 different positions (5 inside the cloud and 15 outside the cloud) are presented in figures 2 to 21. The side-on overpressures inside the cloud initially decays from ΔP_{CJ} to approximately $\Delta P_{CJ}/3$ due to the isentropic expansion of the burned products behind the detonation front. When the latter reaches the edge of the cloud, a secondary expansion wave propagates towards the center of the cloud which results in a further decay and an eventual return to ambient pressure. The dominant pressure loading inside the cloud is due to the positive phase of the side-on overpressure. Indeed, the negative phase is considerably weaker in terms of its maximum amplitude and impulse. Whereas the peak dynamic pressure is approximately one third of the peak side-on overpressure, the duration of the dynamic loading decreases rapidly as one moves towards the center of the cloud.

The side-on overpressures outside the cloud are characterized by a relatively long negative phase. As a consequence, the negative phase impulse is comparable to that of the positive phase in this region. The negative phase also contains a series of secondary shocks and compression waves which emerge as the result of implosions at the center of the cloud and the transmission and reflection of waves at the contact surface between the burned and unburned gases. Finally, the dynamic pressure loading is also important particularly near the edge of the cloud where the peak dynamic pressure is comparable to the peak side-on overpressure.

The main features of the above calculations have been conveniently summarized in tables A-1 and A-2. Table A-1 lists the relevant pressures and impulses for a 10 meter cloud radius at 20 positions ranging from 1 to 150 meters. The variables listed are defined as follows:

RADIUS = radial position from center of cloud (meters)

PMAX = maximum side-on overpressure (atmospheres)

PREF = maximum overpressure which would be generated by normal reflection of the wave (atm)

PDYN = maximum dynamic pressure (atm)

$$= 1/2(\rho u^2)_{Max}$$

PMIN = minimum side-on overpressure (atm)

IPOS = side-on positive phase impulse (atm x msec)

$$= \int_{TARR}^{TARR + TPOS} \Delta P(t)\, dt$$

where: TARR = arrival time of wave

TPOS = time span between arrival of wave and first zero crossing of side-on overpressure (i.e., positive phase duration).

INEG = side-on negative phase impulse (atm x msec)

$$= \int_{TARR + TPOS}^{TARR + TPOS + TNEG} |\Delta P(t)| dt$$

where: TNEG = time span between first and second zero crossings of side-on overpressures (i.e., negative phase duration)

IDYN = dynamic impulse (atm x msec)

$$= \int_{TARR}^{TARR + TREV} \tfrac{1}{2} \rho(t) u^2(t) dt$$

where: TREV = time span between arrival of wave and first flow reversal.

The characteristic times defined above are tabulated in Table A-2 along with the following additional characteristic times and velocity:

TSEC = time span between arrival of wave and secondary shock (msec)

TCONT = time span between arrival of wave and passage of the contact surface separating the burned and unburned gases (msec). If $R < R_c$ this time is zero by definition. If $R > R_c$ and the contact surface never reaches the specified position, TCONT is listed as zero.

VF = wave front velocity (m/sec)

4. SCALING OF RESULTS

The information contained in tables A-1 and A-2 can be presented in a more general non-dimensional form by scaling the position, time, velocity, pressure and impulse variables with respect to a characteristic length $\bar{R}$, velocity $\bar{V}$, and pressure $\bar{P}$. Denoting non-dimensional variables with superscripts (*) the non-dimensionalization may be expressed as follows:

$$R^* = R/\bar{R} \qquad \text{position}$$

$$t^* = t\bar{V}/\bar{R} \qquad \text{time}$$

$$v^* = v/\bar{V} \qquad \text{velocity}$$

$$P^* = P/\bar{P} \qquad \text{pressure}$$

$$I^* = \frac{I\bar{V}}{\bar{R}\bar{P}} \qquad \text{Impulse}$$

a) Scaling with cloud radius

A convenient method of scaling the blast results is to use the cloud radius R_c as a characteristic length such that all results may be represented in terms of the scaled distance R/R_c. Ambient conditions for the pressure and the speed of sound may also be chosen as characteristic quantities such that

$$\bar{R} = R_c$$

$$\bar{V} = c_o$$

$$\bar{P} = P_o$$

and

$$R^* = R/R_c$$

$$t^* = tc_o/R_c$$

$$v^* = v/c_o$$

$$I^* = \frac{Ic_o}{R_cP_o}$$

Non-dimensional versions of tables A-1 and A-2 using cloud radius scaling are presented in table B-1 and B-2. It should also be noted that the same scaling arguments may be applied to convert the pressure traces in figures 2-21 for a 10 meter radius cloud to any other cloud radii. For example, the pressure history at a position R = 40 m for a cloud radius R_c = 20 m (i.e., $R/R_c = 2$) would be identical to that at a position R = 20 m for a cloud radius R_c = 10 m with the exception that the duration in the former case would be twice as long. This scaling procedure is illustrated in Figure 22.

b) Scaling with energy

It is occasionally of interest to compare the blast properties of fuel-air detonations to those of condensed explosives such as TNT. Since solid explosives have a much higher energy release per unit volume than gaseous mixtures, a comparison based on charge radius scaling is not very meaningful. One may, on the other hand, seek a comparison based on the energy, E_D, released during detonation by defining a new characteristic length

$$\bar{R} = R_E = (E_D/P_o)^{1/3}$$

which is commonly referred to as the explosion radius. The characteristic energy, E_D, may be defined as

$$E_D = \rho_i \nu Q$$

where ρ_i = initial density of the fuel-air mixture

ν = initial volume of the fuel-air cloud

Q = energy release per unit mass of mixture.

Following reference [8] the latter is defined here as the difference in enthalpies, at ambient temperature, between the reactants and the burned products

$$Q = h_{To}\ (\text{reactants}) - h_{To}\ (\text{products})$$

For stoichiometric H_2S-air mixtures, the energy release parameter Q = 1962.8 kJ/kg such that for a 10 meter radius cloud R_E = 36.6 m. Using this characteristic length the results may be energy-scaled as shown in tables C-1 and C-2. Finally, using a detonation energy Q = 4200 kJ/kg for TNT the side-on overpressures and impulses may be compared with TNT surface burst data [10] as shown in figures 23 and 24.

BRIEF COMMENT ON APPLICATION OF RESULTS

The ultimate application of any blast calculation is to serve as input to a structural analysis designed to assess the vulnerability of various structures to an accidental explosion. It should of course be emphasized that the simple case of a uniform hemi-spherical cloud considered in this report is a highly idealized one. Consequently, some caution must be exercised in applying the results to realistic spill scenarios which, strictly speaking, would require at least two dimensional modelling. It should also be noted that the loads which structures are subjected to depend not only on the properties of the incident blast but also on the interaction of the latter with the structure itself. The time-dependent pressure distribution on a given structure can be determined either by shock diffraction experiments in a large scale blast simulator or through 2-D and/or 3-D numerical calculations. For engineering purposes, net loads on relatively simple structures may be estimated using approximate methods such as those proposed by Glasstone and Dolan [11]. Without going into any great detail, suffice it to say that these methods require as input the relevant geometric dimensions and drag coefficient for the structure along with the shock velocity, overpressue history and dynamic pressure history of the incident blast. The latter information is readily obtainable from the present report for the case of a hemi-spherical uniform cloud. One final word of caution is that the approximate methods of Glasstone are limited to moderately low overpressures (typically less than 3.5 atm) and should therefore not be applied to regions inside or near the H_2S-air cloud where the overpressures are of course much higher.

1. Sulmistras, A., Moen, I.O. and Saber, A.J., 'Detonations in Hydrogen Sulphide-Air Clouds with Comparisons to Other Fuel-Air Mixtures.' Presented at the Joint Technical Meeting of the Central and Western States Section of the Combustion Institute, San Antonio, Texas, April 22-23, 1985.

2. Moen, I.O., Bjerketvedt, D., Jenssen, A. and Thibault, P.A., 'Transition to Detonation in a Large Fuel-Air Cloud.' Accepted for publication in Combustion and Flame, 1985.

3. Geiger, W., Battelle Institut e.v., Frankfurt, West Germany, private communication to I.O. Moen, 1983.

4. Pförtner, H., Schneider, H., Drenckhahn, W. and Koch, C., 'Flame Acceleration and Pressure Build-Up in Free and Partially Confined Hydrogen-Air Clouds.' Presented at the Ninth International Colloquium on Dynamics of Explosions and Reactive Systems, Poitiers, France, July 1983.

5. Fisk, J.W., Sherman, M.P., Tieszen, S.R. and Benedick, W.B., 'Experimental Facilities to Study Hydrogen Combustion and Detonation.' Published in 'Designing for Hydrogen in Nuclear Power Plants', K.K. Kiyogi, Ed., A.S.M.E., 1984.

6. Boris, J.P., 'Flux-Corrected Transport Modules for Solving Generalized Continuity Equations.' Naval Research Laboratory Memorandum 3237, March, 1976.

7. Gordon, S. and McBride, B., 'Computer Program for Calculations of Complex Chemical Equilibrium Compositions, Rocket Performance, Incident and Reflected Shocks, and Chapman-Jouguet Detonations.' NASA Report SP-273, Washington, D.C., 1976.

8. Moen, I.O., Thibault, P.A. and Funk, J.W., 'Blast Waves from Non-Spherical Fuel-Air Explosions.' Proceedings of the 8th International Symposium on Military Application of Blast Simulation, Spiez, Switzerland, 20-24 June, 1983.

9. Guirao, C.M., Bach, G.E. and Lee, J.H.S., 'On the Scaling of Blast Waves from Fuel-Air Explosions.' Proceedings of the 6th International Symposium on Military Application of Blast Simulation, Cahors, France, 1979.

10. Baker, W.E., Kulesz, J.J., Westine, P.S., Cox, P.A. and Wilbeck, J.S., 'A Manual for Prediction of Blast and Fragment Loading on Structures.' U.S. Department of Energy Report DOE/TIC-11268, Amarillo, Texas, Nov., 1980.

11. Glasstone, S. and Dolan, P.J., 'The Effects of Nuclear Weapons.' Prepared and published by the United States Department of Defense and the United States Department of Energy, 1977.

TABLE A-1

DIMENSIONAL BLAST PROPERTIES

CHARACTERISTIC PRESSURES AND IMPULSES

RADIUS(M)	PMAX(ATM)	PREF	PDMAX	PMIN	IPOS(ATM*MS)	INEG	IDYN
1.000	14.2585	35.917	5.656	-.7936	69.5435	5.3080	.8812
2.500	14.2585	35.917	5.656	-.7073	64.7787	5.3571	1.2929
5.000	14.2585	35.917	5.656	-.4577	54.6684	4.2076	1.9250
7.500	14.2585	35.917	5.656	-.2909	45.3759	2.6491	2.5763
10.000	14.2585	35.917	5.893	-.1605	34.8111	1.6610	7.4131
12.500	5.3546	24.633	5.701	-.2410	23.6805	16.7302	8.7341
15.000	3.5418	14.223	3.082	-.2255	18.5077	16.5826	8.1959
17.500	2.5468	9.169	1.729	-.2243	14.9287	16.2808	7.4559
20.000	1.9450	6.427	1.067	-.2205	13.2050	15.4772	6.1160
22.500	1.5183	4.660	.696	-.1985	12.0268	14.1041	4.6630
25.000	1.2548	3.654	.484	-.1808	11.0731	12.8034	3.6298
27.500	1.0541	2.936	.350	-.1654	10.2257	11.7073	2.8835
30.000	.9075	2.439	.264	-.1508	9.4998	10.7669	2.3293
35.000	.6903	1.752	.157	-.1294	8.2903	9.2801	1.5960
40.000	.5731	1.406	.111	-.1128	7.3379	8.1455	1.1482
50.000	.4144	.967	.059	-.0899	5.9596	6.5432	.6583
75.000	.2292	.502	.018	-.0592	4.0372	4.3821	.2396
100.000	.1534	.326	.008	-.0436	3.0420	3.2927	.1184
125.000	.1128	.236	.004	-.0343	2.4384	2.6370	.0693
150.000	.0881	.182	.002	-.0283	2.0338	2.1990	.0448

TABLE A-2

DIMENSIONAL BLAST PROPERTIES

CHARACTERISTIC TIMES

RADIUS(M)	TARR(MS)	TPOS	TNEG	TSEC	TCONT	TREV	VF(M/SEC)
1.000	.6435	19.5128	10.5922	26.2683	.0000	.5717	1647.25
2.500	1.5583	18.7558	12.4310	.0000	.0000	1.5150	1647.25
5.000	3.0733	18.0854	13.0904	.0000	.0000	2.8300	1647.25
7.500	4.5884	18.6832	14.2956	.0000	.0000	4.3151	1647.25
10.000	6.1034	20.7608	14.7355	.0000	.0000	22.1303	1647.25
12.500	8.4395	22.4098	157.9189	.0000	.8274	22.4098	818.74
15.000	11.5995	21.9945	158.8831	36.1356	4.5833	23.9260	695.70
17.500	15.2634	20.1591	160.1076	35.5290	10.3671	29.1840	617.83
20.000	19.3780	19.6460	161.8413	35.7627	.0000	51.2457	565.55
22.500	23.8665	21.1874	162.5355	37.6186	.0000	31.3844	525.35
25.000	28.6691	22.6607	162.9255	39.6222	.0000	31.6177	498.91
27.500	33.6945	23.7747	163.8677	41.6591	.0000	32.7154	477.79
30.000	38.9691	24.9135	164.8385	43.5278	.0000	33.6059	461.74
35.000	49.9918	27.4281	165.1230	47.1097	.0000	35.4638	436.90
40.000	61.5412	29.4549	165.8519	50.3018	.0000	37.4784	422.89
50.000	85.6732	33.0479	166.8714	55.9147	.0000	40.6776	403.13
75.000	149.6027	39.9444	167.9579	66.1528	.0000	46.2271	378.79
100.000	216.4148	44.5833	168.8052	73.2680	.0000	50.2365	368.36
125.000	284.7500	48.0178	169.2835	78.5338	.0000	52.5315	362.66
150.000	353.9535	50.8656	169.4828	82.7132	.0000	54.8384	359.14

TABLE B-1

NONDIMENSIONAL BLAST PROPERTIES

CHARACTERISTIC PRESSURES AND IMPULSES

RADIUS	PMAX	PREF	PDYN	PMIN	IPOS	INEG	IDYN
.100	14.2585	35.917	5.656	-.7936	2.4083	.1838	.0305
.250	14.2585	35.917	5.656	-.7073	2.2433	.1855	.0448
.500	14.2585	35.917	5.656	-.4577	1.8932	.1457	.0667
.750	14.2585	35.917	5.656	-.2909	1.5714	.0917	.0892
1.000	14.2585	35.917	5.893	-.1605	1.2055	.0575	.2567
1.250	5.3546	24.633	5.701	-.2410	.8201	.5794	.3025
1.500	3.5418	14.223	3.082	-.2255	.6409	.5743	.2838
1.750	2.5468	9.169	1.729	-.2243	.5170	.5638	.2582
2.000	1.9450	6.427	1.067	-.2205	.4573	.5360	.2118
2.250	1.5183	4.660	.696	-.1985	.4165	.4884	.1615
2.500	1.2548	3.654	.484	-.1808	.3835	.4434	.1257
2.750	1.0541	2.936	.350	-.1654	.3541	.4054	.0999
3.000	.9075	2.439	.264	-.1508	.3290	.3729	.0807
3.500	.6903	1.752	.157	-.1294	.2871	.3214	.0553
4.000	.5731	1.406	.111	-.1128	.2541	.2821	.0398
5.000	.4144	.967	.059	-.0899	.2064	.2266	.0228
7.500	.2292	.502	.018	-.0592	.1398	.1518	.0083
10.000	.1534	.326	.008	-.0436	.1053	.1140	.0041
12.500	.1128	.236	.004	-.0343	.0844	.0913	.0024
15.000	.0881	.182	.002	-.0283	.0704	.0761	.0016

TABLE B-2

NONDIMENSIONAL BLAST PROPERTIES

CHARACTERISTIC TIMES

RADIUS	TARR	TPOS	TNEG	TSEC	TCONT	TREV	MF
.100	.0223	.6757	.3668	.9097	.0000	.0198	4.76
.250	.0540	.6495	.4305	.0000	.0000	.0525	4.76
.500	.1064	.6263	.4533	.0000	.0000	.0980	4.76
.750	.1589	.6470	.4951	.0000	.0000	.1494	4.76
1.000	.2114	.7189	.5103	.0000	.0000	.7664	4.76
1.250	.2923	.7761	5.4687	.0000	.0287	.7761	2.36
1.500	.4017	.7617	5.5021	1.2514	.1587	.8286	2.01
1.750	.5286	.6981	5.5445	1.2304	.3590	1.0106	1.78
2.000	.6711	.6803	5.6046	1.2395	.0000	1.7746	1.63
2.250	.8265	.7337	5.6286	1.3027	.0000	1.0868	1.52
2.500	.9928	.7847	5.6421	1.3721	.0000	1.0949	1.44
2.750	1.1668	.8233	5.6747	1.4427	.0000	1.1329	1.38
3.000	1.3495	.8628	5.7084	1.5074	.0000	1.1638	1.33
3.500	1.7312	.9498	5.7182	1.6314	.0000	1.2281	1.26
4.000	2.1312	1.0200	5.7435	1.7420	.0000	1.2979	1.22
5.000	2.9669	1.1445	5.7788	1.9363	.0000	1.4087	1.16
7.500	5.1807	1.3833	5.8164	2.2909	.0000	1.6008	1.09
10.000	7.4944	1.5439	5.8457	2.5373	.0000	1.7397	1.06
12.500	9.8609	1.6629	5.8623	2.7196	.0000	1.8192	1.05
15.000	12.2574	1.7615	5.8692	2.8644	.0000	1.8991	1.04

TABLE C-1

ENERGY-SCALED PARAMETERS

CHARACTERISTIC PRESSURES AND IMPULSES

RADIUS	PMAX	PREF	PDYN	PMIN	IPOS	INEG	IDYN
.027	14.2585	35.917	5.656	-.7936	.6578	.0502	.0083
.068	14.2585	35.917	5.656	-.7073	.6127	.0507	.0122
.137	14.2585	35.917	5.656	-.4577	.5171	.0398	.0182
.205	14.2585	35.917	5.656	-.2909	.4292	.0251	.0244
.273	14.2585	35.917	5.893	-.1605	.3293	.0157	.0701
.341	5.3546	24.633	5.701	-.2410	.2240	.1583	.0826
.410	3.5418	14.223	3.082	-.2255	.1751	.1569	.0775
.478	2.5468	9.169	1.729	-.2243	.1412	.1540	.0705
.546	1.9450	6.427	1.067	-.2205	.1249	.1464	.0579
.615	1.5183	4.660	.696	-.1985	.1138	.1334	.0441
.683	1.2548	3.654	.484	-.1808	.1047	.1211	.0343
.751	1.0541	2.936	.350	-.1654	.0967	.1107	.0273
.819	.9075	2.439	.264	-.1508	.0899	.1018	.0220
.956	.6903	1.752	.157	-.1294	.0784	.0878	.0151
1.093	.5731	1.406	.111	-.1128	.0694	.0770	.0109
1.366	.4144	.967	.059	-.0899	.0564	.0619	.0062
2.049	.2292	.502	.018	-.0592	.0382	.0415	.0023
2.731	.1534	.326	.008	-.0436	.0288	.0311	.0011
3.414	.1128	.236	.004	-.0343	.0231	.0249	.0007
4.097	.0881	.182	.002	-.0283	.0192	.0208	.0004

TABLE C-2

ENERGY-SCALED PARAMETERS

CHARACTERISTIC TIMES

RADIUS	TARR	TPOS	TNEG	TSEC	TCONT	TREV	MF
.027	.0061	.1846	.1002	.2485	.0000	.0054	4.76
.068	.0147	.1774	.1176	.0000	.0000	.0143	4.76
.137	.0291	.1711	.1238	.0000	.0000	.0268	4.76
.205	.0434	.1767	.1352	.0000	.0000	.0408	4.76
.273	.0577	.1964	.1394	.0000	.0000	.2093	4.76
.341	.0798	.2120	1.4938	.0000	.0078	.2120	2.36
.410	.1097	.2080	1.5029	.3418	.0434	.2263	2.01
.478	.1444	.1907	1.5145	.3361	.0981	.2761	1.78
.546	.1833	.1858	1.5309	.3383	.0000	.4847	1.63
.615	.2258	.2004	1.5374	.3558	.0000	.2969	1.52
.683	.2712	.2144	1.5411	.3748	.0000	.2991	1.44
.751	.3187	.2249	1.5500	.3941	.0000	.3095	1.38
.819	.3686	.2357	1.5592	.4117	.0000	.3179	1.33
.956	.4729	.2594	1.5619	.4456	.0000	.3355	1.26
1.093	.5821	.2786	1.5688	.4758	.0000	.3545	1.22
1.366	.8104	.3126	1.5785	.5289	.0000	.3848	1.16
2.049	1.4151	.3778	1.5887	.6257	.0000	.4373	1.09
2.731	2.0471	.4217	1.5967	.6930	.0000	.4752	1.06
3.414	2.6935	.4542	1.6013	.7429	.0000	.4969	1.05
4.097	3.3481	.4811	1.6032	.7824	.0000	.5187	1.04

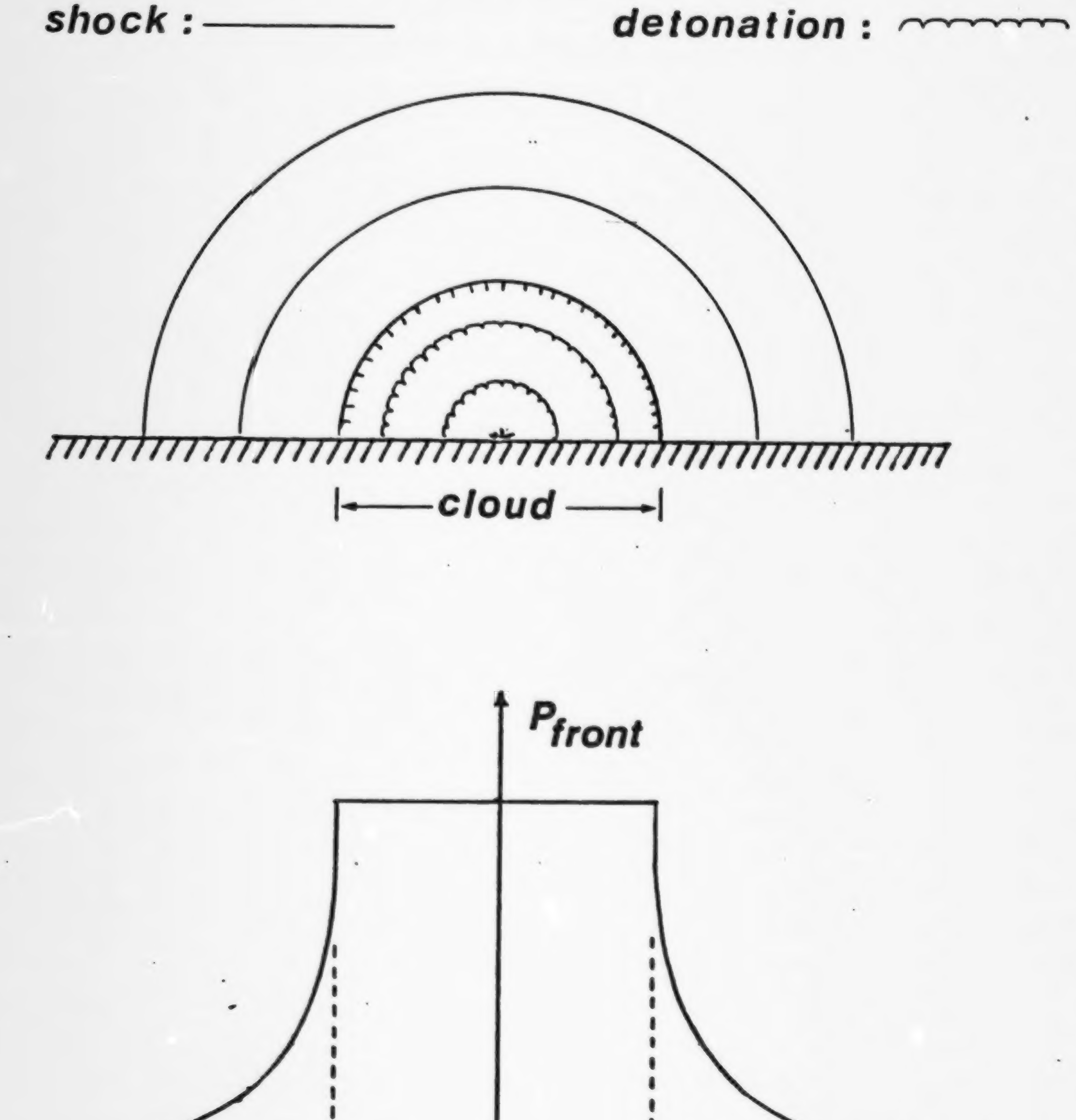

FIGURE 1

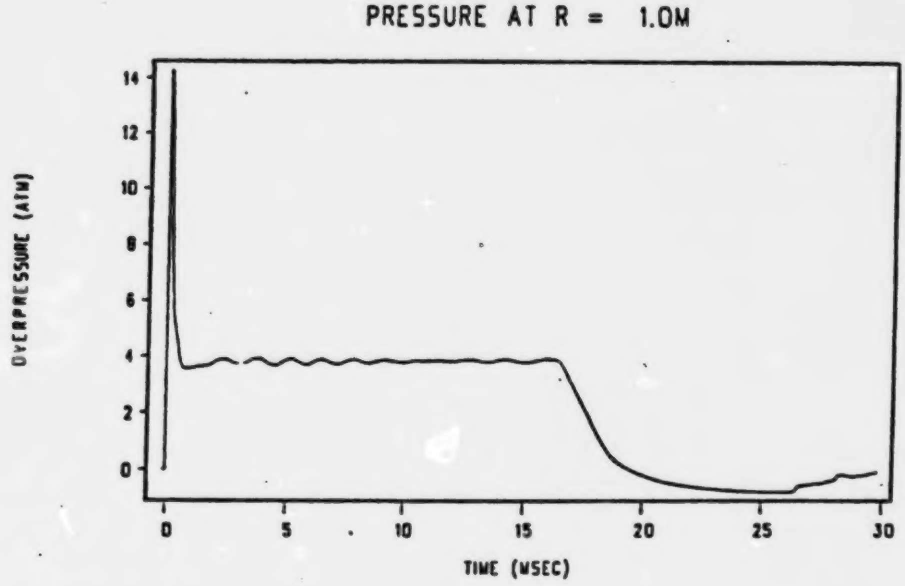
PRESSURE AT R = 1.0M
OVERPRESSURE (ATM)
14
12
10
8
6
4
2
0
0
5
10
15
20
25
30
TIME (MSEC)

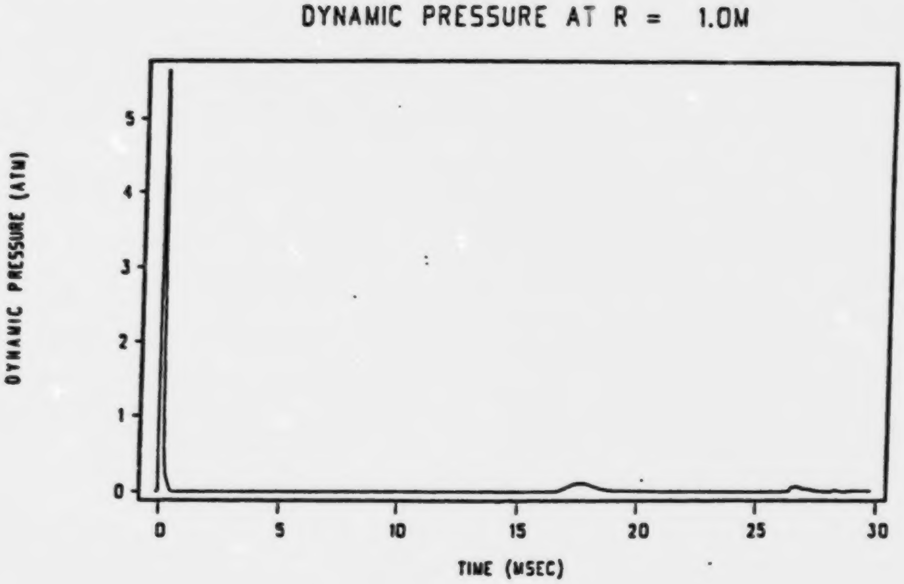
DYNAMIC PRESSURE AT R = 1.0M
DYNAMIC PRESSURE (ATM)
5
4
3
2
1
0
0
5
10
15
20
25
30
TIME (MSEC)

FIGURE 2

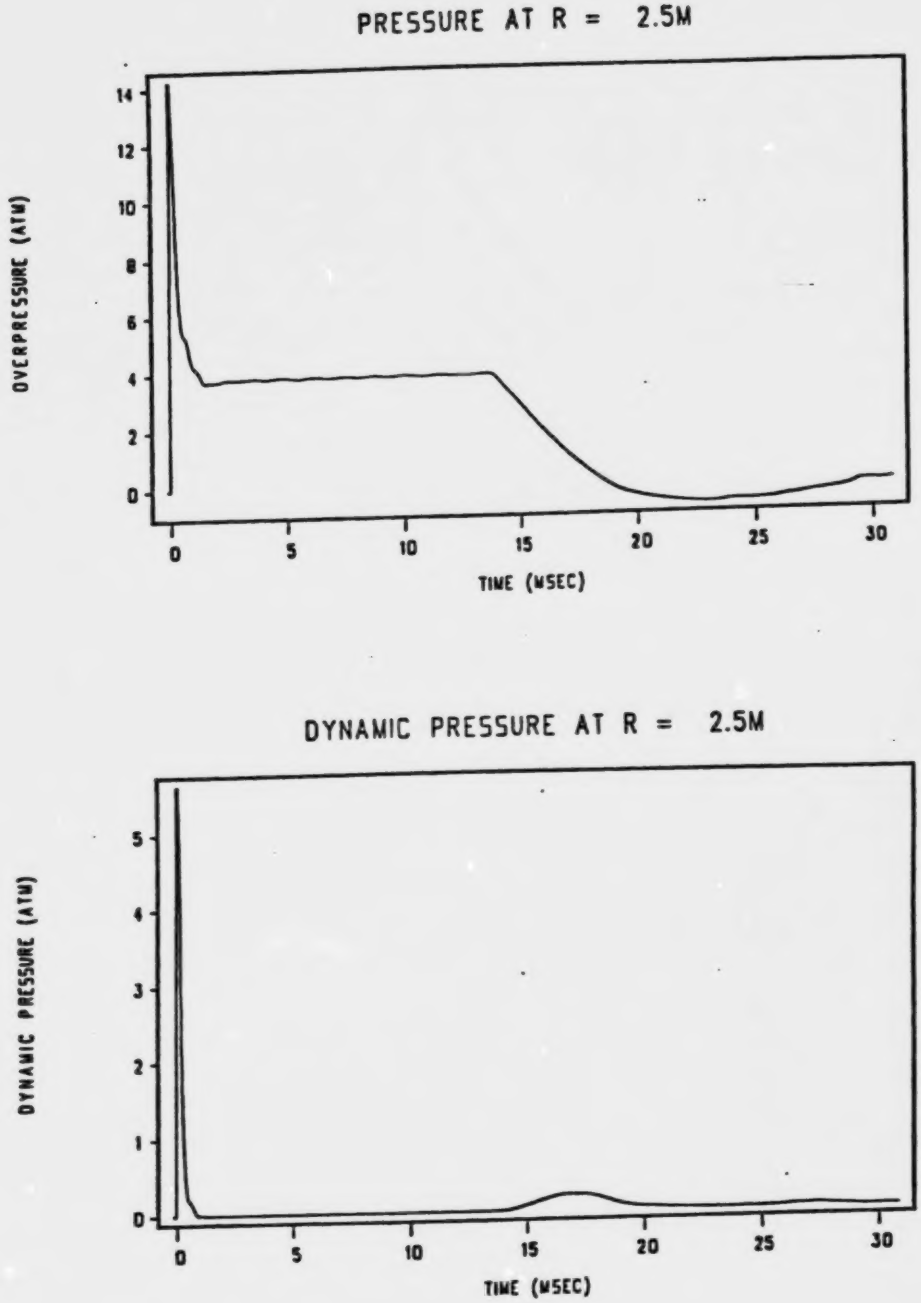
PRESSURE AT R = 2.5M
OVERPRESSURE (ATM)
0
2
4
6
8
10
12
14
TIME (MSEC)
0
5
10
15
20
25
30
DYNAMIC PRESSURE AT R = 2.5M
DYNAMIC PRESSURE (ATM)
0
1
2
3
4
5
TIME (MSEC)
0
5
10
15
20
25
30

FIGURE 3

PRESSURE AT R = 5.0M

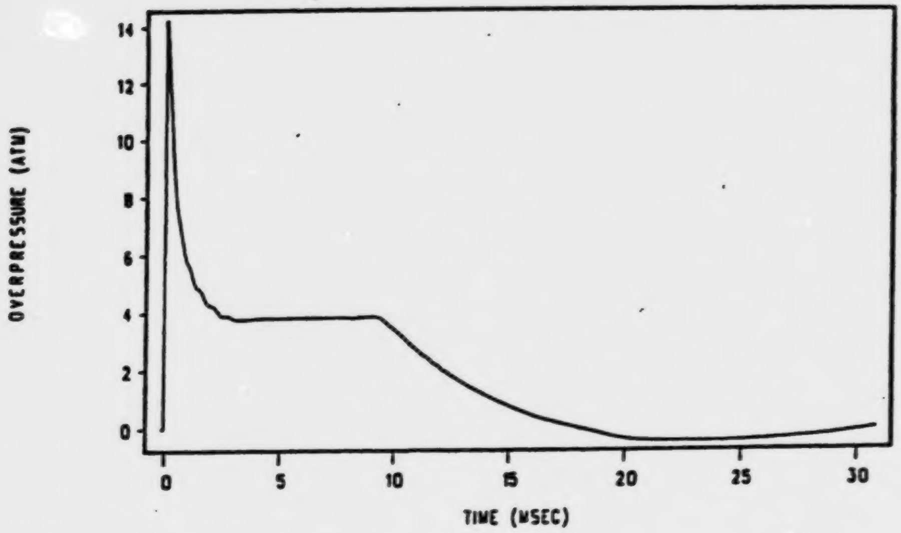

DYNAMIC PRESSURE AT R = 5.0M

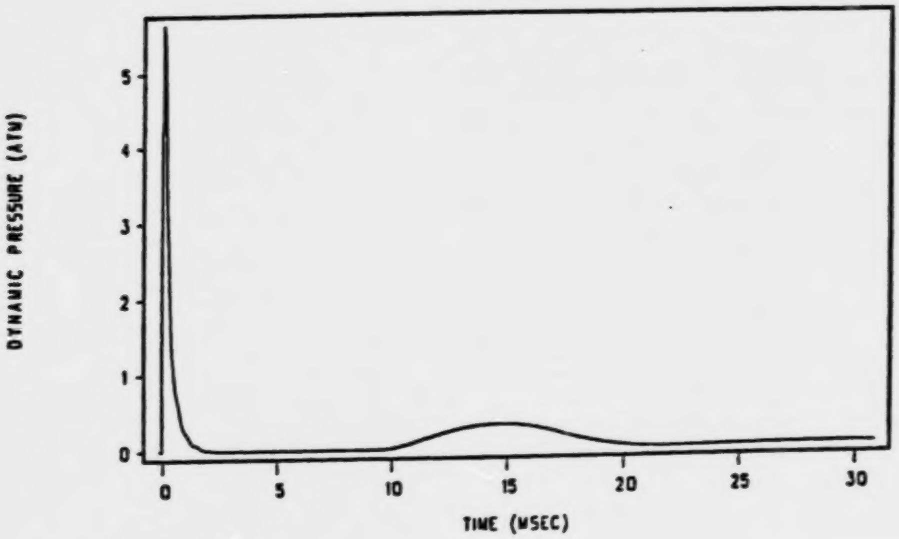

FIGURE 4

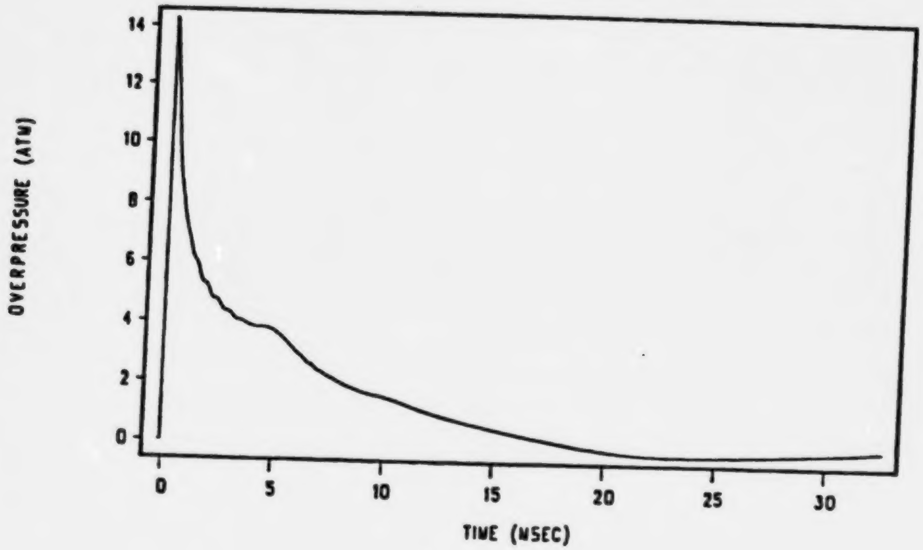

PRESSURE AT R = 7.5M

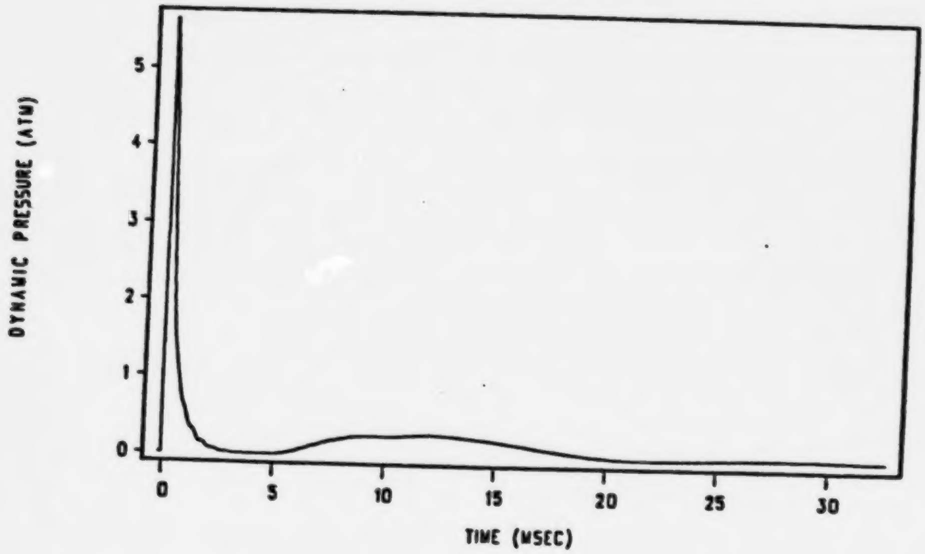

DYNAMIC PRESSURE AT R = 7.5M

FIGURE 5

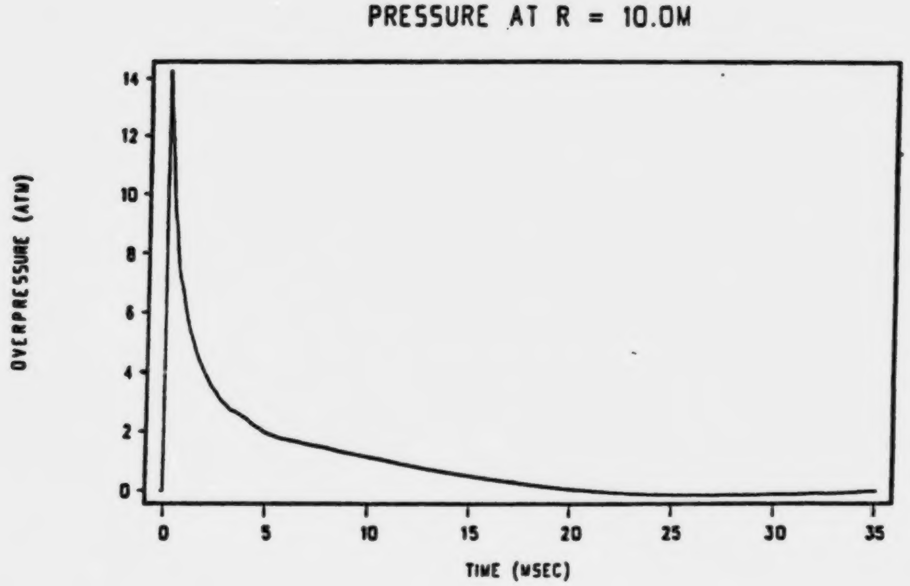
PRESSURE AT R = 10.0M
OVERPRESSURE (ATM)
0
2
4
6
8
10
12
14
TIME (MSEC)
0
5
10
15
20
25
30
35

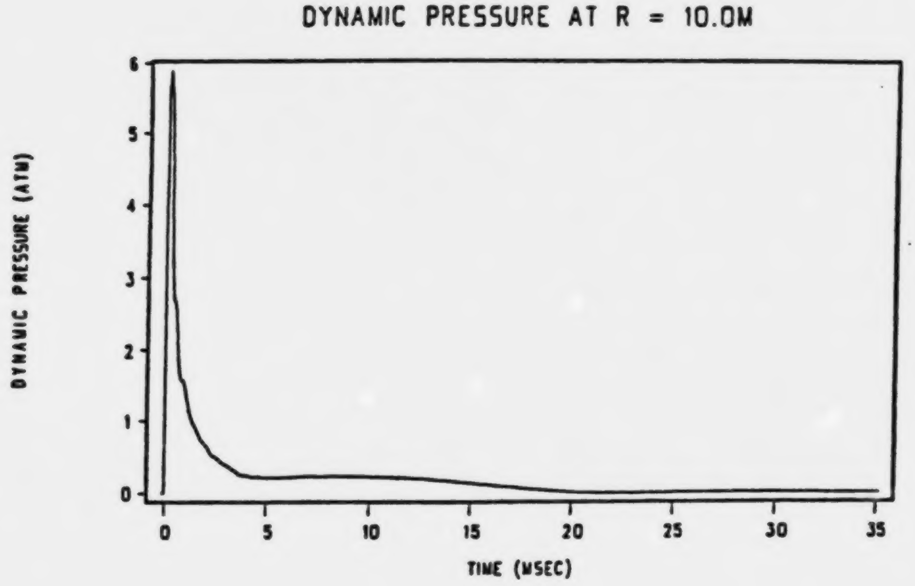
DYNAMIC PRESSURE AT R = 10.0M
DYNAMIC PRESSURE (ATM)
0
1
2
3
4
5
6
TIME (MSEC)
0
5
10
15
20
25
30
35

FIGURE 6

PRESSURE AT R = 12.5M

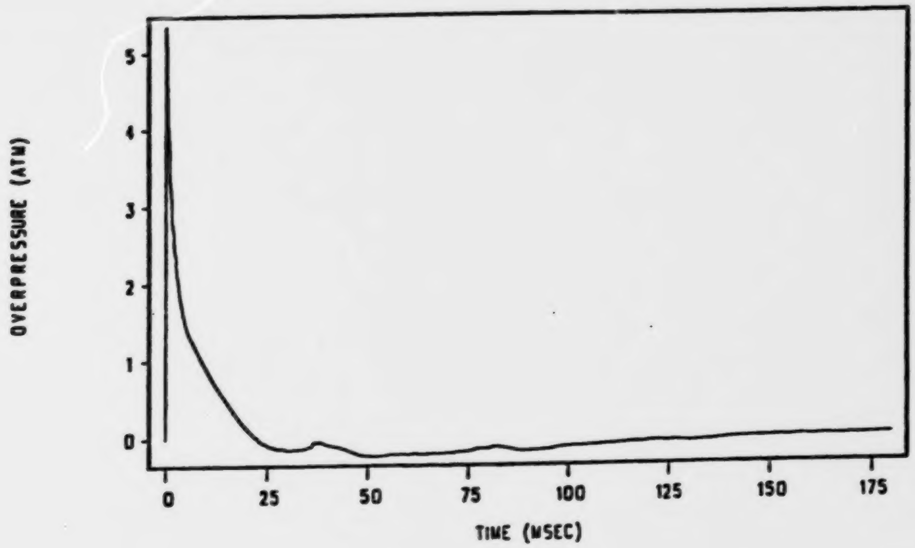

DYNAMIC PRESSURE AT R = 12.5M

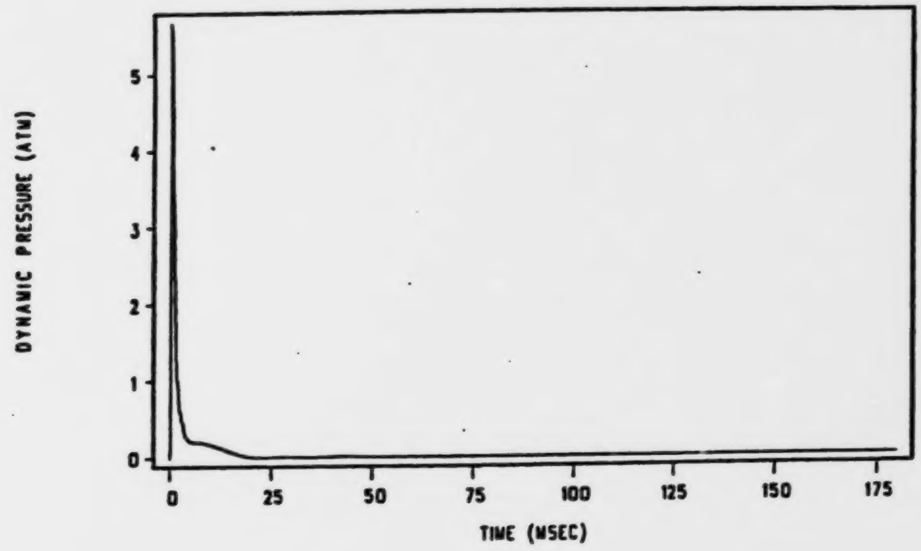

FIGURE 7

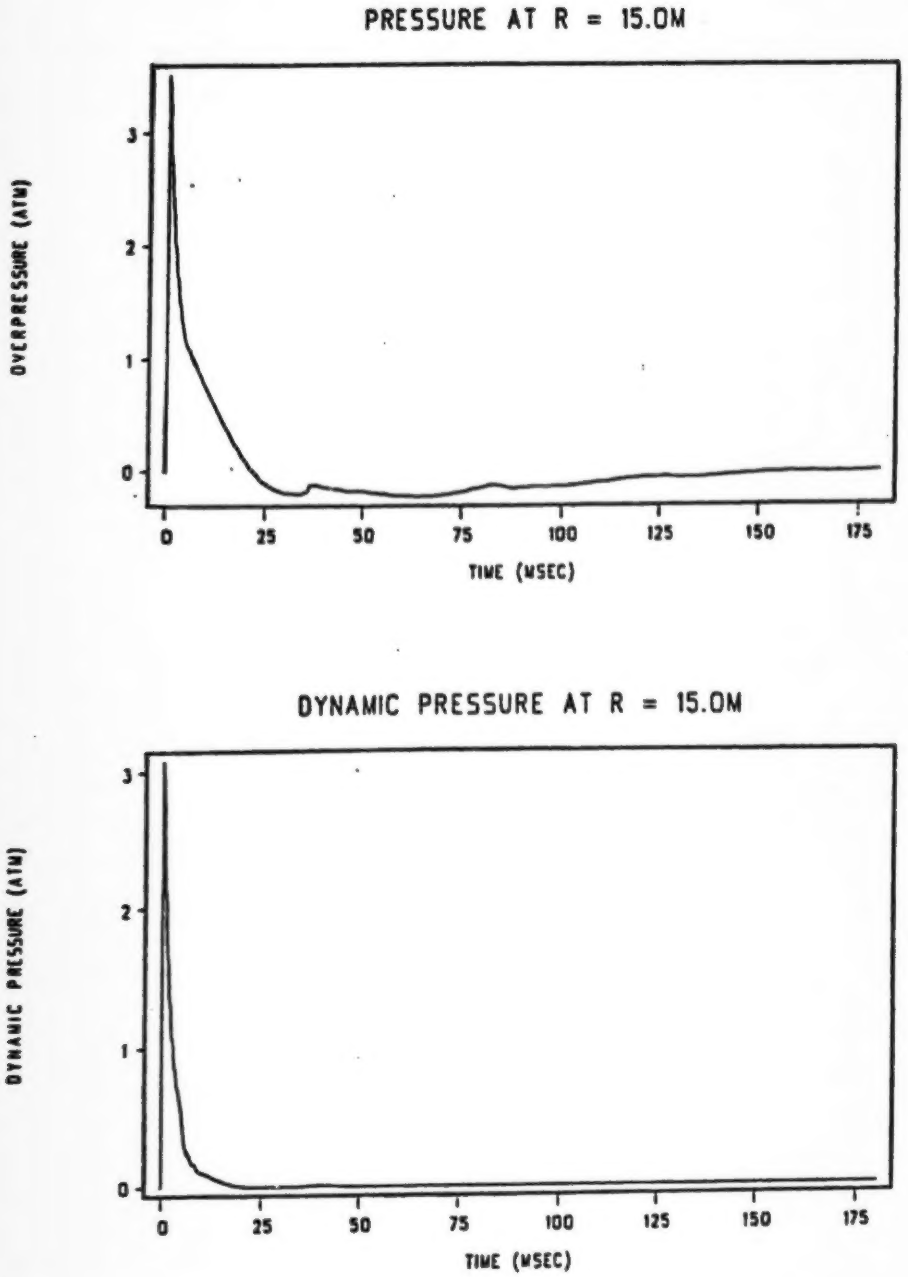

PRESSURE AT R = 15.0M

DYNAMIC PRESSURE AT R = 15.0M

FIGURE 8

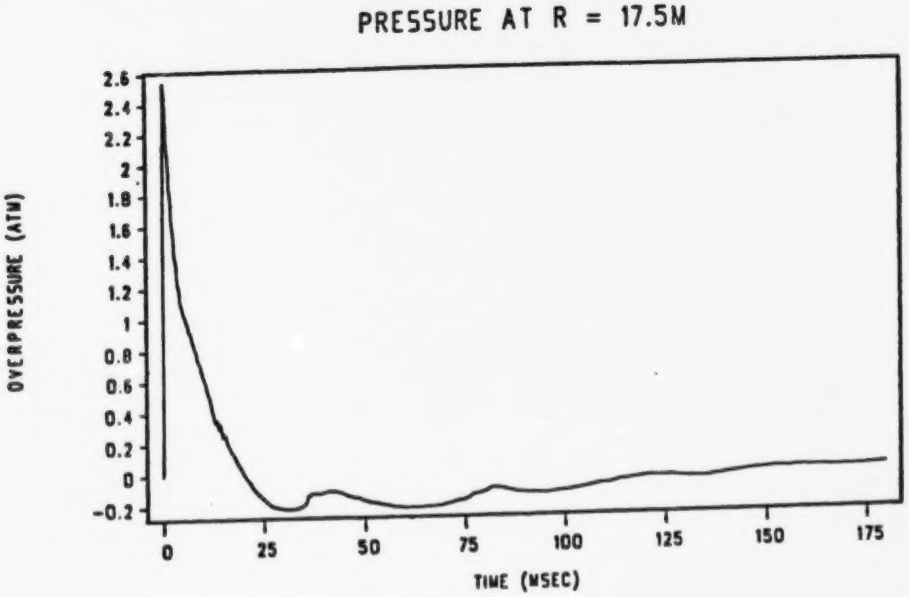
PRESSURE AT R = 17.5M
OVERPRESSURE (ATM)
2.6
2.4
2.2
2
1.8
1.6
1.4
1.2
1
0.8
0.6
0.4
0.2
0
-0.2
0
25
50
75
100
125
150
175
TIME (MSEC)

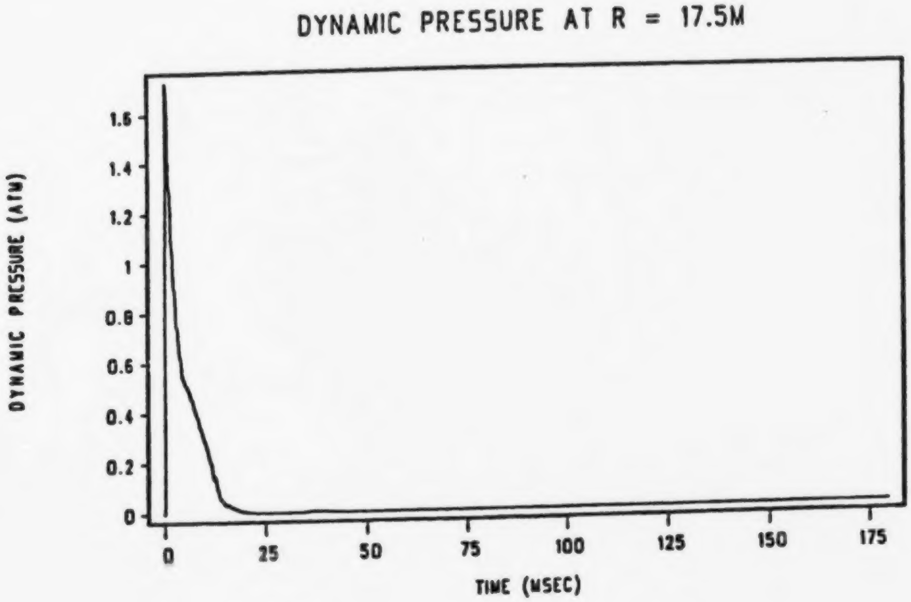
DYNAMIC PRESSURE AT R = 17.5M
DYNAMIC PRESSURE (ATM)
1.6
1.4
1.2
1
0.8
0.6
0.4
0.2
0
0
25
50
75
100
125
150
175
TIME (MSEC)

FIGURE 9

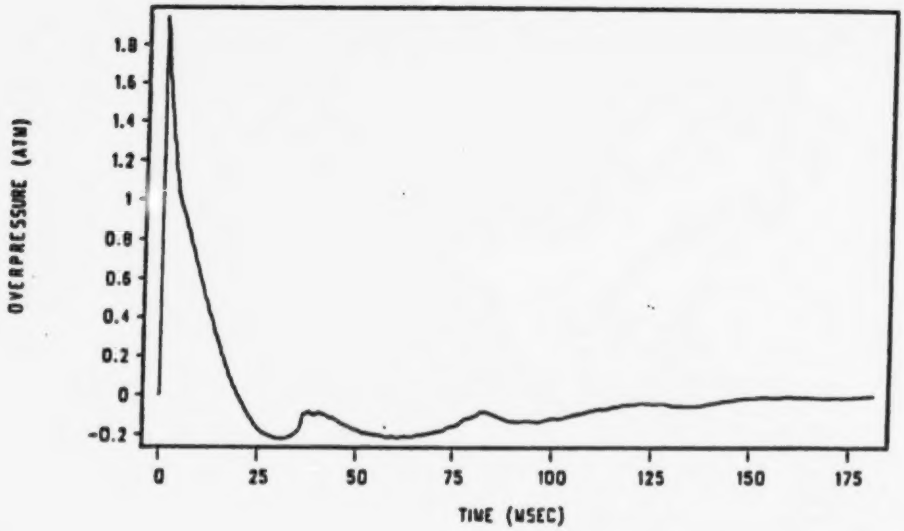

PRESSURE AT R = 20.0M

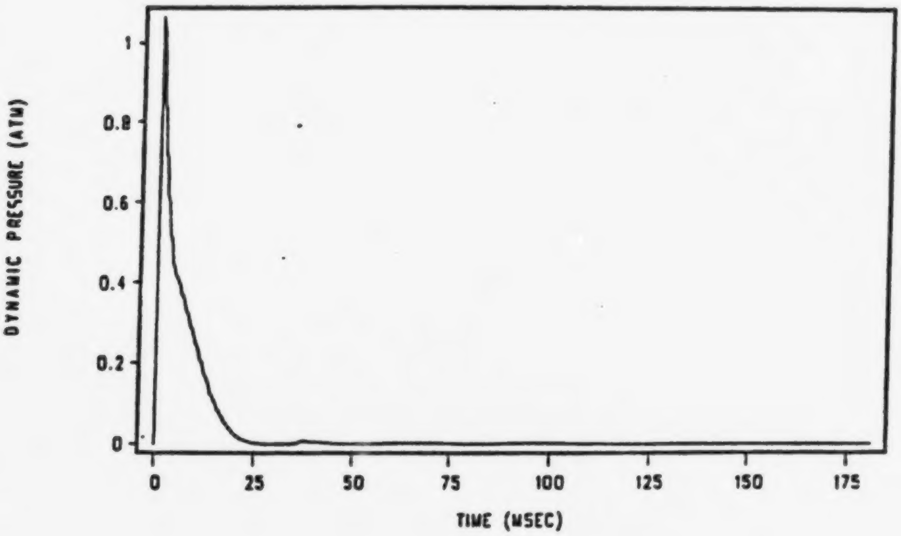

DYNAMIC PRESSURE AT R = 20.0M

FIGURE 10

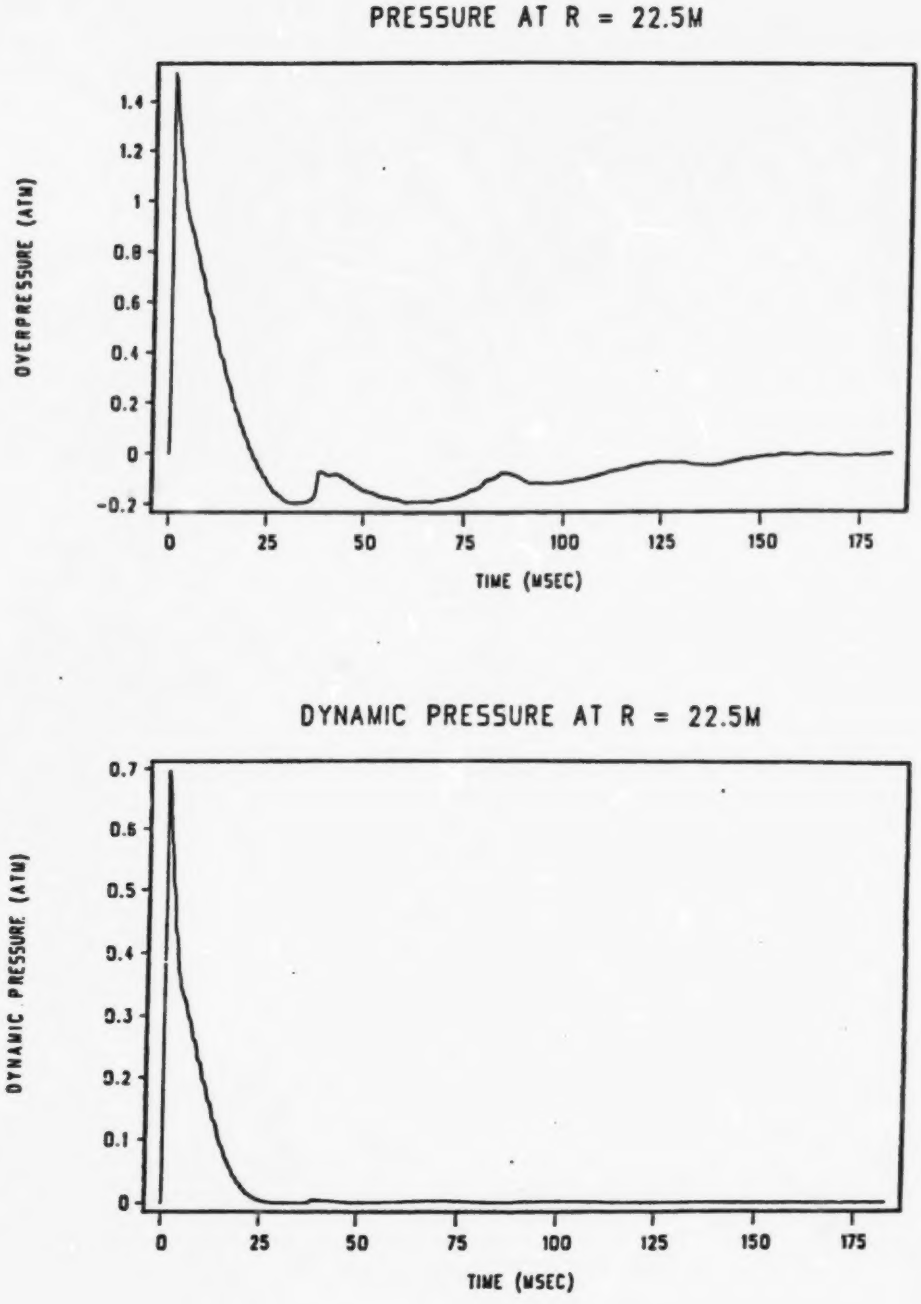
PRESSURE AT R = 22.5M
OVERPRESSURE (ATM)
1.4
1.2
1
0.8
0.6
0.4
0.2
0
-0.2
0
25
50
75
100
125
150
175
TIME (MSEC)
DYNAMIC PRESSURE AT R = 22.5M
DYNAMIC PRESSURE (ATM)
0.7
0.6
0.5
0.4
0.3
0.2
0.1
0
0
25
50
75
100
125
150
175
TIME (MSEC)

FIGURE 11

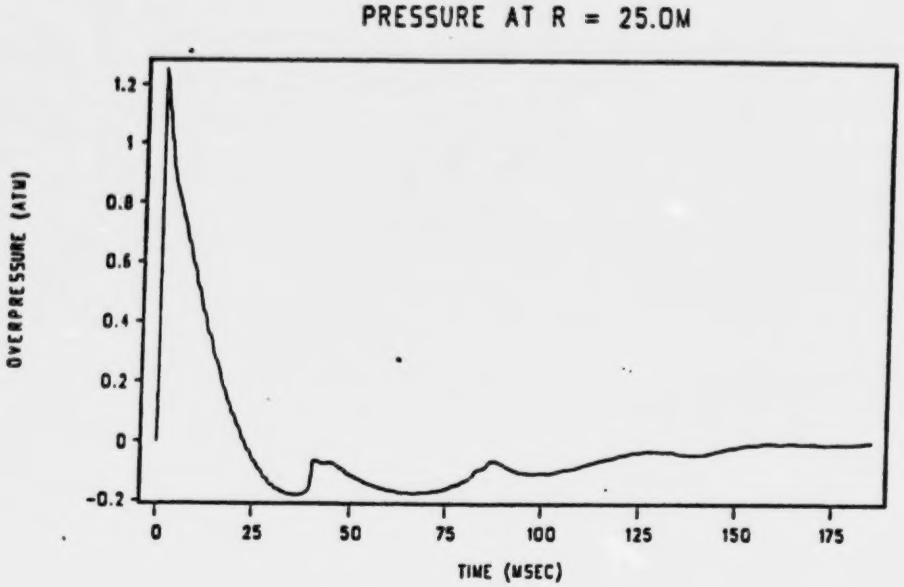
PRESSURE AT R = 25.0M
OVERPRESSURE (ATM)
1.2
1
0.8
0.6
0.4
0.2
0
-0.2
0
25
50
75
100
125
150
175
TIME (MSEC)

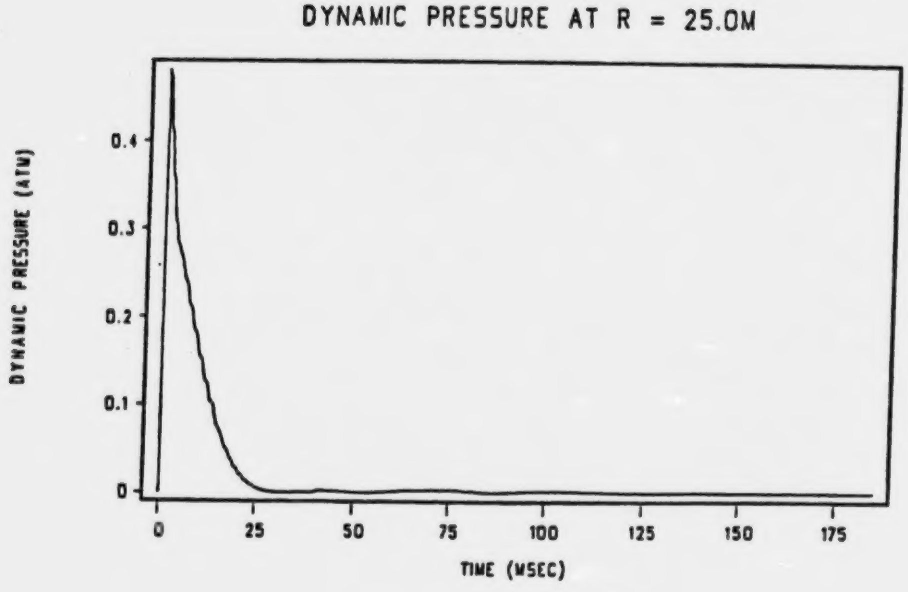
DYNAMIC PRESSURE AT R = 25.0M
DYNAMIC PRESSURE (ATM)
0.4
0.3
0.2
0.1
0
0
25
50
75
100
125
150
175
TIME (MSEC)

FIGURE 12

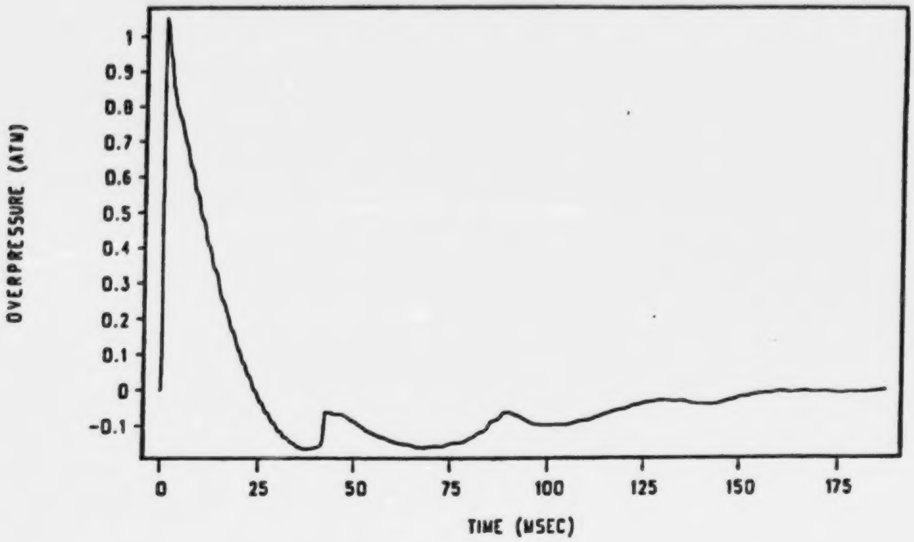

PRESSURE AT R = 27.5M

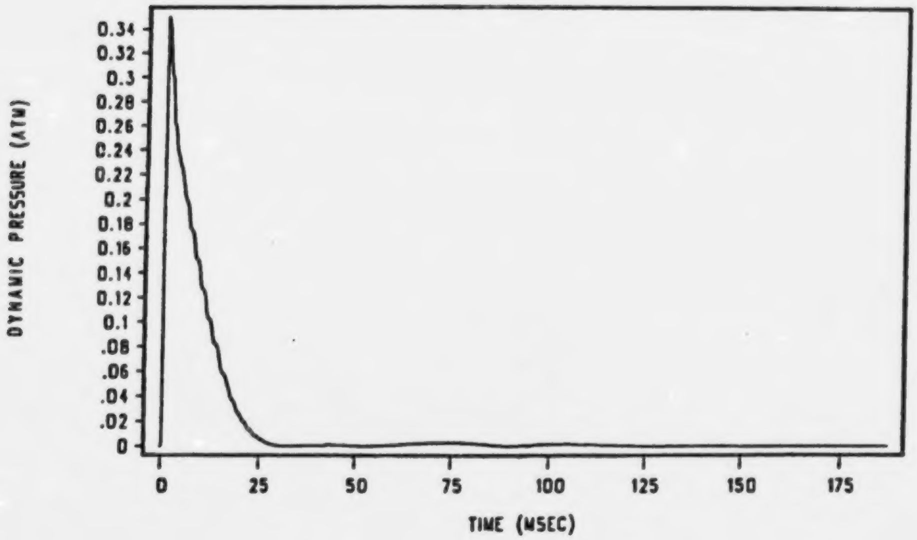

DYNAMIC PRESSURE AT R = 27.5M

FIGURE 13

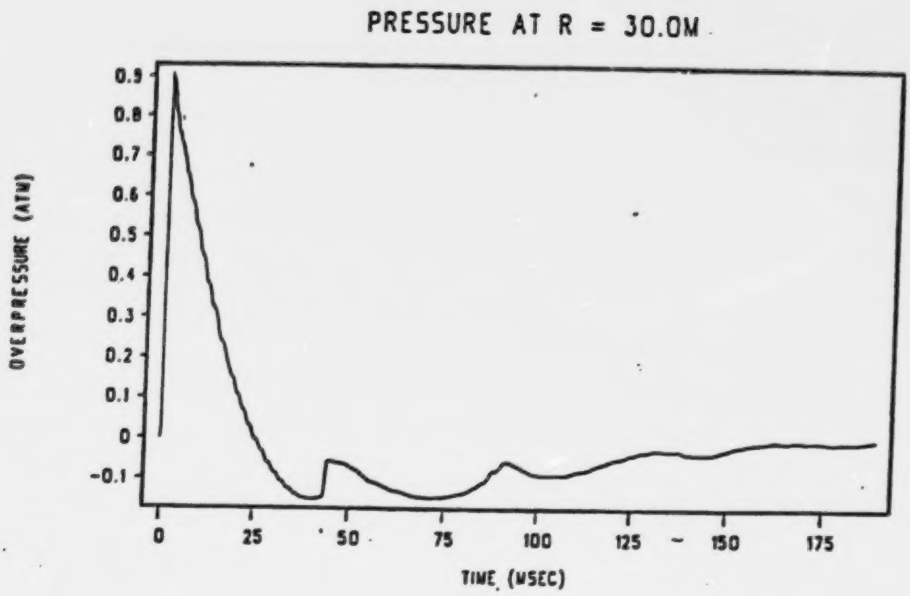

PRESSURE AT R = 30.0M

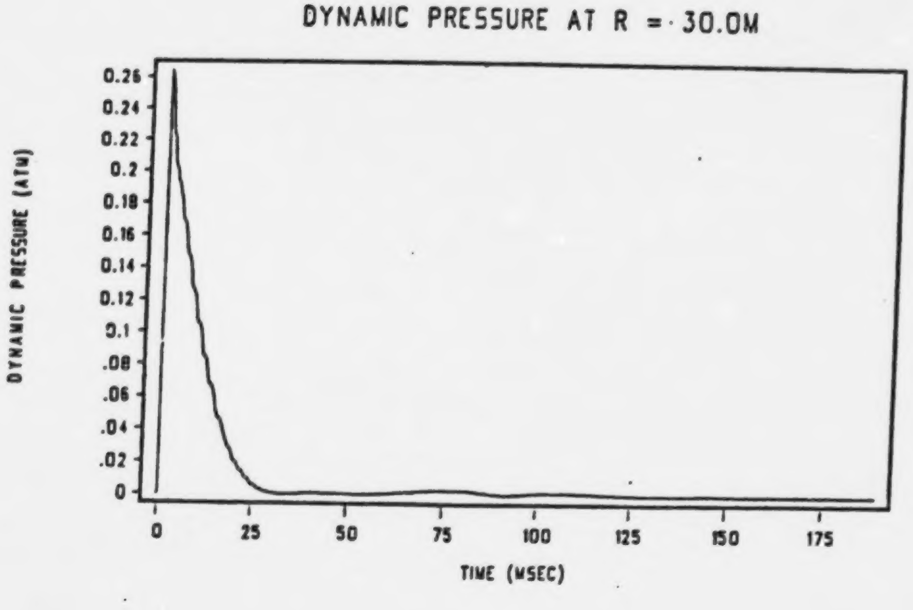

DYNAMIC PRESSURE AT R = 30.0M

FIGURE 14

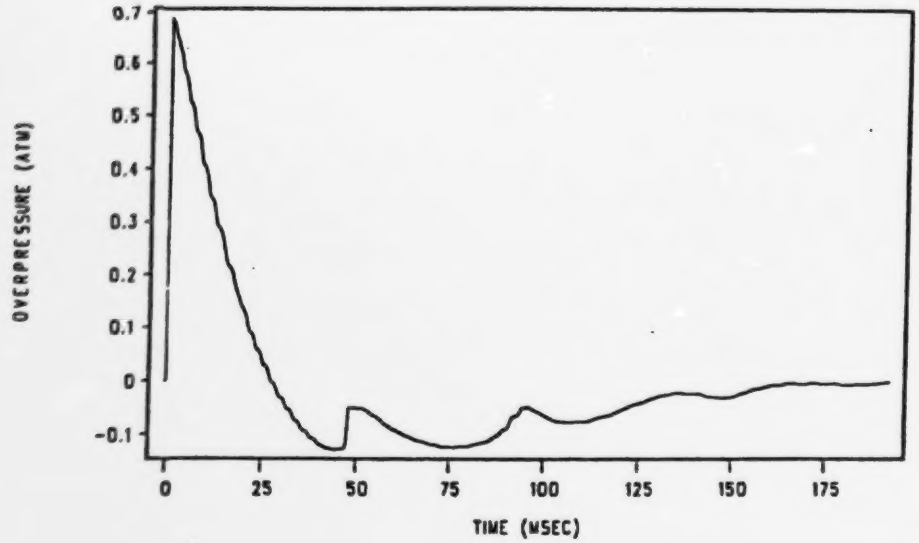
PRESSURE AT R = 35.0M

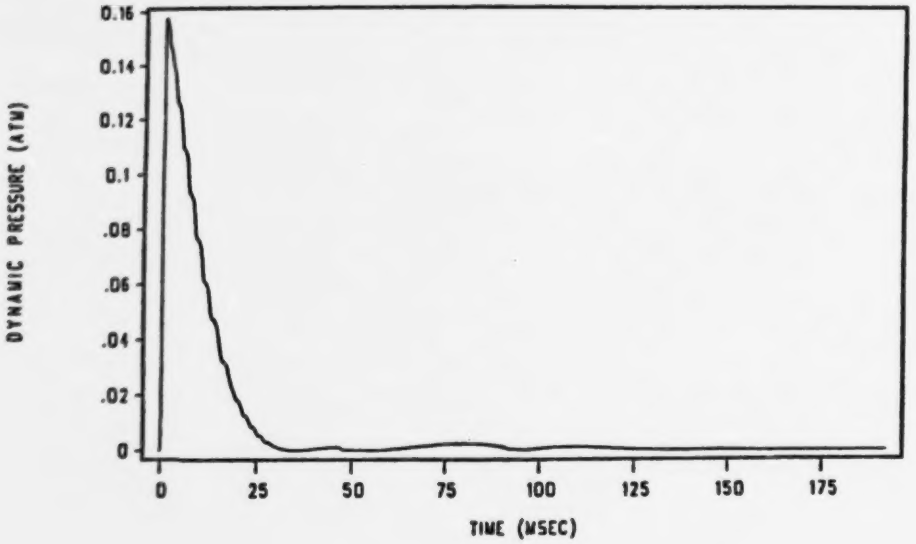
DYNAMIC PRESSURE AT R = 35.0M

FIGURE 15

PRESSURE AT R = 40.0M

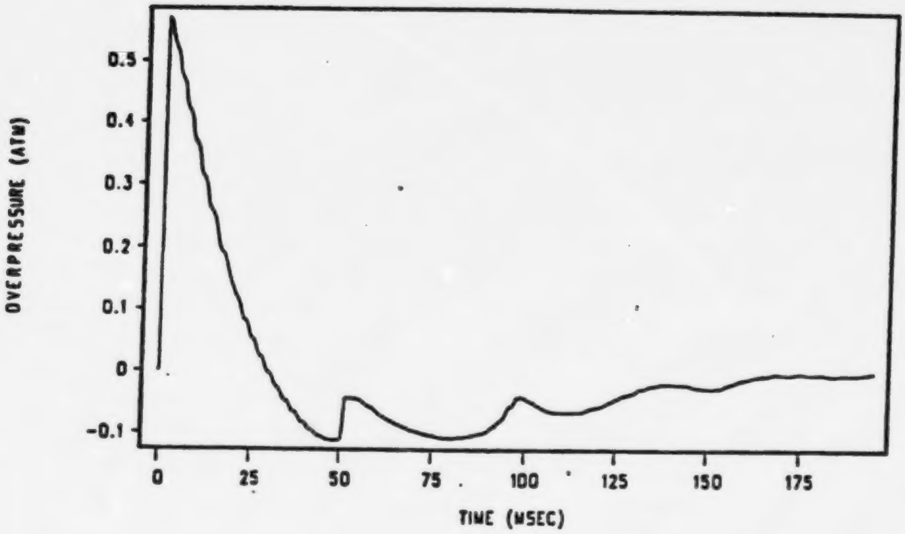

DYNAMIC PRESSURE AT R = 40.0M

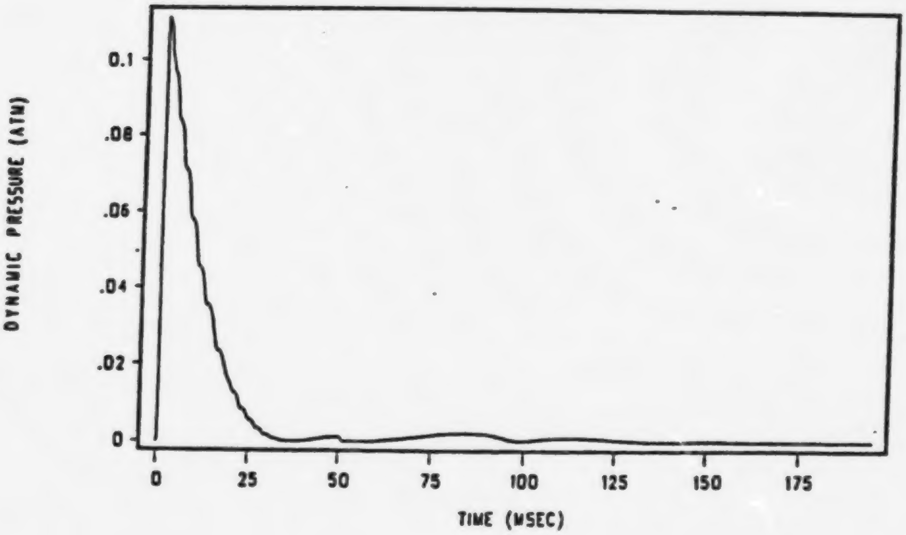

FIGURE 16

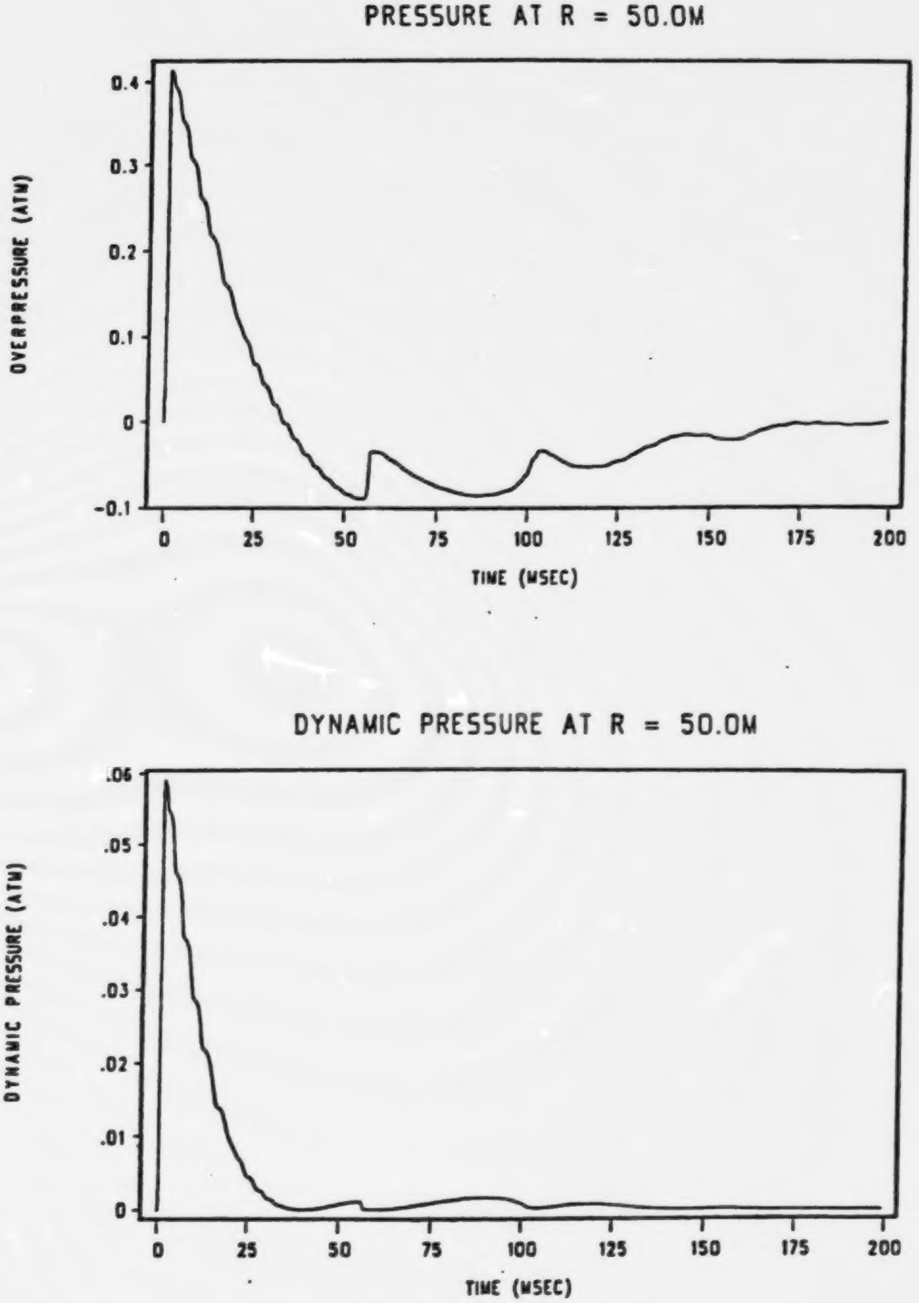
PRESSURE AT R = 50.0M
OVERPRESSURE (ATM)
0.4
0.3
0.2
0.1
0
-0.1
0
25
50
75
100
125
150
175
200
TIME (MSEC)
DYNAMIC PRESSURE AT R = 50.0M
DYNAMIC PRESSURE (ATM)
.06
.05
.04
.03
.02
.01
0
0
25
50
75
100
125
150
175
200
TIME (MSEC)

FIGURE 17

PRESSURE AT R = 75.0M

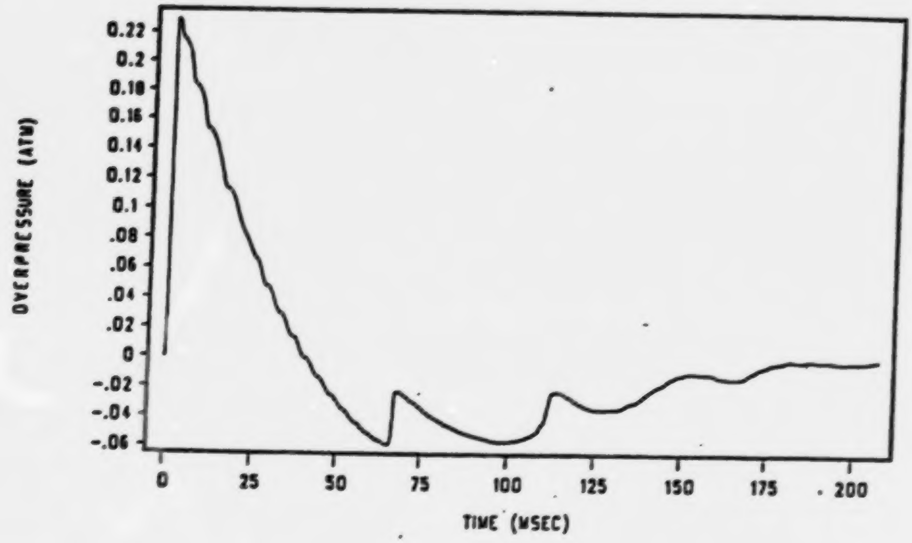

DYNAMIC PRESSURE AT R = 75.0M

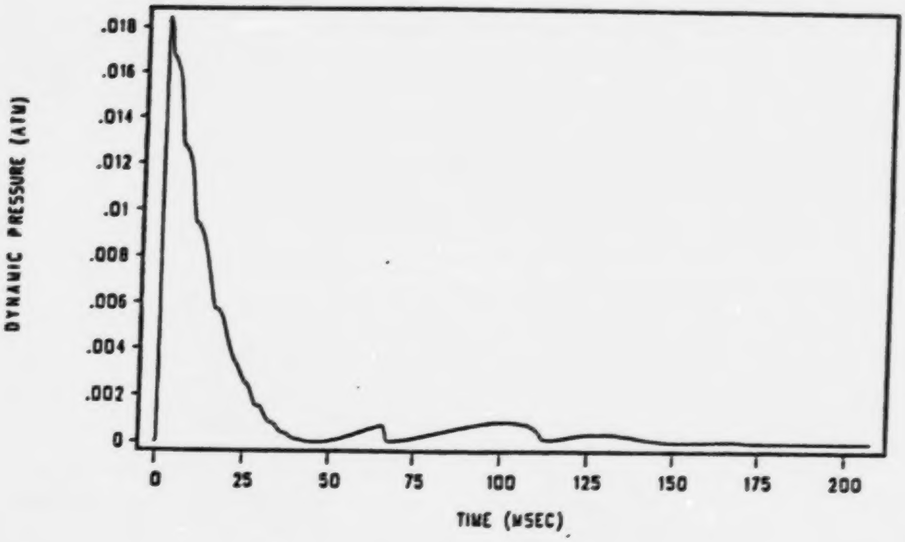

FIGURE 18

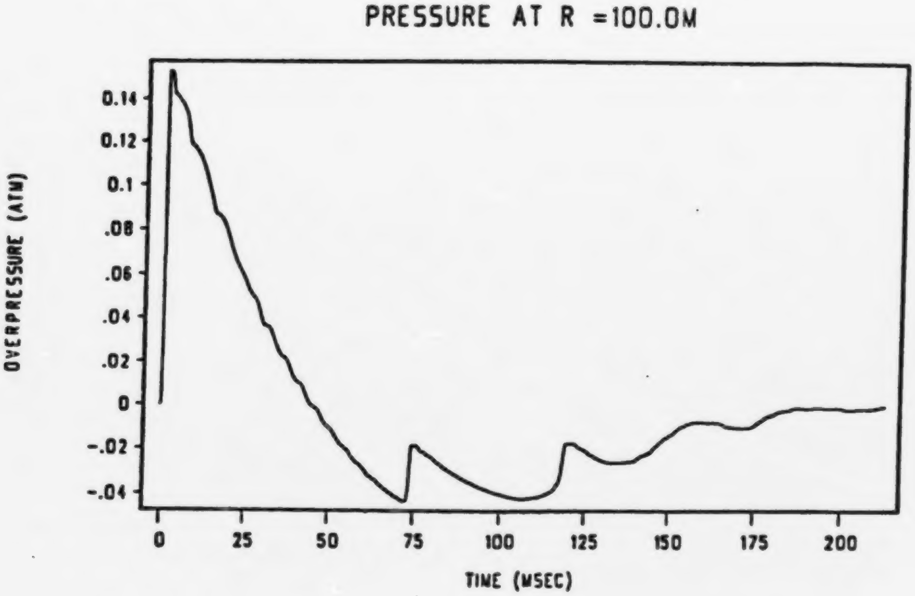
PRESSURE AT R =100.0M
OVERPRESSURE (ATM)
0.14
0.12
0.1
.08
.06
.04
.02
0
-.02
-.04
0
25
50
75
100
125
150
175
200
TIME (MSEC)

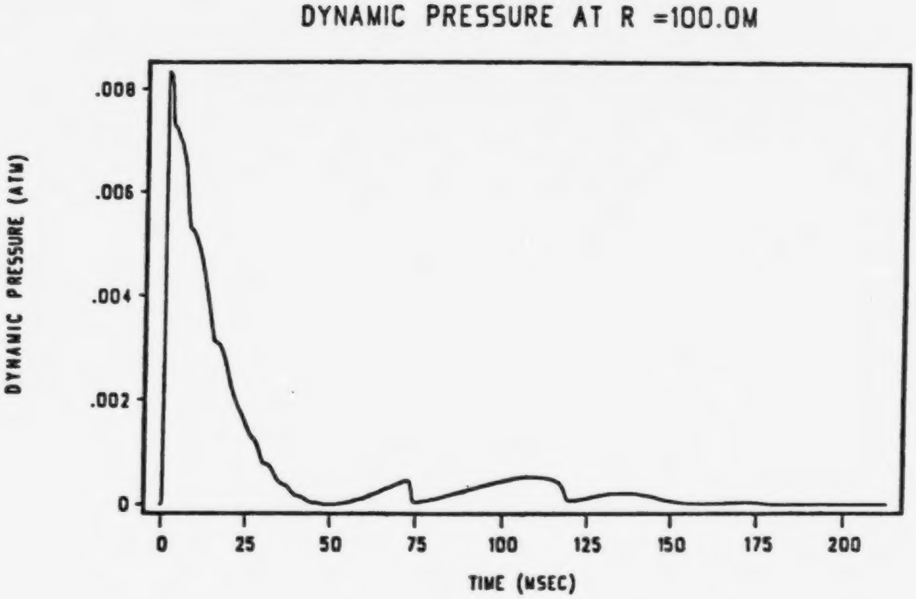
DYNAMIC PRESSURE AT R =100.0M
DYNAMIC PRESSURE (ATM)
.008
.006
.004
.002
0
0
25
50
75
100
125
150
175
200
TIME (MSEC)

FIGURE 19

PRESSURE AT R =125.0M

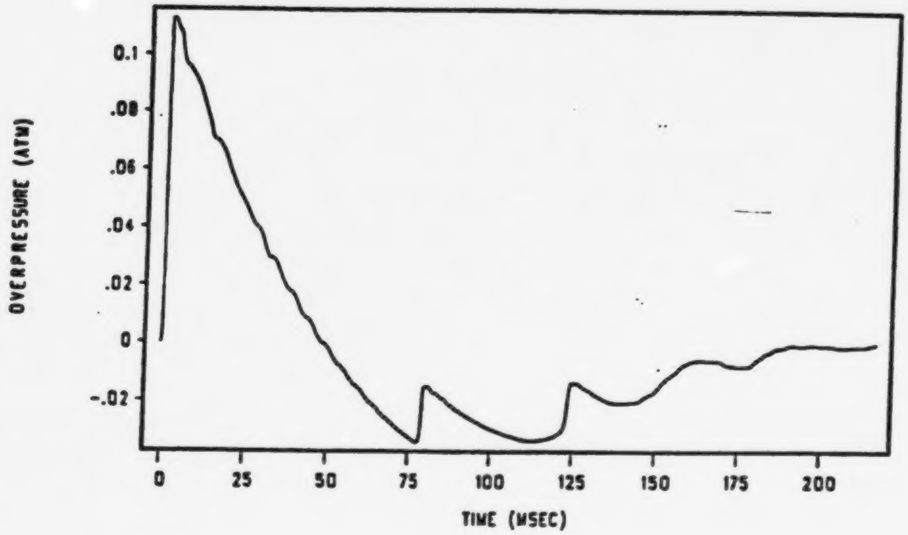

DYNAMIC PRESSURE AT R =125.0M

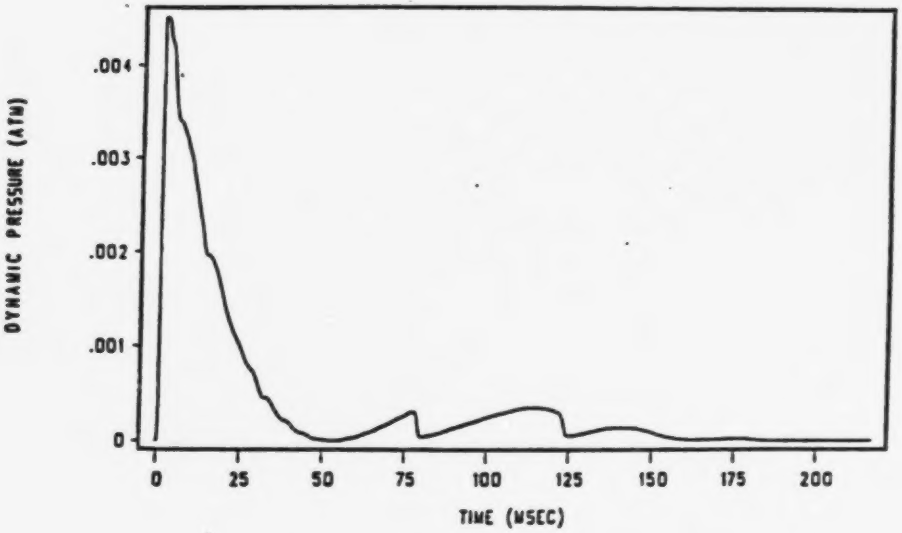

FIGURE 20

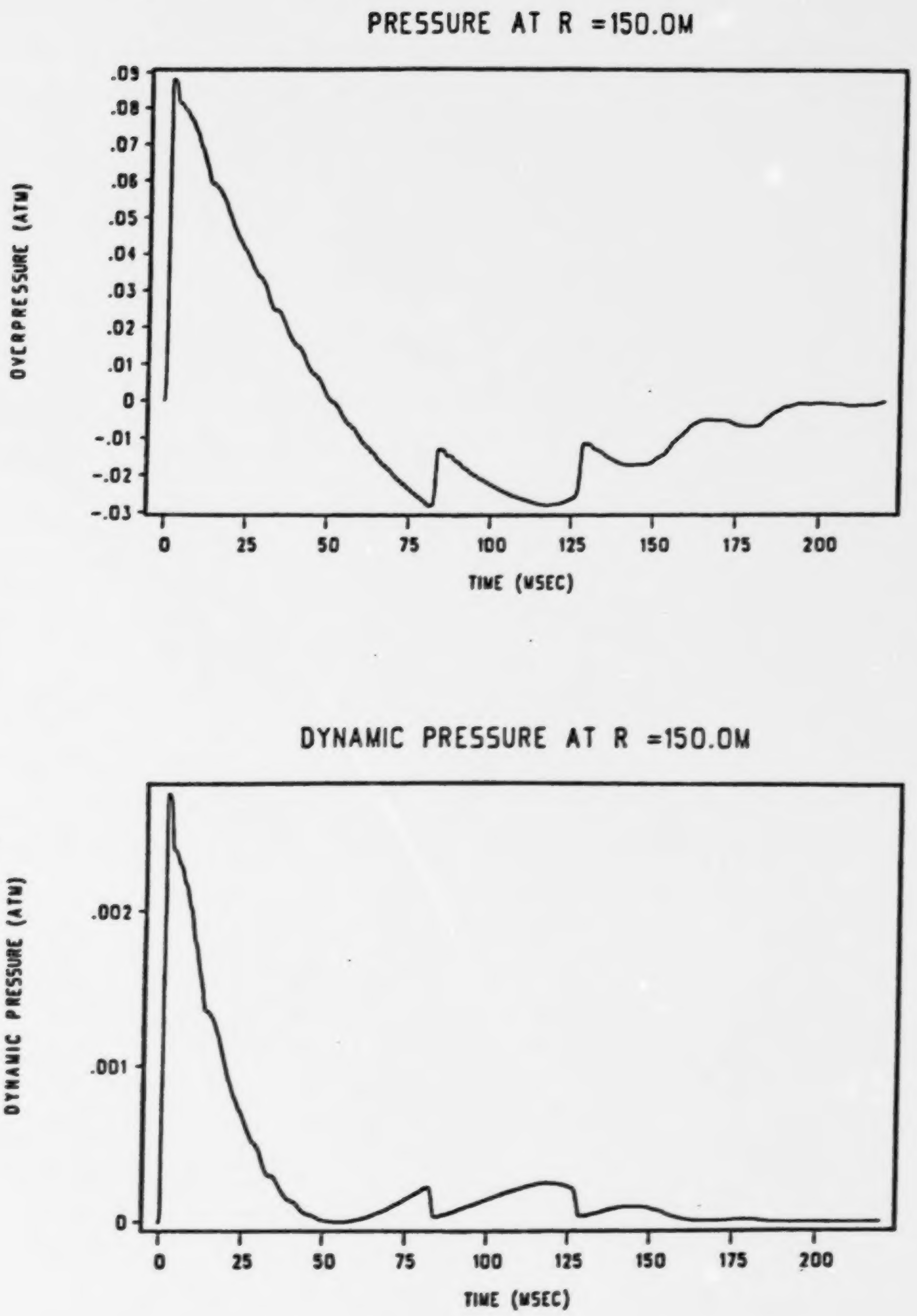
PRESSURE AT R =150.0M
OVERPRESSURE (ATM)
.09
.08
.07
.06
.05
.04
.03
.02
.01
0
-.01
-.02
-.03
0
25
50
75
100
125
150
175
200
TIME (MSEC)
DYNAMIC PRESSURE AT R =150.0M
DYNAMIC PRESSURE (ATM)
.002
.001
0
0
25
50
75
100
125
150
175
200
TIME (MSEC)

FIGURE 21

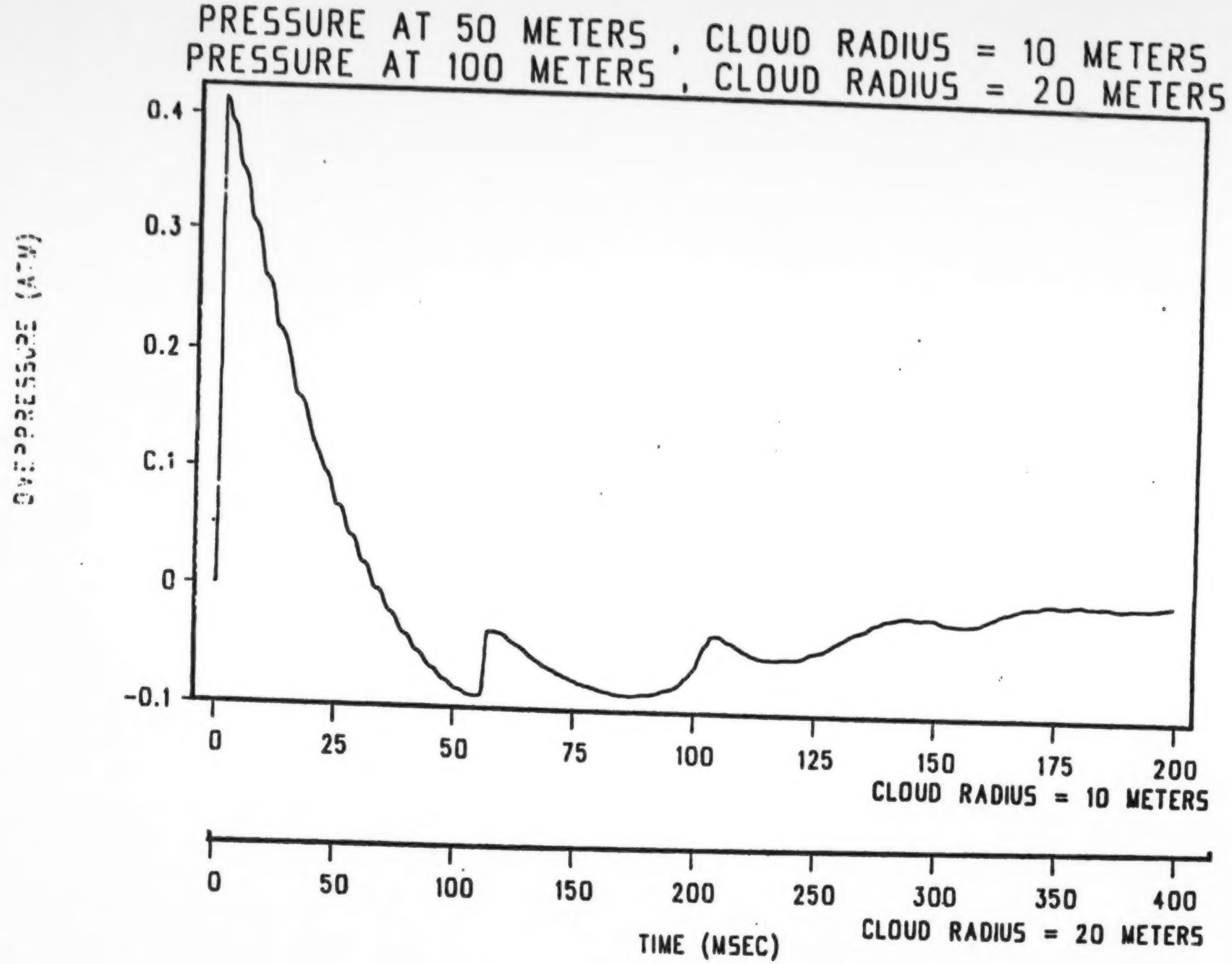
PRESSURE AT 50 METERS , CLOUD RADIUS = 10 METERS
PRESSURE AT 100 METERS , CLOUD RADIUS = 20 METERS
OVERPRESSURE (ATM)
0.4
0.3
0.2
C.1
0
-0.1
0
25
50
75
100
125
150
175
200
CLOUD RADIUS = 10 METERS
0
50
100
150
200
250
300
350
400
CLOUD RADIUS = 20 METERS
TIME (MSEC)

FIGURE 22

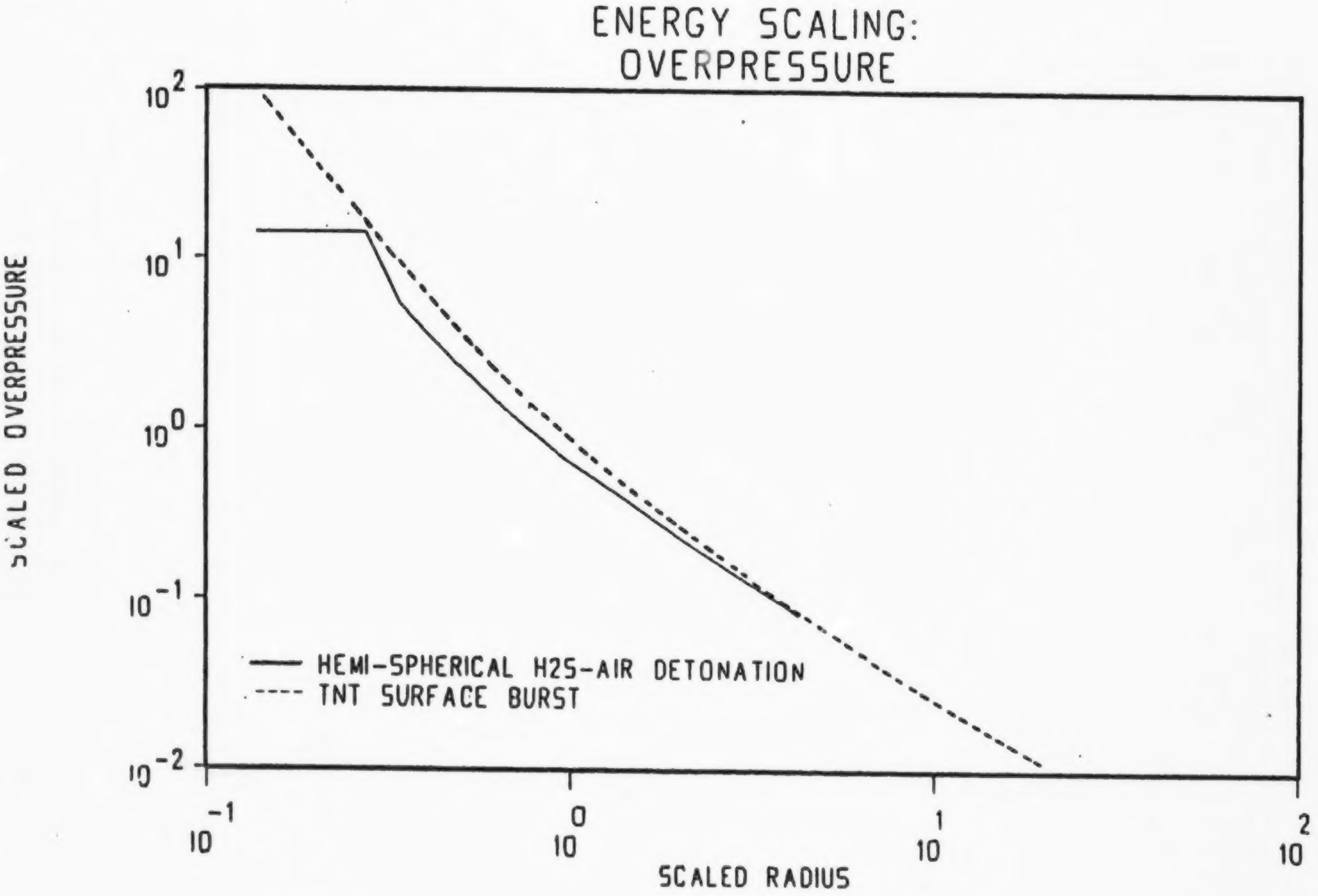
ENERGY SCALING:
OVERPRESSURE
SCALED OVERPRESSURE
10^{2}
10^{1}
10^{0}
10^{-1}
10^{-2}
10^{-1}
10^{0}
10^{1}
10^{2}
SCALED RADIUS
HEMI-SPHERICAL H2S-AIR DETONATION
TNT SURFACE BURST

FIGURE 23

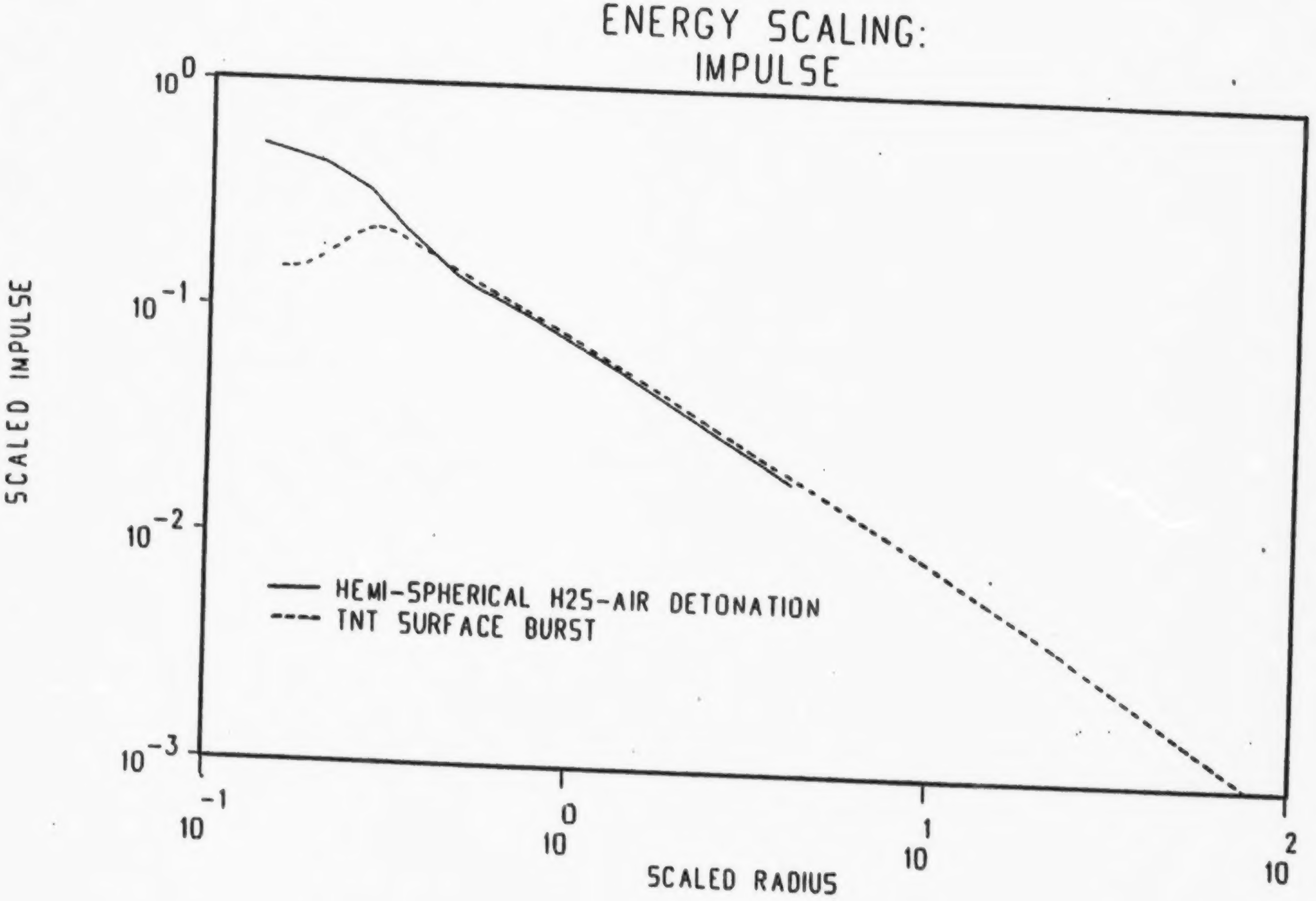
ENERGY SCALING:
IMPULSE
SCALED IMPULSE
10^{0}
10^{-1}
10^{-2}
10^{-3}
10^{-1}
10^{0}
10^{1}
10^{2}
SCALED RADIUS
HEMI-SPHERICAL H2S-AIR DETONATION
TNT SURFACE BURST

FIGURE 24